1102

JAERI 1268

NEANDC(J)-68/U
INDC (JAP)-55/L

Neutron Cross Sections of 28 Fission Product Nuclides adopted in JENDL-1

February 1981

日本原子力研究所
Japan Atomic Energy Research Institute

JAERI 1268

JAERI レポート

この報告書は，日本原子力研究所で行われた研究および技術の成果を研究成果編集委員会の審査を経て，不定期に刊行しているものです．

入手（資料交換による），複製などの問合わせは，日本原子力研究所技術情報部（〒319-11 茨城県那珂郡東海村）あて，お申しこみください．なお，このほかに財団法人原子力弘済会資料センター（茨城県那珂郡東海村日本原子力研究所内）で複写による実費頒布をおこなっております．

JAERI Report

Published by the Japan Atomic Energy Research Institute

Inquiries about the availability of reports and their reproduction should be addressed to the Division of Technical Information, Japan Atomic Energy Research Institute, Tokai-mura, Naka-gun, Ibaraki-ken, Japan.

編集兼発行　日本原子力研究所
印　　刷　三美印刷株式会社

Neutron Cross Sections of 28 Fission Product Nuclides Adopted in JENDL-1

Yasuyuki Kikuchi, Tsuneo Nakagawa, Hiroyuki Matsunobu*,
Masayoshi Kawai**, Sin-iti Igarasi and Shungo Iijima**

Working Group on Fission Product Nuclear Data
Japanese Nuclear Data Committee
Tokai Research Establishment
Japan Atomic Energy Research Institute,
Tokai-mura, Naka-gun, Ibaraki-ken

Received September 1, 1980

This is the final report concerning the evaluated neutron cross sections of 28 fission product nuclides adopted in the first version of Japanese Evaluated Nuclear Data Library (JENDL-1). These 28 nuclides were selected as being most important for fast reactor calculations, and are ^{90}Sr, ^{93}Zr, ^{95}Mo, ^{97}Mo, ^{99}Tc, ^{101}Ru, ^{102}Ru, ^{103}Rh, ^{104}Ru, ^{105}Pd, ^{106}Ru, ^{107}Pd, ^{109}Ag, ^{129}I, ^{131}Xe, ^{133}Cs, ^{135}Cs, ^{137}Cs, ^{143}Nd, ^{144}Ce, ^{144}Nd, ^{145}Nd, ^{147}Pm, ^{147}Sm, ^{149}Sm, ^{151}Sm, ^{153}Eu and ^{155}Eu. The status of the experimental data was reviewed over the whole energy range. The present evaluation was performed on the basis of the measured data with the aid of theoretical calculations. The optical and statistical models were used for evaluation of the smooth cross sections. An improved method was developed in treating the multilevel Breit-Wigner formula for the resonance region. Various physical parameters and the level schemes, adopted in the present work are discussed by comparing with those used in the other evaluations such as ENDF/B-IV, CEA, CNEN-2 and RCN-2. Furthermore, the evaluation method and results are described in detail for each nuclide. The evaluated total, capture and inelastic scattering cross sections are compared with the other evaluated data and some recent measured data. Some problems of the present work are pointed out and ways of their improvement are suggested.

Keywords; JENDL-1, Evaluation, Neutron Cross Sections, Fission Products, Optical Model, Statistical Model, Resonance Parameters, Level Scheme, Capture, Inelastic Scattering, Intercomparison.

* Sumitomo Atomic Energy Industries, Ltd.
** Nippon Atomic Industry Group Co., Ltd.

JENDL-1 に収納された核分裂生成物 28 核種の中性子断面積

菊池康之，中川庸雄，松延広幸*，
川合将義**，五十嵐信一，飯島俊吾**

日本原子力研究所 FP 核データワーキンググループ
シグマ研究専門委員会

1980 年 9 月 1 日　受理

本報告書は，JENDL-1 に収納された核分裂生成物 28 核種の中性子断面積評価の最終報告である。この 28 核種は，^{90}Sr, ^{93}Zr, ^{95}Mo, ^{97}Mo, ^{99}Tc, ^{101}Ru, ^{102}Ru, ^{103}Rh, ^{104}Ru, ^{105}Pd, ^{106}Ru, ^{107}Pd, ^{109}Ag, ^{127}I, ^{131}Xe, ^{133}Cs, ^{135}Cs, ^{137}Cs, ^{143}Nd, ^{144}Ce, ^{144}Nd, ^{145}Nd, ^{147}Pm, ^{147}Sm, ^{149}Sm, ^{151}Sm, ^{153}Eu, ^{155}Eu であり，高速炉計算にとって重要性の高い核種を選んだ。今回の評価はまず実験データの現状を全てのエネルギー範囲に渡って調査し，この実験データと理論計算とを用いて行った。高エネルギー領域では，光学模型および統計模型を用い，共鳴領域では，多準位ブライト・ウィグナー公式を改良した公式を用いた。今回の評価で用いられた物理パラメータとレベルスキームについて，ENDF/B-IV, CEA, CNEN-2, RCN-2 等の価と比較検討した。さらに核種毎に詳細な評価方法を記述し，得られた結果を他の評価値や実験値と比較検討した。また，今回の評価で残された問題点を指摘し，将来への改善方向を示した。

* 住友原子力工業(株)，技術部
** 日本原子力事業(株)，NAIG 総合研究所

Contents

目　　次

1. Introduction

Neutron cross sections of fission products (often abbreviated as F. P. hereafter) have been highly required for predicting the long-term characteristics of fast reactors. Although several works[1~7] were performed on cross section evaluations in early 1970's, there have still remained considerable discrepancies among the evaluated data sets, causing uncertainties of about 1% $\Delta k/k$ in prediction of reactivity and of about 20–30% in sodium void reactivity at a typical burn-up stage of fast reactors[8~11].

Under such a situation, Japanese Nuclear Data Committee (JNDC) started evaluation of F. P. cross sections in Working Group on Fission-Product Nuclear Data in 1970. In the present evaluation, the following 28 nuclides were selected as being most important for fast reactors:

^{90}Sr, ^{93}Zr, ^{95}Mo, ^{97}Mo, ^{99}Tc, ^{101}Ru, ^{102}Ru, ^{103}Rh, ^{104}Ru, ^{105}Pd, ^{106}Ru, ^{107}Pd, ^{109}Ag, ^{129}I, ^{131}Xe, ^{133}Cs, ^{135}Cs, ^{137}Cs, ^{143}Nd, ^{144}Ce, ^{144}Nd, ^{145}Nd, ^{147}Pm, ^{147}Sm, ^{149}Sm, ^{151}Sm, ^{153}Eu, ^{155}Eu.

These 28 nuclides cover about 80% of macroscopic capture reactions by F. P. in an equilibrium core of a large fast reactor.

The first work on evaluation was published[12] in 1974. A set of reactor group constants was produced by the use of these cross sections and various characteristics of fast reactors were examined by Working Group on Fission-Product Group Constants of JNDC[10,11]. In this early evaluation work, the energy range considered was 100 eV to 15 MeV without taking account of the resonance structure. In a large fast reactor, however, the energy range below several keV is still important and therefore the resonance structure should not be ignored in this energy region. The effects of the neutron width fluctuation and the level interference were also ignored in the early work, resulting in overestimation of the capture and inelastic scattering cross sections and in underestimation of the compound elastic scattering cross section.

Taking these drawbacks into consideration, a reevaluation work was performed. In this work, the neutron energy was extended down to 10^{-5} eV so that the revised cross sections should be applicable also to thermal reactor calculations. The general procedure of this reevaluation was reported in Ref. (13). The reevaluated cross sections were adopted in the first version of Japanese Evaluated Nuclear Data Library (JENDL-1)[14]. Lumped group constants were also made[15] on the basis of this new evaluation, and have been used in Japan as the standard F. P. group constants.

Since then there appeared three sets of new evaluation, i. e., the CEA set[16]*, the RCN-2 set[17,18,19] and the CNEN-2 set[20]*. These new evaluations adopted more sophisticated method of evaluation than the present JENDL-1 evaluation. The development of nuclear model for F. P. evaluation was discussed[22,23] in the second IAEA advisory group meeting on fission product nuclear data in Petten, the Netherlands in 1977. Taking account of this new situation, the evaluation of JENDL-1 has been reexamined particularly on the adopted models and parameters.

This report describes the evaluation of 28 F. P. nuclides adopted in JENDL-1 in detail for each nuclide, compares the present results with the other new evaluated data such as ENDF/B-IV, CEA, CNEN-2 and RCN-2, discusses the discrepancies among the evaluated data by comparing the adopted parameters and models, and suggests the way of further improvement of the present evaluation. In Chapter 2, the status of measured data and the general evaluation method are described. Values of parameters used in the evaluation are tabulated. Chapter 3 is devoted to detailed discussion on each nuclide concerning the status of measured data, the evaluation method, comparison with the other evaluations and the encountered problems in the present JENDL-1 data. In Chapter 4, discrepancies among the recent evaluations are reviewed and suggestions are made for further improvement of the present data. The evaluated cross sections are tabulated in Appendix in the form of the averaged values over appropriate energy intervals.

---

* These abbreviations are used by Gruppelaar *et al.*[21]

2. General Description

2.1 Status of Experimental Data

This section describes the status of the experimental data available at present (December 1978). As to the capture data, the status at the time of the present evaluation (July 1975) is also given.

2.1.1 Total Cross Section

The status of total cross section data is shown in TABLE 2.1, in which the number of references on total cross section measurements are given for the thermal, resonance, and fast (>1 keV) energy ranges, and the number of data points and energy range of measurements are also given. The status was surveyed using CINDA 76/77[24] and its Supplement 4.

The thermal data are poor compared with the data in resonance and fast energy ranges. The data in the resonance energy range are comparatively abundant, and exist for 20 nuclides. Measurements in the fast energy range have been performed for 12 nuclides.

TABLE 2.1 Status of the exprerimental data for total cross section

Nuclide	Number of References			σ_T Data Above 1 keV		Comments
	Thermal	Resonance	Fast	Number of Data points	Energy Range	
^{90}Sr	None	None	None			
^{93}Zr	None	1	None			
^{95}Mo	None	None	1	103	130~640 keV	
^{97}Mo	None	None	None			
^{99}Tc	3	5+(1)	3	Many 237	<130 keV 2.5~15 MeV	110 points in 2 eV~130 keV
^{101}Ru	None	1	None			Resonance Parameter
^{102}Ru	None	1	None			Resonance Parameter
^{103}Rh	6	8	9	Many	<15 MeV	8663 pts. below 4.2 keV 242 pts. in 2.5~15 MeV
^{104}Ru	None	1	None			Resonance Parameter
^{105}Pd	None	None	None			
^{106}Ru	None	None	None			
^{107}Pd	None	(1)	None			Resonance Parameter
^{109}Ag	None	3	1	1	14 MeV	σ_T=4.38±0.02 b at 14 MeV
^{129}I	2	1	None			
^{131}Xe	None	None	None			
^{133}Cs	3	5	7	Many 727	<4.5 keV 2.50 keV~15 MeV	7553 pts. in 100 eV~4.5 keV
^{135}Cs	None	1	None			Res. E_0 only (31 pts.)
^{137}Cs	None	1	None			
^{143}Nd	3	3	2	Many 1	<30 keV 14 MeV	11200 points in 65 eV~30 keV
^{144}Ce	None	None	None			
^{144}Nd	None	1	4	Many	<14 MeV	9498 points in 90 eV~29 keV
^{145}Nd	2	3	2	Many 1	<25 keV 14 MeV	13815 points in 31 eV~25 keV
^{147}Pm	4+(1)	4+(1)	1	229	2.5~15 MeV	
^{147}Sm	2	1	None			
^{149}Sm	5	5	2	? 1	<650 keV 14 MeV	
^{151}Sm	2	2	1	Graph	<2.5 keV	
^{153}Eu	2+(1)	3	1	1	2.0 keV	
^{155}Eu	None	None	None			

Numbers in parenthesis show the documentations published since January, 1976.

2.1.2 Capture Data

TABLE 2.2 shows the status of capture data. This includes the thermal neutron cross sections, resonance integrals, resonance parameters and the capture cross sections above 1 keV.

Thermal neutron cross section data are available for all the nuclides except ^{105}Pd and ^{107}Pd. It should be noted, however, that there often exist large discrepancies among the experimental data. Resonance integrals are available for 18 nuclides, but the measured values are not necessarily consistent with the values expected from the resonance parameters. We regarded the resonance integral data as only auxiliary information in the present work.

The resonance parameters were available for 21 nuclides at the time of the present evaluation. After that the parameters of ^{107}Pd became available.

The data for capture cross sections above 1 keV were available for 11 nuclides at the time of the present work. The data for ^{101}Ru, ^{105}Pd, ^{143}Nd, ^{144}Nd and ^{145}Nd were published after this work. The data for ^{103}Rh, ^{109}Ag, and ^{133}Cs are abundant compared with other nuclides, but there exist significant discrepancies among the measured data. For neutron energies above 100 keV, the data were available only for ^{102}Ru, ^{104}Ru, ^{103}Rh, ^{109}Ag, and ^{133}Cs when the evaluation work was performed. However, at present, the data for ^{101}Ru, ^{105}Pd, ^{144}Nd, ^{147}Sm, ^{149}Sm, and ^{153}Eu have been released in this energy range.

2.1.3 Inelastic Scattering Cross Section

The inelastic scattering cross section of F. P. nuclides is an important quantity after the capture cross

TABLE 2.2 Status of the experimental data for neutron capture available up to March, 1980

Nuclide	$\sigma_{a,th}$	Resolved Resonances				$\sigma(n,\gamma)$ Data Above 1 keV		
		RI_γ	N_{res}	E_{max} (eV)	Γ_γ	Number of References	Number of Data Points	Energy Range
^{90}Sr	Yes	No	—	—	—	None		
^{93}Zr	Yes	No	1	110	No	None		
^{95}Mo	Yes	Yes	55	2142	Yes	3+(1)	33+(35)	<200 keV
^{97}Mo	Yes	No	64	1941	Yes	2+(1)	43+(35)	<200 keV
^{99}Tc	Yes	Yes	11	280	Yes	2+(1)	22+(10)	<80 keV, 14.7 MeV
^{101}Ru	Yes	Yes	30+(124)	670 (4483.4)	Yes	1+(1)	434	2.6~550 keV
^{102}Ru	Yes	Yes	3+(121)	1296 (13446)	(Yes)	5+(1)	168	2~500 keV
^{103}Rh	Yes	Yes	276+(97)	4140 (4163)	Yes	34+(1)	Many	<15 MeV
^{104}Ru	Yes	Yes	4+(86)	1055 (11864)	(Yes)	11+(2)	178+(1)	2~950 keV, 3 MeV, 14.5~14.7 MeV
^{105}Pd	Yes	No	58+(85)	808 (3652)	Yes	2+(2)	564+(16)	2.6~800 keV
^{106}Ru	Yes	Yes	—	—	—	None		
^{107}Pd	No	No	(34)	(654)	—	None		
^{109}Ag	Yes	Yes	81	2506	Yes	9	49	<6 MeV
^{129}I	Yes	Yes	5	153	No	None		
^{131}Xe	Yes	No	39	3945	Yes	None		
^{133}Cs	Yes	Yes	160	3500	Yes	10+(3)	162+(26)	<2.6 MeV, 14~15 MeV
^{135}Cs	Yes	Yes	—	—	—	None		
^{137}Cs	Yes	No	—	—	—	None		
^{143}Nd	Yes	Yes	111^B	5503	Yes	(2)	(14)	3~400 keV
^{144}Ce	Yes	Yes	—	—	—	None		
^{144}Nd	Yes	No	35	19407	Yes	(2)	(44)	3~350 keV
^{145}Nd	Yes	Yes	191	4637	Yes	1+(2)	434+(14)	3~400 keV
^{147}Pm	Yes	Yes	38^B	317	Yes	None		
^{147}Sm	Yes	Yes	131^B	1161	Yes	1+(1)	1+(75)	5~350 keV
^{149}Sm	Yes	No	87^B	249	Yes	2+(1)	435+(75)	5~350 keV
^{151}Sm	Yes	Yes	10^B	13	Yes	None		
^{153}Eu	Yes	Yes	76	97	Yes	4+(3)	628+(93)	<350 keV
^{155}Eu	Yes	No	—	—	—	None		

Symbol B indicates that bound level is known to exist besides N_{res}.
Numbers in parenthesis show the data published since January, 1976.

section in reactor calculations. It gives a considerable contribution to the slowing down and spectrum of neutrons, and therefore affects the sodium void coefficient. Hence, it is desirable to evaluate the cross section value as precisely as possible. Against this requirement, the status of the experimental data is poor as shown in TABLE 2.3. The data of total inelastic scattering cross section exist only for ^{99}Tc, ^{103}Rh, and ^{133}Cs, while the differential inelastic scattering cross section has been measured for 7 nuclides, *i. e.*, ^{99}Tc, ^{102}Ru, ^{104}Ru, ^{103}Rh, ^{109}Ag, ^{133}Cs, and ^{144}Nd. In the present evaluation, these experimental data were used only as references.

2.2 Calculation of Smooth Cross Sections

The evaluation of cross sections in the unresolved resonance region and in the high energy region was based on the calculation with the spherical optical model and the statistical theory. When the capture data were available, the calculated cross sections were normalized to these data.

2.2.1 Optical Model

The optical potential papameters adopted are the same as those used in our previous evaluation[12]. These

TABLE 2.3 Status of the experimental data for inelastic scattering cross section

Nuclide	Total Inelastic			Differential Inelastic		
	No. of Refs.	No. of Data pts.	Energy Range	No. of Refs.	No. of Data pts.	Energy Range
^{90}Sr	None			None		
^{93}Zr	None			None		
^{95}Mo	None			None		
^{97}Mo	None			None		
^{99}Tc	1	1	Fiss. Spectrum	3	4	14~15 MeV
^{101}Ru	None			None		
^{102}Ru	None			1	?	Threshold~900 keV
^{103}Rh	5+(1)	2 55 4	Fiss, Fast 180 keV~4.6 MeV 14 keV~15 MeV	12+(2)	5 330	Fiss 120 keV~15 MeV
^{104}Ru	None			1	?	Threshold~900 keV
^{105}Pd	None			None		
^{106}Ru	None			None		
^{107}Pd	None			None		
^{109}Ag	None			4	24	3~18 MeV
^{129}I	None			None		
^{131}Xe	None			None		
^{133}Cs	1	205	550~970 keV	5	185	120 keV~22 MeV
^{135}Cs	None			None		
^{137}Cs	None			None		
^{143}Nd	None			None		
^{144}Ce	None			None		
^{144}Nd	(1)	1	7.0 MeV	(1)	Graph	4.1~7.0 MeV
^{145}Nd	None			None		
^{147}Pm	None			None		
^{147}Sm	None			None		
^{149}Sm	None			None		
^{151}Sm	None			None		
^{153}Eu	None			None		
^{155}Eu	None			None		

Numbers in parenthesis show the documentations published since January, 1976.

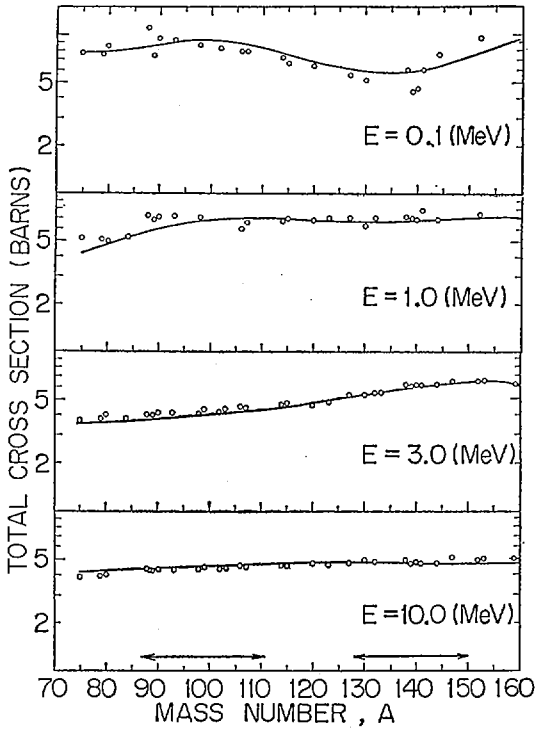

Fig. 2.1 Total cross sections for nuclei in F. P. mass region.

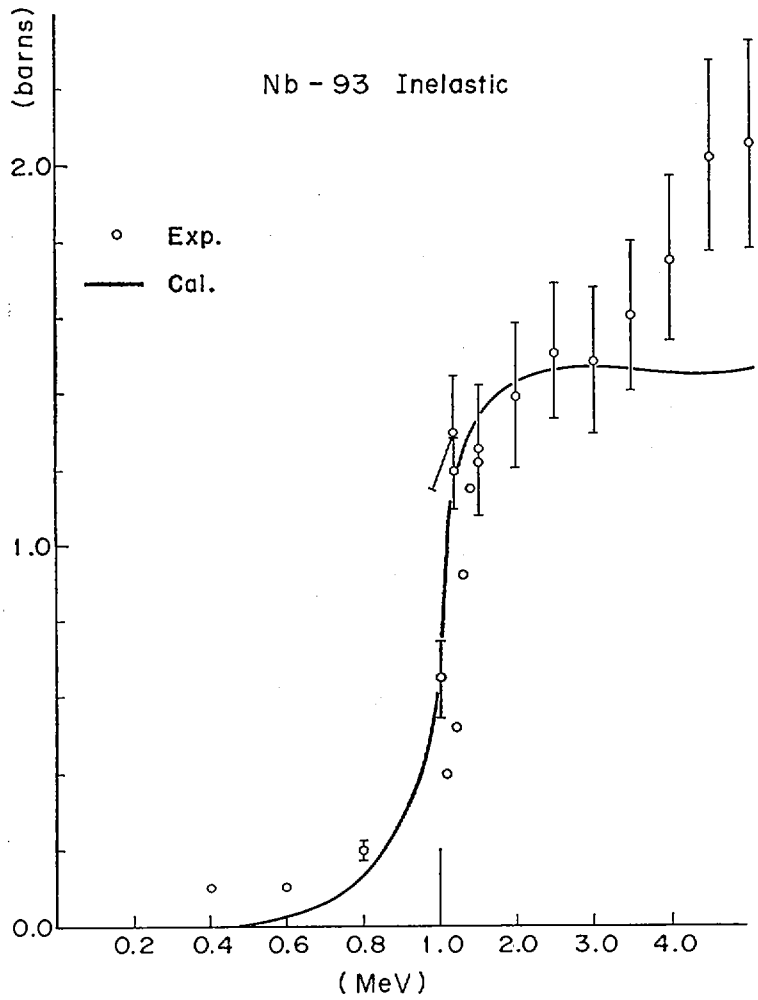

Fig. 2.2 Total elastic scattering cross section of neutrons by ^{93}Nb.

are:

$$V(r)=-(V_0+iW_i)f_1(r)-iW_s f_2(r)-V_{s0}\left(\frac{\hbar}{m_\pi c}\right)^2\frac{1}{r}\left|\frac{df_1(r)}{dr}\right|(\sigma\cdot l) \qquad (1)$$

where

$$f_1(r)=1\Big/\left[1+\exp\left(\frac{r-R_1}{a_0}\right)\right]$$

$$f_2(r)=4\exp\left(\frac{r-R_2}{b}\right)\Big/\left[1+\exp\left(\frac{r-R_2}{b}\right)\right]$$

$V_0=46-0.25E_n$(MeV), for $A<147$

$=52.5-0.25E_n-40(N-Z)/A$(MeV), for $A\geq 147$

$W_I=0.125E_n-0.0004E_n^2$ (MeV)

$W_s=7.0$ MeV, $V_{s0}=7.0$ MeV

$a_0=0.62$ fm, $b=0.35$ fm

$R_1=1.16A^{1/3}+0.6$ fm

$R_2=1.16A^{1/3}+1.1$ fm, for $A<147$

$=1.16A^{1/3}+1.3$ fm, for $A\geq 147$.

Here, m_π is the mass of π-meson and E_n the incident neutron energy in MeV unit in the center of mass system. Other symbols stand for the meanings as commonly used. These potential parameters were obtained so as to reproduce the global trend of the experimental total cross section of nuclides in F. P. mass region as shown in Fig. 2.1. The detail of the procedure is described in Ref. (12). It should be noted that the trend of the real depth is changed at $A=147$.

The validity of these potential parameters was confirmed through comparison between calculated and experimental data on the elastic and inelastic scattering cross sections, the angular distributions of elastically scattered neutrons as shown in Figs. 2.2~2.4 as examples. The s-wave and p-wave strength functions are

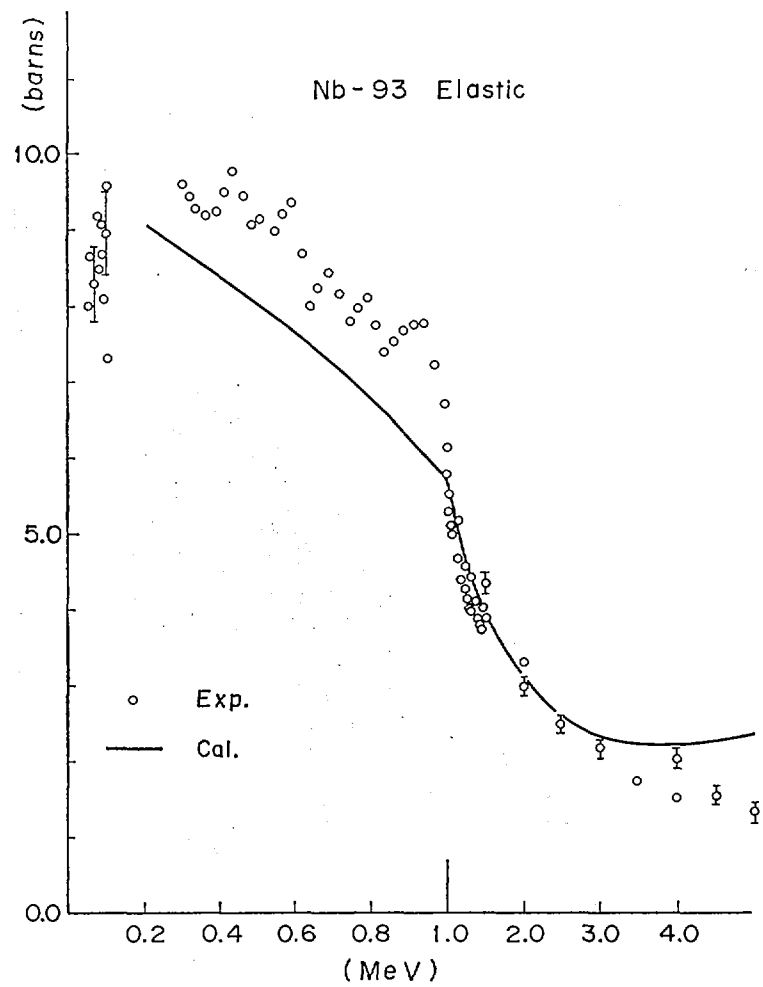

Fig. 2.3 Totat inelastic scattering cross section of neutrons by ^{93}Nb.

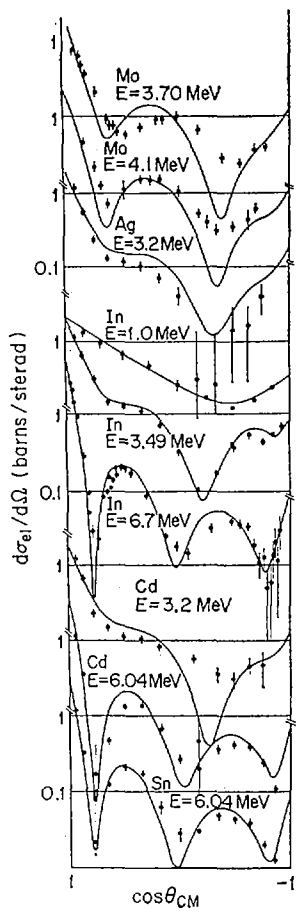

Fig. 2.4 Angular distributions of elastically scattered neutrons from Mo, Ag, In, Cd and Sn.

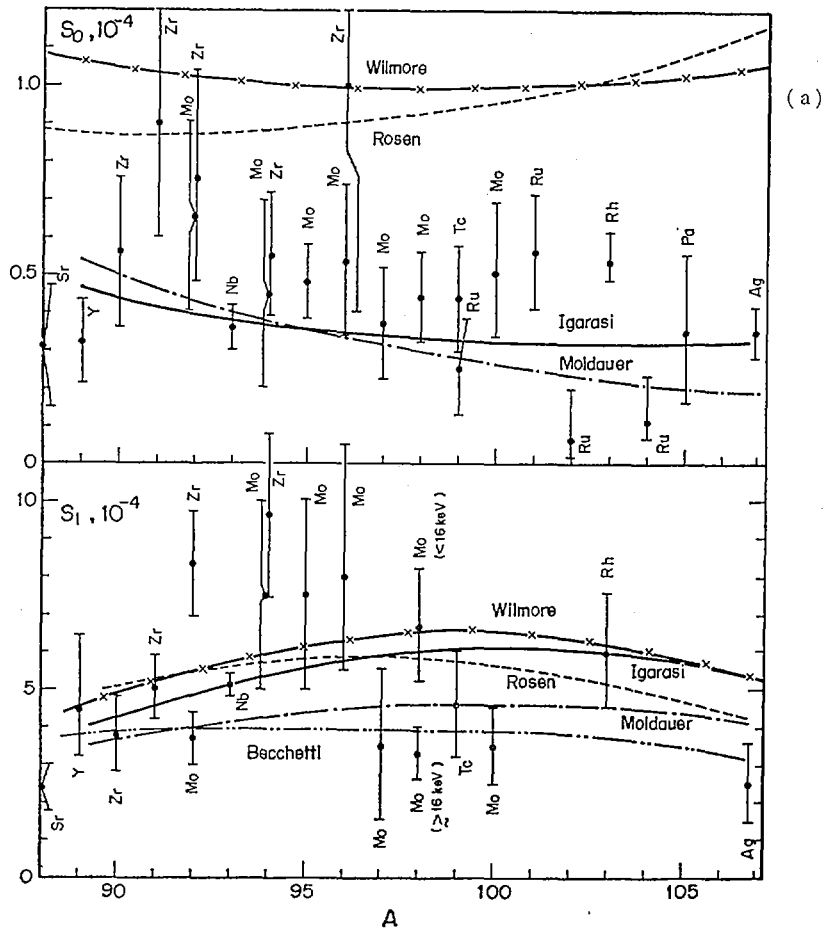

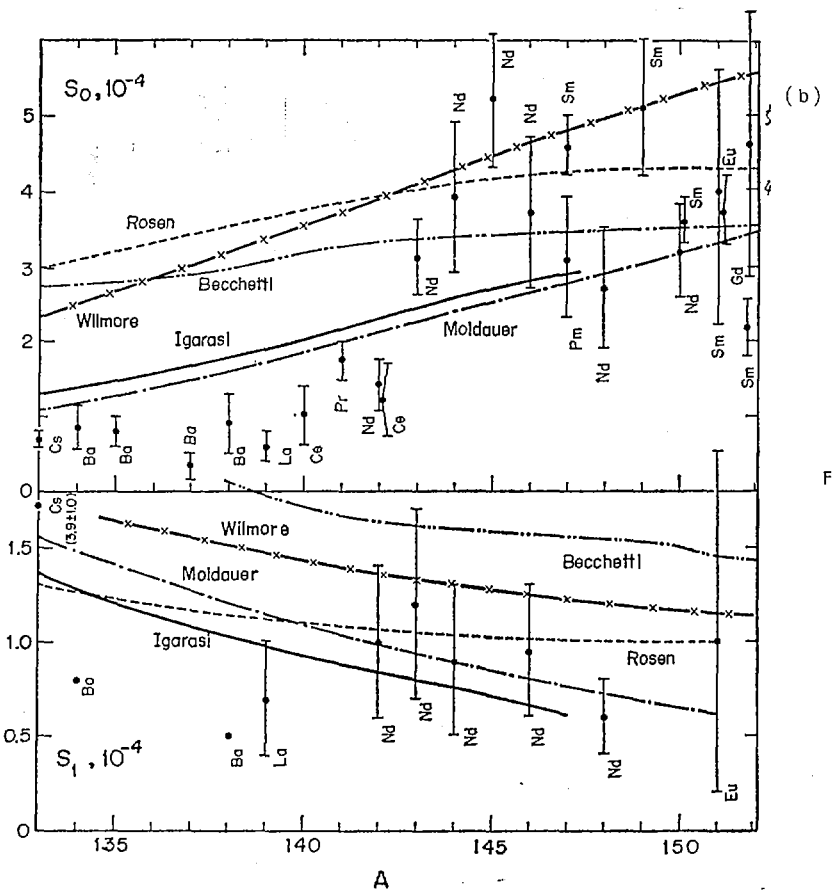

Fig. 2.5 Neutron strength functions calculated by the present optical potential (Igarasi) are compared with the measured values in F. P. mass region as well as with those calculated by the potentials of Moldauer[25], of Wilmore and Hodgson[26], of Becchetti and Greenlees[27] and of Rosen et al.[28]

TABLE 2.4 S-wave and P-wave Neutron Strength Functions in Unit of 10^{-4}

Nuclide		BNL-325[29]	ENDF/B-IV[a]	CEA	CNEN-2[b]	RCN-2[c]	JENDL-1
^{90}Sr	S_0	–	0.50*				0.455
	S_1	–	3.67*				4.17
^{93}Zr	S_0	–	0.41*		0.75		0.401
	S_1	–	4.11*		4.6		4.93
^{95}Mo	S_0	0.35±0.07	0.36*	0.45	0.5	0.8	0.373
	S_1	7±2	4.34*	7.4	5.0	5.0	5.41
^{97}Mo	S_0	0.34±0.06	0.31*	0.5	0.7	0.75	0.352
	S_1	8.0±2.5	4.48*	8.0	6.0	6.0	5.86
^{99}Tc	S_0	0.44±0.14	0.43	0.47	0.44	0.47	0.336
	S_1	4.6±1.4	3.0	6.0	3.9	6.00	6.10
^{101}Ru	S_0	0.56±0.15	0.24*	0.45	0.56	0.56	0.328
	S_1	–	4.57*	7.0	7.3	7.3	6.19
^{102}Ru	S_0	$0.06^{+0.16}_{-0.04}$	0.23*	0.3	0.2	0.322	0.325
	S_1	–	4.55*	5.0	4.5	7.3	6.17
^{103}Rh	S_0	0.54±0.07	0.53	0.475	0.5	0.47	0.324
	S_1	6.0±1.5	4.2	6.0	6.0	6.5	6.12
^{104}Ru	S_0	$0.11^{+0.12}_{-0.04}$	0.21*	0.33	0.34	0.321	0.326
	S_1	–	4.47*	4.0	4.5	7.0	6.04
^{105}Pd	S_0	0.35±0.20	0.20*	0.42	0.45	0.5	0.327
	S_1	–	4.40*	5.5	5.5	5.4	5.94
^{106}Ru	S_0	–	0.20*		0.45		0.332
	S_1	–	4.35*		4.5		5.80
^{107}Pd	S_0	–	0.19*	0.4	0.45	0.4	0.336
	S_1	–	4.24*	5.0	6.0	5.5	5.64
^{109}Ag	S_0	0.50±0.15	1.07**	0.66	0.89	0.6	0.354
	S_1	2.5±1.0	4.85**	3.5	2.9	3.8	5.26
^{129}I	S_0	–	0.80*	0.44		0.8	1.06
	S_1	–	1.87*	2.1		2.0	1.76
^{131}Xe	S_0	–	2.24**				1.22
	S_1	–	1.88**				1.58
^{133}Cs	S_0	0.7±0.1	2.47**	0.85	0.65	0.8	1.42
	S_1	3.9±1.0	1.74**	3.0	3.3	3.9	1.39
^{135}Cs	S_0	–	1.29*	0.8	0.70		1.61
	S_1	–	1.40*	1.7	2.0		1.26
^{137}Cs	S_0	–	1.50*		0.5		1.83
	S_1	–	1.27*		1.0		1.13
^{143}Nd	S_0	3.1±0.5	d)	3.3	3.3	2.7	2.82
	S_1	–		0.8	0.8	1.2	0.82
^{144}Ce	S_0	–	2.40*		3.5		2.97
	S_1	–	0.90*		0.79		0.78
^{144}Nd	S_0	3.9±1.0	2.40*		4.5	3.0	2.97
	S_1	–	0.90*		0.78	0.9	0.78
^{145}Nd	S_0	4.2±0.5	d)	3.5	3.3	3.3	3.19
	S_1	–		0.8	0.5	0.86	0.74
^{147}Pm	S_0	3.1±0.8	d)	3.2	3.4	2.8	3.48
	S_1	–		0.7	0.6	0.71	0.61
^{147}Sm	S_0	4.6±0.4	d)		4.3	4.3	4.02
	S_1	–			1.0	1.8	0.52
^{149}Sm	S_0	5.1±0.9	d)	5.2	5.5	5.1	3.88
	S_1	–		0.6	0.4	1.8	0.54
^{151}Sm	S_0	4.0±1.8	d)	3.5	3.68	3.65	3.80
	S_1	–		0.8	0.5	1.2	0.55
^{153}Eu	S_0	2.5±0.2	3.54***		2.8		4.2
	S_1	0.6±0.4	1.43***		1.0		0.49

TABLE 2.4 (cont.)

Nuclide		BNL-325[29]	ENDF/B-IV[a]	CEA	CNEN-2[b]	RCN-2[c]	JENDL-1
^{155}Eu	S_0	–	d)		2.2		4.13
	S_1	–			0.1		0.49

a) Values were calculated by the present authors from the optical potential parameters used in the ENDF/B-IV evaluation:
*: Moldauer[26]
**: Wilmore and Hodgson[26]
***: Becchetti and Greenlees[27].
b) Obtained from the unresolved resonance parameters.
c) Values used in the strength function model region defined in Table 2.8.
d) Information not obtainable.

also reproduced fairly well as seen in Fig. 2.5. TABLE 2.4 compares the calculated strength functions with the recommended values in BNL-325 3rd edition[29] as well as with the values adopted in the other recent evaluations.

2.2.2 Statistical Model

Neutron capture, compound elastic and inelastic scattering cross sections were calculated with a modified statistical model based on Moldauer's method[30,31] which takes account of the fluctuation in neutron width and the interference among levels. Competition among the reactions was considered in the present model, details of which are given in Ref. (32). Direct capture and collective capture processes were ignored in the present work. This makes a rapid decrease of capture cross section above a few MeV. Other reactions such as $(n, 2n)$, (n, p), *etc.* were ignored. This leads to much overestimation of the inelastic scattering cross section above the threshold energy of these reactions. However, these drawbacks are not thought to be very serious, since the cross sections of fission products little affect the reactor calculations in such a high energy region.

The γ-ray strength function S_γ, the ratio of average radiation width Γ_γ to average s-wave resonance level spacing D_{obs}, is the crucial parameter in determining the capture cross section. The values of Γ_γ and D_{obs} were taken from BNL-325, 2nd edition, Supplement No. 2[33] and the compilation by Baba[34,35], respectively. The unknown data were estimated by interpolation. The energy dependence of Γ_γ was calculated with the Brink-Axel[36] type profile function. The values of S_γ were then adjusted by the capture cross section data when available. The adjustment was made mainly by varying the values of D_{obs}. In some cases where only resonance parameters were known but no capture data existed in keV region, D_{obs} was varied so that the capture cross section obtained by the statistical theory should be connected smoothly with the resonance capture cross section. This procedure will be discussed in section 2.4. Values of Γ_γ, D_{obs} and S_γ thus determined are tabulated in TABLE 2.5, with the values recommended in BNL-325 3rd edition[29] from the resolved resonance parameters as well as those adopted in the other evaluations. In cases of ^{97}Mo, ^{99}Tc and ^{153}Eu, the capture data show gross structure in the unresolved resonance region. In these cases, after adjusting D_{obs} approximately, a curve was drawn through the data points by the eye-guide method to obtain the final evaluated cross section.

TABLE 2.5 Radiation Width, Mean Level Spacing and γ-ray Strength Function in Units of meV, eV and 10^{-4}, respectively

Nuclide		BNL-325[29]	ENDF/B-IV	CEA[f]	CNEN-2[f,g]	RCN-2[f]	JENDL-1
^{90}Sr	Γ_γ	–					205
	D_{obs}	–	d)				12000
	S_γ	–					0.17
^{93}Zr	Γ_γ	–	194		167 (208)		300
	D_{obs}	–	382		320		300
	S_γ	–	5.1		5.2 (6.5)		10
^{95}Mo	Γ_γ	153±6[a]	350	160.5 (299)	171 (210)	154 (265)	180
	D_{obs}	116±0.7[b]	114	89	89	82	69.2
	S_γ	13.2	30.7	18.5 (33.6)	19.2 (23.6)	18.7 (32.3)	26

TABLE 2.5 (cont.) 2

Nuclide		BNL-325[29]	ENDF/B-IV	CEA[f]	CNEN-2[f,g]	RCN-2[f]	JENDL-1
^{97}Mo	Γ_γ	126±7[a]	220	138 (199)	131 (169)	134 (175)	170
	D_{obs}	135±1.3[b]	77.5	65	70	66	72.3
	S_γ	9.3	28.4	21.2 (30.6)	18.7 (24.1)	20.3 (26.5)	23.5
^{99}Tc	Γ_γ	260±5[a]	112	137 (143)	136	130	112
	D_{obs}	27.9±0.4[b]	24.4	18.6	18.5	18.6	16.2
	S_γ	93	45.9	73.6 (76.9)	73.5	70	69.1
^{101}Ru	Γ_γ	173±7[a]	192	174 (194)	160 (172)	172	165
	D_{obs}	33.4±0.3[b]	18.3	16.7	16.4	16.7	13.8
	S_γ	52	105	104 (116)	98 (105)	103	120
^{102}Ru	Γ_γ	—	290	240 (319)	211 (418)	275	165
	D_{obs}	88±10[b]	631	550	550	573	290.5
	S_γ	—	4.60	4.36 (5.8)	3.84 (7.6)	4.8	5.68
^{103}Rh	Γ_γ	156±3[a]	171	162 (161)	189 (184)	161	164
	D_{obs}	12±1[c]	15.9	26.4	35	26.1	26.1
	S_γ	130	108	61.4 (61)	54 (53)	61.7	62.8
^{104}Ru	Γ_γ	—	160	95 (107)	97 (99)	97	165
	D_{obs}	289±23[b]	284	270	270	265	588
	S_γ	—	5.6	3.5 (4.0)	3.6 (3.7)	3.7	2.81
^{105}Pd	Γ_γ	153±5[a]	153	157 (196)	153 (167)	155	155
	D_{obs}	13.6±0.3[b]	9.91	10	10.5	10	11.1
	S_γ	113	154	157 (196)	146 (159)	155	140
^{106}Ru	Γ_γ	—	145		186 (183)		150
	D_{obs}	—	1181		1804		1000
	S_γ	—	1.23		1.03 (1.01)		1.5
^{107}Pd	Γ_γ	—	140	123 (160)	138 (155)	105 (155)	140
	D_{obs}	—	10.3	5.50	11	4.2	10.0
	S_γ	—	136	224 (291)	125 (141)	250 (274)	140
^{109}Ag	Γ_γ	129±2[a]	(140)[e]	132 (125)	128 (125)	129	130
	D_{obs}	44±2[b]	(43.8)[e]	17.9	20.2	17.5	12.7
	S_γ	29	32	74 (70)	63 (62)	74	102
^{129}I	Γ_γ	—	117	68		107	100
	D_{obs}	22.4±1.4[b]	27.4	30.0		30	21.0
	S_γ	—	42.7	22.7		35.7	47.6
^{131}Xe	Γ_γ	114±6[a]	(117)[e]				114
	D_{obs}	55±7[c]	(58.5)[e]				33.2
	S_γ	21	20				34.3
^{133}Cs	Γ_γ	118±17[a]	(110)[e]	127 (158)	124 (127)	125	118
	D_{obs}	20±2[c]	(18.0)[e]	23.4	20	20	23.2
	S_γ	59	61	54 (67.5)	62 (64)	62.5	50.9
^{135}Cs	Γ_γ	—	105	124	123		125
	D_{obs}	—	323	43.1	82		60.0
	S_γ	—	3.25	29	15		20.8
^{137}Cs	Γ_γ	—	95		153 (138)		100
	D_{obs}	—	1213		910		1100
	S_γ	—	0.78		1.68 (1.52)		0.91
^{143}Nd	Γ_γ	72±1[a]	(72)[e]	73 (68)	74 (70)	86 (85)	85
	D_{obs}	32±3[c]	(31)[e]	39	30	35	46.4
	S_γ	23	23.4	18.7 (17.4)	24.7 (23)	24.6 (24.3)	18.3
^{144}Ce	Γ_γ	—	73		59 (58)		90
	D_{obs}	—	1636		785		1000
	S_γ	—	0.45		0.75 (0.74)		0.90
^{144}Nd	Γ_γ	80±12[a]			113 (77)	47 (41)	80
	D_{obs}	540±65[c]	[d]		550	450	700
	S_γ	1.5			2.05 (1.40)	1.04 (0.91)	1.14
^{145}Nd	Γ_γ	52±1[a]	(52)[e]	53 (46)	51 (50)	86 (85)	60
	D_{obs}	19±2[c]	(19.8)[e]	19.2	16.3	19	24.2
	S_γ	27	26.3	28 (24)	31 (31)	45.3 (44.7)	24.8

TABLE 2.5 (cont.) 3

Nuclide		BNL-325[29]	ENDF/B-IV	CEA[f]	CNEN-2[f,g]	RCN-2[f]	JENDL-1
^{147}Pm	Γ_γ	68±3[a]	(68)[e]	67	69	69	66
	D_{obs}	6.8±1.5[c]	(6.6)[e]	5.3	4.7	4.6	4.70
	S_γ	100	103	126	147	150	140
^{147}Sm	Γ_γ	67±2[a]	(63)[e]		84 (83)	100	67
	D_{obs}	7.4±0.7[c]	(6.7)[e]		5.3	6.3	4.26
	S_γ	91	94		158 (157)	159	157
^{149}Sm	Γ_γ	60.5±0.5[a]	(62)[e]	60.5 (56.5)	64 (62)	76	61
	D_{obs}	2.3±0.3[c]	(2.3)[e]	1.95	2.3	2.0	1.63
	S_γ	263	274	310 (290)	278 (270)	380	374
^{151}Sm	Γ_γ	75±4[a]	(75)[e]	78 (76)	96 (95)	96	75
	D_{obs}	1.3±0.2[c]	(1.3)[e]	0.9	1.7	1.72	1.50
	S_γ	577	570	867 (844)	565 (559)	558	500
^{153}Eu	Γ_γ	94±1[a]	94.8		90		94
	D_{obs}	1.3±0.2[c]	1.3		1.05		1.46
	S_γ	723	729		857		644
^{155}Eu	Γ_γ	—	—		129		100
	D_{obs}	—	—		0.92		2.5
	S_γ	—	407		1400		400

a) Obtained by averaging the tabulated Γ_γ with the weight of $(1/\Delta\Gamma_i)^2$.
b) Obtained from the resonance energies in BNL-325 3rd edition[29] by Yoshida and Sasaki.[37]
c) Recommended in BNL-325 3rd edition.[29]
d) Information not available.
e) Only the S_γ-value is given. D_{obs} is deduced by assuming the same Γ_γ as in the resolved or unresolved resonances.
f) The values in the parentheses are for p-wave states.
g) The CNEN-2 evaluation gives J-dependent Γ_γ and the averaged values are given here.

2.2.3 Level Density Formula

The level density is required for both compound and residual nuclei in the statistical model calculation. The level density formula of Gilbert and Cameron[38] was used with a slight modification[32] which was made to take account of parity distribution of low lying discrete levels. The formula is expressed as

$$\rho(E, J, \pi) = P_\pi(E) \cdot R_J(E) \cdot \rho_0(E) \tag{2}$$

$$R_J(E) = \frac{2J+1}{2\sigma_M^2(E)} \exp[-J(J+1)/2\sigma_M^2(E)] \tag{3}$$

$$\rho_0(E) = \rho_G(E) = \frac{\exp[2\sqrt{aU}]}{12\sqrt{2}\,\sigma_M a^{1/4} U^{5/4}} \quad \text{for} \quad E \geq E_x \quad \text{(Fermi gas model)} \tag{4}$$

$$= \rho_T(E) = \rho_G(E_x)\exp[(E-E_x)/T] \quad \text{for} \quad E \leq E_x) \tag{5}$$

(Constant temperature model)

$U = E - \Delta$: effective excitation energy,

$U_x = 2.5 + 150/A$: effective connecting energy,

$E_x = U_x + \Delta$: connecting energy,

$T = U_x / \{\sqrt{a \cdot U_x} - 2\}$: nuclear temperature,

where J is the spin of nucleus, Δ the pairing energy, E the total excitation energy and "a" the level density parameter. The spin cut-off parameter σ_M^2 is

$$\sigma_M^2 = 0.0888\sqrt{a \cdot U} \;.\; A^{2/3} \quad \text{for} \quad E \geq E_x \tag{6}$$

$$= 0.0888\sqrt{a \cdot U_x} \;.\; A^{2/3} = \text{const} \quad \text{for} \quad E \leq E_x. \tag{7}$$

The parity distribution $P_\pi(E)$ is assumed as

$$P_\pi(E) = \frac{f_\pi + 0.5\exp[(E-E_0)/\delta]}{1+\exp[(E-E_0)/\delta} \tag{8}$$

where f_π is the fraction of parity π in low lying discrete levels. The factor $P_\pi(E)$ becomes its theoretical value of one half, with increasing energy E. The parameters E_0 and δ are somewhat arbitrarily determined as

$$E_0 = (E_x + E_c)/2 \tag{9}$$

$$\delta = |E_x - E_c|/2 \tag{10}$$

where E_c is the energy above which levels are treated as overlapping.

TABLE 2.6 Parameters Used in Level Density Formula

Nuclide	Evaluation[a]	Target Nucleus					Compound Nucleus				
		a (MeV^{-1})	Δ (MeV)	E_x (MeV)	σ_M^2 ($E=0$)	S_n (MeV)	a (MeV^{-1})	Δ (MeV)	E_x (MeV)	σ_M^2 ($E=S_n$)	S_n (MeV)
^{90}Sr	JENDL-1	10.55	1.96	6.127	11.8	7.8036	11.24	1.24	5.388	12.9	5.8278
	RCN-2										
	CNEN-2										
	CEA										
	ENDF/B-IV[b]	—	—	—	—	—	—	—	—	—	—
^{93}Zr	JENDL-1	11.38	1.20	5.313	12.5	6.7585	12.16	2.32	6.416	15.5	8.1911
	RCN-2										
	CNEN-2	13.00	(1.2)	5.4	2.5	—	13.40	(2.32)	6.72	26.8	(8.20)
	CEA										
	ENDF/B-IV	11.42	1.2	—	—	—	12.10	2.32	—	15.5	8.1984
^{95}Mo	JENDL-1	11.36	1.28	5.359	12.6	7.3751	12.15	2.40	6.463	16.9	9.1543
	RCN-2	12.9	1.28	6.744	5.1	7.3751	14.0	2.40	7.492	29.8	9.1542
	CNEN-2	12.4	(1.28)	7.08	—[c]	—	14.0	(2.40)	7.5	29.8	(9.15)
	CEA	—	—	—	—	—	12.9	(2.40)	—	17.4	9.15
	ENDF/B-IV	11.9	1.28	—	—	—	12.49	2.40	—	17.1	9.1567
^{97}Mo	JENDL-1	12.93	1.28	5.326	13.6	6.8160	13.55	2.57	6.600	17.1	8.6424
	RCN-2	14.6	1.28	6.896	6.8	6.8161	15.78	2.57	8.124	30.4	8.6424
	CNEN-2	14.55	(1.28)	6.58	—[c]	—	15.7	(2.57)	7.97	30.3	(8.64)
	CEA	—	—	—	—	—	14.7	(2.57)	—	17.9	8.64
	ENDF/B-IV	13.27	1.28	—	—	—	14.39	2.57	—	17.6	8.6422
^{99}Tc	JENDL-1	13.34	1.29	5.305	13.9	8.8797	13.97	0	4.000	18.4	6.5937
	RCN-2	15.80	1.29	6.792	6.6	8.8800	16.38	0	3.142	32.7	6.6000
	CNEN-2	15.60	(1.29)	6.59	—[c]	—	16.40	0	5.3	32.7	(6.60)
	CEA	—	—	—	—	—	15.5	0	—	19.4	6.60
	ENDF/B-IV[b]	—	—	—	—	—	—	—	—	—	—
^{101}Ru	JENDL-1	13.93	1.28	5.265	14.3	6.8055	14.64	2.22	6.191	19.6	9.2162
	RCN-2	16.30	1.28	7.724	—[c]	6.8050	16.20	2.22	6.824	33.9	9.2161
	CNEN-2	15.50	(1.28)	6.58	—[c]	—	16.20	(2.22)	7.32	33.9	(9.22)
	CEA	—	—	—	—	—	15.2	(2.22)	—	20.0	9.22
	ENDF/B-IV	14.95	1.28	—	—	—	14.98	2.22	—	19.8	9.2161
^{102}Ru	JENDL-1	14.64	2.22	6.191	14.8	9.2162	15.25	1.28	5.236	16.9	6.2245
	RCN-2	16.20	2.22	6.824	—[c]	9.2161	17.94	1.28	8.176	—[d]	6.2250
	CNEN-2	16.75	(2.22)	7.52	—[c]	—	18.00	(1.28)	6.58	—[d]	(6.225)
	CEA	—	—	—	—	—	16.50	(1.28)	—	17.7	6.225
	ENDF/B-IV	14.98	2.22	—	—	—	16.21	1.28	—	17.5	6.2475
^{103}Rh	JENDL-1	14.69	0.94	4.896	14.9	9.3097	15.30	0	3.942	20.3	6.9997
	RCN-2	16.50	0.94	5.743	—[c]	9.3120	17.13	0	4.922	35.4	6.9993
	CNEN-2	16.50	(0.94)	6.24	—[c]	—	16.76	0	5.3	35.0	(7.0)
	CEA	—	—	—	—	—	15.80	0	—	20.7	7.0
	ENDF/B-IV[b]	—	—	—	—	—	—	—	—	—	—
^{104}Ru	JENDL-1	16.01	2.52	6.462	15.6	8.9127	16.64	1.28	5.209	17.3	5.9077
	RCN-2	17.00	2.52	8.009	—[c]	8.8870	20.85	1.28	6.869	—[d]	5.9080
	CNEN-2	17.60	(2.52)	7.82	—[c]	—	20.60	(1.28)	6.48	—[d]	(5.91)
	CEA	—	—	—	—	—	19.05	(1.28)	—	18.6	5.91
	ENDF/B-IV	16.56	2.52	—	—	—	18.99	1.28	—	18.7	5.9765
^{105}Pd	JENDL-1	15.16	1.35	5.279	15.3	7.0737	15.93	2.59	6.505	21.0	9.5607
	RCN-2	16.40	1.35	7.748	4.6	7.9041	17.20	2.59	8.047	35.8	9.5610
	CNEN-2	17.25	(1.35)	6.65	—[c]	—	17.15	(2.59)	7.49	35.8	(9.56)
	CEA	—	—	—	—	—	16.30	(2.59)	—	21.1	9.56

TABLE 2.6 (cont.) 2

Nuclide	Evaluation[a]	Target Nucleus					Compound Nucleus				
		a (MeV^{-1})	Δ (MeV)	E_x (MeV)	σ_M^2 ($E=0$)	S_n (MeV)	a (MeV^{-1})	Δ (MeV)	E_x (MeV)	σ_M^2 ($E=S_n$)	S_n (MeV)
	ENDF/B-IV	15.81	1.35	—	—	—	16.08	2.59	—	21.0	9.5474
^{106}Ru	JENDL-1	17.08	2.53	6.445	16.3	8.4647	17.46	1.28	5.182	17.1	5.4587
	RCN-2										
	CNEN-2	17.85	(2.53)	7.73	4.5	—	17.8	(1.28)	6.48	28.4[c]	(5.46)
	CEA										
	ENDF/B-IV	17.09	2.53	—	—	—	17.32	1.28	—	17.0	5.4534
^{107}Pd	JENDL-1	16.57	1.35	5.252	16.1	6.5427	17.01	2.60	6.489	21.4	9.2247
	RCN-2	18.40	1.35	7.173	4.6	6.5420	19.60	2.60	7.887	37.7	9.2250
	CNEN-2	18.00	(1.35)	6.55	—[c]	—	17.85	(2.60)	7.80	36.0	(9.225)
	CEA	—	—	—	—	—	17.90	(2.60)	—	21.9	9.225
	ENDF/B-IV	16.44	1.35	—	—	—	16.69	2.60	—	21.2	9.2275
^{109}Ag	JENDL-1	16.80	1.25	5.126	16.4	9.1882	17.17	0	3.864	22.0	6.8057
	RCN-2	17.80	1.25	6.656	4.8	9.1880	18.38	0	4.458	37.5	6.8055
	CNEN-2	17.85	(1.25)	6.45	—[c]	—	18.05	0	4.4	37.1	(6.805)
	CEA	—	—	—	—	—	17.1	0	—	22.0	6.805
	ENDF/B-IV[b]	—	—	—	—	—	—	—	—	—	—
^{129}I	JENDL-1	15.87	1.20	4.863	17.3	8.8396	14.99	0	3.654	22.4	6.4567
	RCN-2	16.80	1.20	6.310	7.9	8.8400	16.41	0	6.721	—[d]	6.4560
	CNEN-2										
	CEN	—	—	—	—	—	15.30	0	—	22.7	6.45
	ENDF/B-IV	16.78	1.20	—	—	—	15.52	0	—	22.9	6.4984
^{131}Xe	JENDL-1	16.14	1.12	4.765	17.6	6.6056	14.97	2.16	5.796	23.2	8.9361
	RCN-2										
	CNEN-2										
	CEA										
	ENDF/B-IV	16.98	1.12	—	—	—	15.02	2.16	—	23.2	8.9323
^{133}Cs	JENDL-1	16.13	1.04	4.668	17.7	8.9797	14.85	0	3.619	23.5	6.8907
	RCN-2	17.00	1.04	7.136	—[c]	9.0380	16.19	0	4.607	40.4	6.8913
	CNEN-2	16.30	(1.04)	5.44	—[c]	—	16.59	0	4.4	40.9	(6.89)
	CEA	—	—	—	—	—	14.90	0	—	23.6	6.89
	ENDF/B-IV[b]	—	—	—	—	—	—	—	—	—	—
^{135}Cs	JENDL-1	13.55	0.70	4.311	16.3	8.8247	12.35	0	3.603	21.5	6.7687
	RCN-2										
	CNEN-2	15.40	(0.70)	4.60	—[c]	—	14.45	0	3.60	38.2	(6.77)
	CEA	—	—	—	—	—	14.20	0	—	23.1	6.77
	ENDF/B-IV	13.80	0.70	—	—	—	11.52	0	—	20.5	6.6114
^{137}Cs	JENDL-1	11.18	0.85	4.445	15.0	8.2767	12.41	0	3.587	17.5	4.3807
	RCN-2										
	CNEN-2	13.30	(0.85)	2.75	4.1	—	15.60	0	3.9	32.2	(4.38)
	CEA										
	ENDF/B-IV	10.24	0.85	—	—	—	12.16	0	—	17.2	4.3114
^{143}Nd	JENDL-1	18.19	1.18	4.729	19.5	6.1257	19.17	1.94	5.482	25.9	7.8177
	RCN-2	18.28	1.18	3.859	7.8	6.1227	17.72	1.94	5.512	40.9	7.8174
	CNEN-2	17.70	(1.18)	3.28	—[c]	—	17.96	(1.94)	5.54	41.2	(7.82)
	CEA	—	—	—	—	—	16.30	(1.94)	—	24.0	7.82
	ENDF/B-IV[b]	—	—	—	—	—	—	—	—	—	—
^{144}Ce	JENDL-1	15.74	2.09	5.632	18.2	6.8817	16.54	1.17	4.705	18.9	4.7787
	RCN-2										
	CNEN-2	22.90	(2.09)	6.49	2.4	—	24.50	(1.17)	4.67	37.9	(4.78)

TABLE 2.6 (cont.) 3

Nuclide	Evaluation[a)]	Target Nucleus					Compound Nucleus				
		a (MeV^{-1})	Δ (MeV)	E_x (MeV)	σ_M^2 ($E=0$)	S_n (MeV)	a (MeV^{-1})	Δ (MeV)	E_x (MeV)	σ_M^2 ($E=S_n$)	S_n (MeV)
	CEA										
	ENDF/B-IV	17.79	2.09	—	—	—	20.26	1.17	—	20.6	4.6434
	JENDL-1	19.17	1.94	5.482	20.1	7.8177	20.02	1.18	4.715	23.5	5.7597
	RCN-2	17.72	1.94	5.512	7.2	7.8174	20.56	1.18	5.199	39.1	5.7553
^{144}Nd	CNEN-2	17.96	(1.94)	5.64	3.9	—	20.10	(1.18)	5.08	38.7	(5.76)
	CEA										
	ENDF/B-IV[b)]	—	—	—	—	—	—	—	—	—	—
	JENDL-1	20.02	1.18	4.715	20.6	5.7597	17.64	2.10	5.627	24.2	7.5657
	RCN-2	20.56	1.18	5.199	5.7	5.7553	20.20	2.10	6.536	42.5	7.5647
^{145}Nd	CNEN-2	19.3	(1.18)	4.38	—[c)]	—	20.50	(2.10)	6.00	42.8	(7.565)
	CEA	—	—	—	—	—	18.90	(2.10)	—	25.1	7.565
	ENDF/B-IV[b)]	—	—	—	—	—	—	—	—	—	—
	JENDL-1	18.46	0.92	4.440	19.9	7.6737	19.29	0	3.514	26.5	5.9007
	RCN-2	20.20	0.79	4.915	—[c)]	7.674	21.74	0	4.5	46.3	5.902
^{147}Pm	CNEN-2	21.15	(0.92)	5.32	—[c)]	—	21.62	0	4.80	46.1	(5.90)
	CEA	—	—	—	—	—	20.10	0	—	27.1	5.90
	ENDF/B-IV[b)]	—	—	—	—	—	—	—	—	—	—
	JENDL-1	21.41	1.22	4.740	21.5	6.3727	19.01	2.14	5.654	26.5	8.1407
	RCN-2	21.00	1.22	5.198	7.1	6.3730	20.77	2.14	6.358	45.6	8.1402
^{147}Sm	CNEN-2	19.50	(1.22)	5.42	2.8	—	21.15	(2.14)	6.44	46.0	(8.14)
	CEA										
	ENDF/B-IV[b)]	—	—	—	—	—	—	—	—	—	—
	JENDL-1	19.85	1.22	4.727	20.8	5.8727	20.65	2.21	5.710	27.4	7.9867
	RCN-2	23.50	1.22	5.915	6.2	5.8731	24.00	2.21	6.853	48.5	7.9852
^{149}Sm	CNEN-2	22.75	(1.22)	6.02	—[c)]	—	23.71	(2.21)	7.01	48.2	(7.985)
	CEA	—	—	—	—	—	22.60	(2.21)	—	28.7	7.985
	ENDF/B-IV[b)]	—	—	—	—	—	—	—	—	—	—
	JENDL-1	21.26	1.22	4.713	21.7	5.5917	21.32	2.32	5.807	28.5	8.2677
	RCN-2	26.88	1.22	6.806	8.2	5.5960	24.23	2.32	7.611	49.9	8.2580
^{151}Sm	CNEN-2	25.90	(1.22)	6.62	—[c)]	—	24.39	(2.32)	7.82	50.1	(8.27)
	CEA	—	—	—	—	—	23.60	(2.32)	—	30.1	8.27
	ENDF/B-IV[b)]	—	—	—	—	—	—	—	—	—	—
	JENDL-1	21.81	1.10	4.580	22.1	8.5557	21.43	0	3.474	30.0	6.4377
	RCN-2										
^{153}Eu	CNEN-2	25.70	1.10	6.50	—[c)]	—	23.70	0	5.40	51.8	(6.44)
	CEA										
	ENDF/B-IV[b)]	—	—	—	—	—	—	—	—	—	—
	JENDL-1	20.85	0.92	4.388	21.8	8.1767	20.34	0	3.462	29.2	6.3257
	RCN-2										
^{155}Eu	CNEN-2	24.80	(0.92)	6.12	7.2	—	24.20	0	5.10	52.4	(6.33)
	CEA										
	ENDF/B-IV[b)]	—	—	—	—	—	—	—	—	—	—

a) Description for each evaluation

1) JENDL-1 : a, Δ and E_x were taken from Ref. (38), S_n from Ref. (39), $\sigma_M^2(E=0)$ calculated with Eq. (7) and $\sigma_M^2(E=S_n)$ with Eq. (6).

2) RCN-2 : a, Δ, E_x and S_n were taken from Refs. (17), (18) and (19), $\sigma_M^2(E=0)$ is $\sigma_{M,\mathrm{exp}}^2$ in Eq. (13) and taken from Ref. (17), (18) and (19), $\sigma_M^2(E=S_n)$ calculated with Eq. (12).

3) CNEN-2 : a, U_x and $\sigma_{M,\mathrm{exp}}^2$ were obtained through Ref. (20). $\sigma_M^2(E=S_n)$ was calculated with Eq. (12) except for ^{106}Ru where Eq. (13) was used. Δ and S_n were assumed to deduce σ_M^2 and E_x and are given in parentheses.

4) CEA : a, $S_n-\Delta$ and $\sigma_M^2(E=S_n)$ are given in Ref. (16) for only compound nucleus. Δ given in

parentheses was assumed to deduce S_n.

5) ENDF/B-IV : a, Δ for target and compound nuclei and S_n for compound nucleus are given in Ref. (6). E_x is not given and therefore $\sigma_M{}^2(E=0)$ cannot be caculated with Eq.(7). $\sigma_M{}^2(E=S_n)$ was calculated with Eq. (6).

b) Information of level density parameters is not available for this nuclide.

c) $\sigma_M{}^2{}_{,\mathrm{exp}}$ is not given.

d) $\sigma_M{}^2(E=S_n)$ cannot be calculated, because $E_x > S_n$ and $\sigma_M{}^2{}_{,\mathrm{exp}}$ in Eq. (13) is not given for the compound nucleus.

e) $\sigma_M{}^2(E=S_n)$ was calculated from Eq. (13).

As to values of "a" and Δ, we adopted the values recommended by Gilbert and Cameron[38]. TABLE 2.6 gives the adopted parameters with the neutron separation energy taken from a compilation by Wapstra and Gove[39]. The parameters adopted in the other evaluations are also given in TABLE 2.6 for comparison. It should be noted, however, that the adopted formulae are not exactly the same with each other and therefore simple comparison is not allowed. The differences are discussed in the followings:

(1) Parity distribution P_π

All the other avaluations assumed $P_\pi(E)=1/2$.

(2) Spin distribution R_J

The CEA evaluation used Eq. (3). In the RCN-2, CNEN-2 and ENDF/B-IV evaluations, R_J was given as

$$R_J=\frac{2J+1}{2\sigma_M{}^2}\exp\left[-\left(J+\frac{1}{2}\right)^2\Big/2\sigma_M{}^2\right]. \tag{11}$$

(3) Spin cut-off parameter $\sigma_M{}^2$ for $E \geq E_x$

Equation (6) was first derived by Jensen and Luttinger[40] and was used by Gilbert and Cameron[38]. Facchini and Saetta-Menichella[41] gave

$$\sigma_M{}^2=0.146\sqrt{a\cdot U}\ .\ A^{2/3} \tag{12}$$

and argued that Eq. (6) was in error. The choice of Eq. (6) or (12) affects value of the level density parameter "a". If Eq. (12) is used, the value of "a" increases due to Eq. (4) so as to give the same level density at neutron separation energy, and therefore the spin cut off parameter increases by a factor of more than 0.146/0.0888. Equation (6) was adopted in the JENDL-1, CEA and ENDF/B-IV evaluations. On the other hand, the CNEN-2 and RCN-2 evaluations adopted Eq. (12) and gave very large spin cut-off parameters for compound nucleus at the neutron separation energy as seen in TABLE 2.6.

(4) Spin cut-off parameter for $E \leq E_x$

As is evident from Eq. (7), we assumed a constant value for the spin cut-off parameter in the energy region of the constant temperature model and adopted the value $\sigma_M{}^2(E_x)$ calculated at the connecting energy. Consequently the assumed value is considerably larger than the value $\sigma_M{}^2{}_{,\mathrm{exp}}$ expected from the spin distribution of low lying discrete levels. The ENDF/B-IV evaluation adopted Eq. (7) as JENDL-1 did. On the other hand, the RCN-2 and CNEN-2 evlauations assumed

$$\sigma_M{}^2(E)=\sigma_M{}^2{}_{,\mathrm{exp}}+(\sigma_M{}^2(E_x)-\sigma_M{}^2{}_{,\mathrm{exp}})\frac{E}{E_x}. \tag{13}$$

The difference of the spin cut-off parameter in the constant temperature model affects the capture and inelastic scattering cross sections as pointed out by Gruppelaar *et al.*[21]

(5) The level density parameter "a" and E_x

The values of "a" and E_x were searched for so as to reproduce the measured values of the level spacing in all the evaluations except the present work where the recommended values of Gilbert and Cameron[38] were adopted without modification.

2.3 Thermal and Resonance Cross Sections

Cross sections in thermal and resonance regions were calculated from resonance parameters.

2.3.1 Resonance Parameters

The resolved resonance parameters were taken from BNL-325 3rd edition[29] or recent reports on measure-

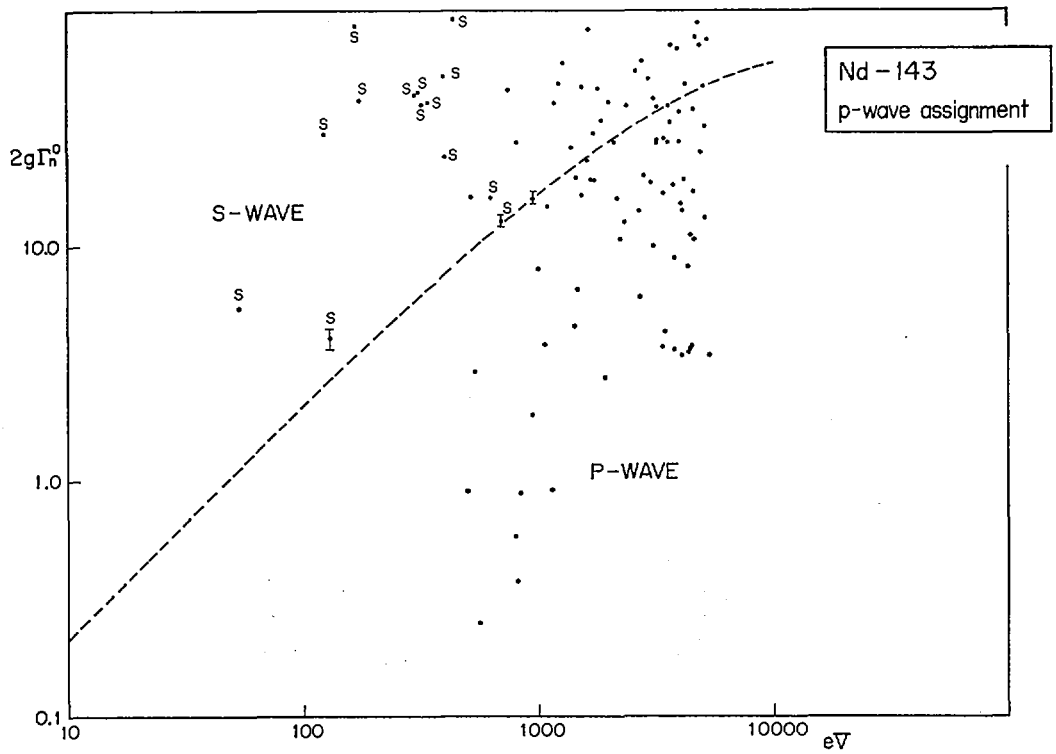

Fig. 2.6 S⁻ and p-wave assignments of ^{143}Nd resonances.

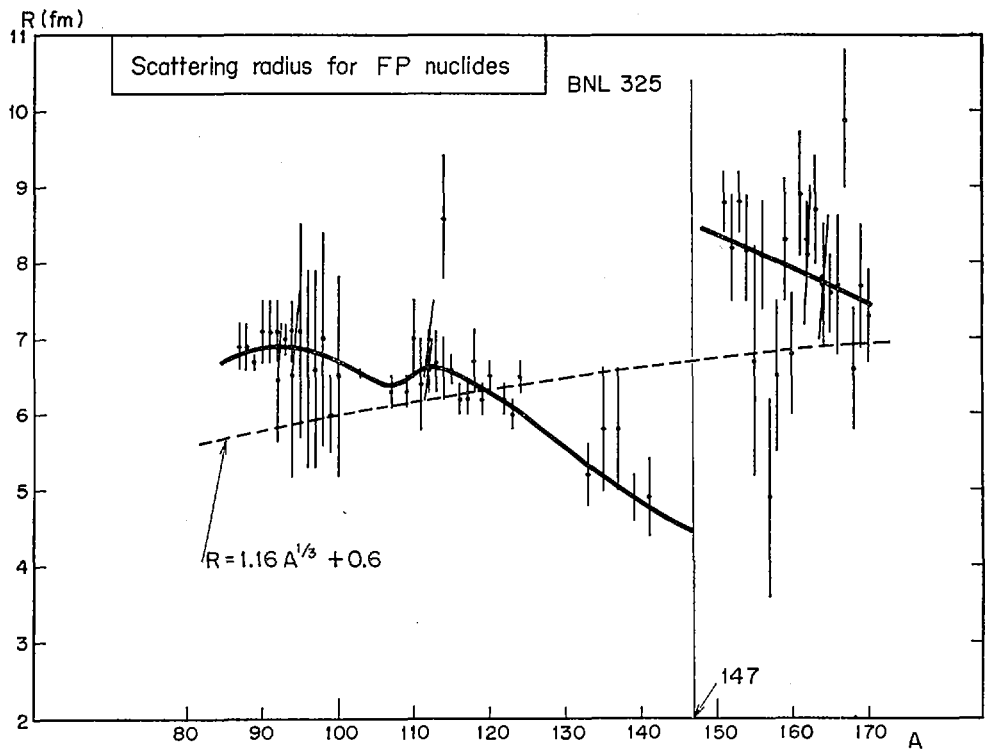

Fig. 2.7 Scattering radii for F. P. nuclides.

TABLE 2.7 Effective Scattering Radius in 10^{-13}cm Unit.

Nuclide	BNL-325	ENDF/B-IV	CEA	CNEN-2	RCN-2	JENDL-1
^{90}Sr	—	5.4051				6.9
^{93}Zr	—	5.4645		7.1		6.9
^{95}Mo	7.1±1.4	5.5034	5.7	6.5017	7.1	7.1
^{97}Mo	6.6±1.3	5.5418	5.8	6.5415	6.6	6.6
^{99}Tc	6.0±0.5	6.91	5.8	6.8	6.8	6.0
^{101}Ru	—	5.6171	5.8	6.6194	6.7	6.65
^{102}Ru	—	5.6355	5.8	6.547	6.6	6.6
^{103}Rh	6.56±0.06	6.56	5.9	5.91	6.56	6.56
^{104}Ru	—	5.6721	5.9	6.5843	6.5	6.6843
^{105}Pd	—	5.6902	5.9	6.6953	6.5	6.4
^{106}Ru	—	5.7084		6.6		6.4
^{107}Pd	—	5.7263	5.9	6.6394	6.5	6.35
^{109}Ag	6.3±0.2	6.3	6.0	6.3	6.3	6.3
^{129}I	—	6.0948	6.3		6.095	5.65
^{131}Xe	—	5.85				5.5
^{133}Cs	5.2±0.4	7.5166	6.4	5.2	5.5	5.2
^{135}Cs	—	6.188	6.4	6.188		5.2
^{137}Cs	—	6.2184		6.22		5.05
^{143}Nd	—	6.3079	6.55	7.3353	5.6	4.65
^{144}Ce	—	6.3228		4.5		4.6
^{144}Nd	—	6.3226		4.6	8.0	4.6
^{145}Nd	—	6.3373	6.6	8.0	5.0	4.55
^{147}Pm	—	6.3663	6.6	7.136	7.14	4.45
^{147}Sm	—	6.3663		5.8	6.366	4.45
^{149}Sm	—	5.093	6.6	5.093	5.09	8.4
^{151}Sm	—	6.4237	6.65	7.463	6.42	8.35
^{153}Eu	8.8±0.4	8.8		8.8		8.8
^{155}Eu	—	6.48		8.0		8.15

ments. For nuclides whose resonances are resolved up to keV region, each level was assigned as either s-wave or p-wave resonance considering the magnitude of Γ_n and the statistics of s- and p-wave levels. The procedure is as follows:

(1) The reduced neutron widths were deduced by assuming that all the resonances belong to s-wave resonances.

(2) The reduced neutron widths were plotted as a function of neutron energy in log-log scale. In this plot, the reduced neutron widths of s-wave resonances scatter around a mean value which is independent of neutron energy. For p-wave resonances, on the other hand, the mean value of the reduced widths must be an increasing function of energy, because the penetration factors were ignored in their deduction.

(3) Taking account of energy dependance of the penetration factor, a line was drawn among the plotted points, and the points lying above the line were assigned to s-wave resonances and those under the line to p-wave ones.

(4) The position of the line was adjusted so that the ratio of s-wave to p-wave resonances should agree with the expectation from the statistics of resonance population.

Fig. 2.6 illustrates the points and the line in the case of ^{143}Nd.

The values of effective scattering radius R were adopted from BNL-325 3rd edition[29] or from the interpolation according to the curve displayed in **Fig. 2.7**. The values are compared in **TABLE 2.7** with the values adopted in the other evaluations. Unresolved resonance parameter representation was not used in the present work, since the resonance self-shielding effect of the fission products are expected to be negligible in the actual reactor calculations. The status of resonance parameters is shown in **TABLE 2.8** for various evaluations.

TABLE 2.8 Status of Resonance Parameters Representation for Various Recent Evaluation Files

Nuclide	Evaluation	Resolved Resonance Region								Upper Energy of Unresolved Resonance Representation** (keV)
		Defined energy range		S-wave resonance			P-wave resonance			
		Minimum (eV)	Maximum (eV)	No[a)]	E_{min}[b)] (eV)	E_{max}[c)] (eV)	No[a)]	E_{min}[b)] (eV)	E_{max}[c)] (eV)	
^{90}Sr	JENDL-1	10^{-5}	6,000*	0	—	—	0	—	—	—
	RCN-2									
	CNEN-2									
	ENDF/B-IV	10^{-5}	6,300*	0	—	—	0	—	—	—
^{93}Zr	JENDL-1	10^{-5}	260	1	110	—	0	—	—	—
	RCN-2									
	CNEN-2	10^{-5}	117	1	110	—	0	—	—	50
	ENDF/B-IV	10^{-5}	347	0	—	—	0	—	—	—
^{95}Mo	JENDL-1	10^{-5}	2,150	19	44.9	2,048	34	110.5	2,112	—
	RCN-2	10^{-3}	2,140	23	−16.0	2,131	33	110.4	2,142	70
	CNEN-2	10^{-5}	2,250	25	−21.2	2,130	30	110.5	2,141	50
	ENDF/B-IV	10^{-5}	2,188	25	44.7	2,131	30	110.4	2,142	—
^{97}Mo	JENDL-1	10^{-5}	1,660	27	70.9	1,795	35	16.3	1,836	—
	RCN-2	10^{-3}	1,950	23	−10.0	1,904	44	16.3	1,941	100
	CNEN-2	10^{-5}	1,950	27	−20.5	1,941	41	16.3	1,904	50
	ENDF/B-IV	10^{-5}	1,980	30	70.9	1,941	34	79.6	1,932	—
^{99}Tc	JENDL-1	10^{-5}	290	11	5.64	280	0	—	—	—
	RCN-2	10^{-3}	1,153	79	5.6	1,115	0	—	—	150
	CNEN-2	10^{-5}	2,105	85	−13.6	2,104	18	61.4	936.6	50
	ENDF/B-IV	10^{-5}	300	12	−6.4	280.9	0	—	—	141.4
^{101}Ru	JENDL-1	10^{-5}	700	22	15.9	670	0	—	—	—
	RCN-2	10^{-3}	677	24	15.7	666	0	—	—	10
	CNEN-2	10^{-5}	680	23	15.9	670	6	325	540	50
	ENDF/B-IV	10^{-5}	120	7	15.9	112.5	0	—	—	—
^{102}Ru	JENDL-1	10^{-5}	1,450	3	166	1,296	0	—	—	—
	RCN-2	10^{-3}	1,578	3	165	1,291	0	—	—	10
	CNEN-2	10^{-5}	1,300	4	−56	1,291	0	—	—	50
	ENDF/B-IV	10^{-5}	1,612	1	1296	—	2	165	415	—
^{103}Rh	JENDL-1	10^{-5}	3,600	87	1.257	4,140	188	34.4	4,128	—
	RCN-2	10^{-3}	4,028	274	1.26	4,015	0	—	—	200
	CNEN-2	10^{-5}	4,150	106	−10.74	4,140	171	34.4	4,128	30
	ENDF/B-IV	10^{-5}	4,150	233	1,257	4,128	42	34.4	1,484	40.4
^{104}Ru	JENDL-1	10^{-5}	1,290	4	226.5	1,055	0	—	—	—
	RCN-2	10^{-3}	1,183	4	224.6	1,050	0	—	—	10
	CNEN-2	10^{-5}	1,190	5	−99.5	1,050	0	—	—	50
	ENDF/B-IV	10^{-5}	1,197	4	224.4	1,055	0	—	—	—
^{105}Pd	JENDL-1	10^{-5}	150	13	11.8	152	0	—	—	—
	RCN-2	10^{-3}	155	17	−2.0	154.7	0	—	—	280
	CNEN-2	10^{-5}	815	61	−4.42	808	0	—	—	50
	ENDF/B-IV	10^{-5}	91.8	9	11.8	86.8	0	—	—	—
^{106}Ru	JENDL-1	10^{-5}	500*	0	—	—	0	—	—	—
	RCN-2									
	CNEN-2	10^{-5}	12,180	6	630	11,130	0	—	—	50
	ENDF/B-IV	10^{-5}	1,570*	0	—	—	0	—	—	—

TABLE 2.8 (cont.) 2

Nuclide	Evaluation	Resolved Resonance Region								Upper Energy of Unresolved Resonance Representation** (keV)
		Defined energy range		S-wave resonance			P-wave resonance			
		Minimum (eV)	Maximum (eV)	No[a)]	E_{min}[b)] (eV)	E_{max}[c)] (eV)	No[a)]	E_{min}[b)] (eV)	E_{max}[c)] (eV)	
^{107}Pd	JENDL-1	10^{-5}	5*	0	—	—	0	—	—	—
	RCN-2	10^{-3}	3.11	1	3.11	—	0	—	—	70
	CNEN-2	10^{-5}	49.1	6	−5.4	48.6	0	—	—	50
	ENDF/B-IV	10^{-5}	16.0*	0	—	—	0	—	—	—
^{109}Ag	JENDL-1	10^{-5}	1,000	81	5.19	2,506	0	—	—	—
	RCN-2	10^{-3}	976	69	5.20	976	0	—	—	100
	CNEN-2	10^{-5}	2,600	68	−19.3	2,587	23	32.63	849	50
	ENDF/B-IV	10^{-5}	1,000	63	5.19	903	0	—	—	—
^{129}I	JENDL-1	10^{-5}	166	5	72.4	153	0	—	—	—
	RCN-2	10^{-3}	153	6	−5.0	153	0	—	—	60
	CNEN-2									
	ENDF/B-IV	10^{-5}	167	5	72.4	153	0	—	—	—
^{131}Xe	JENDL-1	10^{-5}	773	15	14.4	3,945	23	173.6	3,102	—
	RCN-2									
	CNEN-2									
	ENDF/B-IV	10^{-5}	4,000	40	14.4	3,945	0	—	—	—
^{133}Cs	JENDL-1	10^{-5}	1,290	61	5.9	3,422	99	181.5	3,500	—
	RCN-2	10^{-3}	3,512	165	5.9	3,500	0	—	—	1,500
	CNEN-2	10^{-5}	3,520	139	−7.14	3,500	0	—	—	50
	ENDF/B-IV	10^{-5}	3,550	163	5.9	3,500	0	—	—	—
^{135}Cs	JENDL-1	10^{-5}	30*	0	—	—	0	—	—	—
	RCN-2									
	CNEN-2	10^{-5}	463	7	−1.97	460	0	—	—	50
	ENDF/B-IV	10^{-5}	218*	0	—	—	0	—	—	—
^{137}Cs	JENDL-1	10^{-5}	550*	0	—	—	0	—	—	—
	RCN-2									
	CNEN-2	10^{-5}	10,600	11	720	10,408	0	—	—	100
	ENDF/B-IV	10^{-5}	1,533*	0	—	—	0	—	—	—
^{143}Nd	JENDL-1	10^{-5}	4,650	51	−6.0	5,440	60	226.2	5,503	—
	RCN-2	10^{-3}	4,000	91	−5.4	4,022	18	226.2	4,011	50
	CNEN-2	10^{-5}	5,550	112	−6.0	5,503	0	—	—	50
	ENDF/B-IV	10^{-5}	595	18	−6.0	576	0	—	—	—
^{144}Ce	JENDL-1	10^{-5}	500*	0	—	—	0	—	—	—
	RCN-2									
	CNEN-2	10^{-5}	10,400	13	360	9,960	0	—	—	20
	ENDF/B-IV	10^{-5}	1,131*	0	—	—	0	—	—	—
^{144}Nd	JENDL-1	10^{-5}	7,730	15	373.8	18,430	20	733.7	19,407	—
	RCN-2	10^{-3}	12,000	23	−76.0	11,660	33	2,955	11,410	50
	CNEN-2	46	19,700	34	374	19,407	1	4,738	—	60
	ENDF/B-IV	10^{-5}	10,000	19	373.8	9,735	0	—	—	—
^{145}Nd	JENDL-1	10^{-5}	3,600	76	4.04	4,365	109	96	4,637	—
	RCN-2	10^{-3}	2,160	114	−20.0	2,157	0	—	—	50
	CNEN-2	10^{-5}	4,650	193	−6.0	4,637	0	—	—	40
	ENDF/B-IV	10^{-5}	1,457	79	4.35	1,448	0	—	—	—

TABLE 2.8 (cont.) 3

Nuclide	Evaluation	Resolved Resonance Region								Upper Energy of Uuresolved Resonance Represent-ation** (keV)
		Defined energy range		S-wave resonance			P-wave resonance			
		Minimum (eV)	Maximum (eV)	No[a]	E_{min}[b] (eV)	E_{max}[c] (eV)	No[a]	E_{min}[b] (eV)	E_{max}[c] (eV)	
^{147}Pm	JENDL-1	10^{-5}	300	39	− 1.8	316.5	0	—	—	—
	RCN-2	10^{-3}	319	39	− 1.8	316.5	0	—	—	50
	CNEN-2	10^{-5}	320	42	− 1.6	316.5	0	—	—	50
	ENDF/B-IV	10^{-5}	58.1	14	− 1.8	55.7	0	—	—	—
^{147}Sm	JENDL-1	10^{-5}	750	51	− 0.6	1,137	81	40.6	1,161	—
	RCN-2	10^{-3}	402	59	− 3.0	399	0	—	—	70
	CNEN-2	10^{-5}	1,170	128	− 2.2	1,161	0	—	—	50
	ENDF/B-IV	10^{-5}	402	59	− 2.0	399	0	—	—	—
^{149}Sm	JENDL-1	10^{-5}	150	34	− 0.285	179.9	52	15.9	248.7	—
	RCN-2	10^{-3}	151	64	− 0.53	149.5	0	—	—	70
	CNEN-2	10^{-5}	260	92	− 0.285	258.9	0	—	—	15
	ENDF/B-IV	3.508	100	30	− 0.285	99	0	—	—	10
^{151}Sm	JENDL-1	10^{-5}	13.4	11	− 0.015	12.75	0	—	—	—
	RCN-2	10^{-3}	106	65	− 0.12	105.3	0	—	—	70
	CNEN-2	10^{-5}	296.6	121	− 0.12	295.7	0	—	—	4
	ENDF/B-IV	10^{-5}	6.94	8	− 0.015	6.44	0	—	—	—
^{153}Eu	JENDL-1	10^{-5}	98	31	0.457	97.6	41	4.75	96.9	—
	RCN-2									
	CNEN-2	10^{-5}	98	79	− 0.8	97.6	0	—	—	50
	ENDF/B-IV	0.77	97.22	79	− 0.8	97.1	0	—	—	10
^{155}Eu	JENDL-1	10^{-5}	1.25*	0	—	—	0	—	—	—
	RCN-2									
	CNEN-2	10^{-5}	4.1	5	0.19	3.91	0	—	—	50
	ENDF/B-IV	10^{-5}	0.321*	0	—	—	0	—	—	—

a) Number of levels
b) Energy of the lowest level
c) Energy of the highest level
* Upper energy of the $1/v$ cross section
** Upper energy of the strength function model for RCN-2

2.3.2 Multi-level Breit-Wigner Formula

As is well known, the elastic scattering cross section calculated from resonance parameters often takes negative value when a simple sum of single-level Breit-Wigner formula is used. This is caused by disregard of the interference between resonances, and therefore can be avoided if, as allowed in ENDF/B, the multi-level Breit-Wigner formula is adopted. This formula in ENDF/B has an advantage that no additional parameters other than single level parameters are required to calculate the cross section, though the level-level interference is treated approximately for $l \geqq 1$ resonances. In applying this formula, the total angular momentum J must be known for all the levels. For most nuclides, however, the J-values are not always assigned for all the levels considered. In order to overcome this difficulty, a modified multi-level Breit-Wigner formula was developed by estimating statistically the J-values of the unassigned levels. The elastic scattering and capture cross sections are then expressed as follows.

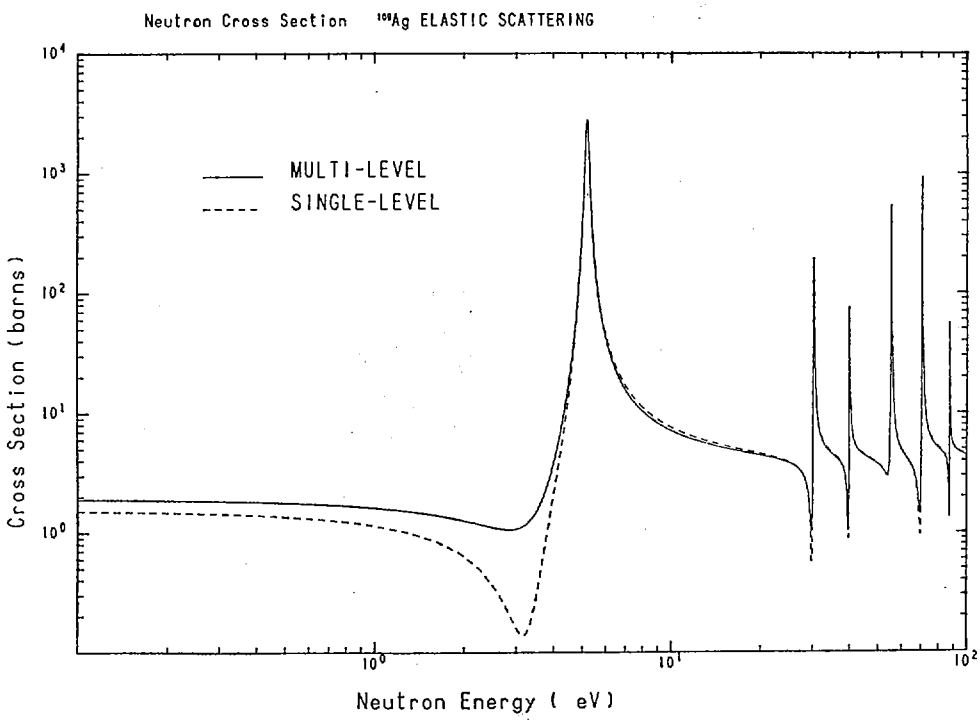

Fig. 2.8 Elastic scattering cross sections of ^{109}Ag calculated with single and multi level Breit-Wigner formulae.

TABLE 2.9 Thermal Capture Cross Section (barns).

Nuclide	BNL-325[29]	ENDF/B-IV		CEA		CNEN-2	RCN-2		JENDL-1	
		Calculated	Adopted	Calculated	Recommended	Calculated[a]	Calculated	Adopted	Calculated	Adopted
^{90}Sr	0.9±0.5	—	0.9						—	0.9
^{93}Zr	1.3~4	—	2.5			1.78			1.34	1.34
^{95}Mo	14.5±0.5	4.81	14.47	4.83	14.5	14.8[b]	14.38[b]	14.38	5.42	14.42
^{97}Mo	2.2±0.7	0.18	2.17	0.2	2.2	2.5[b]	2.30[b]	2.30	0.182	2.18
^{99}Tc	19±2	19.0[b]	19.0	18.15	20.5	20.5[b]	18.2	19.0	17.7	17.7
^{101}Ru	3.1±0.9	3.05	3.10	3.10	5.0	3.0	2.88	2.88	3.34	3.34
^{102}Ru	1.3±0.15	0.012	1.30	0.01	1.35	1.4[b]	0.025	1.31	0.010	1.31
^{103}Rh	150±15	148.2	148.2	148.1	149.1	158.3[b]	147.4	147.4	146.3	146.3
^{104}Ru	0.47±0.2	0.073	0.437	0.09	0.47	0.47[b]	0.011	0.47	0.111	0.411
^{105}Pd	—	2.27	14.0	2.37	12.4	14.7[b]	14.21[b]	14.21	2.49	14.0
^{106}Ru	0.146±0.045	—	0.146			0.148[c]			—	0.146
^{107}Pd	—	—	10.0	—	—	20.8[b,c]	9.98[c]	9.98	—	10.0
^{109}Ag	91±3	90.0	92.0	89.8	91.5	92[b]	89.9	89.9	91.0	91.0
^{129}I	27±3	0.133	27.0	0.13	27.5		27.2[b]	27.2	0.135	27.1
^{131}Xe	90±10	66.9	90.0						68.0	88.0
^{133}Cs	29.0±1.5	16.1	29.5	17.1	29.5	30.1[b]	15.8	29.1	17.0	29.0
^{135}Cs	8.7±0.5	—	8.7	—	8.9	9.0[b,c]			—	8.7
^{137}Cs	0.11±0.033	—	0.11			0.14[c]			—	0.11
^{143}Nd	325±10	313[b]	325	2.3	325	317[b]	325.7[b]	325.7	305[b]	325
^{144}Ce	1.0±0.1	—	1.0			1.128[c]			—	1.0
^{144}Nd	3.6±0.3	2.28	3.6			3.6	3.587[b]	3.587	2.26	3.56
^{145}Nd	42±2	6.79	42.0	6.8	42.8	51.3[b]	42.16[b]	42.16	7.85	41.85
^{147}Pm	181±7	182[b]	182	83	175	198[b]	180.8[b]	180.8	182[b]	182
^{147}Sm	64±5	60.6[b]	64.0			56.5[b]	64.1[b]	64.1	68.2[b]	68.2
^{149}Sm	41000±2000	41191[b]	41191	31050	41500	40637[b]	41000[b]	41000	41500[b]	41500
^{151}Sm	15000±1800	13447[b]	15000	128	15000	15127[b]	15150[b]	15150	12600[b]	15600
^{153}Eu	390±35	—[d]	453			459[b]			71.9	391.9
^{155}Eu	4040±125		4040			3627[c]			—	4040

a) CNEN-2 always adopted the calculated value.
b) Effect of negative resonances included.
c) Adjusted by hypothetical positive resonances.
d) Thermal cross sections are given as point wise data.

TABLE 2.10 Resonance Integrals for Capture (barns)

Nuclide	Compilation of Experiments			Calculated				
	BNL-325[29]	Walker[41]	Iijima et al.[43]	ENDF/B-IV	CEA	CNEN-2	RCN-2	JENDL-1
^{90}Sr	—	—	2.0	0.510				0.49
^{93}Zr	~33	22	1.8	28.2		35.0		30.5
^{95}Mo	105±7	100	106	113	112	121	109	119
^{97}Mo	13±3	15	14.5	16.1	16.8	15.7	17.0	17.1
^{99}Tc	340±20	200	204	353	358	331	353	207
^{101}Ru	85±12	76	73.8	95.2	103	98.5	91.2	107
^{102}Ru	4.1±0.4	4.2	10.6	4.01	4.0	3.79	3.94	4.14
^{103}Rh	1100±50	1100	1070	1048	1046	1030	1047	1034
^{104}Ru	4.6±1.0	4.4	4.6	6.53	6.7	7.51	6.83	7.75
^{105}Pd	90±10	85	80.5	91.8	97	92.0	94.9	94.3
^{106}Ru	2.6±0.6	2.0	1.3	2.08		2.23		2.09
^{107}Pd	—	—	36	69.9	460	255	256	120
^{109}Ag	1450±40	1450	1460	1459	1463	1427	1468	1474
^{129}I	36±4	23	36	36.1	29.2		33.7	44.2
^{131}Xe	—	830	784	877				904
^{133}Cs	415±15	450	440	381	398	378	384	398
^{135}Cs	—	58	80.5	61.6	835	60.0		62.0
^{137}Cs	—	—	0.08	0.488		0.76		0.59
^{143}Nd	—	60	202	204.6	129	125	125.5	134
^{144}Ce	2.6±0.3	2.2	2.62	2.06		2.72		1.55
^{144}Nd	—	3.6	817	5.62		6.4	4.217	5.80
^{145}Nd	240±35	250	306	226	223	226	236.3	266
^{147}Pm	2300±290	2200	2210	2283	2177	2100	2153	2206
^{147}Sm	714±50	600	624	748		736	791	763
^{149}Sm	—	—	3260	3185	3470	3351	3605	3454
^{151}Sm	3300±700	3100	3300	3357	2975	3115	3494	4039
^{153}Eu	1635±200	1500	1430	1550		1396		1529
^{155}Eu	—	—	7000	1856		2180		3218

$$\sigma_{n,\gamma}(E)=\frac{\pi}{k^2}\sum_l\left[\sum_J g_J\sum_\lambda\frac{\Gamma_{n\lambda}\Gamma_{\gamma\lambda}}{(E-E_\lambda)^2+\Gamma_\lambda^2/4}+\bar{g}\sum_\nu\frac{\Gamma_{n\nu}\Gamma_{\gamma\nu}}{(E-E_\nu)^2+\Gamma_\nu^2/4}\right], \tag{14}$$

$$\begin{aligned}\sigma_{n,n}(E)=\frac{\pi}{k^2}\sum_l\Bigg[&4(2l+1)\sin^2\phi_l+\sum_J g_J\sum_\lambda\frac{\Gamma_{n\lambda}^2-\Gamma_{n\lambda}\Gamma_\lambda(1-\cos2\phi_l)+2\Gamma_{n\lambda}(E-E_\lambda)\sin2\phi_l}{(E-E_\lambda)^2+\Gamma_\lambda^2/4}\\&+\bar{g}\sum_\nu\frac{\Gamma_{n\nu}^2\Gamma_{\nu\nu}(1-\cos2\phi_l)+2\Gamma_{n\nu}(E-E_\nu)\sin2\phi_l}{(E-E_\nu)^2+\Gamma_\nu^2/4}\\&+\sum_J g_J\sum_{\lambda\neq\mu}\frac{\Gamma_{n\lambda}\Gamma_{n\mu}[E-E_\lambda)(E-E_\mu)+\Gamma_\lambda\Gamma_\mu/4]}{[(E-E_\lambda)^2+\Gamma_\lambda^2/4]\cdot[(E-E_\mu)^2+\Gamma_\mu^2/4]}\\&+2\sum_J g_J P_J\sum_{\lambda\neq\nu}\frac{\Gamma_{n\lambda}\Gamma_{n\nu}[(E-E_\lambda)(E-E_\nu)+\Gamma_\lambda\Gamma_\nu/4]}{[(E-E_\lambda)^2+\Gamma_\lambda^2/4]\cdot[(E-E_\nu)^2+\Gamma_\nu^2/4]}\\&+\sum_J g_J\frac{P_J(P_JN-1)}{N-1}\sum_{\nu\neq\xi}\frac{\Gamma_{n\nu}\Gamma_{n\xi}[(E-E_\nu)(E-E_\xi)+\Gamma_\nu\Gamma_\xi/4]}{[(E-E_\nu)^2+\Gamma_\nu^2/4]\cdot[(E-E_\xi)^2+\Gamma_\xi^2/4]}.\Bigg]\end{aligned} \tag{15}$$

Here, suffices λ and μ indicate the J-known resonances, ν and ξ the J-unknown resonances. The symbol P_J is the probability that the spin of a resonance is J, and is inversely proportional to D_J, where D_J is the average spacing of levels with spin J. The integer N denotes the number of resonances whose J-values are unknown, and $\bar{g}$ is the average value of the statistical weight factor g_J defined by $\bar{g}=\sum_J g_J P_J$. **Fig. 2.8** shows the elastic scattering cross sections calculated with the single- and multi-level Breit-Wigner formulae.

2.3.3 Thermal Cross Section and Resonance Integral

Thermal neutron cross sections at 2200 m/sec were calculated from the resonance parameters using the above mentioned formula, and were compared with experimental values. The calculated values of capture cross

section are smaller than the measured ones in general. The former values were adjusted to the latter values by adding the background cross sections of $1/v$ form. This assumes that the difference is caused by the contribution from tails of resonances standing far away where resonance parameters are not available in the present work. It should be noted that this adjustment could be made also by assuming negative resonances. The latter procedure were often adopted in the CNEN-2 and RCN-2 evaluations. TABLE 2.9 gives the measured, calculated and adopted thermal capture cross sections as well as those values in the other evaluations.

Capture resonance integrals were calculated including the contributions from the unresolved resonance region. TABLE 2.10 shows the results compared with the other evaluated values.

2.4 Connection between Resonance and Smooth Cross Sections

Resonance cross section should be connected smoothly with the cross section calculated by the statistical theory at some reasonable energy point. We shall call this energy point as the connecting energy. The determination of the connecting energy is often a troublesome problem which we encounter in making a full evaluation. In the followings the method of determining the connecting energy is described according to the data status of resonance parameters at the time of the present evaluation.

(1) No available resonance parameters; ^{106}Ru, ^{107}Pd, ^{135}Cs, ^{137}Cs, ^{144}Ce and ^{155}Eu.

Thermal capture data were available for these nuclides except ^{107}Pd. For these nuclides we set the connecting energy as $E_c = D_{obs}/2$, where D_{obs} is the average level spacing of s-wave resonances adopted in the statistical model calculations. This is based on the following argument. The statistical model calculation gives expectation value of the cross section averaged over resonances. Therefore, when no cross section data are available at all, it will be only the way of estimating the data to apply the statistical model down to the thermal energy. Now suppose the case where only thermal capture cross section is known as the cases of above nuclides. For these nuclides, the thermal cross section values are much smaller than those calculated by the statistical model. Therefore, we may assume that thermal energy locates somewhere at off-resonance region, and the cross section will behave as $1/v$ up to the first resonance. As we do not know the relation between the thermal energy and the first resonance energy, we must estimate the connecting energy statistically so that the connection should be made at the energy point where the probability that the first resonance level appears below this energy is one half. Assuming the random relation between the thermal and the first resonance energy, we took $D_{obs}/2$ approximately as the connecting energy. It is inevitable in this case that the cross section shows a large discontinuity at the connecting energy.

(2) Only a few observed resonance levels; ^{93}Zr, ^{102}Ru, ^{104}Ru and ^{129}I.

For these nuclides we took $E_c = E_{max} + D_{obs}/2$, where E_{max} is the energy of the highest resonance level observed. This choice was based on a similar argument as described just above. A large discontinuity in the cross section can appear also in this case at the connecting energy. Fig. 2.9 shows the case of ^{93}Zr.

(3) Many observed resonance levels; the remaining 17 nuclides.

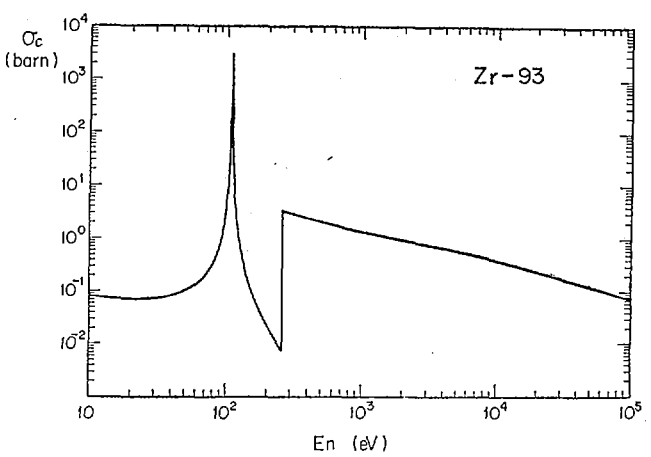

Fig. 2.9 Connection between resonance and smooth cross sections of ^{93}Zr.

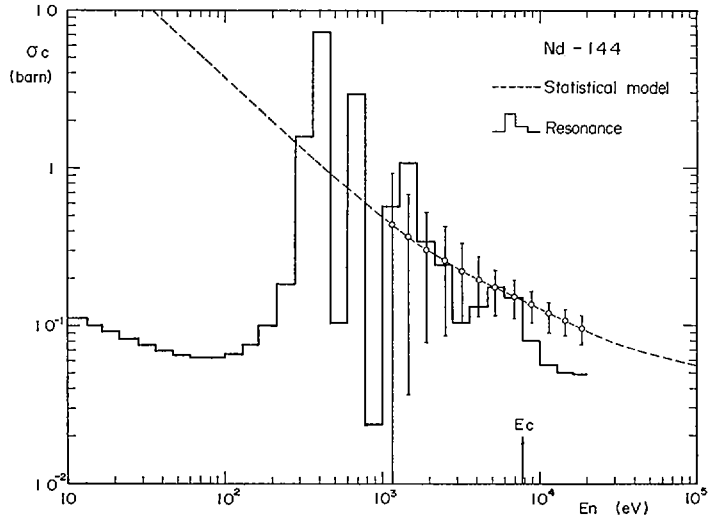

Fig. 2.10 Connection between resonance and smooth cross sections of ^{144}Nd.

TABLE 2.11 Statistical examination at connecting energy

Nuclide	E_c(eV)[a]	ΔE(eV)[b]	Capture			Elastic Scattering		
			A[c]	B[d]	|A|/B	A[c]	B[d]	|A|/B
^{93}Zr	260	250	0.44	1.77	0.25	−0.38	1.64	0.23
^{95}Mo	2150	490	0.045	0.28	0.16	−0.04	0.17	0.24
^{97}Mo	1660	370	0.16	0.37	0.44	−0.26	0.30	0.86
^{99}Tc	290	75	0.04	0.62	0.06	0.14	0.39	0.36
^{101}Ru	700	340	0.094	0.10	0.94	0.65	0.22	2.98
^{102}Ru	1450	450	−0.29	0.75	0.56	0.06	0.54	0.11
^{103}Rh	3600	820	0.015	0.10	0.15	0.17	0.054	3.2
^{104}Ru	1290	930	0.36	0.51	0.70	0.37	0.63	0.58
^{105}Pd	150	21	−0.26	1.01	0.25	−0.26	0.52	0.50
^{109}Ag	1000	220	0.06	0.26	0.23	0.13	0.14	0.92
^{129}I	166	66	−0.32	0.60	0.54	−0.58	0.95	0.60
^{131}Xe	773	175	−0.15	0.45	0.34	−0.27	0.62	0.45
^{133}Cs	1290	290	−0.28	0.21	1.3	−0.60	0.44	1.4
^{143}Nd	4650	1050	−0.01	0.13	0.09	−0.18	0.32	0.59
^{144}Nd	7730	1750	0.007	0.27	0.02	0.48	0.82	0.58
^{145}Nd	3600	820	0.03	0.10	0.30	0.64	0.21	3.0
^{147}Pm	300	22	−0.13	0.45	0.29	0.07	0.87	0.08
^{147}Sm	750	150	−0.08	0.138	0.57	−0.20	0.27	0.73
^{149}Sm	150	50	−0.20	0.25	0.80	0.90	0.55	1.65
^{151}Sm	13.4	5.7	0.44	0.73	0.60	0.43	1.28	0.33
^{153}Eu	98	21	−0.35	0.33	1.05	−0.34	0.54	0.68

a) Connecting energies adopted.
b) Energy range over which the statistical examination was performed.
c) $A=(\bar{\sigma}_r-\sigma_s)/\sigma_s$, where $\bar{\sigma}_r$ is the energy averaged resonance cross section and σ_s the cross section calculated with the statistical model.
d) The ratio of the standard deviation of energy averaged cross section due to the statistical fluctuation of resonance parameters to the expectation value. These values were calculated with the Monte Carlo method.[44]

In this case, the connecting energy is just the upper bound of the resonance region. Hence a special care was paid for missing levels in higher energy region of the resonances. To determine the connecting energy, we performed a statistical examination as follows. We considered the cross section averaged over many resolved resonances. When levels are missing, this average cross section falls off more rapidly as energy increases than that expected theoretically. If the discrepancy between these two is larger than a statistically anticipated value, then we may assume that the levels are really missing in the energy region under consideration. As the statistical criterion we took one standard deviation, which we estimated by Monte Carlo method[44]. We lowered the connecting energy, until the above criterion was satisfied. Thus, the resonances above the connecting energy were abandoned for ^{97}Mo, ^{103}Rh, ^{109}Ag, ^{131}Xe, ^{133}Cs, ^{143}Nd, ^{144}Nd, ^{145}Nd, ^{147}Sm and ^{149}Sm. The case of ^{144}Nd is illustrated in **Fig. 2. 10.** A test was performed at the same time to see if the smooth cross section was connected reasonably with the resonance cross section. The sesult of this test was used as a judgement on selecting the experimental data set for the present evaluation when there existed inconsistency among measured cross sectsons. In case of ^{133}Cs, we used this judgement in our final results. When the capture data were not available, the value of $\bar{\Gamma}_\gamma/D_{obs}$ was varied so as to decrease the discrepancy between the smooth and resonance cross sections at the connecting energy.

TABLE 2. 11 shows the connecting energy thus determined and the results of the statistical test on cross sections. As seen from the table, the discrepancy between the smooth and resonance capture cross sections at the connecting energy is within one standard deviation for most nuclides. On the other hand, the discrepancy is often very large for the elastic scattering cross section, suggesting the existence of fairly large error in the present nuclear model calculation of low energy elastic scattering cross section. This probably reflects the situation that the present global optical potential parameters do not reproduce precisely the neutron strength function and the scattering radius of individual nuclides, though proved to be successful as a general trend. However, the error in the low energy elastic scattering cross section is not very important for reactor calcululation.

2. 5 Level Scheme

Discrete level schemes of target nuclei are important in calculation of the inelastic scattering. They were studied by Nakasima and Murata in the previous work,[12] and these values were adopted in the present work without alteration. Nakasima and Murata surveyed literatures and added new information to those appeared in Nuclear Data Sheets and in Table of Isotopes, 6th edition.[45] The spin-parity assignment was made for unknown levels with theoretical prediction or systematics. The details of the evaluation are given in Ref. (12).

The adopted level schemes are shown in **TABLE 2. 12** with those adopted in the other evaluations. It is observed that the RCN-2, CNEN-2 and CEA evaluations assume more levels than the present JENDL-1 and ENDF/B-IV, some of which may be hypothetical ones. On the other hand, the present level schemes may miss some existing levels. After the present work, Matumoto *et al.*[46] revised the level scheme, and augmented the number of levels for most of these nuclides.

TABLE 2.12 Level schemes of various evaluations in unit of MeV

- o The value in the last line under horizontal bar is the energy above which levels are treated as continuum.
- o The * mark in CEA denotes that the level is hypothetical.

TABLE 2.12.1 ^{90}Sr

JENDL-1		RCN-2	CNEN-2	CEA	ENDF/B-IV	
0	0^+				0	0^+
0.8315	2^+				0.83	2^+
1.6555	0^+				1.69	
1.8921	2^+				1.94	
2.2068	4^+				2.23	
2.5					2.23	

TABLE 2.12.2 ^{93}Zr

JENDL-1		RCN-2	CNEN-2		CEA	ENDF/B-IV	
0	$5/2^+$		0	$5/2^+$		0	$5/2^+$
0.267	$3/2^+$		0.2669	$3/2^+$		0.267	$3/2^+$
0.947	$1/2^+$		0.9471	$1/2^+$		0.940	$1/2^+$
			1.0180	$1/2^+$			
			1.1510	$1/2^+$			
			1.2220	$1/2^+$			
1.425	$5/2^+$		1.4255	$3/2^+$		1.42	$3/2^+$
			1.4356	$1/2^+$			
1.451	$3/2^+$		1.4504	$3/2^+$			
			1.4702	$5/2^+$			
			1.477	$7/2^+$			
			1.597	$5/2^+$			
1.652	$7/2^+$		1.648	$3/2^+$		1.64	$7/2^+$
1.910	$1/2^+$		1.735			1.89	$1/2^+$
1.993	$5/2^+$					2.08	$7/2^+$
2.181	$1/2^+$					2.18	
						2.32	$7/2^+$
2.453	$1/2^+$					2.44	$3/2^+$
2.468	$3/2^+$						
2.605	$1/2^+$						
2.773	$3/2^+$					2.78	$3/2^+$
2.80						2.78	

TABLE 2.12.3 ^{95}Mo

JENDL-1		RCN-2		CNEN-2		CEA		ENDF/B-IV	
0	5/2+	0	5/2+	0	5/2+	0	5/2+	0	5/2+
0.20394	3/2+	0.2039	3/2+	0.2039	3/2+	0.2039	3/2+	0.2039	3/2+
0.76583	7/2+	0.7658	7/2+	0.7658	7/2+	0.7658	7/2+	0.7658	7/2+
0.7862	1/2+	0.7862	1/2+	0.7862	1/2+	0.7862	1/2+	0.7862	1/2+
0.82065	3/2+	0.8207	3/2+	0.8207	3/2+	0.8207	3/2+	0.8207	3/2+
0.9478	9/2+	0.9479	9/2+	0.9479	9/2+	0.9479	9/2+	0.9478	9/2+
1.0391	1/2+	1.039	1/2+	1.0391	1/2+	1.0391	1/2+	1.0391	1/2+
1.059	5/2+	1.057	5/2+	1.0570	5/2+	1.057	5/2+	1.0590	5/2+
1.0741	7/2+	1.074	7/2+	1.0739	7/2+	1.0739	7/2+	1.0741	7/2+
1.2225	5/2+	1.220	3/2+	1.220	3/2+	1.22*	3/2+	1.2225	
		1.250	5/2+	1.250	5/2+	1.25*	5/2+		
1.310	1/2+	1.310	1/2+	1.310	1/2+	1.310	1/2+	1.310	1/2+
1.376	3/2+	1.370	3/2+	1.370	3/2+	1.370	3/2+	1.376	3/2+
1.433	5/2+	1.426	3/2+	1.426	3/2+	1.426	3/2+	1.433	5/2+
		1.440	7/2+	1.440	7/2+	1.44*	7/2+		
		1.470	1/2+	1.470	1/2+	1.47*	1/2+		
1.541	11/2+	1.541	11/2+	1.5412	11/2+	1.5412	11/2+	1.541	11/2+
1.5528	9/2+	1.552	9/2+	1.5518	9/2+	1.5518	(9/2+)	1.5528	9/2+
1.62		1.570	5/2+	1.57	5/2+	1.57*	5/2+		
		1.580	3/2+	1.58	3/2+	1.58*	3/2+		
		1.620	3/2+	1.62	3/2+	1.620	3/2+	1.6202	3/2+
		1.650	7/2-	1.65	7/2-	1.65*	7/2-		
		1.670	5/2+	1.67	5/2+	1.670	(5/2+)	1.670	5/2+
		1.683	9/2+	1.683	9/2+	1.683	(9/2+)	1.683	7/2+
		1.707		1.707	1/2+	1.707	(1/2+)	1.707	1/2+
				1.73	9/2+	1.73*	9/2+		
				1.74	7/2+	1.74*	7/2+		
				1.75	1/2+	1.75*	1/2+		
				1.76	5/2+				
				1.82	9/2-	1.82*	9/2-		
				1.83	3/2+	1.83*	3/2+		
				1.84	11/2+	1.84*	11/2+		
				1.85	5/2+	1.85*	5/2+		
				1.86	3/2+	1.86*	3/2+		
				1.87	7/2+				
				1.91	9/2+	1.91*	9/2+		
				1.92	3/2+	1.92*	3/2+		
				1.938	11/2-	1.938	11/2-	1.938	11/2-
				1.95	5/2+	1.95*	5/2+	1.938	
				1.96	5/2-	1.96*	5/2-		
				1.97	3/2+	1.97*	3/2+		
				2.0		1.978	5/2+		

TABLE 2.12.4 ^{97}Mo

JENDL-1		RCN-2		CNEN-2		CEA		ENDF/B-IV	
0	5/2+	0	5/2+	0	5/2+	0	5/2+	0	5/2+
0.4809	3/2+	0.4809	3/2+	0.4809	3/2+	0.4809	3/2+	0.4809	3/2+
0.6582	7/2+	0.6583	7/2+	0.6583	7/2+	0.6583	7/2+	0.6579	7/2+
0.6796	1/2+	0.6796	1/2+	0.6796	1/2+	0.6796	1/2+	0.6796	1/2+
0.7194	5/2+	0.7193	5/2+	0.7191	3/2+	0.7191	(3/2+)	0.7195	3/2+
0.7211	3/2+	0.7211	3/2+	0.7211	5/2+	0.7211	5/2+	0.7211	3/2+
		0.7530	5/2+						
		0.7950	1/2+						
0.8880	1/2+	0.8810	1/2+	0.8881	1/2+	0.8881	1/2+	0.8882	1/2+
		0.9930	3/2+						
1.0246	7/2+	1.0250	7/2+	1.0246	7/2+	1.0246	7/2+	1.0245	7/2+
1.0926	3/2+	1.0920	3/2+	1.0923	3/2+	1.0923	(3/2+)	1.0926	5/2+
1.1167	9/2+	1.1180	9/2+	1.1175	9/2+	1.1175	9/2+	1.1167	9/2+
		1.1360	3/2+	1.1360	3/2+	1.136	3/2+	1.1360	
		1.1490	9/2+	1.1486	9/2+	1.1486	9/2+	1.1486	
		1.2650	5/2+						
1.2688	7/2+	1.2690	7/2+	1.2686	7/2+	1.2686	7/2+	1.2686	7/2+
								1.2730	3/2+
1.2845	3/2+	1.2840	13/2+	1.2846	3/2+	1.2846	3/2+	1.2840	13/2+
		1.2850	3/2+	1.3600	5/2+	1.36*	5/2+		
1.4095	11/2+	1.4100	11/2+	1.4095	11/2+	1.4095	11/2+	1.4095	11/2+
1.4373	11/2−	1.4370	11/2−	1.4373	11/2−	1.4373	11/2−	1.4373	11/2−
		1.4470	3/2+	1.4600	3/2+	1.460*	3/2+	1.4470	5/2+
1.5156	9/2+	1.5160	9/2+	1.5156	9/2+	1.5156	(9/2+)	1.5156	7/2+
1.54		1.516		1.516	3/2+	1.516*	3/2+		
				1.545	11/2+	1.545	11/2+	1.5452	5/2−
				1.565	7/2−	1.565	7/2−	1.5452	
				1.58	5/2+	1.58*	5/2+		
				1.629	7/2+	1.629	(7/2+)		
				1.64	7/2+	1.64*	7/2+		
				1.66	5/2+				
				1.67	1/2+	1.67*	1/2+		
				1.71	3/2+	1.710	3/2+		
				1.73	5/2+	1.73*	5/2+		
				1.741	5/2+	1.741	5/2+		
				1.7579	1/2+	1.76*	1/2+		
				1.780	7/2+	1.780	7/2+		
				1.79	5/2−	1.79*	5/2−		
				1.82	9/2+	1.82*	9/2+		
				1.83	9/2−	1.83*	9/2−		
				1.858	3/2+	1.858	5/2+		
				1.87	7/2+	1.87*	7/2+		
				1.88	11/2+				
				1.89	1/2+	1.89*	1/2+		
				1.920	13/2+	1.920	(13/2+)		
				1.95		1.93*	5/2+		
						1.95*	7/2−		
						1.96	3/2+		
						1.97*	9/2+		
						1.99*	5/2+		
						2.002	(15/2−)		

TABLE 2.12.5 ^{99}Tc

JENDL-1		RCN-2		CNEN-2		CEA		ENDF/B-IV	
0	9/2+	0	9/2+	0	9/2+	0	9/2+	0	9/2+
0.14051	7/2+	0.1405	7/2+	0.1405	7/2+	0.140	7/2+	0.140	7/2+
0.14263	1/2-	0.1426	1/2-	0.1426	1/2-	0.1426	1/2-	0.142	1/2-
0.18107	5/2+	0.1811	5/2+	0.181	5/2+	0.181	5/2+	0.183	5/2+
				0.250	11/2+	0.250*	11/2+		
				0.350	13/2+	0.350*	13/2+		
0.5091	3/2-	0.5091	1/2-	0.509	3/2-	0.509	3/2-		
0.5343	5/2-	0.5343	3/2-	0.534	5/2+	0.534	(5/2+)	0.534	5/2-
		0.6254	7/2+						
0.6715	5/2-	0.6715	5/2-	0.672	5/2-	0.672	5/2-	0.672	5/2-
0.7263	7/2+	0.7267	11/2+	0.726	7/2+	0.726	(7/2+)		
0.7616	5/2+	0.7617	5/2+	0.762	5/2+	0.762	5/2+	0.762	5/2+
		0.7620	13/2+						
				0.850	1/2+	0.850*	1/2+		
0.9205	3/2+	0.9205	3/2+	0.921	3/2+	0.921	3/2+	0.921	3/2+
				0.950	7/2-	0.950*	7/2+		
1.0040	3/2-	1.0040	3/2-	1.004	3/2-	1.004	3/2-	1.004	3/2-
1.0729	5/2-	1.0730	5/2-	1.073	5/2-	1.073	5/2-	1.073	5/2-
		1.0810	9/2+	1.105	9/2+	1.105*	9/2+		
1.1293	1/2-	1.1290	1/2-	1.130	1/2-	1.130	1/2-		
1.1420	3/2-	1.1420	3/2-	1.142	3/2-	1.142	3/2-	1.142	3/2-
1.199	3/2-	1.199		1.199	3/2-	1.199	3/2-	1.199	1/2-
1.21				1.212				1.287	

TABLE 2.12.6 ^{101}Ru

JENDL-1		RCN-2		CNEN-2		CEA		ENDF/B-IV	
0	5/2+	0	5/2+	0	5/2+	0	5/2+	0	5/2+
0.1271	3/2+	0.1272	3/2+	0.127	3/2+	0.1272	3/2+	0.1272	3/2+
0.3067	7/2+	0.3068	7/2+	0.307	7/2+	0.3068	7/2+	0.3068	7/2+
0.3112	5/2+	0.3113	5/2+	0.311	5/2+	0.3112	5/2+	0.3113	5/2+
0.3254	1/2+	0.3252	1/2+	0.325	1/2+	0.3251	1/2+	0.3252	1/2+
		0.3441	3/2+	0.344	3/2+	0.3441	3/2+	0.3441	
0.4224	3/2+	0.4220	3/2+	0.422	3/2+	0.4220	3/2+	0.4220	3/2+
		0.4623	1/2+	0.462	1/2+	0.4623	1/2+	0.4623	
0.528	11/2−	0.528	11/2−	0.528	11/2−	0.528	11/2−	0.5280	11/2−
0.5447	7/2+	0.5450	7/2+	0.545	7/2+	0.5479	7/2+	0.5450	7/2+
0.6161	7/2+	0.6163	7/2+	0.616	7/2+	0.6162	7/2+	0.6163	7/2+
		0.6235	7/2+	0.623	7/2+	0.6235	7/2+	0.6235	7/2+
		0.6438		0.644	7/2−	0.6438	7/2−	0.6438	7/2+
0.6742	3/2+			0.674	3/2+	0.6742	3/2+	0.6741	
0.720	7/2+			0.720	7/2+	0.7199	7/2+	0.720	9/2+
				0.77	3/2+	0.77*	3/2+		
				0.78	5/2+				
				0.82	1/2+	0.82*	1/2+		
				0.83	7/2+				
0.8426	7/2+			0.843	7/2+	0.8426	7/2+	0.8427	7/2+
				0.87	3/2+	0.87*	3/2+		
				0.88	7/2+	0.88*	7/2+		
				0.89	5/2−	0.89*	5/2−		
0.9111	7/2+			0.912	9/2+	0.9115	9/2+	0.9119	9/2+
0.9282	9/2+			0.929	7/2+	0.9289	7/2+	0.9288	7/2+
0.9381	7/2+			0.938	7/2+	0.9381	7/2+	0.9383	7/2+
				0.959	15/2−	0.959	15/2−	0.959	15/2−
				0.97	5/2+			0.959	
				0.98	1/2+	0.98*	1/2+		
1.0011	11/2+			1.00	11/2+	1.001	11/2+		
1.05				1.20		1.623	19/2−		
						1.861	(15/2+)		
						2.473	23/2−		

TABLE 2.12.7 ^{102}Ru

JENDL-1		RCN-2		CNEN-2		CEA		ENDF/B-IV	
0	0^+	0	0^+	0	0^+	0	0^+	0	0^+
0.4749	2^+	0.475	2^+	0.475	2^+	0.475	2^+	0.475	2^+
0.9437	0^+	0.944	0^+	0.944	0^+	0.944	0^+	0.9437	0^+
1.1032	2^+	1.103	2^+	1.103	2^+	1.103	2^+		
1.1066	4^+	1.107	4^+	1.107	4^+	1.107	4^+	1.106	4^+
1.5219	3^+	1.522	3^+	1.522	3^+	1.522	3^+	1.522	3^+
1.5808	2^+	1.581	2^+	1.581	2^+	1.581	2^+		
		1.603	4^+	1.603	4^+	1.603	4^+	1.600	2^+
1.7990	4^+	1.799	4^+	1.799	4^+	1.799	(4^+)	1.799	3^+
1.8371	0^+	1.837	0^+	1.837	0^+	1.837	0^+		
1.8732	6^+	1.873	6^+	1.873	6^+	1.873	6^+	1.874	5^+
		1.997	5^+	1.997	5^+	(1.997)	(5^+)		
2.0375	2^+	2.037	2^+	2.037	2^+	2.037	2^+	2.040	2^+
2.0441	3^-	2.044	3^-	2.044	3^-	2.044	3^-	2.070	
		2.155	1^+	2.155	1^+	(2.155)	(1^+)	2.155	
2.2192	5^+	2.219	5^+	2.219	5^+	2.219	5^+	2.219	4^+
2.2613	2^+	2.261	2^-	2.261	2^-	2.261	(2^-)	2.261	2^+
2.372	5^-	2.372	5^-	2.372	5^-	2.372	(5^-)		
2.4		2.421	4^+	2.421	4^+	2.421	(4^+)		
		2.442	3^+	2.442	3^+	2.442	(3^+)	2.4419	3^+
		2.471		2.471	1^-	2.471	(4^-)	2.4710	
				2.496		2.614	$(3^+, 4^+)$	2.6144	4^+
						2.650	(6^-)	2.6500	6^-
						2.701	4^+	2.7060	7^-
						2.705	(7^-)	2.7193	4^+
						2.719	4^+	2.8142	4^+
						2.814	4^+	2.8142	
						2.914	4^+		
						2.942	(8^-)		
						3.011	4^+		
						3.387			
						3.434	(9^-)		
						4.056			

TABLE 2.12.8 ^{103}Rh

JENDL-1		RCN-2		CNEN-2		CEA		ENDF/B-IV	
0	1/2$^-$	0	1/2$^-$	0	1/2$^-$	0		0	1/2$^-$
0.040	7/2$^+$	0.0398	7/2$^+$	0.0398	7/2$^+$	0.03978	7/2$^+$	0.040	7/2$^+$
0.093	9/2$^+$	0.0930	9/2$^+$	0.0930	9/2$^+$	0.09304	9/2$^+$	0.093	9/2$^+$
0.298	3/2$^-$	0.2949	3/2$^-$	0.2949	3/2$^-$	0.2949	3/2$^-$	0.297	3/2$^-$
0.360	5/2$^-$	0.3574	5/2$^-$	0.3573	5/2$^-$	0.3573	5/2$^-$	0.362	5/2$^-$
0.537	5/2$^+$	0.5368	5/2$^+$	0.5369	5/2$^+$	0.53685*	(5/2$^+$)	0.538	5/2$^+$
		0.6072	7/2$^+$						
0.651	7/2$^+$	0.6500	5/2$^+$	0.6501	7/2$^+$	0.6501	7/2$^+$	0.650	7/2$^-$
		0.6517	3/2$^+$	0.6514	7/2$^-$	0.6514	7/2$^-$		
0.798	5/2$^+$	0.7980	9/2$^+$	0.7980	9/2$^+$	0.798	9/2$^+$	0.798	3/2$^-$
		0.8031	3/2$^-$	0.8036	3/2$^-$	0.8036	3/2$^-$		
0.843	3/2$^-$	0.8475	7/2$^-$	0.8477	5/2$^-$	0.8477	(5/2$^-$)	0.843	5/2$^-$
0.877	5/2$^-$	0.8806	5/2$^-$	0.8804	5/2$^-$	0.8804	5/2$^-$	0.875	7/2$^-$
0.915	5/2$^-$	0.9200	9/2$^-$	0.9200	9/2$^-$	0.9200	(7/2$^-$)	0.915	9/2$^-$
		0.9680	5/2$^-$	0.968	5/2$^-$	0.968	5/2$^-$		
		1.010	5/2$^+$	1.010	5/2$^+$	1.010*	5/2$^+$		
		1.035	9/2$^+$	1.040	3/2$^+$	1.040*	3/2$^+$	1.043	7/2$^-$
		1.080	7/2$^-$	1.080	7/2$^-$	1.080*	9/2$^-$		
1.102	7/2$^+$	1.107	5/2$^-$	1.1072	5/2$^-$	1.1072	(5/2$^-$)	1.102	7/2$^-$
		1.140	5/2$^+$	1.140	5/2$^+$				
		1.197	9/2$^-$	1.190	7/2$^-$	1.190*	7/2$^-$		
		1.220	3/2$^+$	1.220	3/2$^+$	1.220*	3/2$^+$		
1.247	9/2$^-$	1.252	5/2$^-$	1.2470	5/2$^-$	1.2470	(5/2$^-$)	1.247	5/2$^-$
		1.252	5/2$^+$						
1.270	1/2$^-$	1.277	3/2$^-$	1.2772	3/2$^-$	1.2772	3/2$^-$	1.270	3/2$^-$
1.3		1.2937		1.300	5/2$^+$	1.300*	5/2$^+$	1.387	
				1.310	1/2$^-$	1.310*	1/2$^-$		
				1.330	11/2$^-$	1.330*	11/2$^-$		
				1.380	5/2$^-$				
				1.400	1/2$^+$	1.400	1/2$^+$		
				1.410	3/2$^-$	1.410*	3/2$^-$		
				1.4200	9/2$^+$	1.420*	9/2$^+$		
				1.4380	5/2$^-$	1.438	5/2$^-$		
				1.4650		1.450*	7/2$^-$		
						1.483	7/2$^+$		
						1.500*	3/2$^+$		
						1.510*	5/2$^-$		
						1.540*	1/2$^+$		
						1.560*	5/2$^+$		
						1.580*	9/2$^-$		
						1.598	3/2$^+$		

TABLE 2.12.9 ^{104}Ru

JENDL-1		RCN-2		CNEN-2		CEA		ENDF/B-IV	
0	0^+	0	0^+	0	0^+	0	0^+	0	0^+
0.358	2^+	0.358	2^+	0.358	2^+	0.358	2^+	0.358	2^+
0.889	2^+	0.889	4^+	0.888	4^+	0.888	4^+	0.889	4^+
0.893	4^+	0.893	2^+	0.893	2^+	0.893	2^+	0.889	
0.983	0^+	0.983	0^+	0.988	0^+	0.988	0^+		
1.1		1.242	3^+	1.242	3^+	1.242	3^+		
		1.355	2^+	1.355	2^+	1.355	2^+		
		1.502	4^+	1.502	4^+	1.502	4^+		
		1.516	0^+	1.516	0^+	1.516	0^+		
		1.750	4^+	1.750	4^+	1.750*	4^+		
		1.874	6^+	1.874	6^+	1.874	6^+		
		1.879	3^+	1.879	3^-	1.899	3^-		
		1.971	1^+	1.971	1^+	1.971	1^+		
		1.993	2^+	1.993	2^+	1.993	2^+		
		2.034		2.034	2^-	2.034	2^-		
				2.094	2^+	2.094	2^+		
				2.150	6^+	2.15*	6^+		
				2.160	4^+	2.16*	4^+		
				2.269	3^+	2.269	3^+		
				2.290	2^+	2.290	(2^+)		
				2.350	2^+	2.35*	2^+		
				2.360	5^-	2.36*	5^-		
				2.440	4^+	2.44*	4^+		
				2.450	6^-	2.45*	6^-		
				2.482	2^+	2.482	2^+		
				2.490	3^+	2.490	3^+		
				2.50		2.548	(1, 2)		
						2.823	(2, 3)		
						2.369	(1, 2)		
						3.503	$(1^- \sim 3^-)$		
						3.635	(1, 2)		
						3.713	(1, 2)		
						3.773	$(1^- \sim 3^-)$		

TABLE 2.12.10 ^{105}Pd

JENDL-1		RCN-2		CNEN-2		CEA		ENDF/B-IV	
0	5/2+	0	5/2+	0	5/2+	0	5/2+	0	5/2+
0.2804	3/2+	0.2851	3/2+	0.2805	3/2+	0.2805	3/2+	0.2805	3/2+
0.3062	7/2+	0.3063	7/2+	0.3063	7/2+	0.3063	7/2+	0.3063	7/2+
0.3191	5/2+	0.3192	5/2+	0.3192	5/2+	0.3192	5/2+	0.3192	5/2+
0.3444	1/2+	0.3445	1/2+	0.3445	1/2+	0.3445	1/2+	0.3445	1/2+
								0.4225	3/2+
0.4427	7/2+	0.4422	5/2+	0.4422	5/2+	0.4422	(5/2+)	0.4422	7/2+
0.4890	11/2-	0.4891	11/2-	0.4891	11/2-	0.4891	11/2-	0.4891	11/2-
0.5607	3/2+	0.5608	5/2+	0.5608	3/2+	0.5608	(3/2+)	0.5608	3/2+
0.6444	7/2-	0.6445	7/2-	0.6445	7/2-	0.6445	(7/2-)	0.6445	7/2-
0.6506	3/2+	0.6507	3/2+	0.6507	3/2+	0.6507	3/2+	0.6507	3/2+
0.6731	7/2+	0.6732	1/2+	0.6732	1/2+	0.6732	(1/2+)	0.6732	1/2+
		0.6940	7/2+	0.6940	7/2+	0.694	7/2+		
0.7271	5/2+	0.7272	5/2+	0.7272	5/2+	0.7272	(5/2+)	0.7272	5/2+
0.78	9/2+	0.7813	5/2+	0.7813	5/2+	0.7813	(5/2+)	0.7818	3/2+
		0.7870	1/2+	0.7870	1/2+	0.787	(1/2+)	0.7818	
		0.8500	5/2-	0.8500	5/2-	0.850*	5/2-		
		0.9294	7/2+	0.9294	7/2+	0.9294	7/2+		
		0.9390	1/2+	0.9390	1/2+	0.939	(1/2+)		
0.9623	5/2+	0.9624	3/2+	0.9624	1/2+	0.9624	3/2+		
		0.979	5/2+	0.979	5/2+	0.979	5/2+		
1.0015	5/2+								
		1.040	3/2+	1.040	3/2+	1.040*	3/2+		
		1.072	5/2+	1.072	5/2+	1.072	(5/2-)		
		1.075	1/2+	1.075	1/2+	1.075	(1/2+)		
1.0878	3/2-	1.088	3/2-	1.088	3/2-	1.088	3/2-		
1.12		1.098	5/2+	1.098	5/2+	1.098	(5/2+)		
		1.141	7/2+	1.141	7/2+	1.141	7/2+		
		1.171	7/2-	1.170	7/2-	1.170*	7/2-		
		1.201	3/2+	1.201	3/2+	1.201	3/2+		
		1.220	1/2+	1.220	1/2+	1.220*	1/2+		
		1.250	9/2-	1.250	9/2-	1.250*	9/2-		
		1.263		1.263	5/2+	1.263			
				1.280	3/2+	1.280*	3/2+		
				1.310	3/2-	1.310*	3/2-		
				1.330	9/2+	1.330*	9/2+		
				1.340	7/2+	1.340*	7/2+		
				1.360	5/2-	1.360*	4/2-		
				1.370	3/2-	1.370*	3/2+		
				1.390	5/2+	1.390*	5/2+		
				1.402	5/2-	1.402	5/2-		
				1.410	5/2+	1.410*	5/2+		
				1.420	1/2-	1.420*	1/2-		
				1.50		1.440*	3/2+		
						1.460*	7/2-		
						1.480*	1/2+		
						1.490*	5/2+		

TABLE 2.12.11 ^{106}Ru

JENDL-1		RCN-2	CNEN-2		CEA	ENDF/B-IV	
0	0^+		0	0^+		0	0^+
0.270	2^+		0.2703	2^+		0.270	2^+
0.711	4^+		0.7140	4^+		0.711	4^+
0.791	2^+		0.7927	2^+		0.791	2^+
0.989	0^+		0.9911	0^+		0.989	0^+
			1.0920	4^+		0.989	
			1.1610				
1.772	2^+						
1.888	2^+						
1.91							

TABLE 2.12.12 ^{107}Pd

JENDL-1		RCN-2		CNEN-2		CEA		ENDF/B-IV	
0	5/2+	0	5/2+	0	5/2+	0	(5/2+)	0	5/2+
0.1157	1/2+	0.1157	1/2+	0.1157	1/2+	0.1157	1/2+	0.115	1/2+
0.214	11/2-	0.2140	11/2-	0.2140	11/2-	0.214	(11/2-)	0.214	11/2-
0.3028	5/2+	0.3028	5/2+	0.3028	5/2+	0.3028	3/2+	0.301	5/2+
0.3122	7/2+	0.3122	7/2+	0.3122	7/2+	0.3122	7/2+	0.312	7/2+
0.3482	3/2+	0.3482	5/2+	0.3482	5/2+	0.3482	5/2+		
0.366	9/2+	0.3660	9/2+	0.3660	9/2+	0.366	9/2+	0.367	7/2+
0.3819	3/2+	0.3919	3/2+	0.3819	3/2+	0.3819	3/2+	0.381	3/2+
0.3924	7/2+	0.3924	5/2-	0.3924	5/2+	0.3924	5/2-		
0.412	1/2+	0.4120	1/2+	0.4120	1/2+	0.412	1/2+	0.412	1/2+
0.4712	3/2+	0.4712	3/2+	0.4712	5/2+	0.4712	5/2+	0.471	3/2+
0.5677	5/2+	0.5677	5/2+	0.5677	3/2+	0.5677	3/2+	0.567	5/2+
		0.6200	7/2-	0.6200	7/2-	0.620*	7/2-		
0.6701	5/2+	0.6701	5/2+	0.6701	5/2+	0.6701	5/2+	0.670	5/2+
0.685	7/2-	0.685	7/2+	0.685	7/2-	0.685	7/2+		
0.698	1/2+	0.698	1/2+	0.698	1/2+	0.698	1/2+	0.697	1/2+
0.759	3/2+	0.759	3/2+	0.759	3/2+	0.759	3/2+	0.759	3/2+
0.781	3/2-	0.781	3/2-	0.781	3/2-	0.781	3/2-	0.781	1/2-
0.806	1/2-	0.806	5/2+	0.806	5/2+	0.806	5/2+		
		0.807	5/2-	0.807	5/2-	0.807*	5/2-		
				0.809	1/2+			0.809	5/2+
0.889	1/2+	0.889	1/2+	0.889	1/2+	0.889	1/2+	0.892	1/2+
		0.930	3/2+	0.930	3/2+	0.930*	3/2+	0.892	
		0.950	9/2+	0.950	9/2+	0.950*	9/2+		
		0.980	7/2+	0.980	7/2+	0.980*	7/2+		
1.023	5/2+	1.023	3/2+	1.023	5/2+	1.023	5/2+		
1.07		1.040	3/2+	1.040	3/2+	1.040*	3/2+		
		1.060	3/2-	1.060	3/2-	1.060*	3/2-		
		1.071	3/2+	1.071	3/2+	1.071	3/2+		
		1.102	7/2+	1.102	7/2+	1.102	7/2+		
		1.113	5/2+	1.113	1/2-	1.113	1/2-		
		1.120	1/2+	1.120	1/2+	1.120	1/2+		
		1.149	5/2-	1.149	3/2+	1.149	3/2+		
		1.160	3/2+	1.160	5/2-	1.160	5/2-		
		1.167	1/2+	1.167	1/2+	1.167	1/2+		
		1.214	5/2+	1.214	5/2+	1.214	5/2+		
		1.221		1.221	3/2+	1.221	3/2+		
				1.250	7/2-	1.250*	7/2-		
				1.267	3/2-	1.267	3/2-		
				1.290	9/2+	1.290*	9/2+		
				1.30		1.320*	1/2-		
						1.330*	5/2+		
						1.347	9/2-		
						1.353	7/2+		
						1.370*	1/2+		
						1.380*	5/2-		
						1.402	5/2-		
						1.420*	5/2+		
						1.430*	7/2+		
						1.440*	1/2+		
						1.451	5/2-		
						1.460*	3/2-		
						1.470*	3/2+		
						1.473	7/2-		
						1.480*	3/2+		
						1.490*	9/2+		

TABLE 2.12.13 ^{109}Ag

JENDL-1		RCN-2		CNEN-2		CEA		ENDF/B-IV	
0	1/2$^-$	0	1/2$^-$	0	1/2$^-$	0	1/2$^-$	0	1/2$^-$
0.088032	7/2$^+$	0.0880	7/2$^+$	0.0880	7/2$^+$	0.08803	7/2$^+$	0.088	7/2$^+$
0.1328	9/2$^+$	0.1328	9/2$^+$	0.1328	9/2$^+$	0.1328	9/2$^+$	0.133	9/2$^+$
0.3144	3/2$^-$	0.3114	3/2$^-$	0.3114	3/2$^-$	0.3114	3/2$^-$	0.311	3/2$^-$
0.4153	5/2$^-$	0.4153	5/2$^-$	0.4153	5/2$^-$	0.4153	5/2$^-$	0.415	5/2$^-$
		0.6970	7/2$^+$						
0.7019	3/2$^-$	0.7019	3/2$^-$	0.7019	3/2$^-$	0.7019	3/2$^-$	0.702	3/2$^-$
		0.7070	3/2$^+$	0.7070	1/2$^+$	0.707	1/2$^+$	0.703	
0.7244	3/2$^+$	0.7244	5/2$^+$	0.7244	3/2$^+$	0.7244	(3/2$^+$)		
0.7353	5/2$^+$	0.7353	5/2$^+$	0.7353	5/2$^+$	0.7353	(5/2$^+$)		
		0.8110	3/2$^+$						
0.8398	7/2$^-$	0.8398	1/2$^-$	0.8398	1/2$^-$	0.8398	1/2$^-$		
0.8627	5/2$^-$	0.8627	5/2$^-$	0.8627	5/2$^-$	0.8627	5/2$^-$		
0.8695	5/2$^+$	0.8695	5/2$^+$	0.8695	5/2$^+$	0.8695	5/2$^+$		
0.9110	7/2$^-$	0.9110	7/2$^+$	0.9110	7/2$^+$	0.9110	7/2$^+$		
0.9123	3/2$^+$	0.9123		0.9123	7/2$^-$	0.9123	7/2$^-$		
0.9595				1.02	5/2$^+$	1.02*	5/2$^+$		
				1.04	5/2$^-$	1.04*	5/2$^-$		
				1.0906	7/2$^-$	1.0906	7/2$^-$		
				1.099	3/2$^-$	1.099	3/2$^-$		
				1.13	3/2$^+$				
				1.14	1/2$^+$	1.14*	1/2$^+$		
				1.16	5/2$^-$	1.16*	5/2$^-$		
				1.17	7/2$^-$	1.17*	7/2$^-$		
				1.20	9/2$^+$	1.20	9/2$^+$		
				1.22	7/2$^+$	1.22*	7/2$^+$		
				1.23	1/2$^-$				
				1.26	1/2$^-$	1.26	1/2$^-$		
				1.27	3/2$^+$	1.27*	3/2$^+$		
				1.28	5/2$^+$				
				1.31	7/2$^+$	1.31	7/2$^+$		
				1.324	3/2$^-$	1.324	3/2$^-$		
				1.34	11/2$^-$				
				1.4		1.36*	5/2$^-$		
						1.37*	3/2$^-$		
						1.38*	3/2$^+$		
						1.39*	11/2$^+$		
						1.430	1/2$^+$		
						1.49	5/2$^+$		
						1.510	9/2$^-$		

TABLE 2.12.14 ^{129}I

JENDL-1		RCN-2		CNEN-2	CEA		ENDF/B-IV	
0	$7/2^+$	0	$7/2^+$		0	$7/2^+$	0	$7/2^+$
0.02777	$5/2^+$	0.0278	$5/2^+$		0.0278	$5/2^+$	0.2780	$5/2^+$
0.27842	$5/2^+$	0.2784	$3/2^+$		0.2784	$3/2^+$	0.2784	$3/2^+$
0.48738	$3/2^+$	0.4874	$5/2^+$		0.4874	$5/2^+$	0.4874	$5/2^+$
0.55957	$1/2^+$	0.5597	$5/2^+$		0.5597	$5/2^+$	0.5596	$1/2^+$
		0.5610	$1/2^+$		(0.561)	$(1/2^+)$		
0.69598	$11/2^+$	0.6960	$11/2^+$		0.6960	$11/2^+$	0.6960	
0.72962	$9/2^+$	0.7296	$9/2^+$		0.7296	$9/2^+$	0.7296	
0.7689	$7/2^-$	0.7688	$7/2^+$		0.7689	$7/2^+$	0.7689	
0.8299	$3/2^+$	0.8300	$3/2^+$		0.8299	$3/2^+$		
0.8450	$7/2^-$	0.8450	$7/2^+$		0.8450	$(7/2^+)$	0.8450	
		0.95			0.95*	$9/2^+$		
					1.047	$3/2^+$		
1.0504	$9/2^+$				1.0504	$7/2^+$	1.0504	
1.052	$5/2^+$						1.0504	
					1.09*	$1/2^+$		
1.11175	$3/2^+$				1.1118	$5/2^+$		
					1.18*	$11/2^+$		
1.210	$1/2^+$				1.2042	$5/2^+$		
					1.24*	$11/2^-$		
1.2608	$5/2^+$				1.2608	$3/2^+$		
					1.27*	$7/2^+$		
1.2821	$3/2^+$				1.2821	$5/2^+$		
1.2922	$3/2^+$				1.2922	$3/2^+$		
					1.32*	$9/2^-$		
					1.36*	$1/2^+$		
					1.37*	$3/2^+$		
1.4016	$9/2^+$				1.4016	$9/2^+$		
1.45					1.41*	$5/2^+$		
					1.43*	$3/2^+$		
					1.45*	$7/2^-$		
					1.48*	$3/2^+$		
					1.4835	$1/2^-$		
					1.566	$(3/2^+, 5/2^+)$		
					1.64	$(3/2^+, 5/2^+)$		
					1.741	$1/2^+$		
					1.823	$1/2^+$		
					1.861	$(3/2^+, 5/2^+)$		
					1.963			

TABLE 2.12.15 ^{131}Xe

JENDL-1		RCN-2		CNEN-2		CEA		ENDF/B-IV	
0	3/2+							0	3/2+
0.08016	1/2+							0.080	1/2+
0.16398	11/2-							0.164	11/2-
0.32578	3/2+								
0.36447	5/2+							0.364	5/2+
0.5030	5/2+								
0.6370	5/2+							0.637	7/2+
0.7229	7/2+							0.723	5/2+
0.73								0.806	15/2-
								0.943	

TABLE 2.12.16 ^{133}Cs

JENDL-1		RCN-2		CNEN-2		CEA		ENDF/B-IV	
0	7/2+	0	7/2+	0	7/2+	0	7/2+	0	7/2+
0.0810	5/2+	0.0810	5/2+	0.081	5/2+	0.081	5/2+	0.081	5/2+
0.1605	5/2+	0.1606	5/2+	0.161	5/2+	0.161	5/2+	0.161	5/2+
0.3828	3/2+	0.3839	3/2+	0.384	3/2+	0.384	3/2+	0.384	3/2+
0.4371	1/2+	0.437	1/2+	0.437	1/2+	0.437	1/2+	0.437	1/2+
0.605	11/2-	0.605	11/2-	0.605	11/2-	0.605	11/2-		
0.633	11/2+	0.633	11/2+	0.633	11/2+	0.633	11/2+	0.633	9/2+
0.641	3/2+	0.642	3/2+	0.642	3/2+	0.642	3/2+	0.645	
0.706	7/2+	0.706	7/2+	0.706	7/2+	0.706	(7/2+)		
0.768	9/2+	0.769	9/2+	0.769	9/2+	0.769	(9/2+)		
0.787	7/2+	0.787	7/2+	0.787	7/2+	0.787	7/2+		
0.819	7/2+	0.819	5/2+	0.819	5/2+	0.819	5/2+		
0.873	9/2+	0.872	9/2+	0.872	9/2+	0.872	(9/2+)		
0.917	3/2+	0.917	3/2+	0.917	3/2+	0.917	3/2+		
0.95		0.942		0.942	3/2+	0.942	3/2+		
				0.98	7/2-	0.98*	7/2-		
				1.02	1/2+				
				1.03	9/2-	1.03*	9/2-		
				1.04	7/2+	1.04*	7/2+		
				1.07	3/2+	1.07*	3/2+		
				1.09	3/2+	1.090	3/2+		
				1.12	3/2+				
				1.13	11/2+	1.13*	11/2+		
				1.14	5/2+	1.14*	5/2+		
				1.16	5/2+				
				1.17	9/2+	1.17*	9/2+		
				1.175	5/2-	1.175	5/2-		
				1.20					

TABLE 2.12.17 ^{135}Cs

JENDL-1		RCN-2	CNEN-2		CEA		ENDF/B-IV	
0	7/2+		0	7/2+	0	7/2+	0	7/2+
0.2498	5/2+		0.2497	5/2+	0.2497	5/2+	0.2496	5/2+
0.4082	3/2+		0.4082	3/2+	0.4082	3/2+	0.4082	
0.6086	5/2+		0.6086	5/2+	0.6086	5/2+	0.6086	
0.780	11/2+		0.781	11/2+	0.781	11/2+	0.6086	
			0.88	11/2-	0.88*	11/2-		
			0.92	1/2+	0.92*	1/2+		
0.9817	1/2+		0.9817	3/2+	0.9817	3/2+		
1.0626	3/2+		1.0624	7/2+	1.0624	7/2+		
1.2			1.12	9/2+	1.12*	9/2+		
			1.16	7/2+	1.16*	7/2+		
			1.18	5/2+	1.18*	5/2+		
			1.23	9/2+	1.23*	9/2+		
			1.27	7/2-	1.27*	7/2-		
			1.28	3/2+	1.28*	3/2+		
			1.32	3/2+	1.32*	3/2+		
			1.33	1/2+	1.33*	1/2+		
			1.37	9/2-	1.37*	9/2-		
			1.38	7/2+	1.38*	7/2+		
			1.40					

TABLE 2.12.18 ^{137}Cs

JENDL-1		RCN-2	CNEN-2		CEA	ENDF/B-IV	
0	7/2+		0	7/2+		0	7/2+
0.455	5/2+		0.456	5/2+		0.456	5/2+
0.85	3/2+		0.849	3/2+		0.849	
0.98	5/2+		0.982	3/2+		0.982	
			1.185	3/2+		1.185	
1.49	1/2+		1.490	1/2+		1.490	1/2+
			1.573	3/2+		1.573	
			1.576	3/2+		1.576	
			1.784	3/2+		1.784	
1.87	11/2-		1.870	11/2-		1.870	11/2-
			1.918	3/2+		1.918	
2.07	3/2+		1.942			2.071	3/2+
2.15	1/2+					2.150	1/2+
2.20						2.150	

TABLE 2.12.19 ^{143}Nd

JENDL-1		RCN-2		CNEN-2		CEA		ENDF/B-IV	
0	7/2$^-$	0	7/2$^-$	0	7/2$^-$	0	7/2$^-$	0	7/2$^-$
0.742	3/2$^-$	0.7421	3/2$^-$	0.742	3/2$^-$	0.742	3/2$^-$	0.742	9/2$^-$
1.236	9/2$^-$	1.230	13/2$^+$	1.228	13/2$^+$	1.228	13/2$^+$	1.236	9/2$^-$
1.311	1/2$^-$	1.306	1/2$^-$	1.306	1/2$^-$	1.306	1/2$^-$	1.311	1/2$^-$
1.412	13/2$^+$	1.411	9/2$^-$	1.408	9/2$^-$	1.408	9/2$^-$	1.412	13/2$^-$
		1.432	3/2$^+$	1.432	5/2$^-$	1.432	5/2$^-$		
		1.506	5/2$^+$	1.506	5/2$^+$	1.506	5/2$^+$		
		1.545	3/2$^+$	1.545	3/2$^+$	1.545	3/2$^+$		
1.560	5/2$^-$	1.556	5/2$^-$	1.556	5/2$^-$	1.556	5/2$^-$	1.560	5/2$^-$
		1.608	1/2$^+$	1.605	1/2$^+$	1.605*	1/2$^+$		
				1.660	5/2$^-$	1.660*	5/2$^-$		
				1.680	3/2$^-$				
				1.690	7/2$^+$	1.690*	7/2$^+$		
1.743	7/2$^-$	1.746	9/2$^-$	1.740	9/2$^-$	1.740	9/2$^-$	1.743	7/2$^-$
		1.761	1/2$^+$	1.770	9/2$^-$				
		1.775	3/2$^-$	1.775	1/2$^+$	1.775*	1/2$^+$		
				1.78	3/2$^+$	1.78*	3/2$^+$		
		1.800	3/2$^-$	1.800	3/2$^-$	1.800	3/2$^-$		
				1.82	1/2$^-$	1.82*	1/2$^-$		
				1.83	5/2$^+$				
				1.84	3/2$^-$	1.84*	3/2$^-$		
1.857	3/2$^-$	1.853	3/2$^-$	1.853	3/2$^-$	1.853	3/2$^-$	1.857	3/2$^-$
				1.86	5/2$^-$	1.86*	5/2$^-$		
		1.870	7/2$^-$	1.87	7/2$^-$				
		1.880	3/2$^-$	1.88	1/2$^-$	1.88*	1/2$^-$		
		1.9108		1.89	9/2$^+$	1.89*	9/2$^+$		
1.916	7/2$^-$			1.911	5/2$^-$	1.911	5/2$^-$	1.916	7/2$^-$
				2.0		1.975	3/2$^+$	1.916	
						1.995	3/2$^-$		
						2.005	1/2$^+$		
2.016	7/2$^+$					2.016	(5/2$^-$)		
2.131	1/2$^-$								
2.192	5/2$^-$								
2.261	3/2$^-$								
2.328	3/2$^-$								
2.367	1/2$^-$								
2.45									

TABLE 2.12.20 ^{144}Ce

JENDL-1		RCN-2		CNEN-2		CEA		ENDF/B-IV	
0	0^+			0	0^+			0	0^+
				0.337	1^+			0.695	
0.3975	2^+			0.382	2^+				
				0.485	0^+				
				0.547	3^+				
0.80	4^+			0.814	1^+				
1.00				0.839	4^+				
				0.910	2^+				
				1.044	1^+				
				1.126	0^+				
				1.148	2^+				
				1.201	1^+				
				1.255	3^+				
				1.309	2^+				
				1.320	1^+				
				1.380	0^+				
				1.416	1^+				
				1.430	2^+				
				1.497	1^+				
				1.525					

TABLE 2.12.21 ^{144}Nd

JENDL-1		RCN-2		CNEN-2		CEA	ENDF/B-IV
0	0^+	0	0^+	0	0^+		0
0.6964	2^+	0.6965	2^+	0.697	2^+		0.695
1.3145	4^+	1.315	4^+	1.315	4^+		0.1310
1.5099	3^-	1.511	3^-	1.511	3^-		1.510
1.5600	2^+	1.561	2^+	1.561	2^+		1.560
1.738	2^+						
1.7902	6^+	1.791	6^+	1.791	6^+		1.784
		2.073	2^+	2.073	2^+		
		2.075	0^+	2.075	0^+		
2.085	0^+	2.085	4^+	2.085	2^+		
		2.093	5^-	2.093	5^-		
2.11	2^-	2.109	4^+	2.110	2^+		2.100
		2.179	1^+	2.179	2^+		
2.1856	1^-	2.186	1^-	2.186	1^-		2.184
		2.205	4^+	2.205	4^+		
		2.218	6^+	2.218			
2.287	4^+	2.2951					
2.37	2^+						2.360
2.50							2.360

TABLE 2.12.22 ^{145}Nd

JENDL-1		RCN-2		CNEN-2		CEA		ENDF/B-IV	
0	7/2⁻	0	7/2⁻	0	7/2⁻	0	7/2⁻	0	7/2⁻
0.067	3/2⁻	0.0672	3/2⁻	0.067	3/2⁻	0.067	3/2⁻	0.067	3/2⁻
0.072	5/2⁻	0.0724	5/2⁻	0.0722	5/2⁻	0.0722	5/2⁻	0.072	5/2⁻
		0.5066	3/2⁺	0.513	5/2⁻	0.513	5/2⁻		
		0.6576	9/2⁻	0.657	3/2⁻	0.657	3/2⁻	0.657	3/2⁻
0.749	5/2⁻	0.7482	9/2⁻	0.749	9/2⁻	0.749	9/2⁻		
		0.7803	3/2⁻	0.779	3/2⁻	0.779	3/2⁻	0.781	1/2⁻
		0.8407	5/2⁺						
		0.9202	1/2⁻	0.919	1/2⁻	0.919*	1/2⁻		
0.92	9/2⁻	0.9205	9/2⁻	0.921	9/2⁻	0.921*	9/2⁻	0.920	9/2⁻
		0.9340	5/2⁻	0.934	5/2⁻	0.934*	5/2⁻		
1.054	3/2⁻	1.0510	7/2⁺	1.052	3/2⁻	1.052	3/2⁻	1.052	3/2⁻
		1.0850	5/2⁺						
		1.1120	11/2⁺	1.109	9/2⁻	1.109	9/2⁻		
1.155	9/2⁺	1.1500	5/2⁻	1.151	5/2⁻	1.151	5/2⁻	1.152	9/2⁺
		1.1612		1.2133	9/2⁻	1.2133	9/2⁻		
				1.248	7/2⁻	1.248	7/2⁻	1.248	5/2⁻
				1.284	3/2⁻	1.284	3/2⁻	1.284	3/2⁻
				1.331	5/2⁻	1.331	5/2⁻	1.331	7/2⁻
1.39	7/2⁻			1.395	3/2⁻	1.395	(3/2⁻)	1.390	3/2⁻
1.40				1.46	11/2⁻	1.46*	11/2⁻		
				1.48	7/2⁻	1.48*	7/2⁻		
				1.527	5/2⁻	1.527	5/2⁻	1.527	5/2⁻
				1.55	1/2⁻	1.55*	1/2⁻		
				1.578	7/2⁻	1.578	7/2⁻		
				1.593	3/2⁻	1.593	(3/2⁻)	1.594	1/2⁻
				1.62	3/2⁻	1.62*	3/2⁻		
				1.63	5/2⁻	1.63*	5/2⁻		
				1.67	7/2⁻	1.67*	7/2⁻		
				1.681	3/2⁻	1.681	3/2⁻		
				1.714	11/2⁻	1.714	11/2⁻		
				1.745	1/2⁻	1.745	1/2⁻		
				1.80		1.760	5/2⁻	1.760	7/2⁻
						1.77*	9/2⁻	1.760	
						1.78*	5/2⁻		
						1.79*	3/2⁻		
						1.82*	9/2⁻		
						1.846	(13/2⁺)		
						1.86*	7/2⁻		
						1.87*	5/2⁻		
						1.885	3/2⁻		

TABLE 2.12.23 ^{147}Pm

JENDL-1		RCN-2		CNEN-2		CEA		ENDF/B-IV	
0	7/2+	0	7/2+	0	7/2+	0	7/2+	0	7/2+
0.0911	5/2+	0.0911	5/2+	0.091	5/2+	0.091	5/2+	0.0911	5/2+
		0.4082	9/2+						
0.4105	3/2+	0.4106	3/2+	0.4112	3/2+	0.4112	3/2+	0.4105	3/2+
				0.450	9/2+				
0.4893	7/2+	0.4893	7/2+	0.4901	5/2+	0.4901	5/2+	0.4892	7/2+
0.5310	5/2+	0.5311	5/2+	0.5319	5/2+	0.5319	5/2+	0.5309	5/2+
				0.55	1/2+				
				0.60	11/2+	0.60*	9/2+		
		0.6328	1/2+						
		0.6413	3/2+						
		0.6493	11/2-	0.65	3/2+				
		0.6672	11/2+						
0.6804	3/2+	0.6804	7/2+	0.6808	7/2+	0.6808	7/2+		
0.6859	5/2+	0.6861	5/2+	0.6874	5/2+	0.6874	5/2+	0.6858	5/2+
0.72		0.7307		0.70	9/2+			0.6858	
				0.7235	3/2+	0.7235	3/2+		
				0.75	5/2+	0.75*	11/2+		
				0.75		0.85*	1/2+		

TABLE 2.12.24 ^{147}Sm

JENDL-1		RCN-2		CNEN-2		CEA	ENDF/B-IV	
0	7/2-	0	7/2-	0	7/2-		0	7/2-
0.1212	5/2-	0.1230	5/2-	0.121	5/2-		0.1218	5/2-
0.1974	3/2-	0.1973	3/2-	0.197	3/2-		0.1981	3/2-
0.713	11/2-	0.7155	11/2-	0.713	3/2-		0.713	11/2-
0.7988	3/2-	0.7988	3/2-	0.799	3/2-		0.799	3/2-
0.808	13/2+	0.808	3/2-	0.808	1/2+		0.808	13/2+
		0.900	1/2+					
0.925	11/2+	0.925	3/2+	0.925	1/2+		0.925	11/2+
1.007	1/2-	1.007	1/2-	1.007	1/2-		1.007	1/2-
1.029	11/2+	1.029	11/2+	1.029	1/2+		1.029	11/2+
1.054	5/2+	1.054	5/2+	1.054	5/2+		1.054	5/2+
1.065	5/2+	1.065	5/2+	1.065	5/2+		1.065	5/2+
1.077	7/2-	1.077	7/2-	1.077	5/2-		1.077	3/2-
1.103	9/2-	1.103	9/2-	1.116			1.103	9/2-
1.166	11/2-	1.166	11/2-				1.166	11/2-
1.180	7/2-	1.180					1.180	7/2-
1.20							1.180	

TABLE 2.12.25 ^{149}Sm

JENDL-1		RCN-2		CNEN-2		CEA		ENDF/B-IV	
0	7/2⁻	0	7/2⁻	0	7/2⁻	0	7/2⁻	0	7/2⁻
0.0225	5/2⁻	0.0225	5/2⁻	0.0225	5/2⁻	0.0225	5/2⁻	0.022	5/2⁻
0.2772	3/2⁻	0.2770	5/2⁻	0.2770	7/2⁻	0.2770	7/2⁻	0.277	3/2⁻
0.2857	9/2⁻	0.2859	9/2⁻	0.2859	9/2⁻	0.2859	9/2⁻	0.286	9/2⁻
0.3502	3/2⁻	0.3500	3/2⁻	0.350	3/2⁻	0.350	3/2⁻	0.350	3/2⁻
0.398	1/2⁻	0.3963	1/2⁻	0.393	1/2⁻	0.393	1/2⁻	0.398	1/2⁻
0.5286	3/2⁻	0.5285	3/2⁻	0.5285	3/2⁻	0.5285	3/2⁻	0.529	3/2⁻
0.5583	5/2⁺	0.5584	5/2⁻	0.5584	5/2⁻	0.5584	5/2⁻	0.558	5/2⁺
0.566	9/2⁻	0.5908	9/2⁻	0.5905	9/2⁻	0.5905	9/2⁻	0.582	9/2⁻
				0.606	3/2⁻	0.606	3/2⁻		
0.640	5/2⁻	0.6367	7/2⁻	0.6364	7/2⁻	0.6364	7/2⁻		
0.65		0.6490	3/2⁺	0.649	3/2⁺	0.649	3/2⁺	0.650	5/2⁻
		0.6640	11/2⁻	0.660	11/2⁻	0.660	11/2⁻		
		0.6770	5/2⁻	0.677	5/2⁻	0.677	5/2⁻		
		0.6950	3/2⁻	0.695	1/2⁻	0.695	1/2⁻		
		0.7100	3/2⁻	0.709	3/2⁻	0.709	3/2⁻		
		0.722		0.722	5/2⁺	0.722	5/2⁺		
				0.76	3/2⁻	0.76*	3/2⁻		
				0.77	5/2⁻				
				0.785	5/2⁻	0.785	5/2⁻		
				0.814	7/2⁺	0.814	7/2⁺		
				0.82	9/2⁻	0.82*	9/2⁻		
				0.8304	5/2⁺	0.8304	5/2⁺		
				0.8332	1/2⁺	0.8332	1/2⁺		
				0.85	7/2⁺			0.853	
				0.86	1/2⁻	0.86*	1/2⁻	1.970	
				0.87	3/2⁻	0.87*	3/2⁻		
				0.88	7/2⁻	0.88*	7/2⁻		
				0.881	3/2⁺	0.881	3/2⁺		
				0.885	11/2⁻	0.885	11/2⁻		
				0.90	3/2⁺				
				0.91	5/2⁻	0.91*	5/2⁻		
				0.92	1/2⁻	0.92*	1/2⁻		
				0.93	5/2⁺	0.93*	5/2⁺		
				0.94	3/2⁻				
				0.95	1/2⁻	0.95*	1/2⁻		
				0.953	7/2⁻	0.953	7/2⁻		
				0.96	9/2⁻	0.96*	9/2⁻		
				0.968	5/2⁻	0.968	5/2⁻		
				0.97	7/2⁺				
				0.98	1/2⁺	0.98	1/2⁺		
				1.0		0.989	9/2⁺		
						0.99*	11/2⁺		
						1.009	7/2⁻		
						1.04	3/2⁺		

TABLE 2.12.26 ^{151}Sm

JENDL-1		RCN-2		CNEN-2		CEA		ENDF/B-IV	
0	5/2⁻	0	5/2⁻	0	5/2⁻	0	5/2⁻	0	7/2⁻
0.00482	7/2⁻	0.0048	3/2⁻	0.0048	3/2⁻	0.00482	3/2⁻	0.005	7/2⁻
0.06582	3/2⁻	0.0658	7/2⁻	0.0658	7/2⁻	0.06583	7/2⁻	0.066	3/2⁻
0.0697	5/2⁻	0.0697	5/2⁻	0.0697	5/2⁻	0.06970	5/2⁻	0.070	5/2⁻
0.09153	1/2⁺	0.0915	9/2⁺	0.0916	9/2⁺	0.09155	9/2⁺	0.092	1/2⁺
0.10485	5/2⁻	0.1048	3/2⁻	0.1048	3/2⁻	0.10483	3/2⁻	0.105	5/2⁻
		0.1479	13/2⁺	0.1479	13/2⁺	0.1479	13/2⁻		
0.16772	5/2⁺	0.1678	5/2⁺	0.1678	5/2⁺	0.16777	5/2⁺	0.168	5/2⁺
0.16839	7/2⁻	0.1684	5/2⁻	0.1684	5/2⁻	0.16840	5/2⁻	0.168	7/2⁻
		0.1754	9/2⁻	0.1754	9/2⁻	0.17538	9/2⁻		
0.20898	7/2⁻	0.2090	7/2⁻	0.2090	7/2⁻	0.20901	7/2⁻	0.209	7/2⁻
				0.22	3/2⁻	0.22*	3/2⁻		
				0.23	7/2⁻				
				0.2456	7/2⁺	0.2456	7/2⁺		
		0.2611	11/2⁻	0.2611	11/2⁻	0.2611	11/2⁻		
				0.27	9/2⁺				
				0.28	1/2⁻	0.28*	1/2⁻		
		0.2850	1/2⁻	0.2850	1/2⁻	0.28497	1/2⁻		
		0.2948	9/2⁻	0.2948	9/2⁻	0.2948	9/2⁻		
		0.3026	5/2⁻	0.3025	5/2⁻	0.30255	5/2⁻		
0.3067	3/2⁻	0.3068	3/2⁺	0.3068	3/2⁺	0.30680	3/2⁺	0.307	3/2⁻
		0.3138	1/2⁺	0.3134	1/2⁺	0.31338	1/2⁺		
		0.3153	3/2⁻	0.3153	3/2⁻	0.31529	3/2⁻		
0.3239	3/2⁺	0.3239	7/2⁺	0.3240	7/2⁺	0.32395	7/2⁺	0.324	3/2⁺
				0.33	9/2⁻	0.33*	9/2⁻		
				0.334	3/2⁺	0.334*	3/2⁺		
				0.336	7/2⁻				
				0.34	5/2⁻	0.34*	5/2⁻		
0.34487	7/2⁺	0.3449	3/2⁺	0.3449	3/2⁺	0.34493	3/2⁺	0.345	7/2⁺
0.35		0.3576		0.35	5/2⁺			0.345	
				0.355	7/2⁺	0.355*	7/2⁺		
				0.3576	1/2⁺	0.35762	1/2⁺		
				0.36	3/2⁺	0.36*	3/2⁺		
				0.365	3/2⁻				
				0.37	7/2⁻	0.37*	7/2⁻		
				0.375	11/2⁻	0.375*	11/2⁻		
				0.38	5/2⁺	0.38*	5/2⁺		
				0.385	9/2⁺				
				0.386	17/2⁺	0.386	17/2⁺		
				0.39	1/2⁻	0.39*	1/2⁻		
				0.392	9/2⁻	0.392*	9/2⁻		
				0.50		0.395*	3/2⁺		
						0.39557	5/2⁺		
						0.405	7/2⁻		
						0.41560	5/2⁻		
						0.42373	7/2⁺		
						0.44606	5/2⁺		
						0.44964	1/2⁻		
						0.47035	3/2⁻		
						0.43024	7/2⁻		
						0.50295	1/2⁺		
						0.50428	5/2⁺		
						0.52148	3/2⁺		
						0.704			
						0.741	3/2⁺		
						0.774	5/2⁺, (3/2⁺)		
						0.823	3/2⁺		
						0.878	5/2⁺		
						0.923	3/2⁺		

TABLE 2.12.27 ^{153}Eu

JENDL-1		RCN-2	CNEN-2		CEA	ENDF/B-IV	
0	$5/2^+$		0	$5/2^+$		0	$5/2^+$
0.08337	$7/2^+$		0.083	$7/2^+$		0.08337	$7/2^+$
0.09743	$5/2^-$		0.097	$5/2^-$		0.09743	$5/2^+$
0.10318	$3/2^+$		0.103	$3/2^+$		0.10318	$3/2^+$
0.15161	$7/2^-$		0.152	$7/2^-$		0.151607	$7/2^-$
0.17285	$5/2^+$		0.173	$5/2^+$		0.17285	$5/2^+$
0.1914	$9/2^+$		0.193	$9/2^+$		0.1914	$9/2^+$
			0.235	$9/2^-$			
0.268	$7/2^+$		0.270	$7/2^+$			
			0.322	$11/2^-$			
			0.325	$11/2^+$			
			0.396	$9/2^+$			
0.6346	$1/2^-$		0.400			0.6346	$1/2^+$
0.6364	$3/2^-$					0.6350	$3/2^+$
0.682	$5/2^-$					0.6820	$5/2^+$
0.6943	$1/2^-$					0.6940	$3/2^+$
0.7064	$3/2^-$					0.7070	$5/2^-$
0.71						0.7153	

TABLE 2.12.28 ^{155}Eu

JENDL-1		RCN-2	CNEN-2		CEA	ENDF/B-IV	
0	$5/2^+$		0	$5/2^+$		0	$5/2^+$
0.075	$7/2^+$		0.0786	$7/2^+$		0.0750	$7/2^+$
0.10435	$5/2^-$		0.1043	$5/2^-$		0.1044	$5/2^-$
0.17	$7/2^-$		0.1690	$7/2^-$		0.1700	$7/2^-$
0.2462	$3/2^+$		0.2457	$3/2^+$		0.2462	$3/2^+$
0.31	$5/2^+$		0.3073	$5/2^+$		0.31	$5/2^+$
			0.3570	$11/2^-$			
			0.3914	$7/2^+$			
0.76	$1/2^-$		0.453			0.76	$1/2^-$
0.87	$5/2^+$					0.87	$5/2^+$
1.09	$3/2^+$					1.09	$3/2^+$
1.27	$5/2^-$					1.27	$5/2^-$
1.45						1.27	

3. Discussion on Each Nuclide

Deatiled discussions are made in this chapter on each nuclide: The first subsection reviews the status of experimental data at the time of the evaluation and at present (October 1978)*. In the second subsection, the evaluation procedure is described on the resonance parameters, thermal cross sections, background cross sections, statistical examination at the connecting energy, adopted level scheme, parameters used in the statistical model calculation and measured capture cross section data used for normalization. The last subsection is devoted to discussion on various problems found in the present evaluation and left in part for future work, and to intercomparison with the other recent evaluations such as ENDF/B-IV, CEA, CNEN-2 and RCN-2.

Since an excellent intercomparison of the recent evaluated data was already published by Gruppelaar *et al.*[21] on capture cross section, the present discussion puts emphasis on the intercomparison of the total and inelastic scattering cross sections for which attention was paid in the evaluation less than for the capture cross section. It is to be noted that detailed intercomparison was difficult due to lack of precise information on ENDF/B-IV evaluation.

Following general characteristics are pointed out here:

(1) The optical potential parameters adopted in the other evaluations are shown in TABLE 3. 1. It is seen that the present potential set, often called Igarasi potential, has very often been used in the European evaluations.

(2) When the calculation with the resonance parameters alone does not well reproduce the experimental thermal capture cross section, the $1/v$ background correction was applied in the JENDL-1 and ENDF/B-IV evaluations, while some hypothetical negative levels were often assumed in the RCN-2 and CNEN-2 evaluations as seen in TABLE 2. 8. Consequently the cross section of the former is higher than that of the latter up to the first positive resonance.

(3) The JENDL-1 and ENDF/B-IV evaluations ignored $(n, 2n)$ and $(n, 3n)$ reactions, while the CNEN-2 and RCN-2 took account of them. Therefore the inelastic scattering cross section decreases abruptly above the threshold energy of the $(n, 2n)$ reaction in the RCN-2 and CNEN-2 evaluations.

3. 1 Strontium-90

3. 1. 1 Status of experimental data

The capture cross section measured in the pile spectrum by Zeisel[49] is the only available experimental data. Though Zeisel gave the value of 0.8 ± 0.5 barns, BNL-325 3rd edition[29] recommends 0.9 ± 0.5 barns. Neither resonance parameters nor smooth cross sections have so far been measured.

3. 1. 2 Evaluation

As for thermal capture cross section, the value recommended in BNL-325 3rd edition was adopted. The $1/v$ behavior was assumed for the capture cross section up to 6 keV corresponding to a half of the mean level spacing used in the statistical model calculation. The elastic scattering cross section below 6 keV was calculated with the effective scattering radius of 6. 9 fm

All the cross sections were calculated in the energy region above 6 keV with the optical and statistical models, since no experimental data were available. The radiation width and mean level spacing were determined by examining the systematic trends in the neighboring nuclides.

3. 1. 3 Discussion

The total, capture and inelastic scattering cross sections are shown in Figs.3. 1. 1~3. 1. 3, respectively.

* A systematic survey of experimental data was completed at October 1978. However, data released after this data are partly included in this report.

TABLE 3.1 Optical Potential Parameter Sets Adopted in the Other Evaluations

Nuclide	RCN-2	CNEN-2	CEA	ENDF/B-IV
^{90}Sr	—	—	—	B
^{93}Zr	—	A	—	B
^{95}Mo	C	A	A	B
^{97}Mo	C	A	A	B
^{99}Tc	A	E	A	I
^{101}Ru	A	E	A	B
^{102}Ru	A	E	A	B
^{103}Ru	A	E	A	I
^{104}Ru	A	E	A	B
^{105}Pd	C	E	A	B
^{106}Ru	—	E	—	B
^{107}Pd	C	E	A	B
^{109}Ag	B	E	A	F
^{129}I	A	—	A	B
^{131}Xe	—	—	—	F
^{133}Cs	A	A	A	F
^{135}Cs	—	A	A	B
^{137}Cs	—	A	—	B
^{143}Nd	A	A	A	H
^{144}Ce	—	A	—	B
^{144}Nd	A	A	—	B
^{145}Nd	A	A	A	H
^{147}Pm	A	A	A	H
^{147}Sm	D	A	—	H
^{149}Sm	D	A	A	a)
^{151}Sm	D	A	A+F	H
^{153}Eu	—	A	—	G
^{155}Eu	—	A	—	H

A : The present potential often called Igarasi potential
B : Moldauer[25] C : Smith *et al.*[47]
D : Rosen *et al.*[28] E : Perrey and Buck[48]
F : Wilmore and Hodgeson[26]
G : Becchetti and Greenlees[27]
H : Coupled channel potential. Precise information is not available.
I : Livolsi[232]
a) : Information not available.

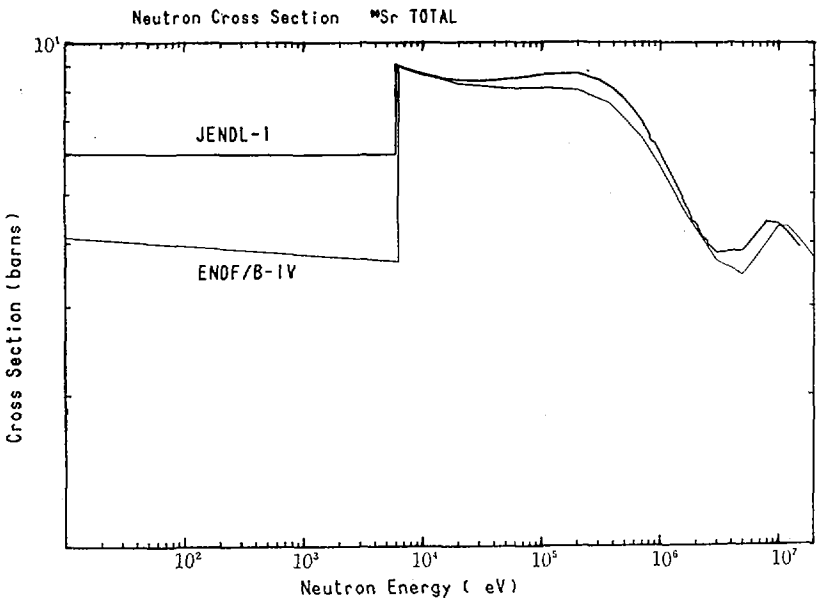

Fig. 3.1.1 Total cross sections of ^{90}Sr.

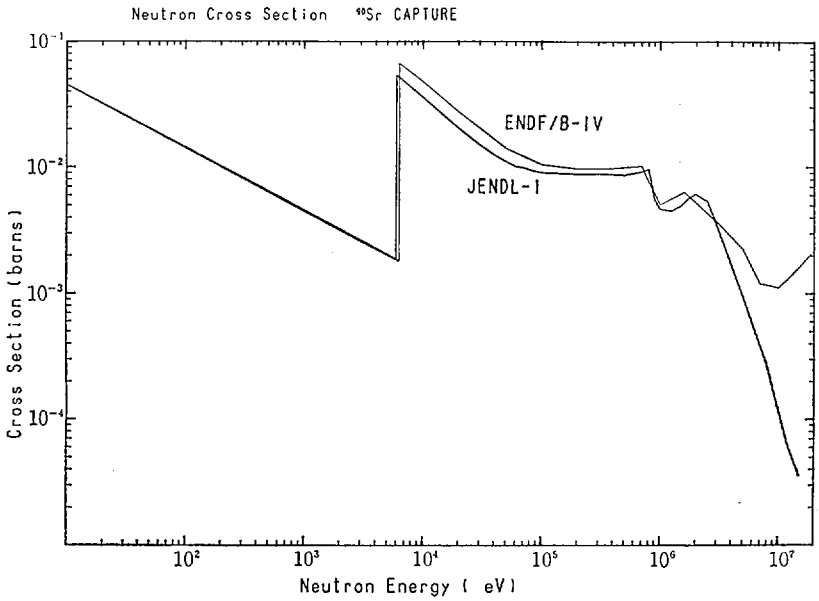

Fig. 3.1.2 Capture cross sections of ^{90}Sr.

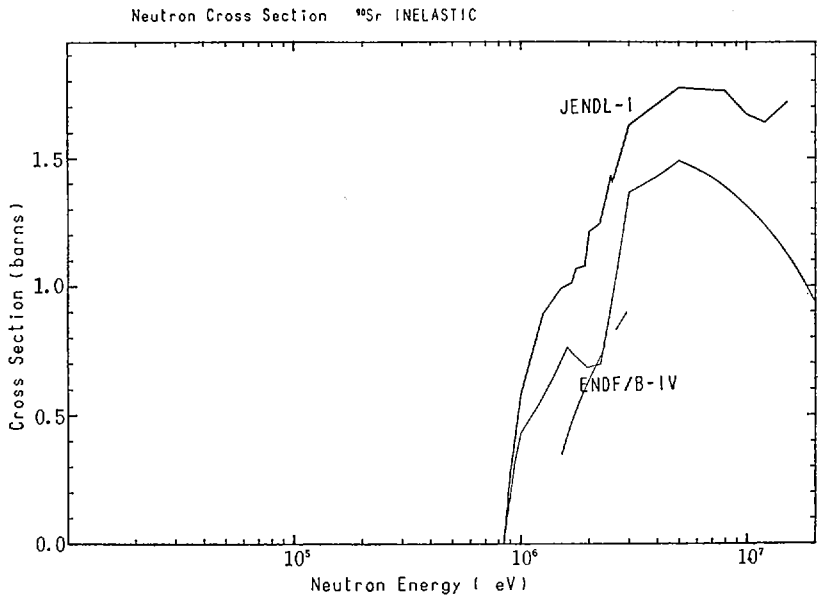

Fig. 3.1.3 Inelastic scattering cross sections of ^{90}Sr.

ENDF/B-IV is the only other evaluation for this nuclide.

The total cross section of JENDL-1 is higher than that of ENDF/B-IV. This is caused by the difference of optical potential parameters in the energy region above 6 keV, and by the considerable difference of the effective scattering radius below 6 keV as seen in TABLE 2.7.

On the other hand, the JENDL-1 evaluation gives lower value for the capture cross section. As to the inelastic scattering cross section, the value of JENDL-1 is higher than that of ENDF/B-IV, probably due to the difference of the optical potential.

3.2 Zirconium-93

3.2.1 Status of experimental data

The thermal capture cross section was measured by Pomerance[50] with a pile oscillator. The uncertainty of the data is large and the cross section is reported to fall into the range from 1.3 to 4 barns. The neutron width of 110 eV level was deduced from the transmission experiment by Block *et al.*[51] No other quantities have so far been measured.

BNL-325 3rd edition[29] recommends these experimental data. It also recommends the cepture resonance integral of 33 barns, whose experimental basis is not clear.

3. 2. 2 Evaluation

We adopted the neutron width deduced by Block *et al.*[51] for 110 eV level. The radiation width was estimated to be 300 meV from the systematic study on the neighboring nuclides. The thermal cross sections and the capture resonance integral were calculated from the resonance parameters of 110 eV level. The value of 1. 34 barns for the capture cross section falls within the uncertainty of the experimental value. Hence no background cross section of $1/v$ type was applied for this nuclide. The effective scattering radius of 6. 9 fm was assumed in calculation of the elastic scattering.

The resonance cross section formula was applied up to 260 eV, i. e., $E_R+D_{obs}/2$, where the mean level spacing D_{obs} of 300 eV was estimated also from the systematic trends of neighboring nuclides and was used in the statistical model calculation.

All the cross sections were calculated with the optical and statistical models in the energy region above 260 eV. The γ-ray strength fuection was obtained from the radiation width and the mean level spacing mentioned above. Twelve discrete excited levels were considered up to 2. 773 MeV and the levels were assumed to be continuum above 2. 8 MeV.

3. 2. 3 Discussion

The total, capture and inelastic scattering cross sections are compared with those of ENDF/B-IV and CNEN-2 in **Figs. 3. 2. 1～3. 2. 3**, respectively. As seen in **TABLE 2. 8**, the ENDF/B-IV evaluation did not adopt the resonance parameters of 110 eV level but gave a smooth curve to represent this resonance.

The total cross sections of JENDL-1 and CNEN-2 agree fairly well with each other in the energy range above 100 keV, while the ENDF/B-IV evaluation gives the lower value in this energy range probably due to the difference of the optical potential parameters. The lower value of ENDF/B-IV below 100 eV is caused by its lower effective scattering radius as seen in **TABLE 2. 7**. Below 50 keV, the CNEN-2 evaluation gives considerably high value calculated from their unresolved resonance parameters whose s-wave strength function is about twice as large as those adopted in JENDL-1 and ENDF/B-IV.

The thermal capture cross sections are given in **TABLE 2. 9** for each evaluation. They lie within the large uncertainty of the experimental data. The capture resonance integrals of the three evaluations agree fairly well with the recommended value of BNL-325 3rd edition. In the smooth region above 260 eV, JENDL-1 gives the highest capture cross section by assuming the largest radiation width. (See **TABLE 2. 5**)

As to the inelastic scattering cross section, the JENDL-1 and ENDF/B-IV evaluations give similar energy

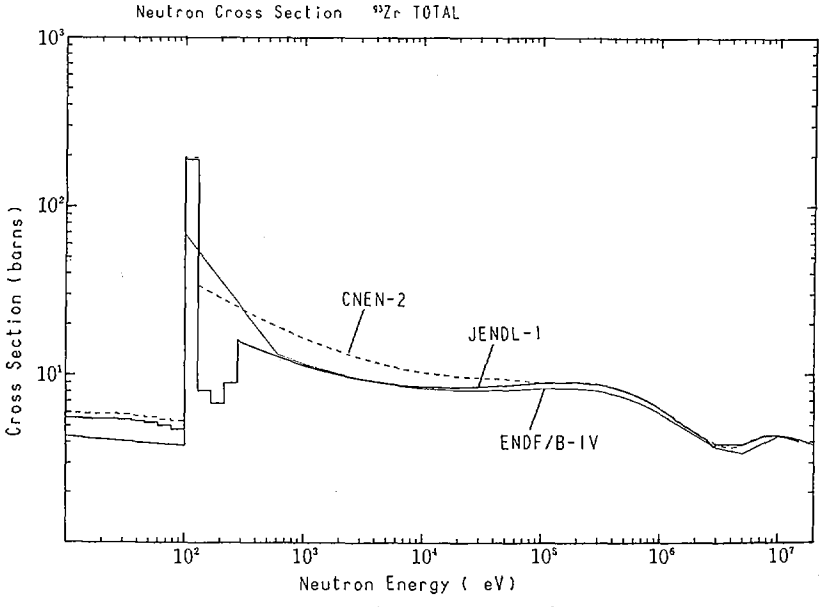

Fig. 3. 2. 1 Total cross sections of ^{93}Zr.

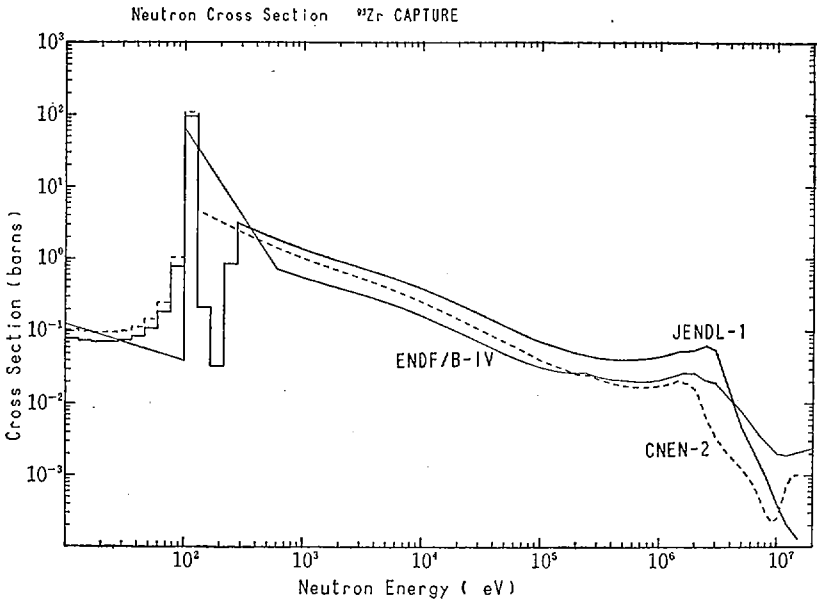

Fig. 3.2.2 Capture cross sections of ^{93}Zr.

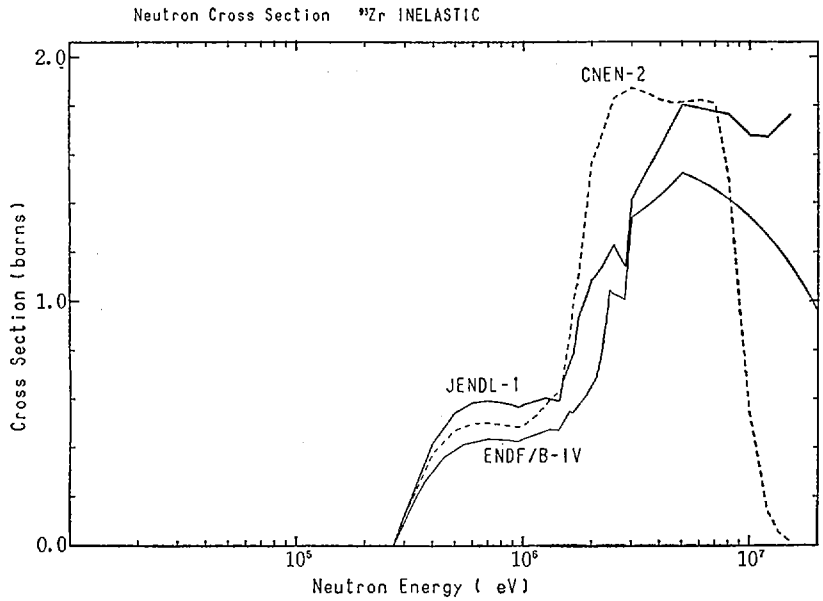

Fig. 3.2.3 Inelastic scattering cross sections of ^{93}Zr.

dependence, though the absolute value of JENDL-1 is a little higher probably due to the difference of the optical potential as observed in the total cross section. The CNEN-2 evaluation adopted 7 levels more than JENDL-1 in the energy range between 1 and 1.6 MeV as seen in TABLE 2.12.2, and assumed continuum levels above 1.735 MeV. This may explain the rapid increase of the inelastic scattering cross section of CNEN-2 above 1 MeV. However, these added levels are probably hypothetical ones.

3.3 Molybdenum-95

3.3.1 Status of experimental data

The thermal capture cross section was measured by Tattersall *et al.*[52] and by Pomerance[53] before 1960. No new data have been reported. BNL-325 recommended $\sigma_{n,\gamma}{}^{th}=14.5\pm0.5$ barns in both 2nd[33] and 3rd[29] editions on the basis of these two experiments. Tattersal *et al.* also measured the resonance integral for capture and gave R.I.$=100\pm20$ barns. BNL-325 3rd edition recommends 105 ± 7 barns whose basis is not clear.

A considerable number of experiments have been reported on the resonance parameters. BNL-325 2nd edition compiled the parameters measured till 1966 and recommended the values of 14 resonances up to 1,413

eV. ENDF/B-IV seems to have adopted most of these recommended values. After 1966 some new experiments have been made. Particularly Weigmann *et al.*[54] measured the resonances in the energy range up to about 2 keV. Recently Musgrove *et al.*[55] extended the resolved resonance region up to 4 keV but his data were not available at the time of the present evaluation.

As for the capture cross section above keV region, the data of Kapchigashev and Popov[56] were the only available data at the time of the present work. After that, two measurements have been reported by Musgrove *et al.*[55] and by Hockenbury *et al.*[57]* The total cross section was measured by Divadeenam *et at.*[58] and Hockenbury *et al.*[57]*

3.3.2 Evaluation

As to the resonance parameters, two sets of new data by Shwe and Coté[59] and by Weigmann *et al.*[54] were taken into consideration as well as those recommended in BNL-325 2nd edition. The resonance parameters deduced by Weigmann *et al.* were mainly adopted, with the assumption of $\Gamma_\gamma=180$ mVe. The values of orbital angular momentum were assigned from the value of $\Gamma_n\Gamma_\gamma/\Gamma$, when no assignment was made by the experimenters. Thus the resonance parameters were determined for 53 levels up to 2,112 eV, 19 of which were assigned as s-wave resonances.

The thermal capture cross section was calculated trom these resonance parameters. The calculated value of 5.42 barns is much lower than 14.5±0.5 barns recommended in BNL-325. The large discrepancy might be caused by our disregard of possible negative resonances. The difference was given as the background cross section whose energy dependence was assumed to be $1/v$ form. The elastic scattering cross section was calculated with the effective scattering radius of 7.1 fm.

The statistical examination was made whether the resonance cross sections connect reasonably with the smooth cross sections calculated with the optical and statistical models. It was found that both cross sections joined at the upper bound of resonances within the standard deviation due to the statistical fiuctuation of the resonance parameters. Therefore the connecting energy was taken at 2,150 eV.

The cross sections were calculated in the energy region above 2,150 eV with the optical and statistical models. The γ-ray strengh function was adjusted so that the calculated capture cross section might reproduce the experimental data of Kapchigashev and Popov[56], which were the only available data at the time of the present evaluation. Fourteen discrete levels were taken into account up to the energy of 1.55 MeV and levels were assumed to be overlapping in the energy region above 1.62 MeV.

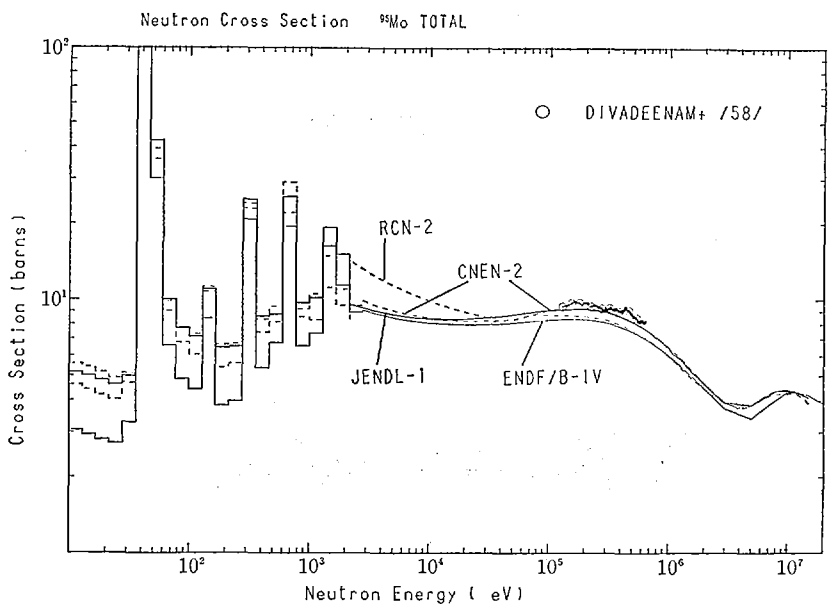

Fig. 3.3.1 Total cross sections of ^{95}Mo.

* The numerical data of Hockenbury *et al.* was not published.

3. 3. 3 Discussion

The total, capture and inelastic scattering cross sections of the present evaluation are compared with the experimental data and the other evaluated data in **Figs. 3. 3. 1～3. 3. 3**, respectively.

As for the total cross section, the present values calculated with the optical model well reproduce the exprimental data of Devadeenam *et al.*[58], while the optical potential parameters were determined from the global trend of the total cross sections in the mass region $A=70\sim160$. This suggests the applicability of the present optical potential. The CNEN-2 evaluation also adopted present potential parameters. The ENDF/B-IV evaluation gives the lowest value. The highest values of RCN-2 below 30 keV are obtained with the strength function model which uses the s-wave strength function more than twice as large as that used in JENDL-1 and the recommended value in BNL-325 3rd edition as shown in **TABLE 2. 4.**

The calculated thermal capture cross section was about one third of the experimental value. Though the $1/v$ correction was applied in the present JENDL-1 evaluation, such a large difference may be caused more probably by existence of negative resonances. The resonance integral for capture was calculated from the resonance parameters and the $1/v$ background cross section. The calculated values of all the evaluations fall within the uncertainty of the experimental data of Tattersall *et al.*[52] as shown in **TABLE 2. 10.**

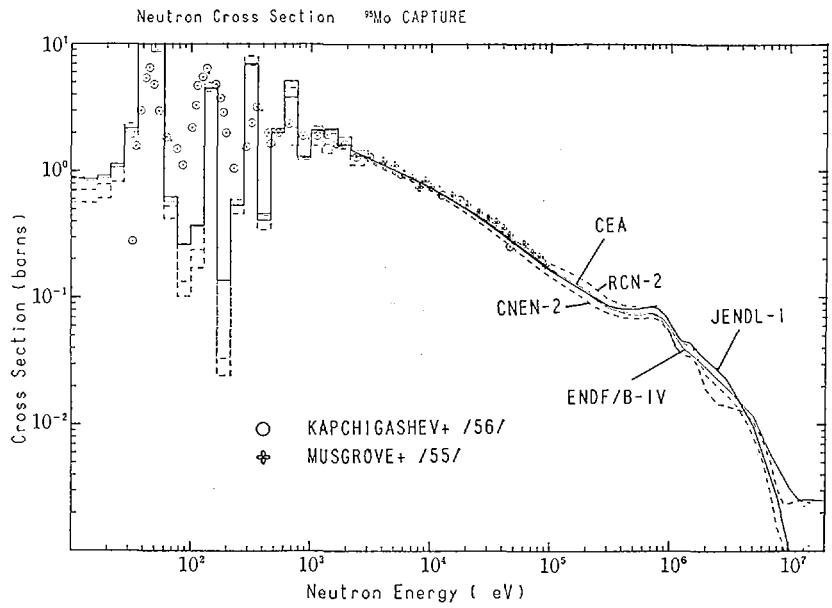

Fig. 3.3.2 Capture cross sections of ^{95}Mo.

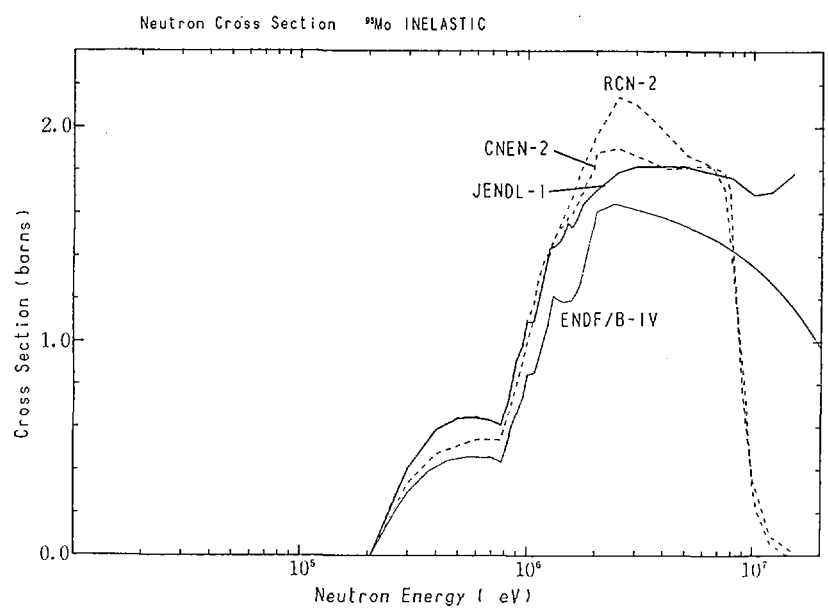

Fig. 3.3.3 Inelastic scattering cross sections of ^{95}Mo.

As was pointed out by Gruppelaar *et al.*[21], it was not possible to reproduce the experimental data of Kapchigashev and Popov[56] both below 40 keV and at 47 keV with the statistical model calculation. Then we adjusted γ-ray strength function so that the calculated curve might pass the middle of these data points. The recent data of Musgrove *et al.*[55] seem to support this decision. The RCN-2 evaluation took account of valence capture effect and also gave the larger radiation widths for p-wave resonances than for s-wave ones as seen in TABLE 2.5. The valency effect was not considered in the present work.

The inelastic scattering cross section of JENDL-1 agrees fairly well with that of CNEN-2. The ENDF/B-IV gives the lowest value as in the case of the total cross section probably due to the adopted optical potential. The data of RCN-2 are lower than those of JENDL-1 below 1 MeV. The data of RCN-2 and CNEN-2 become larger than those of JENDL-1 above 1.2 MeV. This may be partly attributed to their adopting more discrete levels, some of which are hypothetical ones. Recently Matsumoto *et al.*[46] added 5 levels betwen 1.62 MeV and 1.94 MeV in their revised level scheme. This may change the cross section of JENDL-1 in this energy range.

3.4 Molybdenum-97

3.4.1 Status of experimental data

The thermal capture cross section was measured by Pomerance[53] in 1952. BNL-325 3rd edition[29] recommends $\sigma_{n,\gamma}{}^{th}=2.2\pm0.7$ barns on the basis of the datum of Pomerance taking account of the difference of the standard cross section of gold. BNL-325 3rd edition also recommends R.I.$=13\pm3$ barns whose experimental basis is not clear.

Numerous experiments have been made on the resonance parameters. BNL-325 2nd edition[33] compiled the data measured till 1966 and recommended the parameters for 9 resonances up to 1,255 eV. ENDF/B-IV seems to have adopted most of these recommended parameters. At the time of the present evaluation, two other experimental data ware available, *i.e.*, the data of Schwe and Coté[59] and Weigmann *et al.*[54] The latter reported the $g\Gamma_n\Gamma_\gamma/\Gamma$ values of 63 resonances up to 1,940 eV. After the present evaluation, Musgrove *et al.*[55] gave the parameters for the levels up to 3,500 eV.

The capture cross sections measured by Kapchigashev and Popov[56] were the only available data in keV region at the time of present work. After that, the data of Musgrove *et al.*[55] became available for the capture cross section. Recently Hockenbuy *et al.*[57]* reported the measurements of the total and capture cross sections.

2.4.2 Evaluation

In the present work, two sets of new data on the resonance parameters, *i.e.*, by Shwe and Coté[59] and by Weigmann *et al.*[54] were compared with each other and with those in BNL-325 2nd edition. The data by Weigmann *et al.* were mainly adopted with assuming $\Gamma_\gamma=170$ meV for levels whose radiation width was not given. The values of orbital angular momentum were assigned from the value of $\Gamma_n\Gamma_\gamma/\Gamma$, when no assignment was given by the experimenters. The resonance parameters were thus obtained up to 1,836 eV for 62 levels, 27 of which were assigned as s-wave resonances.

The thermal capture cross section calculated from these parameters is 0.18 barns which is much smaller than the value of 2.2 barns recommended in BNL-325 3rd edition. The difference was corrected by the background cross section of $1/v$ type. The elastic scattering cross section was calculated with the effective scattering radius of 6.6 fm.

The statistical examination suggests that some levels might be missed in the energy range above 1,700 eV. Therefore the connecting energy was set at 1,660 eV.

The cross sections above 1,660 eV were calculated with the optical and statistical models. The γ-ray strength function was so adjusted that the calculated capture cross section reproduced the experimental data of Kapchigashev and Popov[56]. It was found, however, that the experimental data had a structure which could not be reproduced with the present model calculation. Finally the cross section was drawn with the eye-guide

* The numerical data of Hockenbury *et al.* were not published.

method below 10 keV.

The lowest 13 discrete levels were adopted up to 1.52 MeV and the levels were assumed to distribute continuously in the energy range above 1.54 MeV.

3.4.3 Discussion

The total, capture and inelastic scattering cross sections are compared with the other evaluated data as well as the experimental data in Figs. 3.4.1~3.4.3, respectively.

No experimental data are available for the total cross section, but the same tendencies as those in ^{95}Mo are observed among the various evaluated data: The ENDF/B-IV gives the lowest values, and the RCN-2 shows apparent discontinuity near 100 keV where the strength function model is connected to the optical model. The s-wave strength function of the RCN-2 evaluation is more than twice as large as that of the JENDL-1 evaluation and the recommended value in BNL-325 3rd edition as seen in TABLE 2.4.

As is evident in TABLE 2.9, there exists a large discrepancy between the thermal capture cross section calculated from the resonance parameters and the experimental data. To avoid this difficulty, the JENDL-1 and ENDF/B-IV evaluations adopted the $1/v$ background cross section, while the CNEN-2 and RCN-2 evalua-

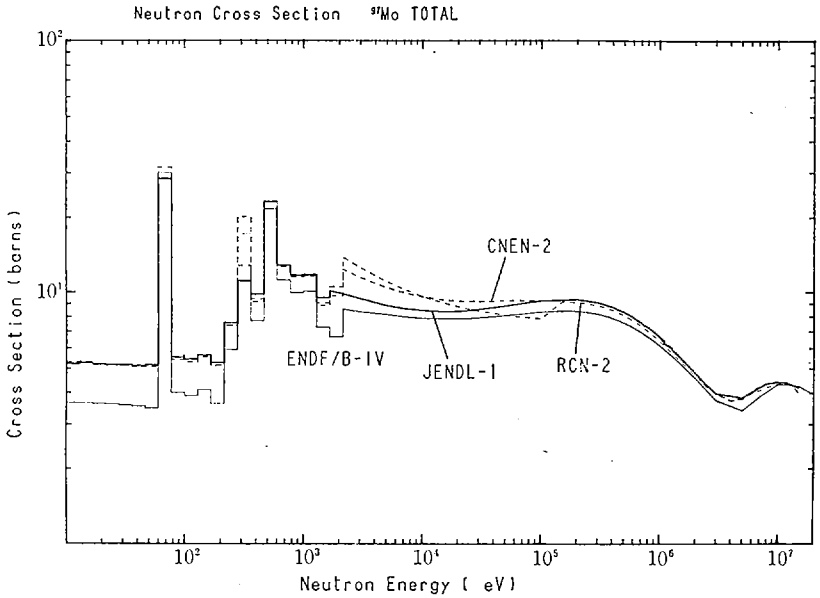

Fig. 3.4.1 Total cross sections of ^{97}Mo.

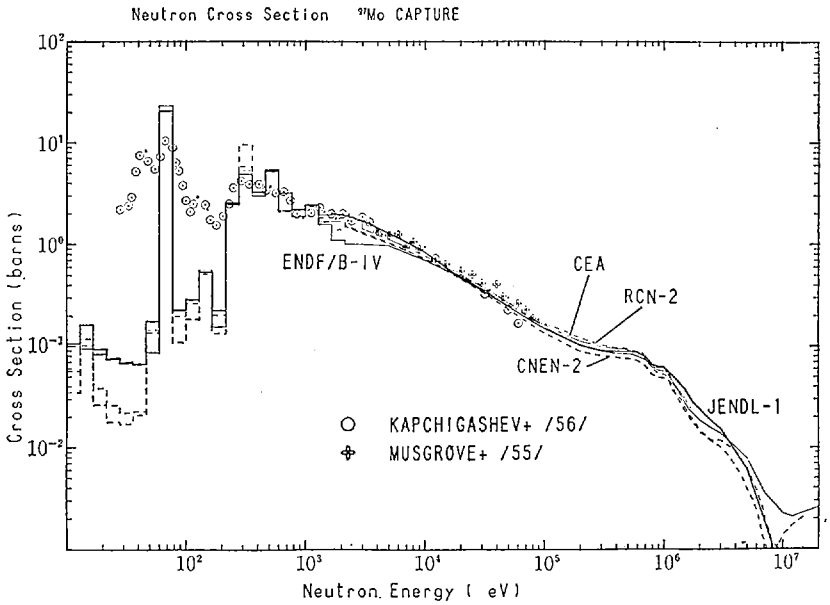

Fig. 3.4.2 Capture cross sections of ^{97}Mo.

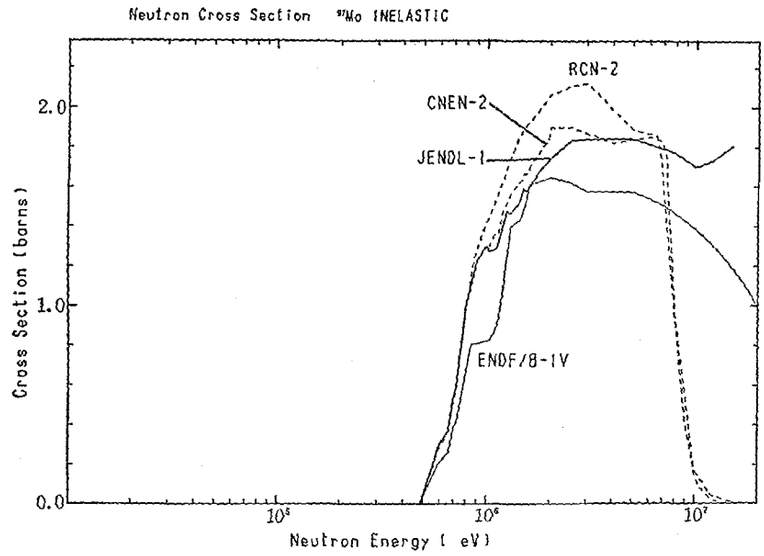

Fig. 3.4.3 Inelastic scattering cross sections of ^{97}Mo.

tions adjusted the calculated thermal cross section by assuming a negative resonance. For such a large difference, assumption of a negative resonance might be more reasonable. The capture resonance integral calculated from the resonance parameters and the background cross section is 17.1 barns in JENDL-1, which is slightly larger than the recommended value in BNL-325 3rd edition. It should be noted, however, that all the other evaluations give higher values than the BNL-325 recommendation whose experimental basis is not clear.

As pointed out in section 2.2.2, the optical and statistical model calculation could not reproduce the structure of the measured capture cross section of Kapchigashev and Popov[56] below 10 keV. The JENDL-1 evaluation adopted the eye-guide method below 10 keV, while the CNEN-2, RCN-2 and CEA evaluations extrapolated the model calculation and consequently gave the lower values than the measured ones. The ENDF/B-IV gives extremely low values below 20 keV whose energy dependence cannot be expected from the statistical model. Recent data of Musgrove *et al.*[55] agree with those of Kapchigashev and Popov below 20 keV but are a little higher above 20 keV, where most of the evaluated curves agree fairly well with the new data of Musgrove *et al.*

As for the inelastic scattering cross section, ENDF/B-IV gives the lowest values, RCN-2 gives the highest ones and the values of JENDL-1 and CNEN-2 lie in the middle agreeing fairly well with each other. The highest values in the RCN-2 evaluation may be attributed to its adopting 0.753, 0.795 and 0.993 MeV levels which were not taken in the other evaluations because of no exprimental evidence[46]. The lowest values of ENDF/B-IV may be caused by the adopted optical potential parameters which gives the lowest value also for the total cross section.

3.5 Technetium-99

3.5.1 Status of experimental data

The thermal capture cross section was measured by Pomerance[60] and by Tattersall *et al.*[52] BNL-325 3rd edition[29] recommends $\sigma_{n,\gamma}{}^{th}=19\pm2$ barns on the basis of the results by Pomerance. The resonance integral for absorption was reported to be 60 ± 20 barns by Tattersall *et al.* The total cross section at 0.0253 eV was measured by Hay and Pattenden[61] and by Watanabe and Reeder.[62]

The resonance parameters were deduced from the experiments on the total cross section by Pattenden[63] and by Watanabe and Reeder. Particularly Watanabe and Reeder gave the parameters for 12 levels from -6.4 eV to 280 eV by applying both the area and shape analyses. They calculated the capture resonance integral from their parameters and gave 340 ± 20 barns, which was adopted in BNL-325 3rd edition. On the other hand, Chou and Werle[64] gave the parameters of two low lying levels on the basis of their measurements on the capture cross section with a slowing-down time spectrometer. Discrepancies are considerably large

among the parameters obtained from the three experiments mentioned above. BNL-325 3rd edition recommends the parameters of 11 levels from 5.64 to 280 eV, on the basis of these three experiments and an experiment made at ORNL[65] whose numerical results have not yet been published. After the present evaluation, Adamchuk *et al.*[66] reported the parameters of 79 levels up to 1,144 eV. It was pointed out,[67] however, that some levels were missed in the data of Adamchuk *et al.*

At the time of the present evaluation, the only available experimental data of the smooth capture cross section were those measured by Chou and Werle up to 50 keV. After the present work, Little and Block[67] gave the capture cross section up to 80 keV. The total cross section was measured by Watanabe and Reeder in the energy range below 1 keV, by Harvey[68] from 2 eV to 130 keV and by Foster and Glasgow[70] from 2.5 MeV to 15 MeV.

3.5.2 Evaluation

The resonance parameters recommended in BNL-325 3rd edition were adopted in the present work, since it took account of all the available experimental data at the time of the evaluation. For the levels whose radiation width was not given in BNL-325, the value of 112 meV was assumed according to the analysis by Watanabe and Reeder.[62] A negative resonance deduced by Watanabe and Reeder with the shape analysis was not taken into account. All the eleven levels were assumed to be s-wave resonances.

The thermal capture cross section calculated from these resonance parameters is 17.7 barns which agrees with the recommended data of BNL-325 within the quoted error. The elastic scattering cross section was calculated with the effective scattering radius of 6.0 fm. From the statistical examination mentioned in section 2.4, no levels seemed to be missing. The connecting energy was set at 290 eV by adding nearly $D_{obs}/2$ to the highest resonance energy of 280 eV.

The cross sections were calculated with the optical and statistical models in the energy range above 290 eV. Fourteen discrete levels were taken into consideration up to 1.199 MeV, and the levels were assumed to be overlapping above the energy of 1.21 MeV. The γ-ray strength function was adjusted so that the calculated capture cross section might reproduce the experimental data of Chou and Werle[64]. From the γ-ray strength function thus determined, we obtained the mean level spacing of 16.2 eV which agrees with the value obtained from the resolved resonances, if we assume $\Gamma_\gamma = 112$ meV. As described in section 2.2.2, the calculated cross section could not reproduce the structure in the measured data of Chou and Werle below 3 keV. The present cross section was obtained by the eye-guide method in this energy range.

3.5.3 Discussion

The total, capture and inelastic scattering cross sections are shown in **Figs. 3.5.1~3.5.3** with the experi-

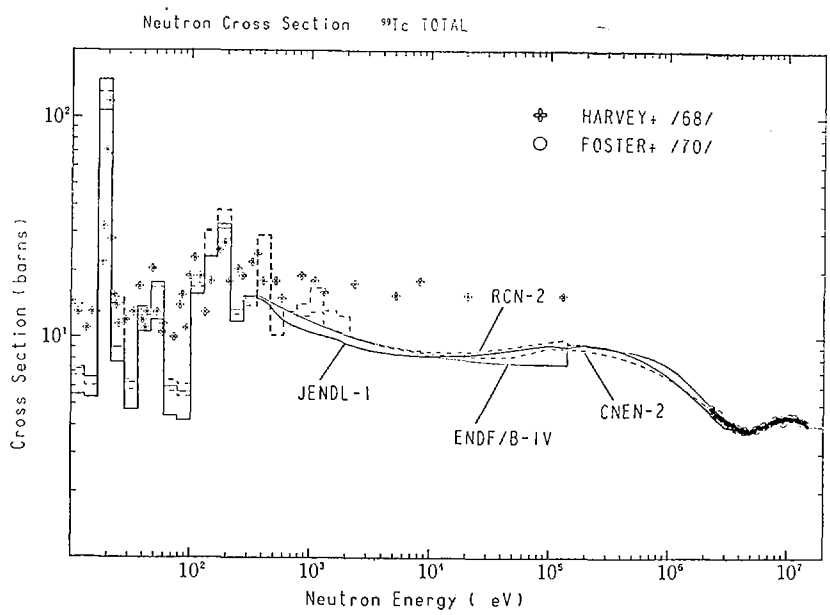

Fig. 3.5.1 Total cross sections of ^{99}Tc.

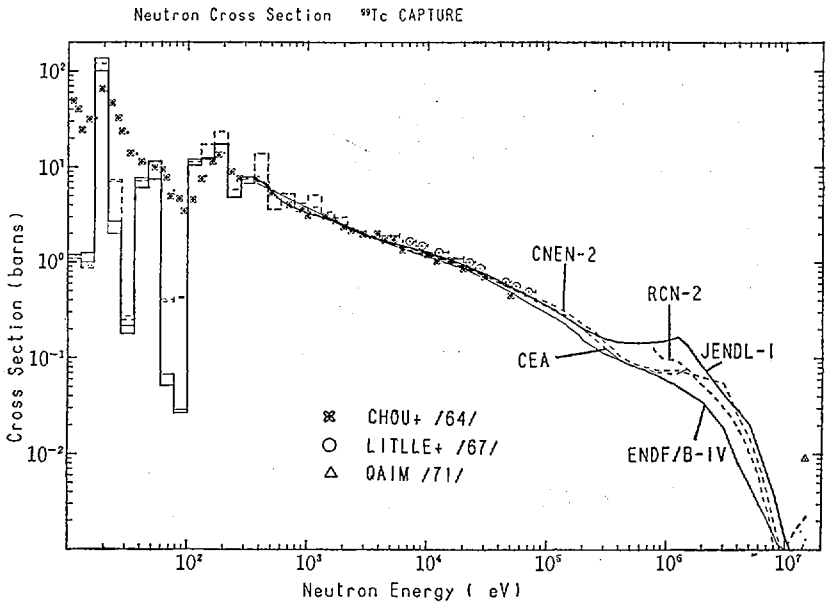

Fig. 3.5.2 Capture cross sections of ^{99}Tc.

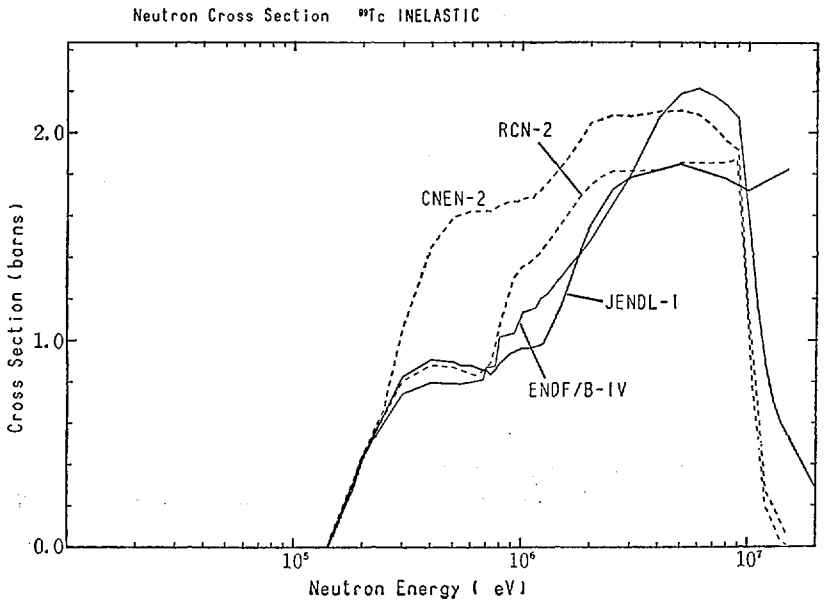

Fig. 3.5.3 Inelastic scattering cross sections of ^{99}Tc.

mental data and with the other evaluated data. As seen in TABLE 2.8, much more resonance levels were adopted in RCN-2 and CNEN-2.

The total cross sections of all the evaluations reproduce fairly well the measured data of Foster and Glasgow[70] above 2 MeV, while they cannot at all reproduce the measured data of Harvey below 100 keV. The data of ENDF/B-IV show apparent discontinuity at 141 keV where the cross section calculated from the unresolved resonance parameters is connected to the smooth cross section. The RCN-2 evaluation adopted the same optical potential parameters as JENDL-1.

The calculated thermal capture cross sections in all the evaluations fall within the uncertainty of the measured data as seen in TABLE 2.9. The JENDL-1 evaluation adopted no background cross section, while the RCN-2 and CEA evaluations adopted a small $1/v$ correction, and the ENDF/B-IV and CNEN-2 evaluations took a negative resonance. The capture cross sections of all the evaluations well reproduce the data of Chou and Werle[64] below 80 keV. However, recent measurements by Little and Block[67] give a little higher values than all the evaluations. The evaluated cross sections deviate from one another above a few hundred keV. This is partly due to the difference in the inelastic scattering cross section as will be mentioned later.

As pointed out by Gruppelaar *et al.*[21], the calculated inelastic scattering cross section is sensitive to the

adopted level scheme of the target nucleus in the case of ^{99}Tc, because the ground state spin is high ($9/2^+$) and therefore the inelastic transfer is limited to states of high spin. As is seen in TABLE 2.12.5, the level scheme adopted in JENDL-1 has few high spin states up to 1.2 MeV. Hence the inelastic scattering is restrained and the capture is enhanced. On the other hand, the CEA and CNEN-2 evaluations adopted two hypothetical high spin states at 250 and 350 keV: this probably makes the inelastic scattering cross section twice as large as the other evaluated data and decreases the capture cross section above 250 keV. The RCN-2 evaluation has two more high spin states than JENDL-1 above 750 keV. This level scheme might explain the rapid increase in inelastic scattering cross section and abrupt decrease in capture cross section of the RCN-2 data. It should be noted, however, that the revised level scheme by Matsumoto *et al.*[46] becomes very analogous to that of RCN-2. Hence the same tendency is expected, if this revised level scheme is used.

3.6 Ruthenium-101

3.6.1 Status of experimental data

The thermal capture cross section and the capture resonance integral were measured twice by Halperin *et al.*[72,73] BNL-325 recommends $\sigma_{n,\gamma}{}^{th}=3.1\pm0.9$ barns and R.I.$=85\pm12$ barns on the basis of their old data[72] in both 2nd[33] and 3rd[29] editions, though their new data[73] are $\sigma_{n,\gamma}{}^{th}=5.23$ barns and R.I.$=79.1$ barns, respectively.

BNL-325 2nd edition recommended the resonance parameters of 11 levels up to 460 eV on the basis of measurements made till 1965. Since then Coceva *et al.*[74] made the isotope and spin assignment for Ru resonances up to 560 eV with their capture γ-ray measurements, and Priesmeyer and Jung[75] deduced the neutron widths to 22 resonances up to 670 eV from their transmission measurements. The recommendation in BNL-325 3rd edition is mainly based on these two measurements. After its release, Macklin and Halperin[76] gave the $g\Gamma_n\Gamma_\gamma/\Gamma$ values from 2,650 to 4,500 eV.

At the time of the present evaluation, no experimental data were available above resonance region. Recently, however, the capture cross section was measured by Hockenbury *et al.*[77] between 20 eV and 150 keV and Macklin and Halperin[76] between 3 and 700 keV.

3.6.2 Evaluation

The resonance parameters deduced by Priesmeyer and Jung[75] were mainly adopted* for 22 levels up to 670 eV. For the levels whose radiation width was not given explicitly by Priesmeyer and Jung, the value of 165 meV was adopted, which was assumed by them in deducing the neutron widths. However, for the 52.3 eV level we adopted the recommended value of 190 meV in BNL-325 2nd edition. The connecting energy was set at 700 eV, as the statistical examination showed no level missing.

The thermal capture cross section calculated from these resonance parameters is 3.34 barns which agrees well with the recommended value of 3.1 ± 0.9 barns in BNL-325 but is smaller than the new experimental value of Halperin *et al.*[73] However, no background correction were made for this nuclide. The elastic scattering cross section was calculated with the effective radius of 6.65 fm.

The cross sections were calculated with the optical and statistical models in the energy range between 700 eV and 15 MeV. Fourteen discrete levels were adopted up to 1.0011 MeV and the levels were treated as continuum above 1.05 MeV. The γ-ray strength function was determined from the values of neighboring nuclides.

3.6.3 Discussion

The total, capture, and inelastic scattering cross sections of the JENDL-1 evaluation are shown in **Figs. 3.6.1~3.6.3** with the other evaluated data and the experimental data. The ENDF/B-IV evaluation adopted the resonance parameters up to 112.5 eV, while the other evaluations took the parameters up to 670 eV.

The total cross section of ENDF/B-IV is smaller than the others in all the energy range. The RCN-2 and CNEN-2 evaluations give higher values in the low energy region where they use the strength function

* The resonance energies were taken from their preliminary report[78].

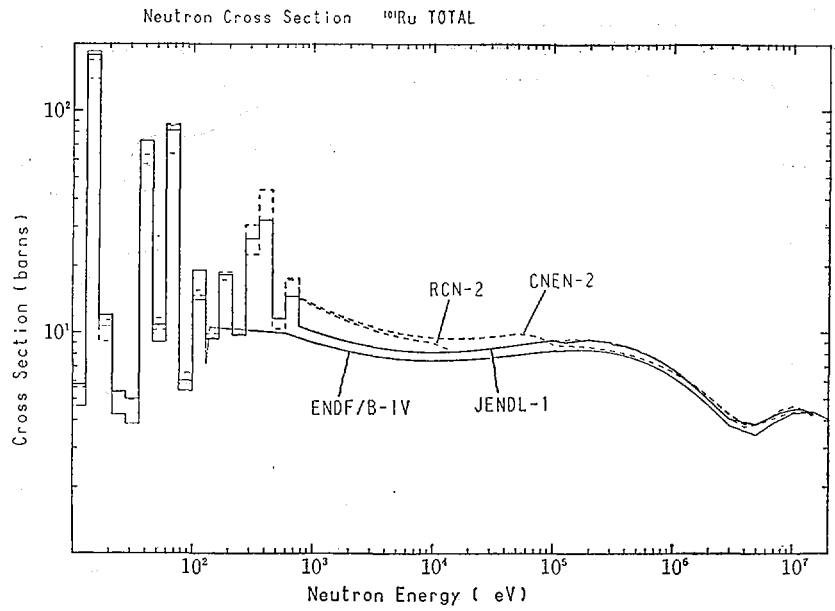

Fig. 3.6.1 Total cross sections of ^{101}Ru.

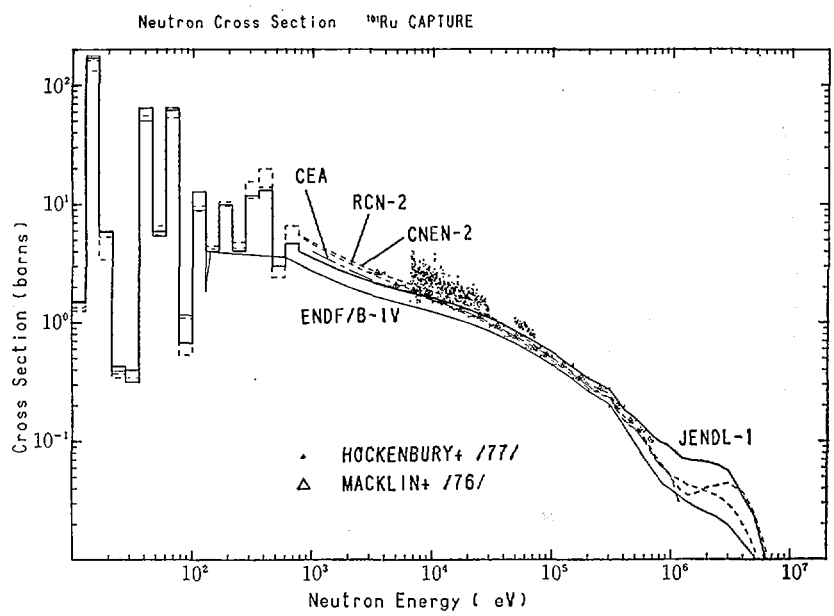

Fig. 3.6.2 Capture cross sections of ^{101}Ru.

model and the unresolved resonance representation, respectively. The RCN-2 evaluation adopted the same optical potential as JENDL-1.

In all the evaluations, the thermal capture cross sections calculated from the resonance parameters are a little smaller than the newly measured datum of Halperin *et al.*[73], though they agree with their old value[72]. However, the quality of the new measurement of Halperin *et al.* is not clear due to lack of their error assignment. The calculated capture resonance integrals are a little higher than the measured ones in all the evaluations.

All the evaluations of capture cross section are based on the theoretical calculation above the resonance region, since no experimental capture data were available at the times of each evaluation. Nevertheless the calculated cross sections agree fairly well with the recent measurements except those of ENDF/B-IV which are considerably lower in all the energy region. Particularly the data of RCN-2 and CNEN-2 agree very well with the data of Macklin ard Halperin[76], while those of JENDL-1 are a little lower in the energy region below 10 keV and a little higher above a few hundred keV. On the other hand, the data of Hockenbury *et al.*[77] are a little higher than all the evaluated values. The cross section of JENDL-1 is the highest in the energy region above 50 keV among all the evaluated data. This is partly caused by the competition with its

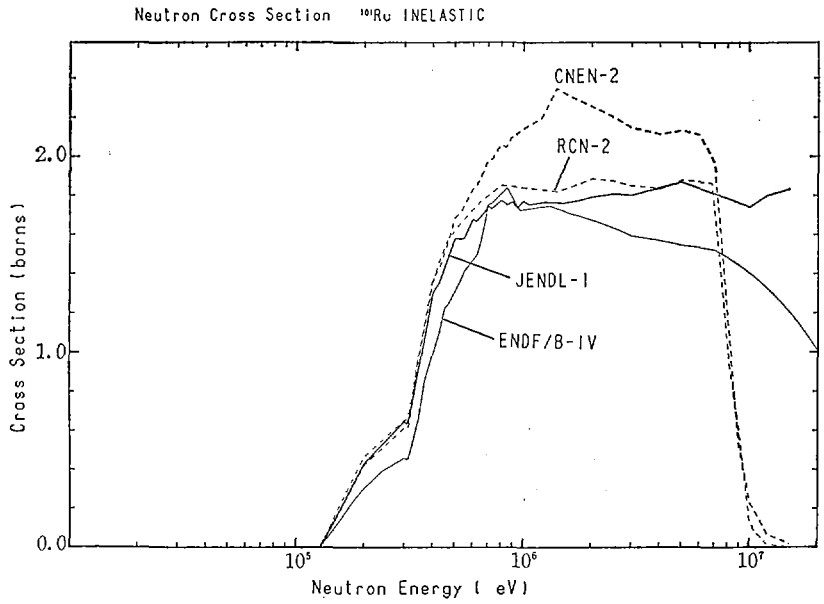

Fig. 3.6.3 Inelastic scattering cross sections of ^{101}Ru.

rather small inelastic scattering cross section which will be discussed later. An obvious dip observed in the CNEN-2 evaluation near 1 MeV may be also attributed to the competition with the inelastic scattering. In the JENDL-1 evaluation, the adopted γ-ray strength function shown in TABLE 2.5 gives smaller value of D_{obs} than that obtained from the resolved resonances, if we assume $\Gamma_\gamma = 165$ meV.

As to the inelastic scattering cross section, the data of JENDL-1 are smaller than those of RCN-2 and CNEN-2 above 300 keV. This is probably caused by our omitting some discrete levels such as 0.3441, 0.4623, 0.6235 and 0.6432 MeV levels and by our adopting a lower value of level density parameter "a" as seen in TABLE 2.12.6 and 2.6, respectively. The large value of the CNEN-2 evaluation may be partly attributed to its adopting 9 hypothetical levels between 700 keV and 1 MeV. The lowest value of ENDF/B-IV may be caused by the adopted optical potential which gives the lower total cross section than the other evaluated data. It should be noted that Matsumoto *et al.*[46] recently revised the level scheme adopted in JENDL-1 by adding the above mentioned levels which were already adopted in the other evaluations. With these revised level scheme, it is expected that the inelastic scattering cross section of JENDL-1 will be a little increased above 300 keV, and the capture cross section will be decreased.

3.7 Ruthenium-102

3.7.1 Status of experimental data

The thermal capture cross section was measured by Katcoff and Williams[79], by Lantz[80] and by Ishikawa[81]. The measured values scatter between 1.23 and 1.50 barns. BNL-325 3rd edition[29] recommends 1.30±0.15 barns on the basis of these measurements. The capture resonance integral was measured by Lantz, by Ricabarra *et al.*[82] and by Van der Linden *et al.*[83] Their results agree with one another within the quoted errors. BNL-325 3rd edition recommends 4.1±0.4 barns.

As to the resonance parameters, BNL-325 2nd edition[33] recommended the parameters of only one level at 200 eV on the basis of the measurements by Bolotin and Chrien[84]. Recently, however, Priesmeyer and Jung[75] pointed out that this level belonged to ^{101}Ru, and they gave the neutron widths to three new levels at 165.3, 415.2 and 1,296 eV. BNL-325 3rd edition recommends their parameters. After its publication, Macklin and Halperin[76] gave the resonance parameters in the energy range from 2.66 to 12 keV.

The capture cross section was measured at 24 keV by Macklin *et al.*[85] and by Murty *et al.*[86], and at 190 keV by Lyon and Macklin[87] at the time of the evaluation. Recently Hockenbury *et al.*[77] measured the capture cross section between 20 eV and 150 keV and Macklin and Halperin[76] between 3 and 600 keV. No experimental data are available on the elastic and inelastic scattering cross sections.

3.7.2 Evaluation

The neutron widths obtained by Priesmeyer and Jung[75] were adopted for the three resonances with assuming $\Gamma_\gamma = 165$ meV, which was assumed by Priesmeyer and Jung in their deducing the neutron widths. All the three levels were assumed to be s-wave resonances.

The thermal capture cross section calculated from these parameters becomes 0.0104 barns which is much smaller than the smallest measured value of Lantz[80]. We assumed the value of 1.3 barns according to BNL-325 3rd edition and corrected the difference by applying the $1/v$ type background cross section. The thermal elastic scattering cross section was calculated with the effective radius of 6.6 fm.

The resonance cross section was calculated up to 1,450 eV corresponding to $E_{max} + D_{obs}/2$, where the mean level spacing D_{obs} was obtained in the statistical model calculation as described below.

The cross sections were calculated with the optical and statistical models in the energy range above 1,450 eV. Thirteen discrete levels were considered up to 2.37 MeV and levels were assumed to be overlapping above 2.4 MeV. It was found that the energy dependence of the calculated capture cross section was considerably different from that of the measured data at the time of the evaluation as shown in **Fig. 3.7.2**. Hence we took the data of Macklin *et al.*[85] and of Murty *et al.*[86] at 24 keV, which agree with each other, but abandoned the datum of Lyon and Macklin[87] at 190 keV. The γ-ray strength function was so determined that the calculated capture cross section became 350 millibarns at 24 keV. From the γ-ray strength function thus obtained, the mean level spacing was deduced to be 290.5 eV with assuming $\Gamma_\gamma = 165$ meV.

3.7.3 Discussion

The total, capture and inelastic scattering cross sections are compared with the other evaluated data and the experimental data in **Figs. 3.7.1～3.7.3**, respectively.

As to the total cross section, the JENDL-1 and RCN-2 evaluations, which used the same optical potential parameters, give the highest values, while the ENDF/B-IV evaluation gives the lowest value. The cross section of CNEN-2 is as low as that of ENDF/B-IV in the unresolved resonance region below 50 keV and becomes as high as that of JENDL-1 above 1 MeV. The smaller value of ENDF/B-IV in the resonance region is evidently caused by its smaller effective scattering radius as shown in **TABLE 2.7**.

The thermal capture cross section calculated with the resonance parameters is less than 1/100 of the measured value as seen in **TABLE 2.9**. Such a large discrepancy may be more reasonably explained by ignorance of negative resonances, though all the evaluations except CNEN-2 apply the $1/v$ background cross section. The capture resonance integral calculated from the resonance parameters and the background cross section agrees witn the measured data within quoted errors. In the energy region above 2 keV, all the evaluations seem to rely on the measured data of Macklin *et al.*[85] and of Murty *et al.*[86] at 24 keV and to abandon the data of

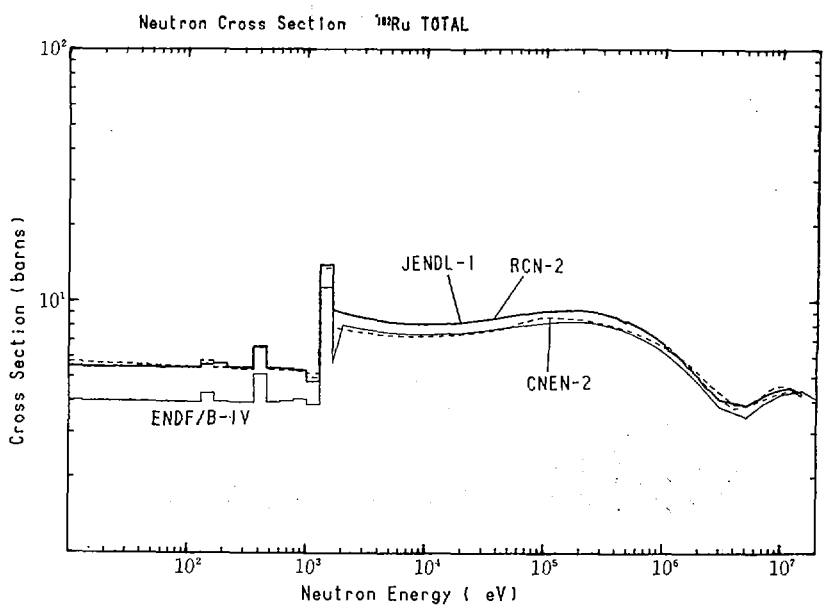

Fig. 3.7.1 Total cross sections of ^{102}Ru.

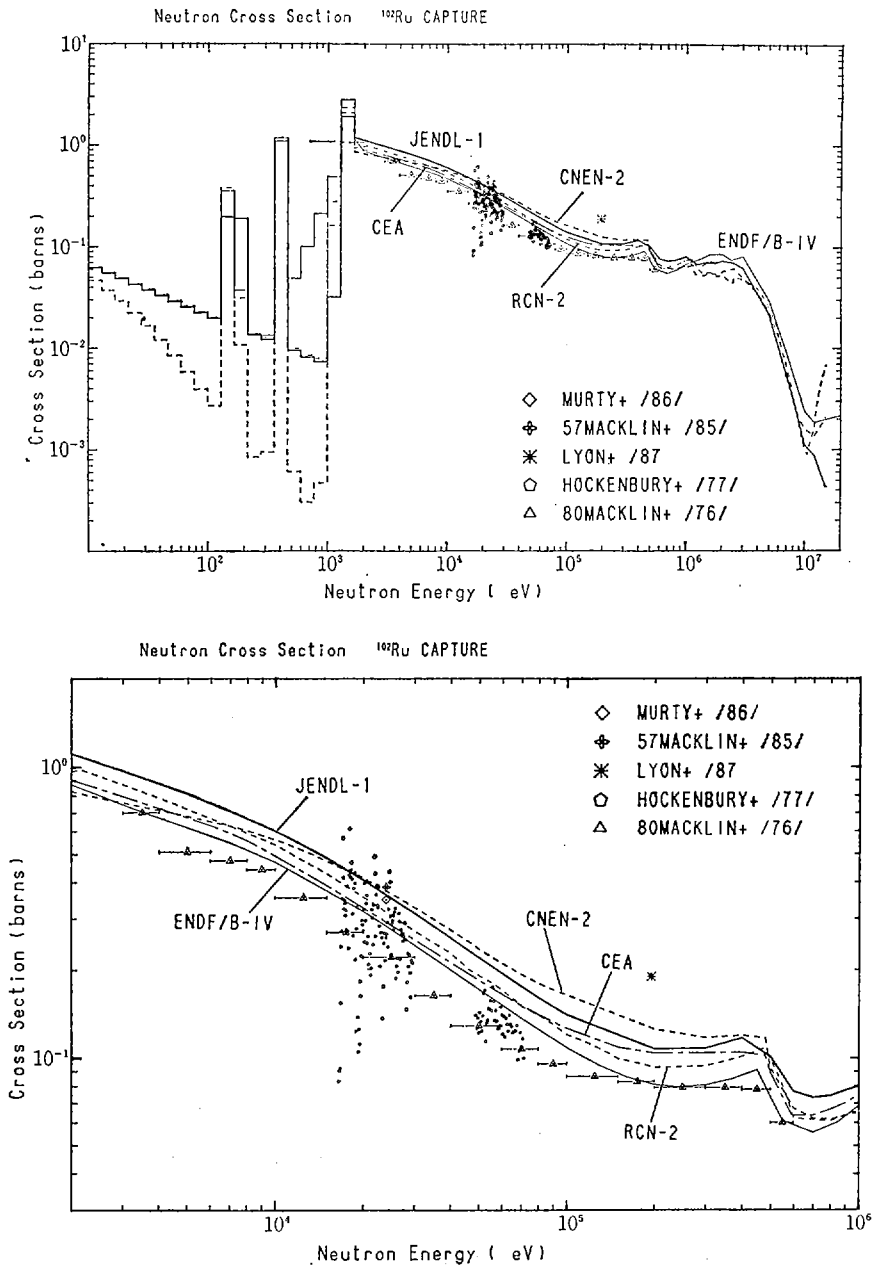

Fig. 3.7.2 Capture cross sections of ^{102}Ru.

Lyon and Macklin[87] at 190 keV. However, recent measurements by Hockenbury *et al.*[77] and by Macklin and Halperin[76] give lower values than the evaluated curves: The data of JENDL-1 are about 30% larger than those of Macklin and Halperin. These new measurements should be considered in future work. Above 1 MeV the data of ENDF/B-IV are the largest and those of CNEN-2 the smallest. This is probably due to the competition with the inelastic scattering process.

As to the inelastic scattering cross section, ENDF/B-IV gives the smallest values, CNEN-2 the largest, and the values of JENDL-1 and RCN-2 lie between these two extreme values. The difference might be mostly caused by the difference of the optical potential as seen in the total cross section, since little discrepancies are observed in the level scheme shown in TABLE 2.12.7.

3.8 Rhodium-103

3.8.1 Status of experimental data

Experimental data are numerous for this nuclide. The thermal capture cross sections were measured by several experiments for production of 4.35 min ^{104m}Rh and 42 sec ^{104g}Rh. BNL-325 recommends $\sigma_{n,\gamma}{}^{th}=150$

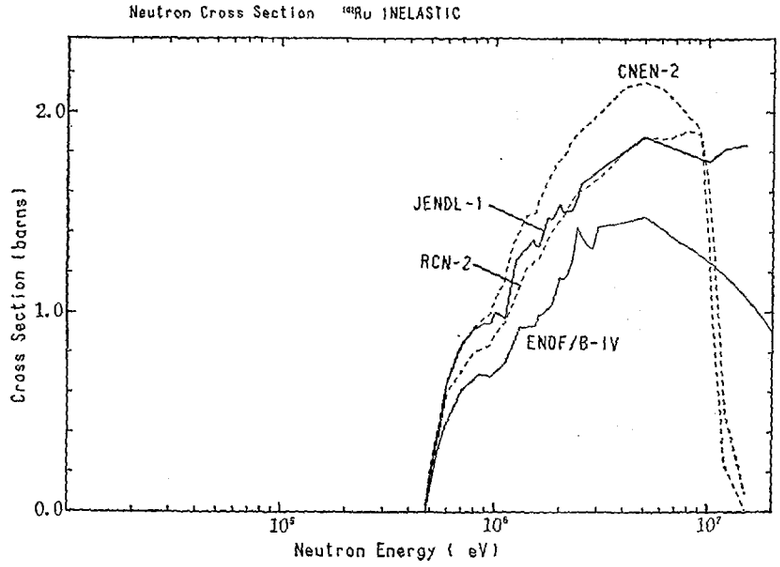

Fig. 3.7.3 Inelastic scattering cross sections of ^{102}Ru.

± 5 barns [$\sigma_{n,\gamma}{}^{th}(^{104m}Rh)=11\pm1$ barns and $\sigma_{n,\gamma}{}^{th}(^{104g}Rh)=139\pm7$ barns] in both 2nd[33] and 3rd[29] editions. After its 3rd edition was published, Dilg and Mannhart[88] deduced $\sigma_{n,\gamma}{}^{th}=144.8\pm0.5$ barns from their measurements of the total cross section with the ultracold TOF spectrometer. The total cross section in the thermal energy region is also given by Dilg and Mannhart $\sigma_T(E)=(22.17\pm0.10)/\sqrt{E}$ (ev)$+1.3$ barns.

The resonance capture integral has been measured since 1950. Walker and Copley[89] gave R. I.(^{104m}Rh) $=81\pm8$ barns and R. I.(^{104g}Rh)$=1,094\pm60$ barns, and Köhler and Schneider[90] R. I.(^{104m}Rh)$=78\pm7$ barns and R. I.(^{104g}Rh)$=1,054\pm74$ barns. BNL-325 3rd edition recommends R. I.$=1,100\pm50$ barns. Recently, however, Hüttel[91] and Van der Linden *et al.*[83] reported R. I.(^{104m}Rh)$=610\sim650$ barns, which is not consistent with the old measurements.

As to the resonance parameters, BNL-325 2nd edition recommended the values for 47 levels up to 1,270 eV on the basis of measurements before 1967. In 1969 Ribon *et al.*[92] deduced the parameters for 273 levels up to 4,140 eV. Taking account of these new data, BNL-325 3rd edition recommends the parameters for 276 resonances. After BNL-325 3rd edition was published, Carlson and Fricke[93] and Haste and Thomas[94] made spin assignments, and Macklein and Halperin[76] gave the resonance parameters between 2,644 and 4,263 eV.

The measured capture data cover almost all the energy range above resolved resonances. The ratio of ^{104m}Rh production to ^{104}Rhg production cross sections were also measured. The measured data agree fairly well with one another except near 14.5 MeV, where the discrepancy of a factor of 20 was reported among the measured data as seen in Fig. 3.8.2. The total cross section was measured by several experimenters below 600 keV and above 2.6 MeV, but the measured data show the discrepancy of 10% below 600 keV. As to the inelastic scattering, the differential cross section and ^{103m}Rh production cross section have been measured, but the measurements of the excitation function of total inelastic scattering have not so far been reported except the cross section at 6 MeV measured by Wilenzick *et at.*[95]

3.8.2 Evaluation

The resonance parameters were taken from the recommended values in BNL-325 3rd edition. For the levels whose radiation width was not given, it was assumed to be 164 meV for s-wave resonances and 159 meV for p-wave ones, according to the evaluation by Zakharova *et al.*[96] The s- and p-wave assignment was made with the method described in section 2.3.1. Thus 87 levels were assigned as s-wave resonances and 188 levels as p-wave ones.

The thermal capture cross section calculated from these parameters is 146 barns which agrees with the recommended value of BNL-325 within the quoted error. Hence no background correction was applied. The effective scattering radius of 6.56 fm was taken from the recommendation of BNL-325. The statistical examination suggested that levels were missing above 3.6 keV, and the connecting energy was set at 3.6 keV.

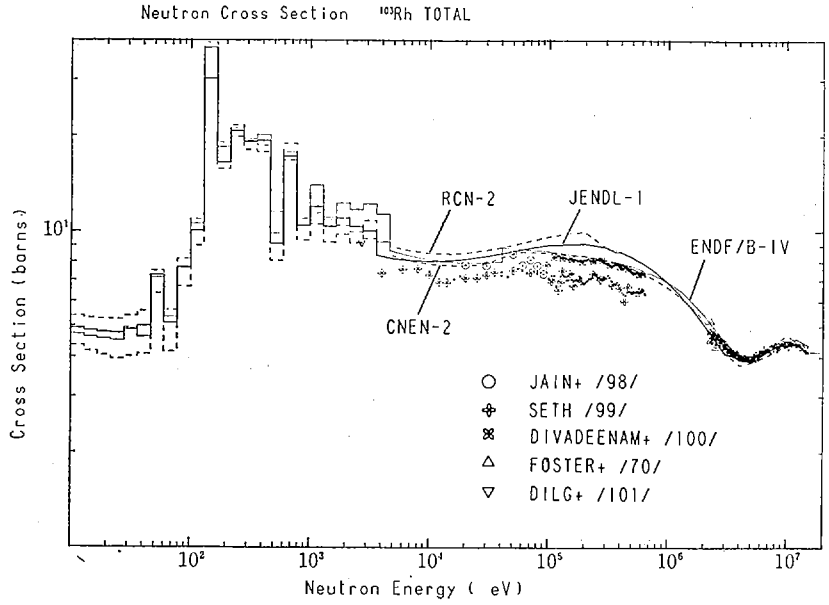

Fig. 3.8.1 Total cross sections of ^{103}Rh.

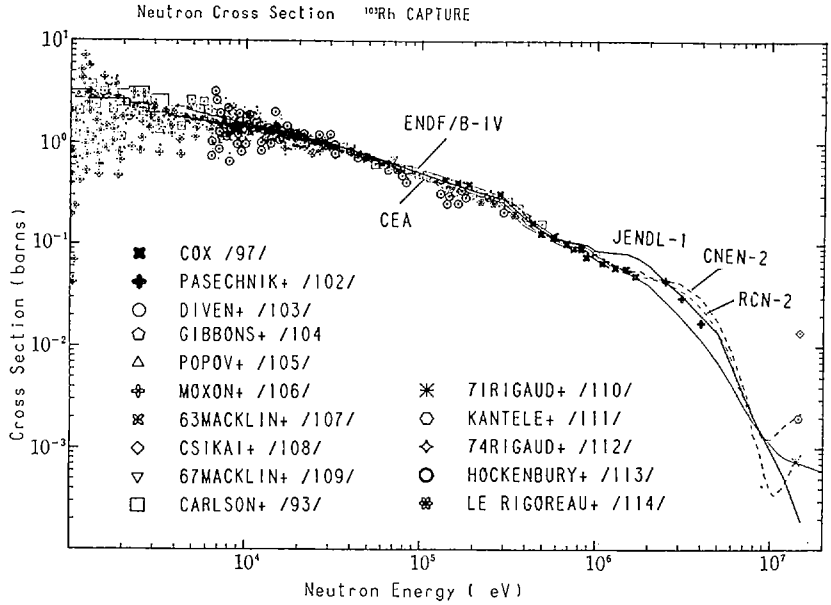

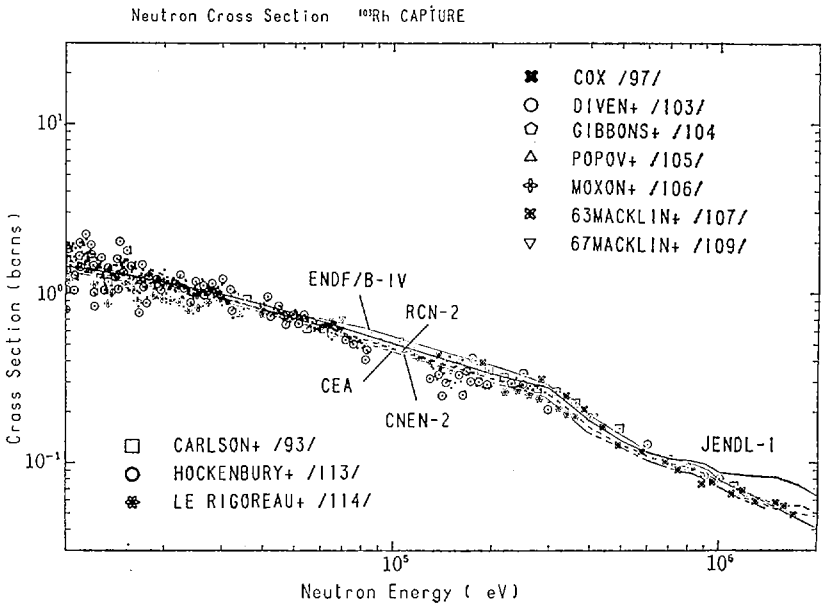

Fig. 3.8.2 Capture cross sections of ^{103}Rh.

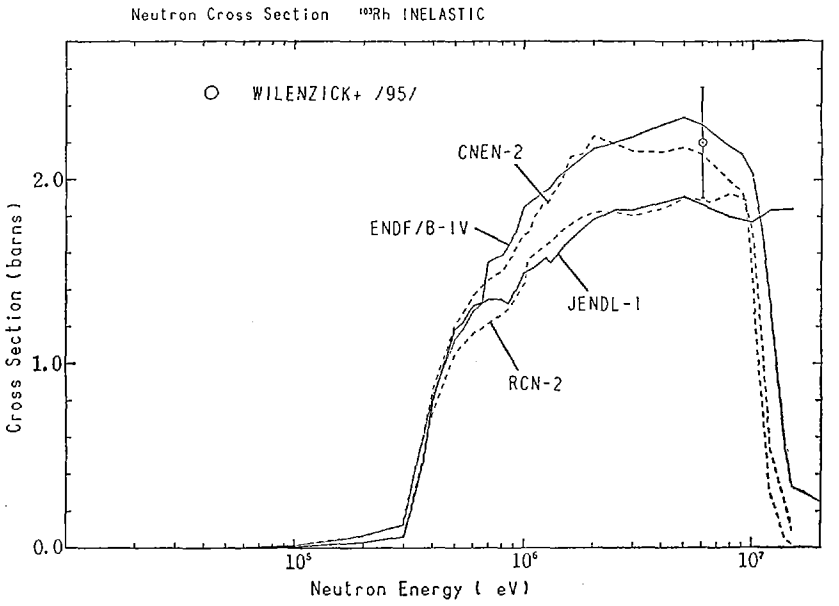

Fig. 3.8.3 Inelastic scattering cross sections of ^{103}Rh.

The cross sections were calculated with the optical and statistical models in the energy range above 3.6 keV. The γ-ray strength function was determined so that the calculated value at 140 keV might be 0.44 barns based on the measurements of Cox[97]. Fourteen discrete levels were adopted and levels were assumed to be overlapping above 1.3 MeV.

3.8.3 Discussion

The total, capture and inelastic scattering cross sections are shown with the other evaluated data as well as the selected measured data in **Figs. 3.8.1~3.8.3**, respectively.

The total cross sections of JENDL-1 and RCN-2 are larger than the measured data by 10~20% between 50 keV and 1 MeV, while those of CNEN-2 and ENDF/B-IV agree with the data of Divadeenam[100] which are higher than those of Seth[99].

The capture resonance integral calculated from the resonance parameters is 1,034 barns which is a little smaller than the recommended value of BNL-325. In the energy region between 10 keV and 1 MeV the evaluated capture cross sections agree with each other within scatters of the measured data. The mean level spacing D_{obs} falls between 16 and 35 eV in the various evaluations, when it is deduced from the γ-ray strength function used in the statistical model calculation and the radiation width assumed in the resolved resonances. These values are much larger than the recommended value $D_{obs}=12\pm1$ eV in BNL-325. However we suspect that the recommeded value of BNL-325 may be too small, because all the levels seem to be assumed as s-wave ones. If the present s- and p-wave assigenments are assumed, the mean level spacing becomes 47.5 eV. Therefore we conclude that the value of 16~35 eV is reasonable, taking in into account that the present s- and p-wave assigenments may assume too many p-wave resonamces in spite of their larger probability of missing. The discrepancy of capture cross section above 1 MeV may be partly due to difference in the inelastic scattering cross section.

As to the inelastic scattering, the cross sections of JENDL-1 and RCN-2 are lower than those of ENDF/B-IV and CNEN-2 which agree with the measured datum of Wilenzik *et al.*[95] at 6 MeV. The energy dependence of the JENDL-1 cross section is different from the others above 500 keV. This is due to difference in the level scheme as seen in **Table 2.12.8.** Recently Matsumoto *et al.*[46] revised the level scheme. It was reported[22] that the inelastic scattering cross section is increased by 4% at 1 MeV with this new level scheme.

3.9 Rethenium-104

3.9.1 Status of experimental data

Two experiments[115,116] have been reported on the thermal activation cross section and the resonance integral.

BNL-325 adopted $\sigma_{n,\gamma}{}^{th}=0.47\pm0.20$ barns and R. I.=4.6 barns in both 2nd[33] and 3rd[29] editions on the basis of the experimental data of Lantz.[116]

The resonance parameters were measured by Priesmeyer and Jung[75] with the natural and isotopic Ru samples. They reported the resonance parameters for 4 levels up to the energy of 1,055 eV on the basis of isotope assignment of resonances by Coceva *et al.*[74] BNL-325 3rd edition adopted these parameters with modifying the resonance energies on the basis of the data of Coceva *et al.* After its release, Macklin and Halperin[76] gave the resonance parameters between 2.66 and 12 keV.

The capture cross section had been measured by 7 authors at 4 energy points by the time of the present work. Evident discrepancy is observed at 24.5 keV as shown in **Fig. 3.9.2**: One trend is represented by higher values of Macklin *et al.*[85] and of Murty *et al.*[86], and the other by lower value of Chaubey and Sehgal.[117] After the present evaluation, data of Anand *et al.*[118], of Hockenbury *et al.*[77] and of Macklin and Halperin[76] became available. All of them support the higher value at 24.5 keV. No available experimental data exist for other cross sections except for the $(n, 2n)$ reaction cross section near 14 MeV.

3.9.2 Evaluation

The resonance parameters reported by Priesmeyer and Jung[75] were adopted* with $\Gamma_\gamma=165$ meV which was assumed by them in deducing the neutron widths. The thermal capture cross section calculated from these parameters is 0.111 barns, which is smaller than the value recommended in BNL-325 2nd and 3rd editions. The difference was corrected by applying the $1/v$ type background cross section. The thermal elastic scattering cross section was also calculated from these parameters with the effective scattering radius of 6.6843 fm. The connecting energy point with the smooth cross sections was set at 1,290 eV which is higher than the highest resonance energy by nearly a half of mean level spacing used in the statistical model calculations.

The cross sections were calculated in the energy region above 1.29 keV with the statistical and optical models. The γ-ray strength function was adjusted so that the calculated capture cross section might reproduce the experimental data of Murty *et al.*[86] at 24.5 keV. The lower value reported by Chaubey and Sehgal[117] was abandoned. Four discrete levels were taken into account up to 0.983 MeV and the levels were assumed to be continuum above 1.1 MeV.

3.9.3 Discussion

The total, capture and inelastic scattering cross sections are shown with the measured and the other evaluated data in **Figs. 3.9.1~3.9.3**, respectively.

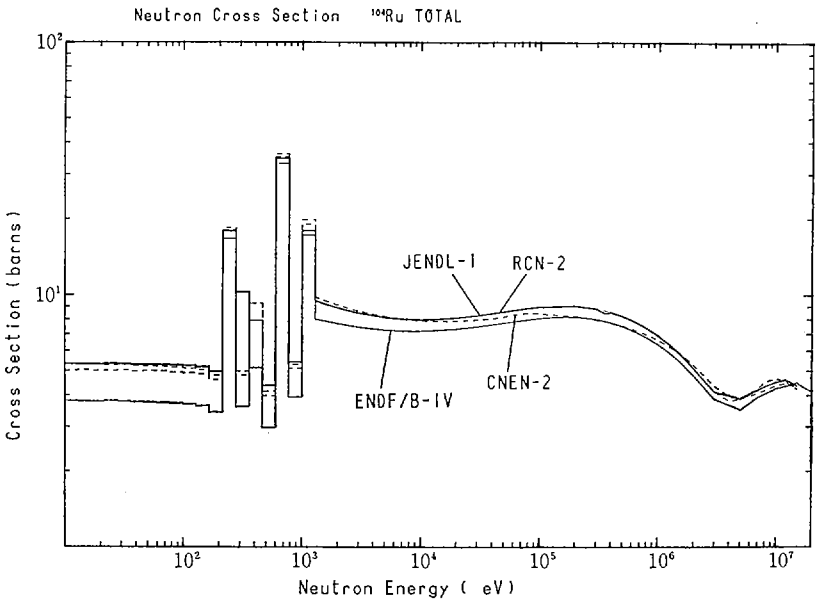

Fig. 3.9.1 Total cross sections of ^{104}Ru.

* The resonance energies were taken from their preliminary report[78].

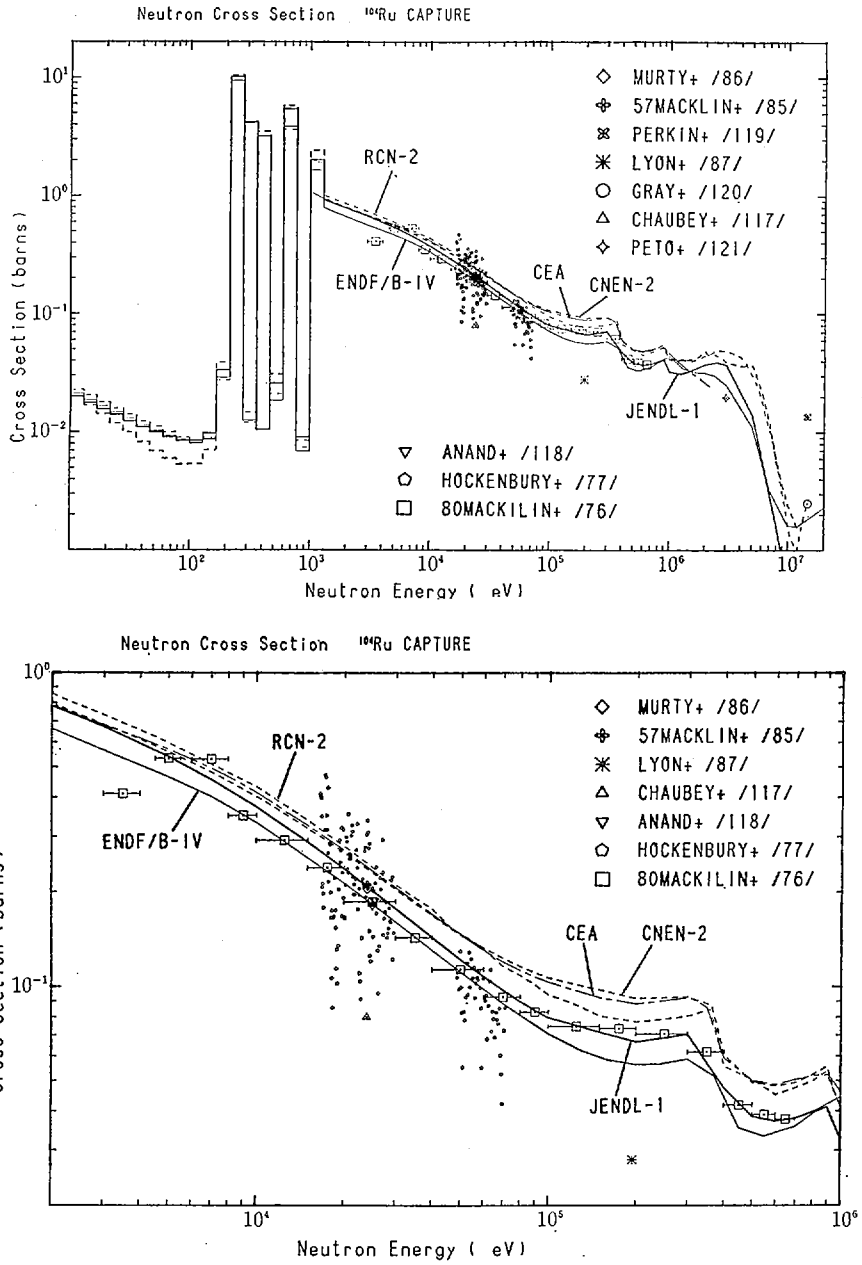

Fig. 3.9.2 Capture cross sections of ^{104}Ru.

As to the total cross section in the energy region above 1.5 keV, the values of JENDL-1 and RCN-2, which were calculated with the same optical potential parameters, are the highest, the ENDF/B-IV evaluation gives the lowest value and the curve of CNEN-2 lies between the two extremes. The lowest value of ENDF/B-IV below 200 eV is evidently caused by their adopting a smaller effective scattering radius.

The thermal capture cross section becomes much smaller than the experimental values as seen in TABLE 2.9, when it is calculated from the resolved resonance parameters. All the evaluations except CNEN-2 applied the $1/v$ type background cross section, though such a large discrepancy may be caused by ignoring negative resonances. The calculated values of capture resonance integral are considerably larger than the measured ones for all the evaluations. More precise measurements are required for the resonance parameters of this nuclide.

In the energy region above resolved resonances, the evaluated cross sections are considerably discrepant among themselves. The data of JENDL-1 excellently reproduce the recent experimental data of Macklin and Halperin[76] which were not available at the time of the present evaluation. The data of RCN-2, CNEN-2 and CEA take a little higher values and those of ENDF/B-IV lower value than those of JENDL-1. All the evaluations abondoned the datum of Chaubey and Sehgal.[117] None of the evaluated data can reproduce the measured data of Lyon and Macklin[87] at 195 keV. In MeV region, the lowest value of ENDF/B-IV agree

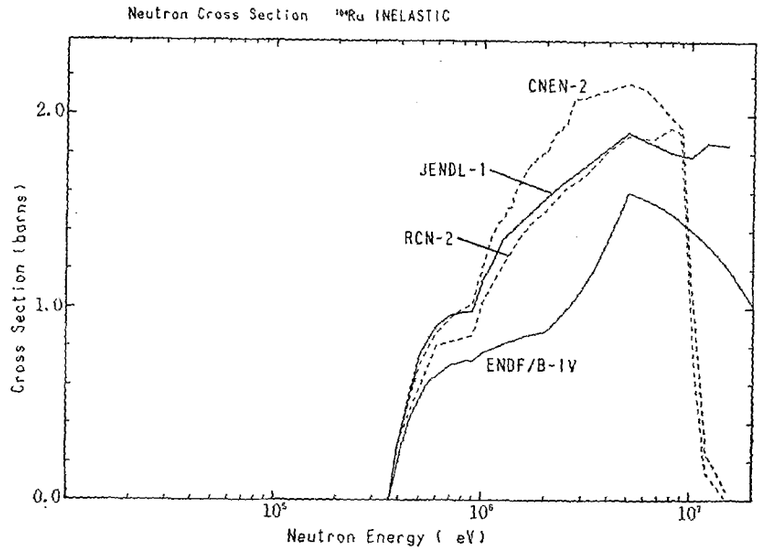

Fig. 3.9.3 Inelastic scattering cross sections of ^{104}Ru.

with the measured datum of Petö *et al.*[121] within its quoted error, while all the other evaluations give considerably higher values.

In the present JENDL-1 evaluation, the mean level spacing becames 588 eV from the value of the γ-ray strength function used in the statistical calculation, if we take $\Gamma_\gamma = 165$ meV. This value of the mean level spacing is about twice as large as that expected from the spacings of the resolved resonances. It should be noted, however, that recent measurements by Hockenbury *et al.*[77] reported $\Gamma_\gamma = 60$ meV, with which the mean level spacing becomes 214 eV.

The inelastic scattering cross sections are also discrepant among the various evaluations. The JENDL-1 and ENDF/B-IV evaluations assume 4 and 2 discrete levels, respectively, while RCN-2 and CNEN-2 adopted much more discrete levels, some of which must be hypothetical. This difference may cause the difference of the cross section shape above 980 keV. The lowest value of ENDF/B-IV is probably attributed to its optical potential which gives the lowest total cross section. The difference below 900 keV between JENDL-1 and RCN-2, which adopted the same potential parameters, may be caused by the difference of the γ-ray strength function as seen in TABLE 2.5.

3.10 Palladium-105

3.10.1 Status of experimental data

No experimental data are available either on the thermal cross sections or the resonance integral, though considerable number of experiments have been reported on the resonance parameters. BNL-325 3rd edition[29] recommended $\sigma_{n,\gamma}{}^{th} = 14$ barns and R. I. $= 90 \pm 10$ barns on the basis of some calculation.

As to the resonance parameters, BNL-325 2nd edition[33] recommended the neutron width for 14 levels, for 5 of which the capture width was also recommended, on the basis of several experiments made until 1965. Since then only one experiment by Yamamuro *et al.*[122] has been reported on the resonance parameters. On the other hand, Coceva *et al.*[74] and Wetzel and Thomas[123] made spin assignment for many levels but did not give the resonance parameters. Consequently BNL-325 3rd edition gave the resonance energies and their spin for more than 50 levels up to 800 eV mainly based on the work by Coceva *et al.* but gave the resonance parameters only for 11 levels up to 141 eV. ENDF/B-IV took these recommended parameters. Very recently Macklin *et al.*[124] gave the values og $g\Gamma_n\Gamma_\gamma/\Gamma$ in the energy range between 2.6 and 3.6 keV.

At the time of the present work no experimental data were available in the energy range above resonance region. After that two new experiments were reported on the capture cross section in keV region by Macklin *et al.*[124] and by Hockenbury *et al.*[113]

3. 10. 2 Evaluation

We compared the resonance parameters recommended in BNL-325 2nd edition with the new experimental results by Yamamuro *et al.*[122], and found good agreement. For 9 resonances to which Yamamuro *et al.* gave the parameters, their deduced parameters were adopted. The parameters recommended in BNL-325 2nd edition were adopted for the remaining 5 resonances. The radiation widths were assumed to be 155 meV to the levels whose radiation width is not known experimentally. Thus the parameters were determined to 14 resonances up to 150 eV.

The thermal capture cross setion calculated from the present parameters is 2. 49 barns. This value seems to be too small considering the cross sections of natural palladium and the other Pd isotopes, though no experimental data exist for this isotope. We assumed the thermal capture cross section of 14 barns according to the recommendation in BNL-325 3rd edition, and applied the $1/v$ type correction. The elastic scattering cross section was calculated with the effective scattering radius of 6. 4 fm. The connecting energy was set at 150 eV.

The cross sections were calculated with the optical and statistical models in the energy range above 150 eV. Fifteen discrete levels were considered up to 1. 0878 MeV and levels were assumed to be overlapping above 1. 12 MeV. As no experimental data existed at the time of the present evaluation, the γ-ray strength function was obtained from the radiation width and the mean level spacing of the resolved resonances.

3. 10. 3 Discussion

The total, capture and inelastic scattering cross sections are compared with the measured data and the other evaluated curves in Figs. 3. 10. 1~3. 10. 3, respectively. As is evident from TABLE 2. 8, the CNEN-2 evaluation adopted the resolved resonance parameters for 61 levels up to 808 eV, for most of which the parameters have not been given experimentally as mentioned in section 3. 10. 1.

The energy dependences of the total cross section are fairly discrepant among the various evaluations. The CNEN-2 value is the highest in the unresolved resonance region below 50 keV and becomes the lowest in the energy region above 100 keV. The cross section of ENDF/B-IV shows a strange structure between 300 keV and 1 MeV. The value of JENDL-1 is the highest above 100 keV.

The thermal capture cross sections seem to be too small for all the evaluations, when they are calculated from the resonance parameters of positive resonances. As no measured data exist for this nuclide, the uncertainties of the $1/v$ correction or negative resonance parameters must be large. The calculated capture resonance integrals agree with the measured data of natural palladium.

In the energy region above resolved resonances, the capture cross sections of all the evaluations agree very well with the recent measurements of Hockenbury *et al.*[113] and Macklin *et al.*[124], though these data were not available for most of evaluations including JENDL-1. The γ-ray strength function was determined from

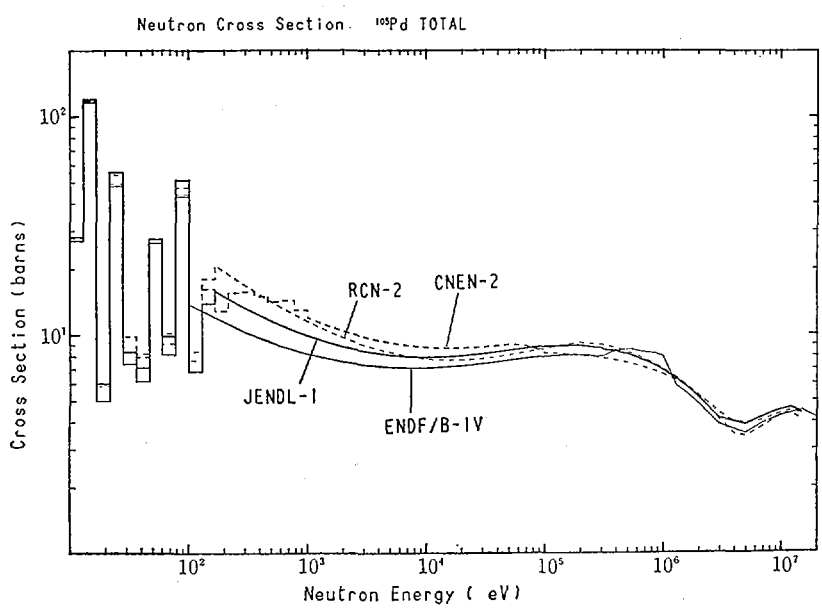

Fig. 3. 10. 1 Total cross sections of ^{105}Pd.

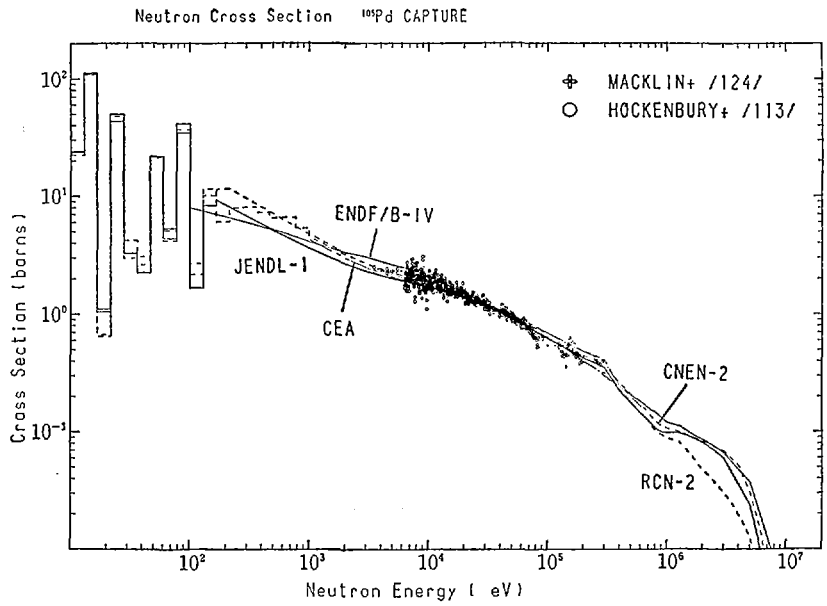

Fig. 3.10.2 Capture cross sections of ^{105}Pd.

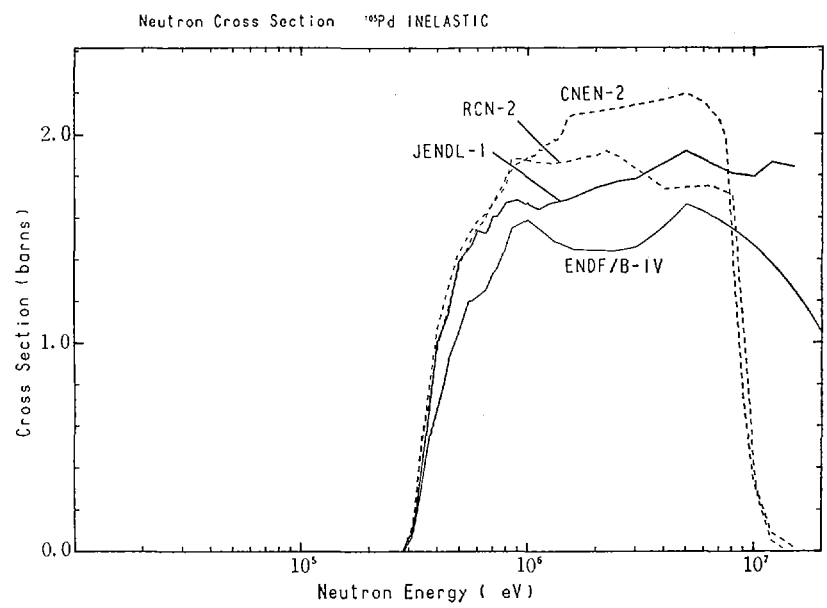

Fig. 3.10.3 Inelastic scattering cross sections of ^{105}Pd.

the resolved resonance parameters as seen in TABLE 2.5. Therefore the excellent agreements between the calculated and measured values suggest that the resonance parameters are also reliable. The lowest value of the RCN-2 evaluation above 1 MeV was explained by Gruppelaar *et al.*[21] that the low spin cut off parameters adopted in RCN-2 enhanced the inelastic scattering cross section in the continuum region and decreased the capture cross section for a nuclide of a low target spin (5/2 for ^{105}Pd). However, no such enhancement is observed in the inelastic scattering cross section of RCN-2 as will be discussed later.

The inelastic scattering cross sections of JENDL-1, RCN-2 and CNEN-2 agree with one another in the energy up to 600 keV, where nearly the same level schemes are assumed in these three evaluations as seen in TABLE 2.12.10. Above 650 keV, the JENDL-1 evaluation misses some discrete levels and gives lower cross section. Matsumoto *et al.*[46] added some levels in this energy region in their revised level scheme, and the cross section is expected to increase with this new level scheme. Above 1.25 MeV, no special enhancement is observed in the cross section of RCN-2 as is seen Fig. 3.10.3.

3.11 Ruthenium-106

3.11.1 Status of experimental data

Two experiment[125,126] on the thermal capture cross section and the resonance integral are the only available data. BNL-325 2nd[33] and 3rd[29] editions recommended $\sigma_{n,\gamma}{}^{th}=0.146\pm0.045$ barns on the basis of the newer experiment by Werner and Eastwood[125]. As to the resonance integral BNL-325 3rd edition recommends R. I. $=2.6\pm0.6$ barns, while the measured datum of Werner and Eastwood is R. I. $=2.0\pm0.6$ barns. Neither resonance parameters nor smooth cross sections have been measured.

3.11.2 Evaluation

As for the thermal capture cross section, the measured value of Werner and Eastwood[125] was adopted. As no resonance parameters are known, the $1/v$ type cross section was assumed for the capture cross section in the energy range up to 500 eV which corresponds to a half of the mean level spacing used in the statistical model calculation. The elastic scattering cross section was calculated with the effective scattering radius of 6.4 fm.

The cross sections were calculated with the optical and statistical models in the energy range above 500 eV. The γ-ray strength function was estimated from the trends of neighboring nuclides. Six discrete levels were considered in the energy region up to 1.888 MeV and levels were assumed to be continuum above 1.91 MeV.

3.11.3 Discussion

The total, capture and inelastic scattering cross sections are compared with the values of ENDF/B-IV and CNEN-2 in **Figs. 3.11.1~3.11.3**, respectively. The CNEN-2 evaluation adopts 6 hypothetical resonances between 630 eV and 11.13 keV as seen in **TABLE 2.8**.

The total cross sections of JENDL-1 and CNEN-2 agree with each other in the energy above 12 keV, while the value of ENDF/B-IV is lower in this energy region.

As to the capture cross section, the value of the resonance integral is 2.09 barns in JENDL-1, when calculated from the $1/v$ cross section and the smooth cross section obtained by the statistical model. This value agrees very well with the measured value of Werner and Eastwood.[125] This suggests that no resonance exists at some low energy and that reasonable values are adopted in JENDL-1 for the parameters used in the statistical model, such as the mean level spacing and the radiation width. On the other hand, the ENDF/B-IV evaluation applies the $1/v$ cross section up to 1,230 eV corresponding to D_{obs}, not $1/2D_{obs}$, and gives some structure below 5 keV probably to reproduce the resonance integral. The increase of the capture cross section of JENDL-1

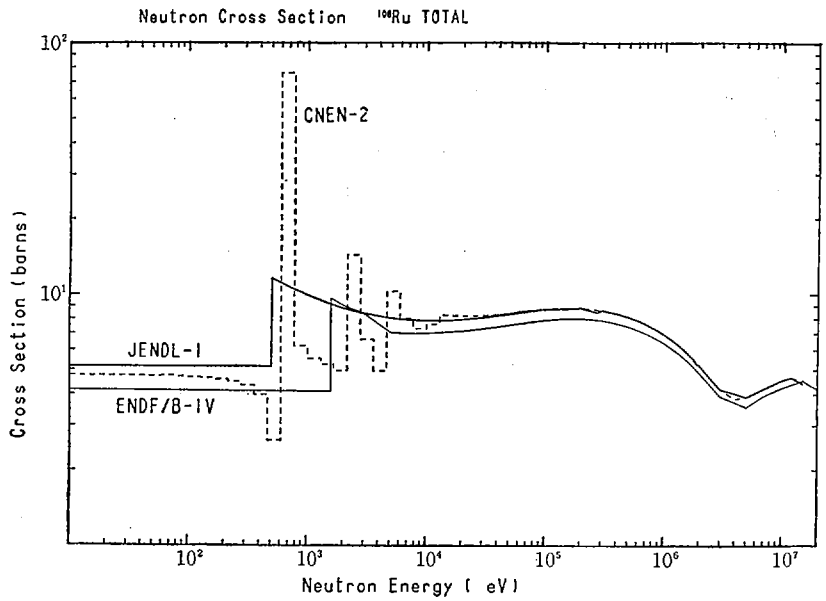

Fig. 3.11.1 Total cross sections of ^{106}Ru.

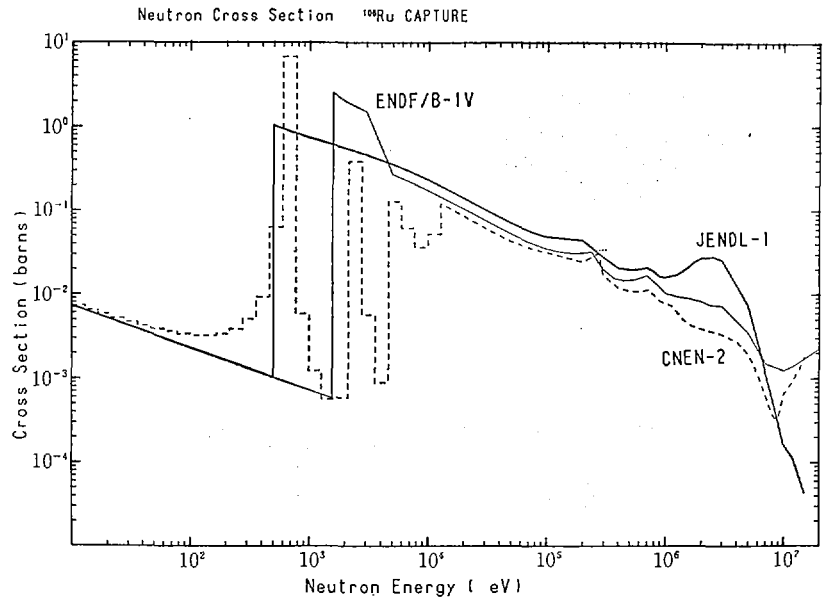

Fig. 3.11.2 Capture cross sections of ^{106}Ru.

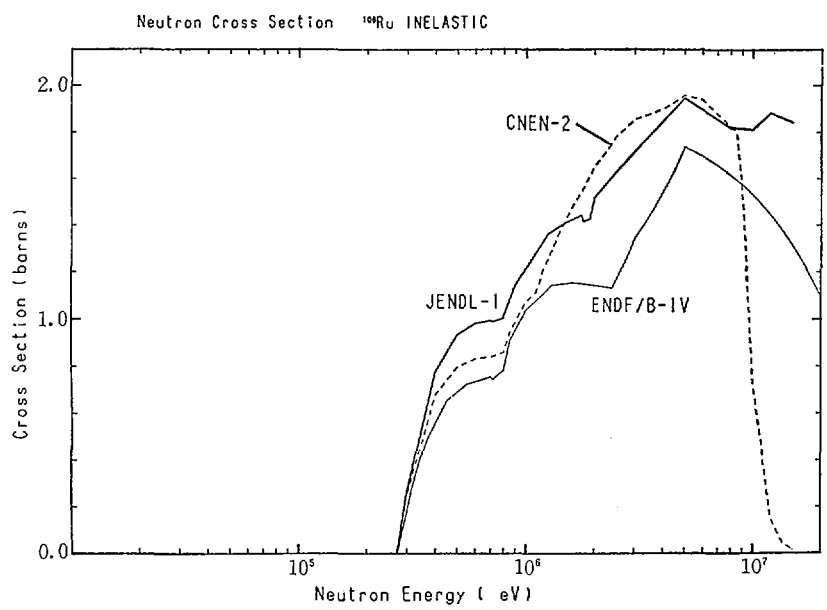

Fig. 3.11.3 Inelastic scattering cross sections of ^{106}Ru.

between 1 and 2 MeV can be explained as competition with the inelastic scattering.

The energy dependences of the inelastic scattering cross section are analogous among the three evaluations in the energy region up to 1 MeV where the same level schemes are assumed. Above 1 MeV, the treatment of levels is different as seen in TABLE 2. 12. 11: JENDL-1 assumes only two discrete levels at 1. 77 and 1. 89 MeV, while CNEN-2 and ENDF/B-IV assumes the continuum levels above 1. 16 and 0. 99 MeV, respectively. It is probable that some levels are missed in JENDL-1 between 1 and 1. 77 MeV. This may decrease the inelastic scattering cross section and enhance the capture cross section between 1 and 2 MeV for JENDL-1.

3. 12 Palladium-107

3. 12. 1 Status of experimental data

At the time of the present evaluation, no experimental data were available on the thermal capture cross sections, resonance integrals, resonance parameters and the smooth cross sections. Very recently Singh *et al.*[127] made neutron capture and transmission measurements and gave the resonance parameters for 34 levels up to 645 eV. Their deduced average parameters are:

$$D_{obs}=10.7\pm1.5\,\text{eV},\ \Gamma_\gamma=125\pm1.5\,\text{meV},\ S_o=\left(0.56^{+0.16}_{-0.12}\right)\times10^{-4}.$$

3.12.2 Evaluation

As no experimental data exist on the thermal cross sections, the thermal capture cross section was assumed to be 10 barns according to the estimation by Garrison and Roos[128] and the $1/v$ type cross section was applied up to 5 eV corresponding to a half of the mean level spacing used in the statistical model calculation. The elastic scattering cross section was calculated with the effective scattering radius of 6.35 fm.

The cross sections were calculated with the optical and statistical models above 5 eV. Nineteen discrete levels were taken into account up to 1.023 MeV and the levels were assumed to be continiuum above 1.07 MeV. The γ-ray strength function was estimated by study the systematic trends of the neighboring nuclides.

3.12.3 Discussion

The total, capture and inelastic scattering cross sections of the various evaluations are compared with one another in Figs. 3.12.1~3.12.3, respectively. As is seen in TABLE 2.8, the CNEN-2 and RCN-2 evaluations

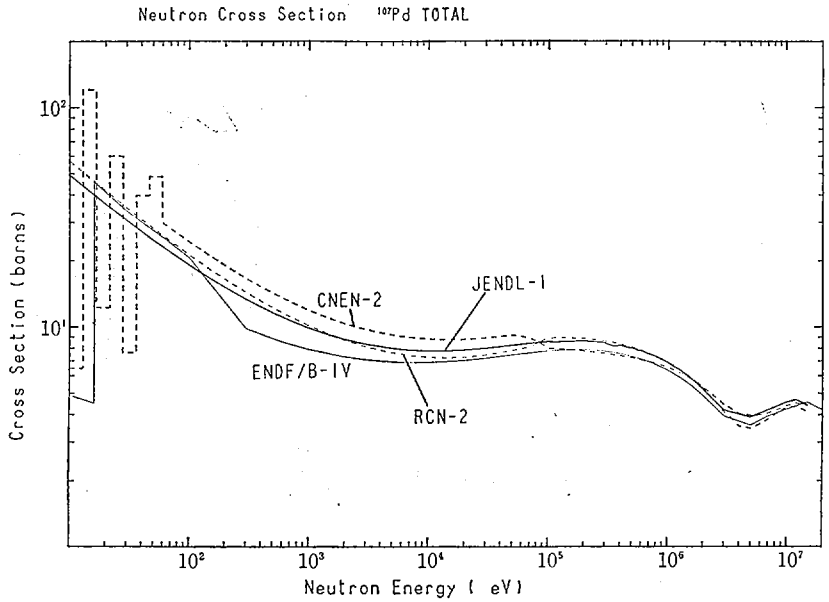

Fig. .12.1 Total cross sections of ^{107}Pd.

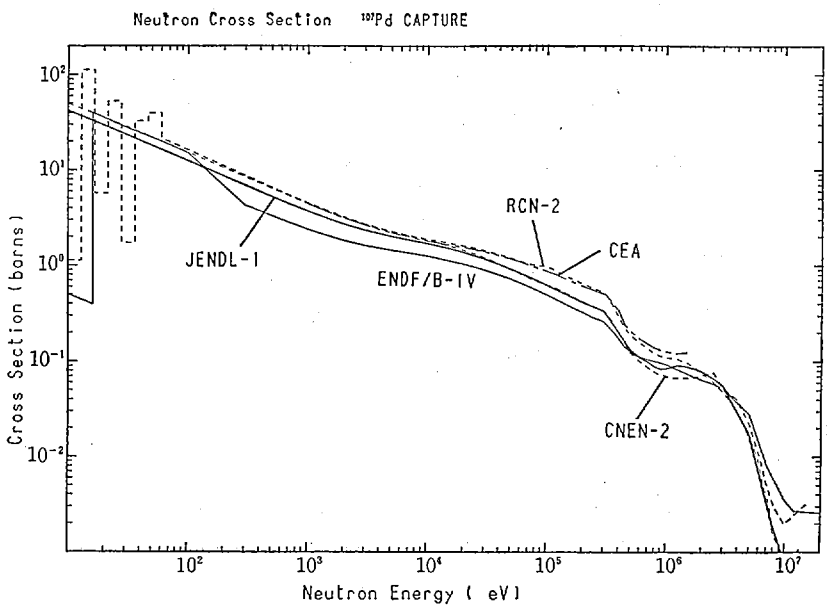

Fig. 3.12.2 Capture cross sections of ^{107}Pd.

adopted hypothetical resonances.

As to the total cross section, the JENDL-1 evaluation gives the highest values in the energy region above 100 keV. The ENDF/B-IV values are the lowest in all the energy region. This may be due to their adopting Moldauer potential[25] which gives the smallest s-wave strength function in this mass region as is evident in TABLE 2.4. The cross section of CNEN-2 is the highest in the unresolved resonance region below 100 keV where the CNEN-2 evaluation adopted the largest s-wave and p-wave strength functions as seen in TABLE 2.4, but becomes the lowest above 100 keV.

The value of the thermal capture cross section was estimated to be about 10 barns for all the evaluations except CNEN-2 which assumed 20.8 barns. However, the thermal capture cross section becomes about 1.8 barns when it is calculated from the resonance parameters recently obtained by Singh *et al.*[127] The resonance capture cross section calculated from their parameters is compared with that from the hypothetical parameters of CNEN-2 and with the smooth cross section of JENDL-1 in Fig. 3.12.4. Singh *et al.* deduced the capture resonance integral of 87 barns for 34 resonances, which agrees fairly well with the value of JENDL-1.

The γ-ray strength functions adopted in JENDL-1, CNEN-2 and ENDF/B-IV agree fairly well with the value of 1.17×10^{-4} obtained from Γ_γ and D_{obs} of Singh *et al.*, while the CEA and RCN-2 evaluations assume

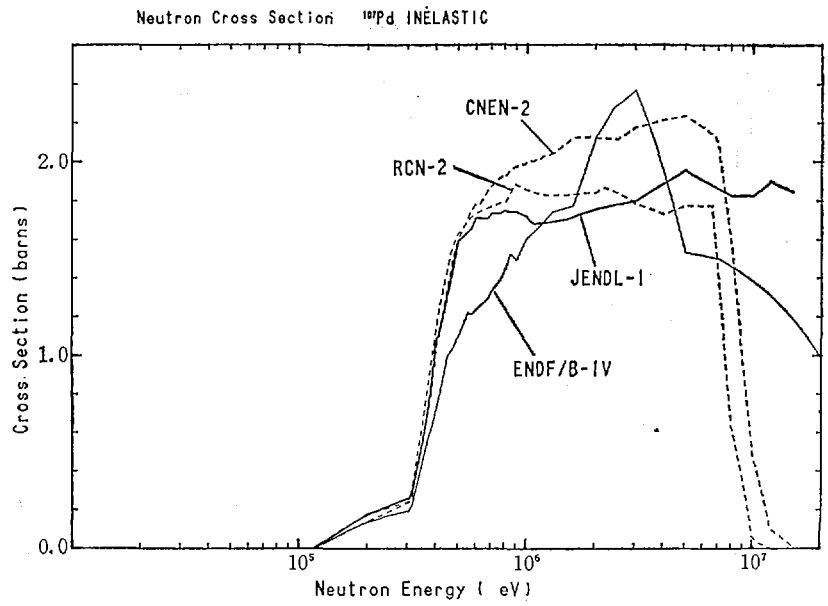

Fig. 3.12.3 Inelastic scattering cross sections of ^{107}Pd.

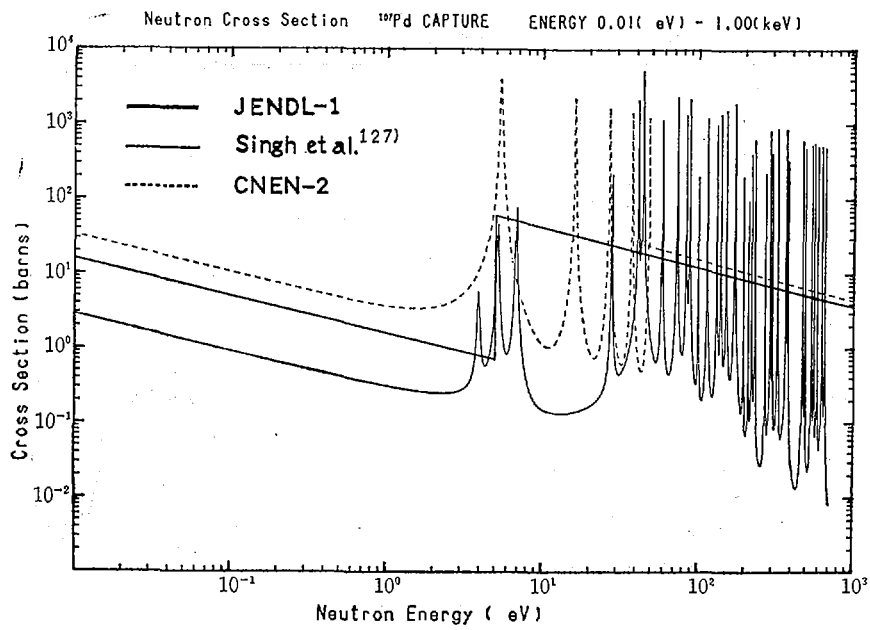

Fig. 3.12.4 Resonance cross sections of ^{107}Pd.

higher values as shown in TABLE 2. 5. This difference of S_γ-values can explain the discrepancies in the capture cross section below 1 MeV. The lowest value of ENDF/B-IV may be attributed to its low neutron strength function. The evident increase of the JENDL-1 and CNEN-2 above 1 MeV may be caused by their adopting large spin cut-off parameters for nuclides of low target spin ($5/2^+$) as pointed out by Gruppelaar *et al.*[21]

The inelastic scattering cross section is small below 0. 3 MeV because of large difference between the spins of low lying excited states and the target spin. The cross sections of JENDL-1, RCN-2 and CNEN-2 agree well with one another in the energy region up to 0. 5 MeV where nearly the same level schemes were assumed for the three evaluations. Above 0. 5 MeV the CNEN-2 and RNC-2 evaluations adopted some hypothetical discrete levels as seen in TABLE 2. 12. 12, and consequently give higher values than that of JENDL-1. The ENDF/B-IV evaluation adopted smaller number of the discrete levels and give the lowest value. The structure of the ENDF/B-IV cross section above 1. 5 MeV cannot be understood.

3. 13 Silver-109

3. 13. 1 *status of experimental data*

A considerable number of experiments have been reported on the thermal capture cross section for both 24 sec ^{110g}Ag and 290 day ^{110m}Ag production. BNL-325 3rd edition[29] recommends $\sigma_{n,\gamma}{}^{th}=91\pm3$ barns [$\sigma_{,n\gamma}{}^{th}$ (^{110g}Ag)$=89\pm4$ barns and $\sigma_{n,\gamma}{}^{th}$(^{110m}Ag)$=4.5\pm0.2$ barns] on the basis of the experimental data. Experimental data are scarce for the resonance integral. Tattersall *et al.*[52] and Van der Linden *et al.*[83] gave R. I.$=1,870\pm200$ barns and $1,161\pm70$ barns, respectively. BNL-325 3rd edition recammends R. I.$=1,450\pm40$ barns which agrees with the recommended value by Walker.[42]

Experimental data are numerous on the resonance parameters. BNL-325 2nd edition recommended the parameters of 34 resonances up to 622 eV on the basis of 16 sets of experimental data measured till 1966. After that a few new experiments have been reported. Particularly Pattenden and Joly[129] extended the upper energy of resolved resonances up to 2, 600 eV. Based on these new experimental data, BNL-325 3rd edition recommends the parameters of 81 resonances, only 21 of which the radiation width is given.

Experimental data are available in the energy range above resonances. However, obvious systematic discrepancies are observed among them as shown in Fig. 3. 13. 2. The data of Weston *et el.*[130] are by about two times higher than those of Kononov and Stavisskii.[131] The datum of Furr[132] agrees with the data of Weston *et al.*, while the datum of Chaubey and Sehgal[117] supports the data of Kononov and Stavisskii.

The total coss section was measured below 30 keV by Chrien[133] and at 14 MeV by Dukarevich *et al.*[134] As to the inelastic scattering, Augustyniak *et al.*[135] measured the ^{110m}Ag production cross section.

3. 13. 2 Evaluation

The resonance parameters recommended in BNL-325 3rd edition were adopted for 81 levels up to 2, 506 eV. For the levels whose capture width is not given, we assumed the value of 130 meV which was obtained by averaging the capture widths of 21 levels recommended in BNL-325.

The value of thermal capture cross section calculated from these resonance parameters is 91 barns which agrees quite well with the value of 91 ± 3 barns recommended in BNL-325. Hence no background cross section was applied. The thermal elastic scattering cross section was calculated with the effective scattering radius of 6. 3 fm.

The resonance capture cross section decreases with increasing energy above 1 keV more abruptly than expected from the statistical theory. After the statistical examination mentioned in section 2. 4, it was assumed that some levels were missing above 1 keV, and the connecting energy was determined to be 1 keV.

The cross sections above 1 keV were obtained by the optical and statistical model calculations. Seventeen discrete levels were considered up to 1. 4 MeV and the levels were assumed to be continuum above 1. 45 MeV. The γ-ray strength function was determined so that the calculated capture cross section might reproduce the experimental data. However, there are obvious systematic discrepancies among the existing experimental data as described in the previous section. We adopted the data of Weston *et al.*[130], since these data join smoothly with the cross section in the resolved resonance region.

3. 13. 3 Discussion

The total, capture and inelastic scattering cross sections are shown with the measured data as well as the other evaluated data in Figs. 3. 13. 1～3. 13. 3, respectively.

The energy dependece of the total cross section is very different from one another among the four evaluations. None of the evaluated curves reproduce the measured data of Chrien[133] below 30 keV, though all the evaluated values agree with the measured datum of Dukarevich *et al.*[134] at 14 MeV. The value of JENDL-1 seems to be a little too low in the energy range below 100 keV from the view point of connection with the resonance cross section. This low value is caused by underestimation of the s-wave strength function as seen in TABLE 2. 4.

The measured values of the thermal capture cross section and the resonance capture integral are quite well reproduced by the calculation with the resonance parameters in all the evaluations as seen in TABLES 2. 9 and 2. 10.

As to the capture cross section above resonance region, there exist large discrepancies among the evaluated data: The JENDL-1 evaluation relied on the high values of Weston *et al.*[130] and ENDF/B-IV adopted the low value of Kononov and Stavisskii.[131] The RCN-2, CNEN-2 and CEA evaluations probably relied on the

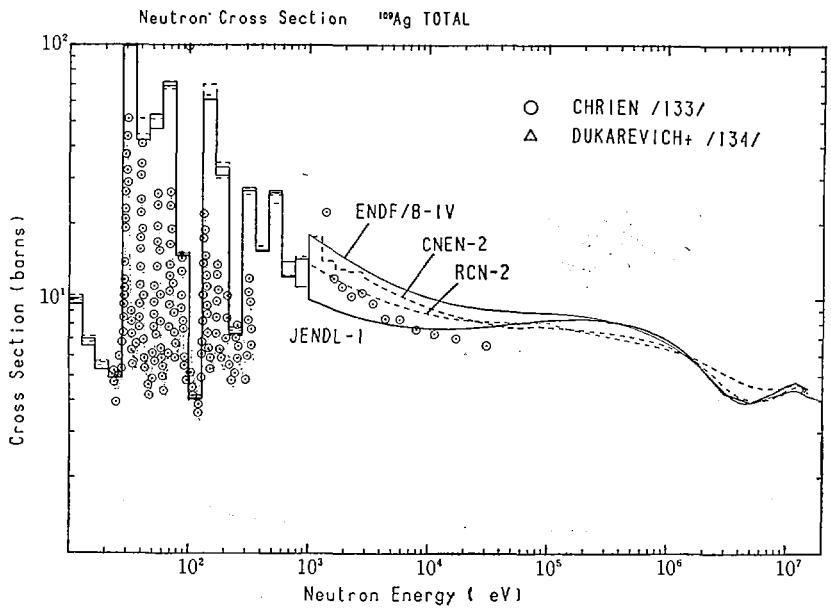

Fig. 3.13.1 Total cross sections of ^{109}Ag.

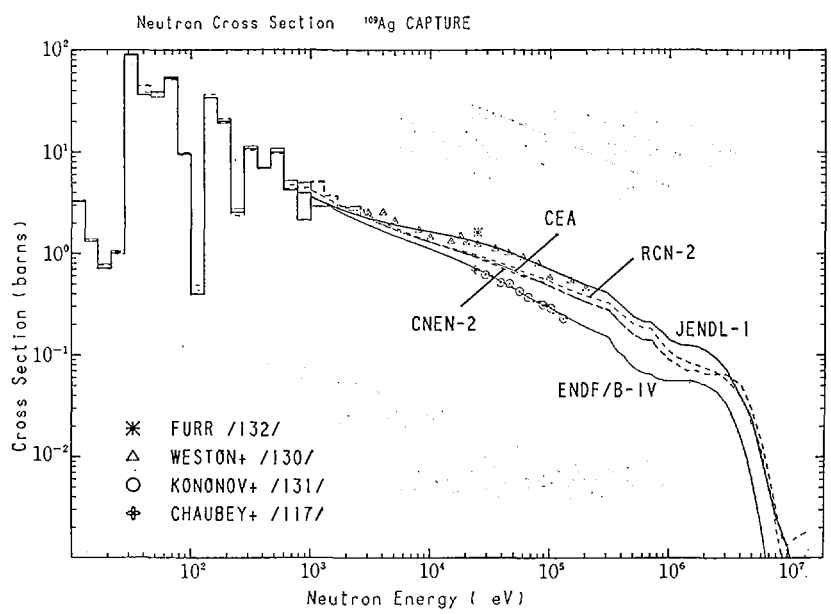

Fig. 3.13.2 Capture cross section of ^{109}Ag.

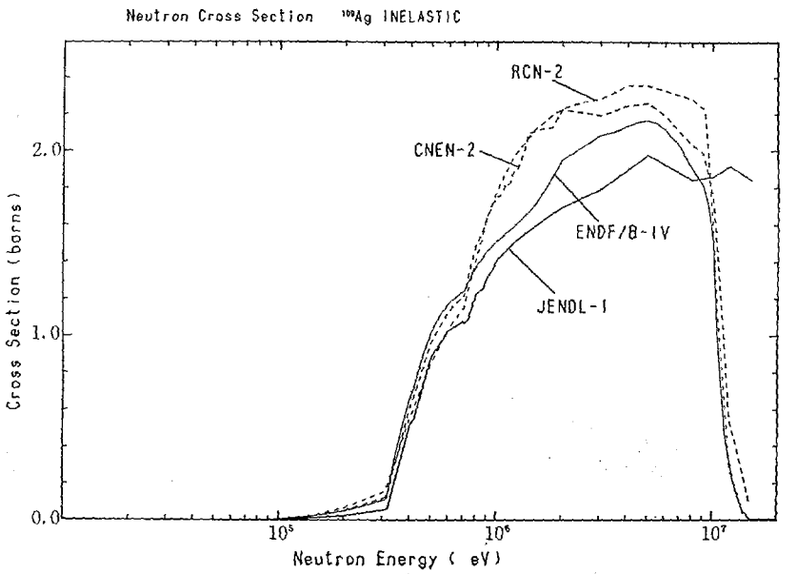

Fig. 3.13.3 Inelastic scattering cross sections of ^{109}Ag.

values of Kononov and Stavisskii renormalized by Ribon *et al.*[16] and gave the middle values. The value of ENDF/B-IV must be too low, because, as its evaluators admitted[136] by themselves, the capture cross section of natural silver cannot be reproduced with such a low capture value of ^{109}Ag. Gruppelaar *et al.*[21] argued from the integral measurements in STEK that the values of JENDL-1 were too high.

The discrepancies are also large in the inelastic scattering cross sections. The value of JENDL-1 is the smallest particularly in the energy range where the levels are assumed as overlapping. As pointed out by Gruppelaar *et al.*[21], this might be caused by our adopting a high spin cut-off parameter which decreases the population of low spin states relatively and therefore decreases the inelastic scattering cross section for nuclides of low target spin ($1/2^-$ for ^{109}Ag).

3.14 Iodine-129

3.14.1 Status of experimental data

The thermal capture cross section was measured by Purkayastha and Martin[137], by Roy and Wuschke[138] and by Eastwood *et al.*[139] The experimental values scatter between 26.7 barns[138] and 35 barns.[137] BNL-325 2nd edition[33] recommended 28±3 barns. After that Wilkey and Willard[140] found the existence of a metastable state in ^{130}I and measured the branching ratio of the activation cross section. Based on this result, BNL-325 3rd edition[29] recommends $\sigma_{n,\gamma}{}^{th}=27\pm3$ barns [$\sigma_{n,\gamma}{}^{th}$ (9 min ^{130m}I)$=18\pm2$ barns and $\sigma_{n,\gamma}{}^{th}$ (12.4 hr ^{130g}I)$=9\pm1$ barns]. The absorption resonance integral was reported to be 36±4 barns by Roy and Wuschke.[138]

The total cross section was measured in the low energy region by Harvey *et al.*[141], by Block *et al.*[142] and by Pattenden.[143] The resonance parameters were deduced for 5 levels between 72.4 eV and 154 eV by Harvey *et al.* and by Pattenden. No experimental works have so far been reported in the fast neutron range except on the $(n, 2n)$ reaction cross section at 15 MeV.

3.14.2 Evaluation

The resonance parameters were determined for 5 levels from 72.4 eV to 153 eV by averaging the experimental data of Γ_n reported by Harvey *et al.*[141] and by Pattenden[143] with the assumption of $\Gamma_\gamma=100$ meV. These parameters are nearly the same as those recommended in BNL-325 3rd edition.

This set of parameters gives the thermal capture cross section of 0.135 barns which is mucn lower than the experimental values (26.7±35 barns). This discrepancy was corrected by adding the $1/v$ type background cross section so that the capture cross section at 0.0253 eV might be 27 barns as recommended in BNL-325 3rd edition. The connecting energy was determined to be 166 eV according to the relation $E_c=E_{max}+1/2D_{obs}$ as described in section 2.4. The effective scattering radius was assumed to be 5.65 fm.

The cross sections were calculated with the optical and statistical models in the energy region above 166 eV. Seventeen discrete levels were adopted up to 1.4 MeV and the continuum levels were applied above 1.45 MeV. The γ-ray strength function was obtained from the resolved resonance parameters.

3.14.3 Discussion

The total, capture and inelastic scattering cross sections are compared with the other calculated data in Figs. 3.14.1~3.14.3, respectively.

The total cross section of JENDL-1 is the highest particularly in the energy range below 60 keV, since the largest s-wave strength function was used in the JENDEL-1 evaluation as seen in TABLE 2.4. This value of 1.06×10^{-4} may be too large, taking it into account that the value of S_0 is recommended as 0.6×10^{-4} for ^{127}I in BNL-325 3rd edition. The RCN-2 evaluation adopted the same optical potential parameters as JENDL-1 above 60 keV, but used the lower value as the s-wave strength function below 60 keV, which agrees with that of ENDF/B-IV.

The thermal capture cross section is less than 1/100 of the experimental value for all the evaluations, when it is calculated from the resonance parameters. This discrepancy is probably caused by missing of some levels

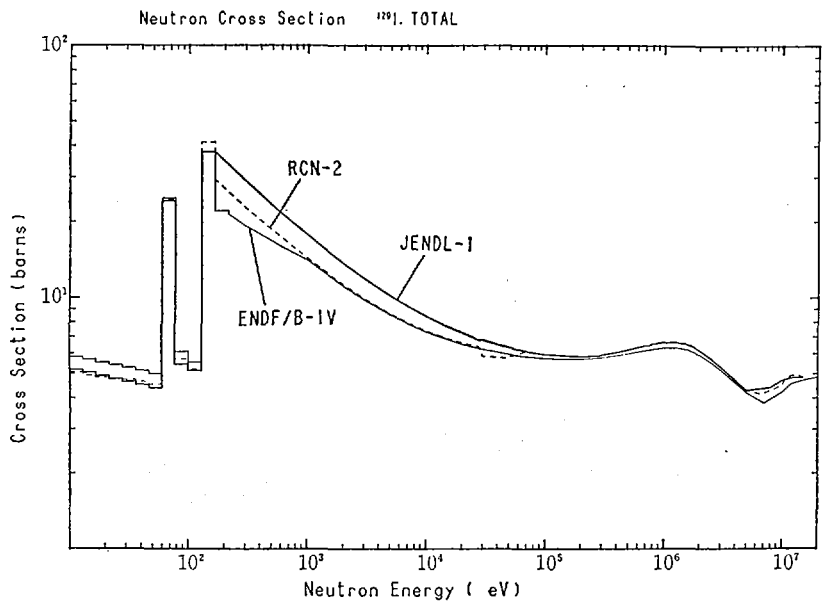

Fig. 3.14.1 Total cross sections of ^{129}I.

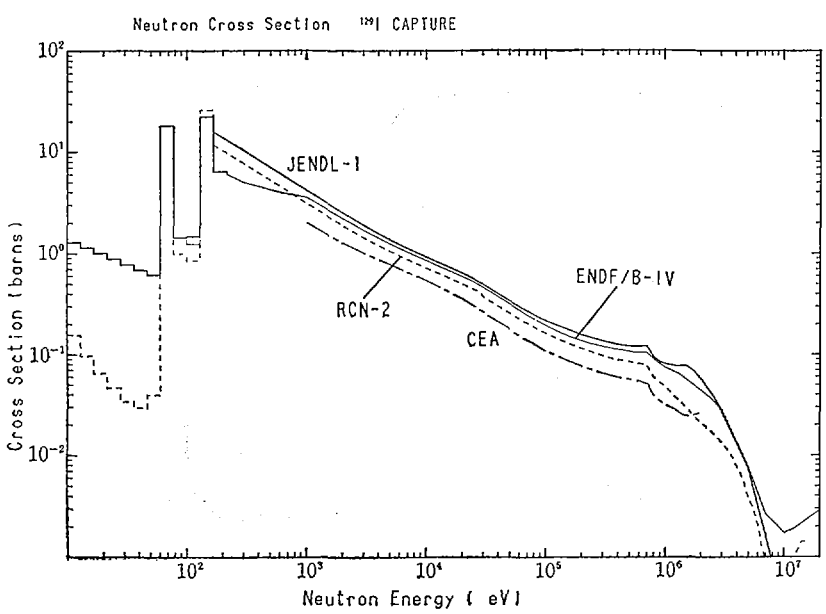

Fig. 3.14.2 Capture cross sections of ^{129}I.

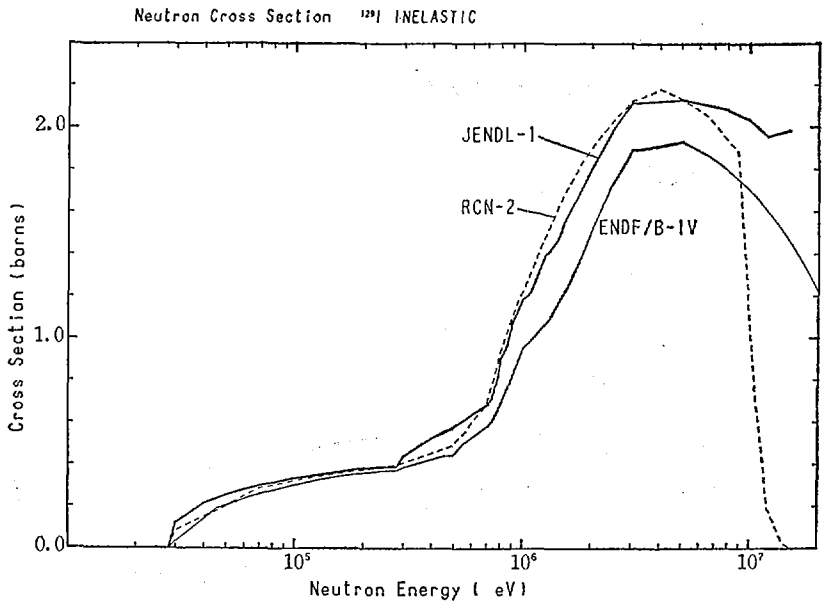

Fig. 3.14.3 Inelastic scattering cross sections of ^{129}I.

located below the lowest level of 72.4 eV presently adopted, because it is hardly expected from the statistical ditribution of resonance energies that there exists no level up to 72.4 eV and do exist 5 levels between 72.4 eV and 153 eV. Nevertheless, the $1/v$ correction was applied in the JENDL-1 and ENDF/B-IV evaluations, and a negative resonance was assumed in the RCN-2 evaluation. The calculated resonance integral for capture of JENDL-1 is a little larger than the measured value of Roy and Wuschke[138], while the calculated values of the other evaluations show good agreement with the measured value.

As to the capture cross section above resonance region, the values of JENDL-1 and ENDF/B-IV are the highest, the cross section of CEA is the lowest and the RCN-2 evaluation gives the middle value. Gruppelaar *et al.*[21] concluded from their integral tests at STEK facilities that even the RCN-2 cross section was too high. If that is the case, it might be necessary to decrease the γ-ray strength function which was obtained from the resolved resonance parameters of only 6 levels.

The inelastic scattering cross sections are analogous to one another among all the evaluations. The rapid increase in the value of JENDL-1 above 280 keV is caused by spin and parity assignment of $5/2^+$ to 0.278 MeV level, while the RCN-2 evaluation assigned $3/2^+$ to this level. It is to be noted, however, that Matsumoto *et al.* assigned $3/2^+$ to this level in their revised evaluation[46]. Therefore it is expected that the discrepancy of the inelastic scattering cross section between 280 an 550 keV will disappear, if the revised level scheme is used.

3.15 Xenon-131

3.15.1 Status of experimental data

The thermal capture cross section was measured in the pile spectrum by Eastwood and Brown[144] and by MacNamara and Thode.[145] BNL-325 2nd edition recommended 110 ± 20 barns on the basis of these experimental data. BNL-325 3rd edition recommends 90 ± 10 barns which is lower than both of the experimental results. The reason of this change is not clear. The resonance integral has not so far been measured.

The resonance parameters were obtained by Mann *et al.*[146] and by Ribon.[147] Particularly Ribon gave the parameters for 39 levels up to 4 keV. BNL-325 3rd edition seems to have taken the experimental data of Ribon. However, BNL-325 gives Γ values for 27 levels and Γ_γ values only for 7 levels, while Ribon gave the former for 30 levels and the latter for 23 levels.

No experimental data are available in the fast neutron region except on $(n, 2n)$ and (n, p) reaction cross sections near 14 MeV.

3.15.2 Evaluation

The resonance parameters recommended in BNL-325 3rd edition were adopted in the present work. For the levels whose radiation width is not given, the average value of 114 meV was assumed. The s- and p-wave assignment was made with the method described in section 2.3, and 15 levels were assigned as s-wave resonances and the remaining 24 levels as p-wave resonances.

As for the thermal capture cross section, the value of 90 barns recommended in BNL-325 3rd edition was tentatively assumed in the present work, though its experimental basis is not clear. The thermal capture cross section is 68 barns, when it is calculated from the resonance parameters. The difference was corrected by appyling the $1/v$ type background cross section. The effective scattering radius of 5.5 fm was assumed in calculating the elastic scattering cross section.

The results of the statistical examination suggest that some levels are missing in the energy region above 800 eV. The connecting energy was thus determined to be 773 eV.

The cross sections above 773 eV were obtained by the optical and statistical model calculations. Seven discreate levels were considered up to 723 keV and the continuum levels were assumed above 950 keV. The γ-ray strength function was determined so that the calculated capture cross section might join the average resonance cross section smoothly at 773 eV.

3.15.3 Discussion

The total, capture and inelastic scattering cross sections of JENDL-1 are compared with those of ENDF/B-IV in **Figs. 3.15.1~3.15.3**, respectively. The ENDF/B-IV evaluation adopted the resonances up to 4 keV, while we assumed level missing in the enengy rarge above 773 eV.

The resonance cross sections of ENDF/B-IV are much smaller than those of JENDL-1. The resonance parameters of ENDF/B-IV are reported[148] to have been taken from the measurements by Ribon[147], but the correction due to isotopic abundance was not made. Hence the neutron widths are underestimated in ENDF/B-IV by a factor of 4.72, *i.e.*, an inverse of the isotopic abundance of ^{131}Xe (21.18%). As a result of the present s- and p-wave assignment of resonances, the level spacing of the assigned s-wave resonances becomes very odd: For example, there are 6 levels below 300 eV and no levels between 800 and 1,500 eV. This may suggest that the present s- and p-wave assignment is in error.

The total cross sections of both evaluations agree with each other in the energy range above 500 keV, while the values of ENDF/B-IV are higher below 500 keV because of larger s- and p-wave strength functions as seen in **TABLE 2.4**.

The capture cross section of JENDL-1 is much higher than that of ENDF/B-IV above resonance region. This is caused by our adopting a larger value of the γ-ray strength function than that of ENDF/B-IV as seen

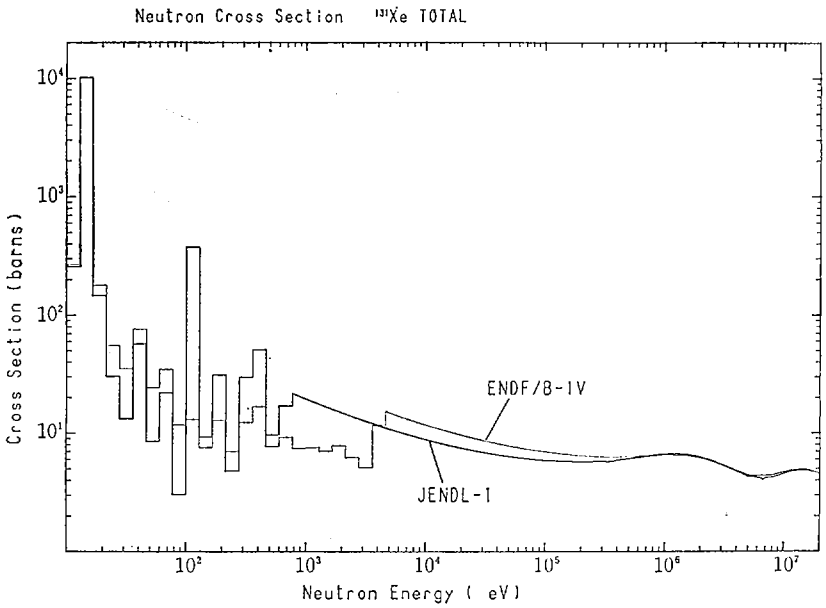

Fig. 3.15.1 Total cross sections of ^{131}Xe.

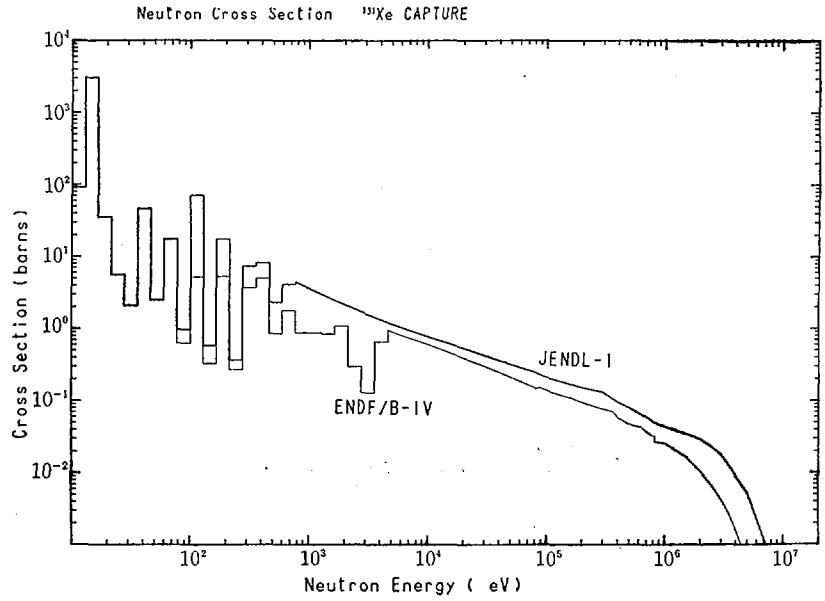

Fig. 3.15.2 Capture cross sections of ^{131}Xe.

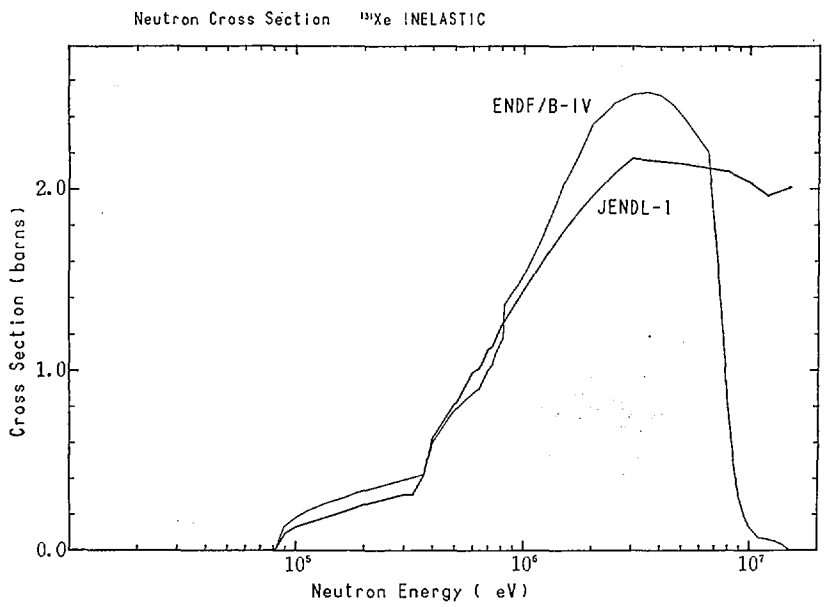

Fig. 3.15.3 Inelastic scattering cross sections of ^{131}Xe.

in TABLE 2.5. The present γ-ray strength function gives $D_{obs}=33$ eV by assuming $\Gamma_\gamma=114$ meV. This value of D_{obs} is consistent with that obtained from the lowest four levels, but is too small if we take account of all the levels up to 800 eV. Hence the γ-ray strength function may be overestimated in JENDL-1. The D_{obs} value of ENDF/B-IV is consistent with that recommended in BNL-325 3rd edition. Gruppelaar *et al.*[21] argued from the integral measurements at STEK facilities that the preferable capture cross section lies between both extremes of JENDL-1 and ENDF/B-IV.

The inelastic scattering cross section of JENDL-1 is lower than that of ENDF/B-IV below 500 keV. This is partly caused by the difference of the neutron strength functions as mentioned above.

3.16 Cesium-133

3.16.1 *Status of experimental data*

Experimental data are numerous for this nuclide. The thermal capture cross section has been measured by more than 10 experimenters. The measured values scatter between 26 and 47 barns. BNL-325 recommends $\sigma_{n,\gamma}{}^{th}=29.0\pm1.5$ barns in both 2nd[33] and 3rd[29] editions. The recently measured data by Steinnes[149] and by

Widder[150] agree with this recommended value within the quoted errors. The cross section of 2.9 hr ^{134m}Cs production was also measured. BNL-325 3rd edition recommends $\sigma_{n,\gamma}{}^{th}(^{134m}Cs)=2.5\pm0.2$ barns on the basis of the measured data. The capture resonance integral has been measured by about 10 experimenters. The measured values lie in the range from 320 to 500 barns, and BNL-325 3rd edition recommends R. I. $=415\pm15$ barns. The recently measured data by Steinnes[149], by Alian[151] and by Van der Linden *et al.*[152] agree with this value within the quoted errors. The measured values of the resonance integral for ^{134m}Cs production are between 29 and 35 barns. The total cross section in the thermal energy range was measured only by Hickman[153] who reported the cross section curve up to 4 eV and gave $\sigma_T{}^{th}=33\pm1$ barns.

The resonance parameters were deduced by several experimenters. BNL-325 2nd edition recommended the parameters up to 3.5 keV on the basis of the data of Landon and Sailor[154], of Harvey *et al.*[155] and of Garg *et al.*[156] Particularly Gerg *et al.* gave the neutron widths in the energy range between 126 eV and 3,500 eV. Since then Jung and Priesmeyer[157] deduced the parameters for 21 resonances in the energy range from 5.9 to 591 eV with the area analysis method. Thomas *et al.*[158] assigned the resonance spins for 12 resonances between 5.90 eV and 359 eV. Taking account of these measurements, BNL-325 3rd edition recommends the neutron widths for 160 resonances, but gives the capture widths only for 5 resonances. After publication of BNL-325 3rd edition, Riehs and Thomas[159] assigned the spin values for 29 resonances between 22.6 eV and 795.7 eV. Hockenbury *et al.*[57] recently reported the parameters for 7 levels between 47.5 eV and 295.5 eV.

There are more than 10 measurements on the capture cross section in the energy range from 1 keV to 15 MeV. However, there exist two different trends in the experimental data as shown in **Fig. 3.16.2**. The data of Popov and Shapiro[105] are by about 20% lower than those of Kompe[160] in the energy range between 13 and 40 keV. The datum of Yamamuro *et al.*[161] at 24 keV supports the data of Popov and Shapiro, while the datum of Booth *et al.*[162] gives even a higher value than those of Kompe. Recently Yamamuro and Asami[163] reported the measured data between 3 and 240 keV, which agree very well with those of Popov and Shapiro.

The total cross section was measured by Dilg and Vonach[101] at 2.7 keV, by Barnard *et al.*[164] between 250 keV and 1.2 MeV, by Foster and Glasgow[70] between 2.5 and 15 MeV and by Angeli *et al.*[165,166] at 14.5 MeV. As to the inelastic scattering cross section, Kikuchi[167] measured the excitation functions in the energy range from 550 to 970 keV for 6 excited levels, the energies of which are 633, 641, 768, 787, 819 and 873 keV. Some experimental data are also available for the differential inelastic scattering cross section. Two sets of experiments were reported on the elastic scattering cross section.

3.16.2 Evaluation

The resonance parameters recommended in BNL-325 3rd edition were adopted in the present work. For the levels whose radiation width is not given, we assumed $\Gamma_\gamma=118$ meV which was derived by averaging the values of 5 levels given in BNL-325 taking account of the quoted errors. We assigned 61 levels as the s-wave resonances and the remaining 99 levels as the p-wave ones with the method described in section 2.3.

The thermal capture cross section calculated from these parameters is 17.0 barns which is smaller than the value of 29.0 barns recommended in BNL-325 3rd edition. The difference was corrected by the $1/v$ type background cross section. The elastic scattering cross section was calculated with the effective scattering radius of 5.2 fm. The result of the statistical examination suggests that some levels are missing above 1.3 keV. The connecting energy was thus set at 1.3 keV.

The smooth cross sections were obtained by the spherical optical and statistical model calculations. The γ-ray strength function was adjusted so that the calculated capture cross section might reproduce the trend of the experimental data of Popov and Shapiro[105], which were adopted in the present work because of their smooth connection with the resonance cross sections as seen in **Fig. 3.16.2**.

3.16.3 Discussion

The total, capture and inelastic scattering cross sections are illustrated with the other evaluated data and selected measured data in **Figs. 3.16.1~3.16.3**, respectively.

The present optical potential reproduces very well the measured total cross sections of Barnard *et al.*[164] and of Foster and Glasgow[70], while the potentials of ENDF/B-IV and RCN-2 overestimate the total cross section

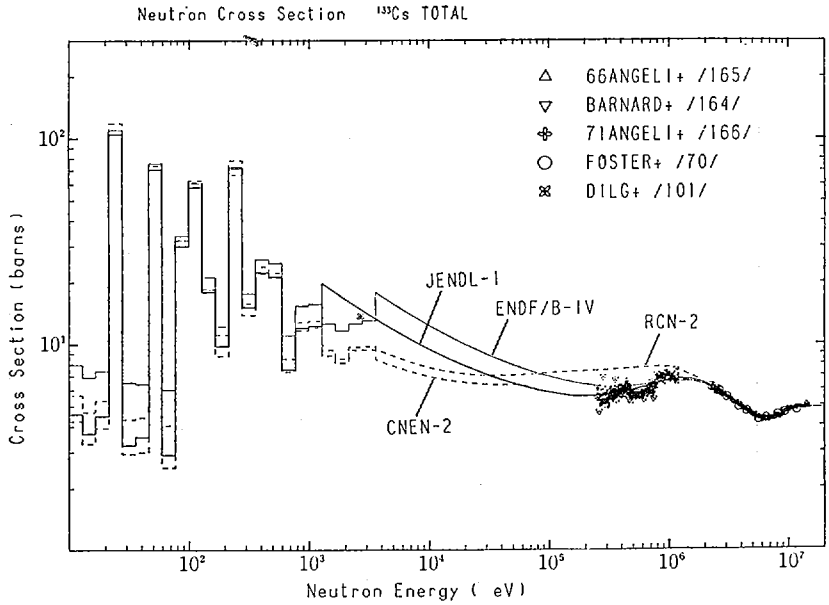

Fig. 3.16.1 Total cross sections of ^{133}Cs.

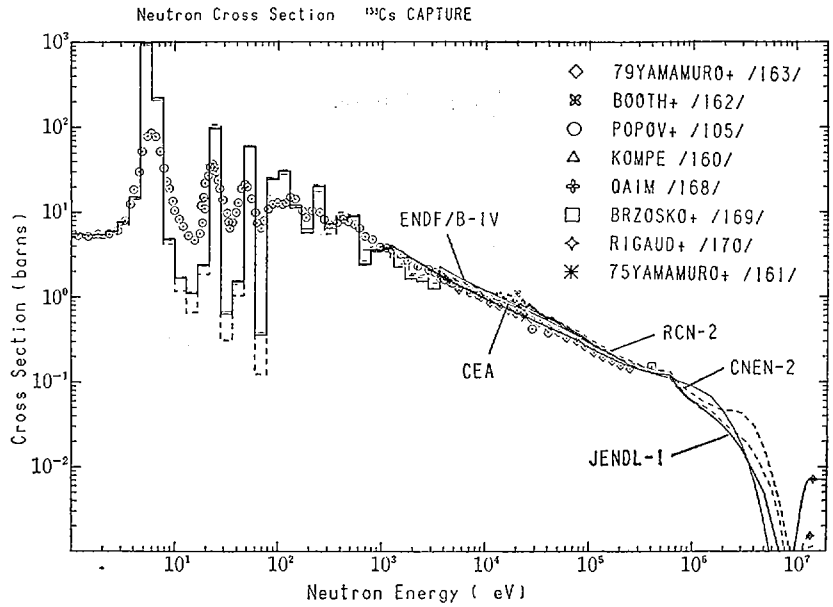

Fig. 3.16.2 Capture cross sections of ^{133}Cs.

below 1 MeV.

The capture resonance integral calculated from the resonance parameters and the $1/v$ background cross section is 398 barns, which falls within the uncertainty of the measured data. As is mentioned in section 3. 16. 1, two trends of the measured data exist in the capture cross section below 100 keV. The present JENDL-1 evaluation is based on the lower values of Popov and Shapiro[105] and of Yamamuro *et al.*[161], while the ENDF/B-IV, CNEN-2 and RCN-2 evaluations are based on the higher values of Kompe[160]. The values of CEA agree with the data of Popov and Shapiro below 10 keV and with those of Kompe above 30 keV. The recent data of Yamamuro and Asami[163] agree very well with the curve of JENDL-1. The difference between ENDF/B-IV and the other evaluations above 650 keV is probably caused by the different treatment of the inelastic scattering in this energy region, as pointed out by Gruppelarr *et al.*[21] The difference between JENDL-1 and CNEN-2 above 1 MeV is difficult to be understood, because both the evaluations use the same optical potential and give very similar inelastic scattering cross section as seen in Fig. 3.16.3.

As to the inelastic scattering cross section, the RCN-2 and ENDF/B-IV evaluations give higher values below 600 keV. This may be reflection of their larger total cross section in this energy region. As also pointed out by Gruppelaar *et al.*, ^{133}Cs has a high ground state spin ($7/2^+$), but has excited states of rather low

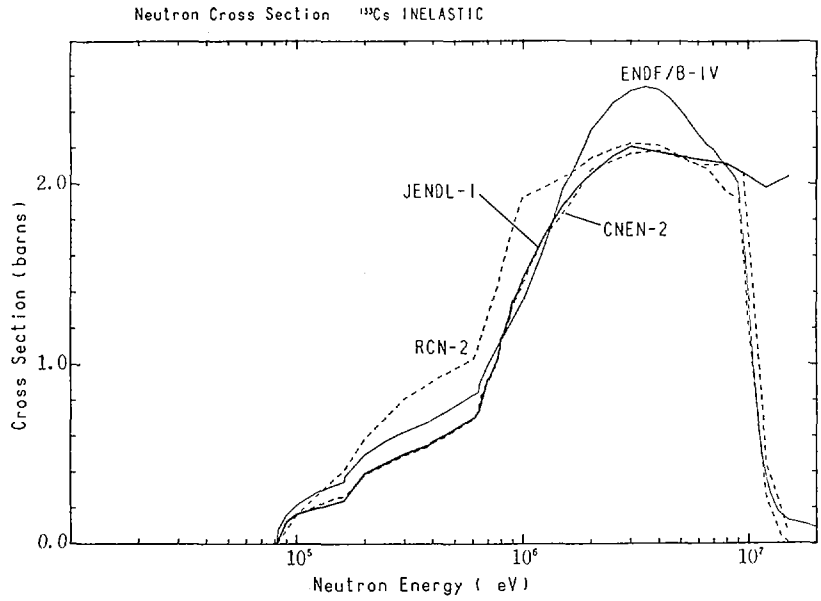

Fig. 3.16.3 Inelastic scattering cross sections of ^{133}Cs.

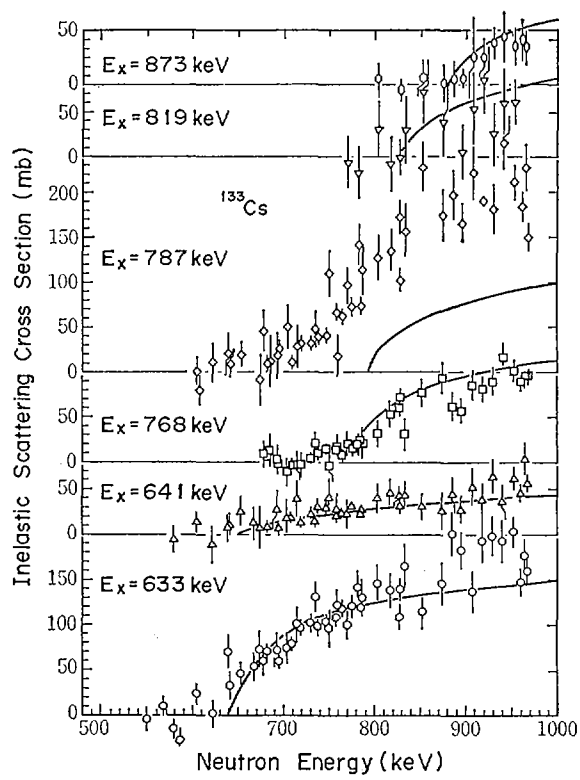

Fig. 3.16.4 Partial inelastic scattering cross sections of ^{133}Cs.

spin up to 600 keV. Therefore the inelastic scattering is rather suppressed below 600 keV. On the other hand, many high spin states exist above 600 keV and the inelastic scattering is enhanced. In ENDF/B-IV, the levels above 645 keV are treated as continuum, and the fluctuation of population of the high spin states is ignored. Hence the increase of the inelastic scattering cross section above 600 keV is rather moderate and this affects also the energy dependence of the capture cross section.

The excitation functions of the inelastic scattering to the 633, 641, 768, 787, 819 and 873 keV levels are shown in Fig. 3.16.4 with the measured data by Kikuchi[167]. Agreement between JENDL-1 and the measured data is fairly satisfactory except for the 787 keV level, where the evaluated data of JENDL-1 are much lower.

3.17 Cesium-135

3.17.1 Status of experimental data

The experimental data are very scarce. The thermal capture cross section and the resonance integral measured by Baerg *et al.*[171] are the only practically available experimental data. Jung *et al.*[172] tried to measure the resonance parameters using the mixture sample of ^{133}Cs, ^{135}Cs and ^{137}Cs but failed to distinguish the resonances of ^{135}Cs from those of ^{137}Cs. No other experimental data are available.

3.17.2 Evaluation

The value of thermal capture cross section was taken from the experimental data of Baerg *et al.*[171], *i.e.*, $\sigma_{n,\gamma}{}^{th}=8.7$ barns. As no resonance parameters are known, the $1/v$ type cross section was applied for the capture cross section up to 30 eV, which corresponds to a half of the level spacing used in the statistical model calculation. The elastic scattering cross section was calculated with the effective scattering radius of 5.2 fm.

The cross sections were calculated with the optical and statistical models in the energy range above 30 eV. The radiation width and the mean level spacing were estimated from the trends of neighboring nuclides. We took 6 discrete levels up to 1.06 MeV and assumed the continuum levels above 1.2 MeV.

3.17.3 Discussion

The total, capture and inelastic scattering cross sections are shown with the ENDF/B-IV and CNEN-2 data in Figs. 3.17.1~3.17.3, respectively. The CNEN-2 evaluation assumed hypothetical resonance levels below 460 eV.

As to the total cross section, the results of the present potential (JENDL-1 and CNEN-2) are a little higher than the result of Moldauer potential[25] (ENDF/B-IV) in the high energy region. The structure in ENDF/B-IV between 10 and 100 eV is caused by that of the capture cross section.

The value of the capture resonance integral calculated from the JENDL-1 cross section is 62.02 barns which agrees well with 61.7±2.3 barns obtained by Baerg *et al.*[171] This may suggest the reasonable connection between the $1/v$ and the smooth cross section. The ENDF/B-IV evaluation seems to have adjusted the cross section value between 10 and 100 eV so as to obtain the reasonable value of the resonance integral. Above 100 eV, the ENDF/B-IV gives very low capture cross section, by assuming much larger value of D_{obs} than the other evaluations. Gruppelaar *et al.*[21] pointed out that the value of D_{obs} in ENDF/B-IV must be too large comparing with D_{obs} of N-magic nuclide ^{136}Cs.

As to the inelastic scattering cross section, the ENDF/B-IV gives the lowest value in the continuum region.

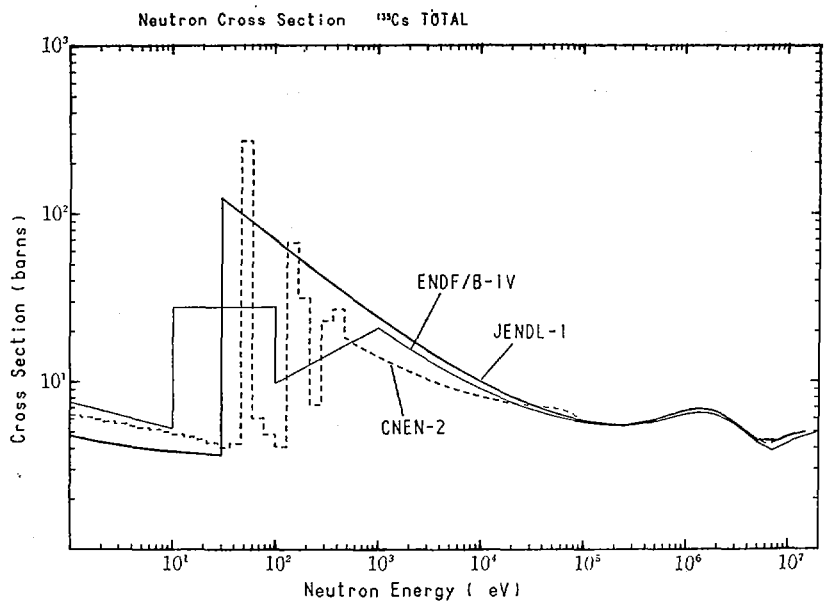

Fig. 3.17.1 Total cross sections of ^{135}Cs.

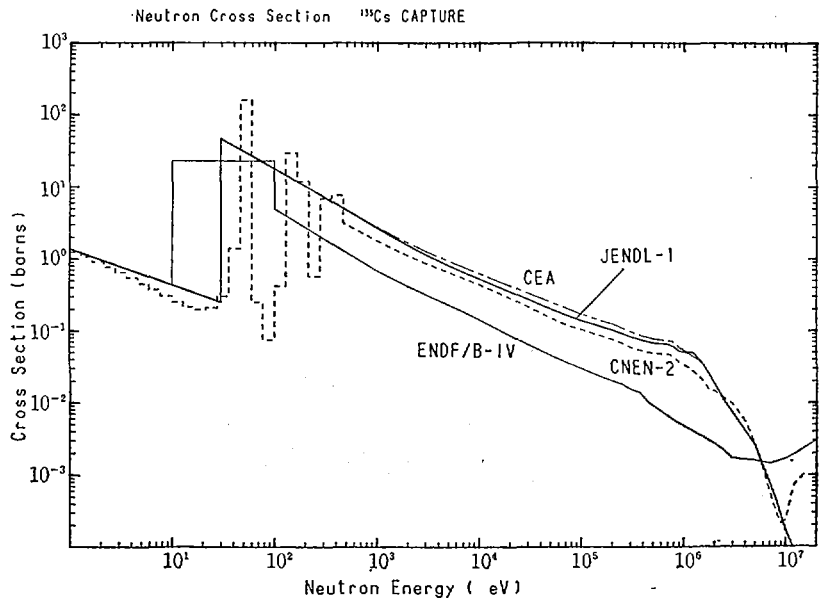

Fig. 3.17.2 Capture cross sections of ^{135}Cs.

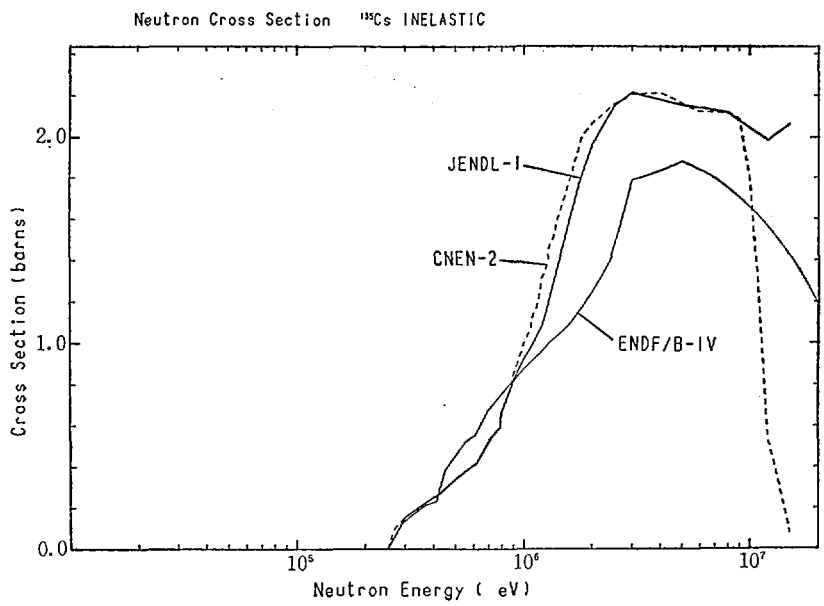

Fig. 3.17.3 Inelastic scattering cross sections of ^{135}Cs.

On the other hand, the value of CNEN-2 is a little larger than that of JENDL-1 probably due to assuming some hypothetical discrete levels.

3.18 Cesium-137

3.18.1 Status of experimental data

The experimental data are very scarce. The thermal capture cross section measured by Stupegia[173] is the only practically available experimental datum. The recommendation of BNL-325 is based on this datum in both 2nd[33] and 3rd[29] editions. The resonance parameters measured by Jung *et al.*[172] were not distinguished from those of ^{135}Cs and could not be used in the present work. No other experimental data have been reported.

3.18.2 Evaluation

The value of thermal capture cross section was taken as 0.11 barns on the basis of the experimental datum of Stupegia.[173] As no resonance parameters are known, the $1/v$ type cross section was applied to the capture cross section up to 550 eV which corresponds to a half of the mean level spacing used in the statistical model

calculation. The elastic scattering cross section was calculated with the effective scattering radius of 5.05 fm.

The cross sections were calculated in the energy range above 550 eV with the optical and statistical models. The mean level spacing and the radiation width were estimated from the trends of neighboring nuclides. Seven discrete levels were adopted and the levels were assumed to be continuum above 2.15 MeV.

3.18.3 Discussion

The total, capture and inelastic scattering cross sections are shown with the other evaluated data in **Figs. 3.18.1～3.18.3**, respectively. The CNEN-2 evaluation adopted 11 resolved resonances which are probably hypothetical ones.

The total cross sections of the three evaluations agree well with one another in the energy region above 100 keV. The total cross section of CNEN-2 is very low in the unresolved resonance region between 10 and 100 keV because of the very low s-wave strength function as seen in **TABLE 2.4.**

The capture cross sections of JENDL-1 and CNEN-2 agree fairly well with each other in the energy region above 10 keV, while ENDF/B-IV gives much lower values between 10 keV and 3 MeV and shows strange energy dependence below 5 keV and above 1 MeV.

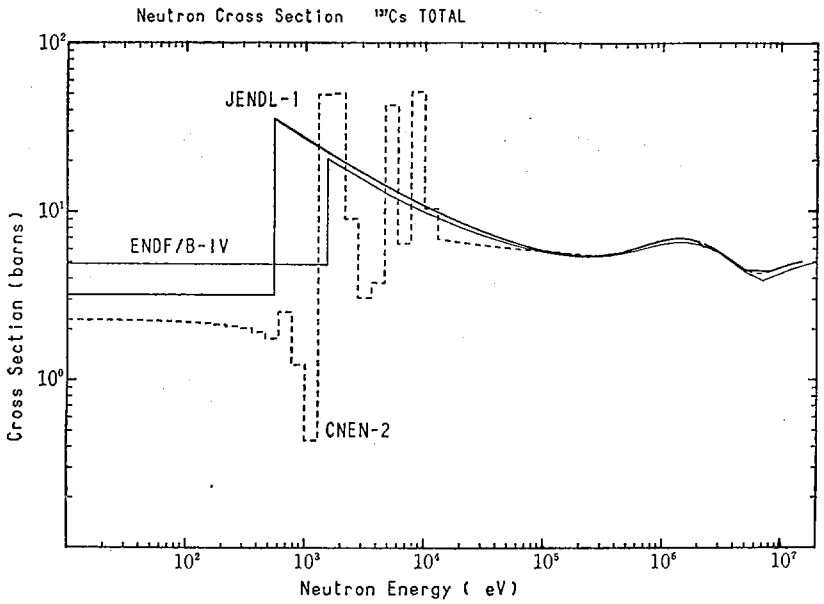

Fig. 3.18.1 Total cross sections of ^{137}Cs.

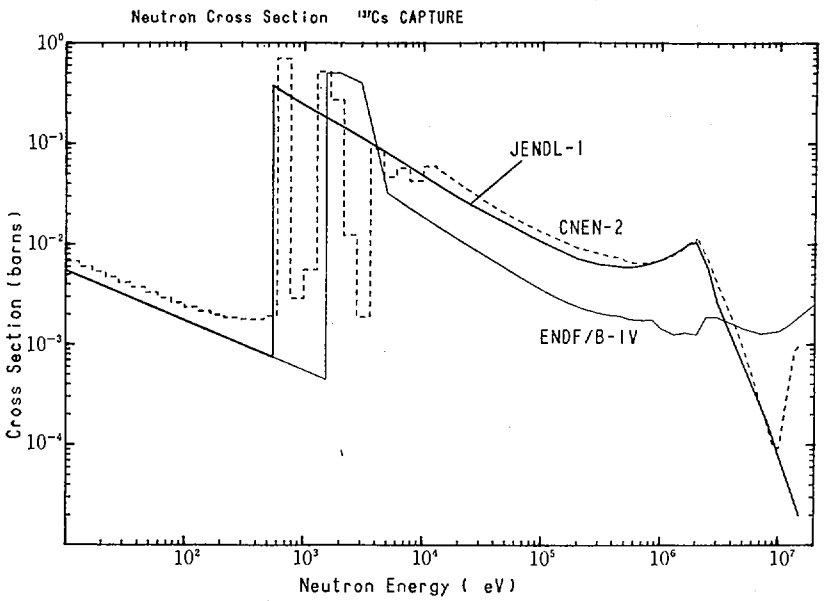

Fig. 3.18.2 Capture cross sections of ^{137}Cs.

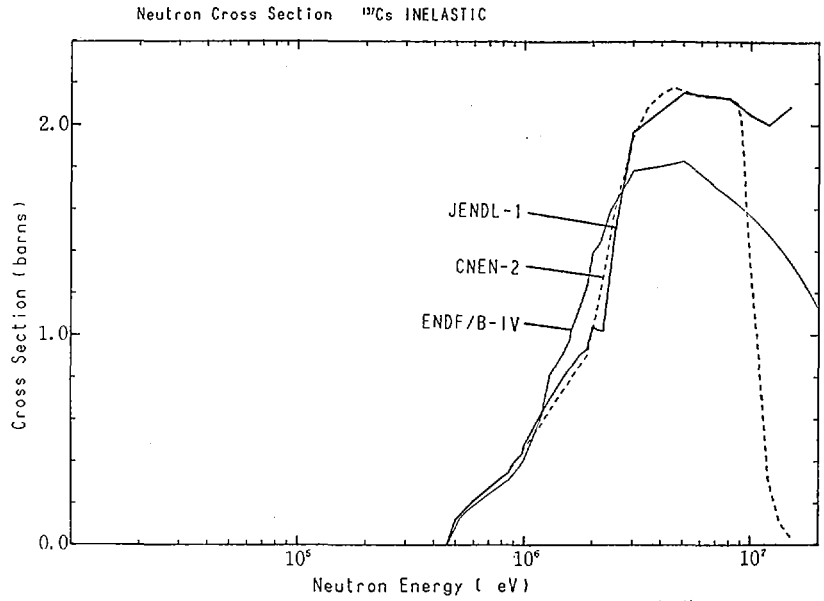

Fig. 3.18.3 Inelastic scattering cross sections of ^{137}Cs.

As to the inelastic scattering cross section, the JENDL-1 and CNEN-2 evaluations give very analogous results, while the values of ENDF/B-IV are different. The decrease of the JENDL-1 values above 2 MeV is caused by our adopting two levels which are hardly excited because of their large difference of spin values ($3/2^+$ and $1/2^+$) from that of the ground state ($7/2^+$).

3.19 Neodymium-143

3.19.1 Status of experimental data

A considerable number of experiments have been reported on the thermal capture cross section. BNL-325 2nd edition[33] recommended $\sigma_{n,\gamma}{}^{th}=335\pm10$ barns on the basis of 4 experiments made by 1960. BNL-325 3rd edition[29] recommends 325 ± 10 barns, possibly based on the recommendation by Walker[42] who took account of a new datum of Cabell and Wilkins.[174] Recently, however, Vertebny *et al.*[175] gave 338 ± 8 barns. The capture resonance integral was measured by Tattersall *et al.*[52] who reported R.I.$<$50 barns. The thermal scattering cross section was reported to be 80 barns by Vertebny *et al.* The total cross section at the thermal neutron energy was measured by Hay[176] and by Vertebny *et al.* but the results are very discrepant.

Experimental data are numerous for resonance parameters. BNL-325 2nd edition recommended the parameters for 7 levels up to 190 eV on the basis of 5 experiments made by 1963. Since then Karzhavina *et al.*[177], Migneco *et al.*[178], Rohr *et al.*[179] and Tellier[180] gave the parameters in higher energy region. The resonance spins have been assigned by Alves *et al.*[181], by Cauvin *et al.*[182], and by Stolovy *et al.*[183] Based on these new experimental data, BNL-325 3rd edition recommends the neutron widths for 112 levels up to 5,503 eV, 39 of which are given the radiation widths. After the present evaluation, Musgrove *el al.*[194] gave the radiation widths for many resonances in keV region, most of which are p-wave ones, from their capture measurements. Several measurements have been made on the α-emission widths.

At the time of the present evaluation, no experimental data were available for total, capture, elasitc and inelastic scattering cross sections above resonance region. Recently the capture cross section was measured by Musgrove *et al.*[184] in the energy range between 2.5 and 25 keV and by Nakajima *et al.*[185] from 5 to 400 keV. These two sets of data agree fairly well with each other. It was also reported that the total and capture cross sections had been measured by Hockenbury *et al.*[57]* up to 100 keV.

3.19.2 Evaluation

As to the resonance parameters, we compared the experimental data of Tellier,[180] Rohr *et al.*[179] and the

* Numerical results of these measurements were not published.

data adopted in ENDF/B-III with one another. We mainly adopted the neutron widths of Tellier, but added two levels including a negative resonance appeared in the other experiments. As the result, the adopted data agree with those recommended in BNL-325 3rd edition which was not published at the time of the present decision. For the levels whose radiation width is not given, the value of 85 meV was assumed according to the evaluation of ENDF/B-III. The s-wave and p-wave assignment was made by considering the magnitude of the reduced neutron width and theoretically expected distribution of levels as described in section 2. 3. 1. Thus the resonance parameters were determined for 111 levels, 51 of which were assigned as s-wave resonances.

The thermal capture cross section calculated from the resonance parameters is 305 barns which is a little lower than the recommended value of 325±10 barns in BNL-325 3rd edition. The difference was corrected by applying the $1/v$ type cross section. The elastic scattering cross section was calculated with the effective scattering radius of 4. 65 fm. The (n, α) cross section was ignored in the present work.

According to the statistical examination described in section 2. 4, some levels seem to be missing above 4. 7 keV, and the connecting energy was set at 4. 65 keV.

The cross sections were calculated in the energy region above 4. 65 keV with the optical and statistical models. The γ-ray strength function was determined so that the calculated capture cross section might connect smoothly with the resonance cross section. Fourteen discrete levels were taken into account up to the energy of 2. 37 MeV and levels were assumed to be continuum in the energy region above 2. 45 MeV.

3. 19. 3 Discussion

The total, capture and inelastic scattering cross sections are shown with the other evaluated data and the experimental data in **Figs. 3. 19. 1～3. 19. 3**, respectively.

The total cross sections of JENDL-1, RCN-2 and CNEN-2 are slightly lower than that of ENDF/B-IV in the energy region above 100 keV. Below 100 keV, the values of JENDL-1 and RCN-2 are about 40% lower than the others. This reflects the difference of the strength function. The present optical potential gives $S_0=2.8\times10^{-4}$, while the CNEN-2 adopted $S_0=3.3\times10^{-4}$ in the unresolved resonance region below 100 keV.

The thermal capture cross section calculated from the resonance parameters is a little too low in JENDL-1, even though a negative resonance was taken into account. Though the $1/v$ background cross section was applied, it may be preferable to adjust the parameters of the negative resonance. The capture resonance integral calculated from the resonance parameters is considerably higher than the measured value of Tattersall *et al.*[52] in each of the four evaluations.

The capture cross section of JENDL-1 in the energy region above 4. 5 keV is 20% lower than the recently measured data of Musgrove *et al.*[184] and of Nakajima *et al.*[185], with which the evaluated values of RCN-2, CNEN-2 and ENDF/B-IV agree very well. The γ-ray strength function was so determined in the present

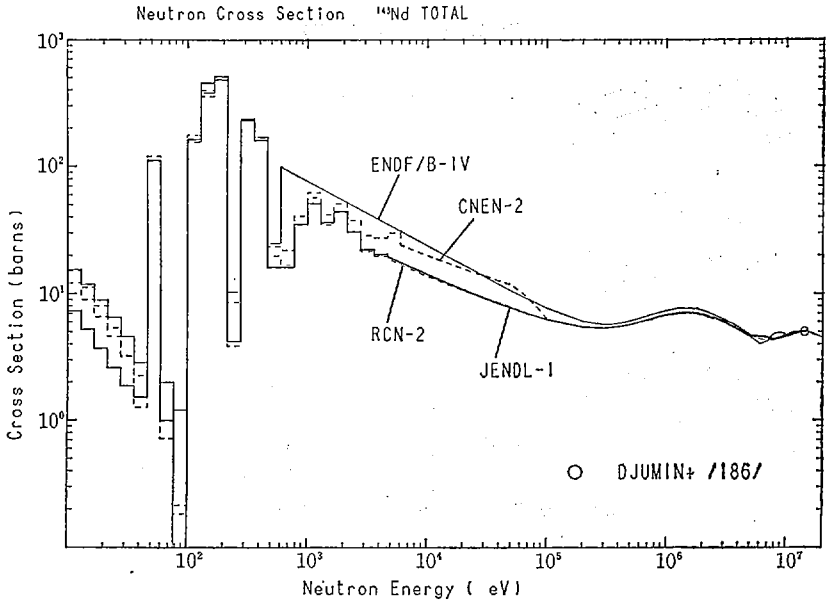

Fig. 3. 19. 1 Total cross sections of ^{143}Nd.

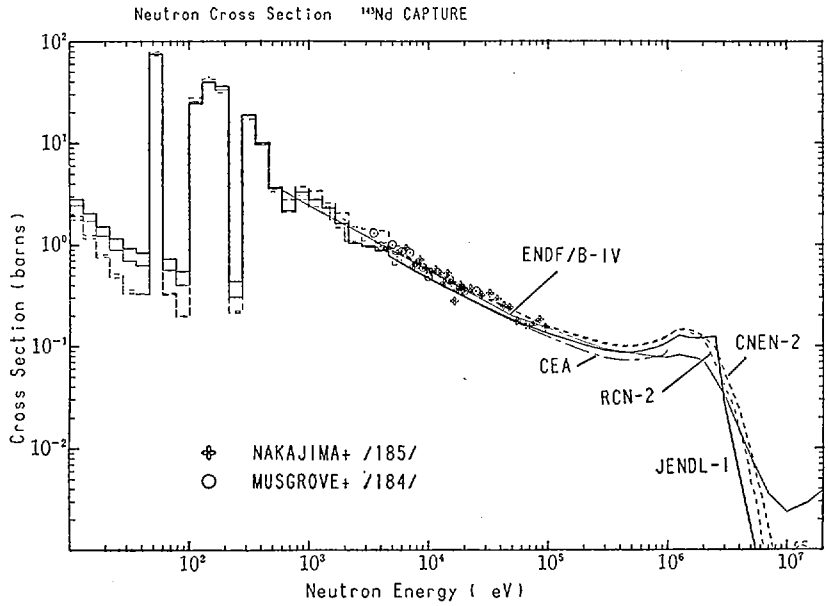

Fig. 3.19.2 Capture cross sections of ^{143}Nd.

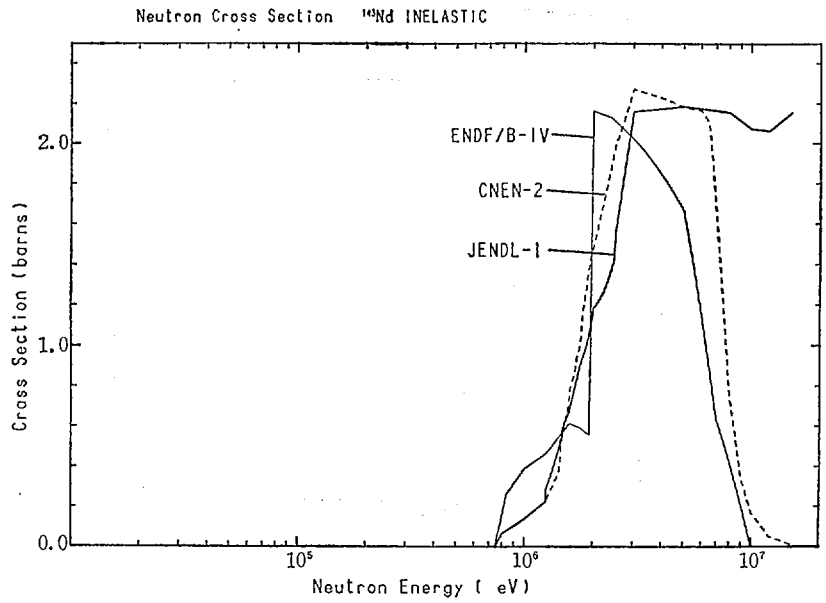

Fig. 3.19.3 Inelastic scattering cross sections of ^{143}Nd.

work that the calculated capture cross section connected smoothly to the resonance cross section based on the parameters of Tallier[180]. Recently, however, Musgrove *et al.* deduced the parameters from their capture measurements for many p-wave resonances which were not found by Tellier in his transmission measurements. Therefore the capture cross section calculated from Tellier's parameters must be too low, resulting underestimation of the present γ-ray strength function. The present l-assignment of the resonance levels must be also in error and all the levels must be reassigned as s-wave resonances. After reassignment of l, the staircase plot of the levels gives $D_{obs} \fallingdotseq 35$ eV, which will give more appropriate value of S_γ. The difference among the evaluations above 1 MeV may be attributed to the different calculation models.

As to the inelastic scattering, the value of JENDL-1 agrees fairly well with those of RCN-2 and CNEN-2 up to 1.5 MeV. RCN-2 and CNEN-2 adopted more discrete levels and give higher value in the energy range above 1.5 MeV. On the other hand, ENDF/B-IV gives much higher value below 1.5 MeV, probably due to coupled channel effects.

3.20 Cerium-144

3.20.1 Status of experimental data

The thermal capture cross section and the resonance integral were measured by Lantz[187]. BNL-325 adopted the data of Lantz in both 2nd[33] and 3rd[29] editions. No other experimental data are available.

3.20.2 Evaluation

For the thermal capture cross section, we adopted the data of Lantz[187] which gives $\sigma_{n,\gamma}{}^{th}=1.0\pm0.1$ barns. Since no resonance parameters are known, the $1/v$ law was assumed for the capture cross section up to 500 eV, which corresponds to a half of the mean level spacing used in the statistical model calculation. The elastic scattering cross section was calculated by assuming the effective scattering radius of 4.6 fm.

The cross sections were calculated in the energy range above 500 keV with the optical and statistical models. Two discrete levels were adopted and the levels were assumed to be continuum in the energy range above 1 MeV. The level spacing and the radiation width were determined by taking account of the trends of neigh-

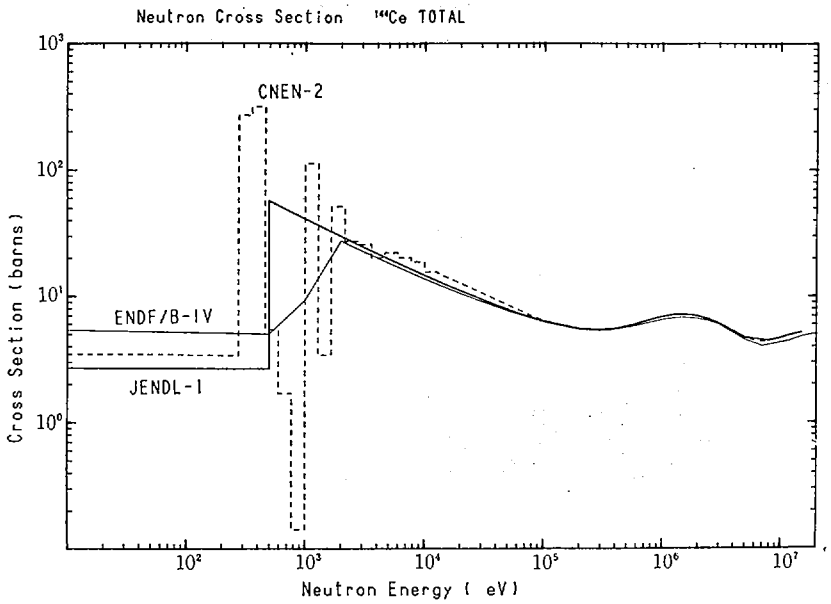

Fig. 3.20.1 Total cross sections of ^{144}Ce.

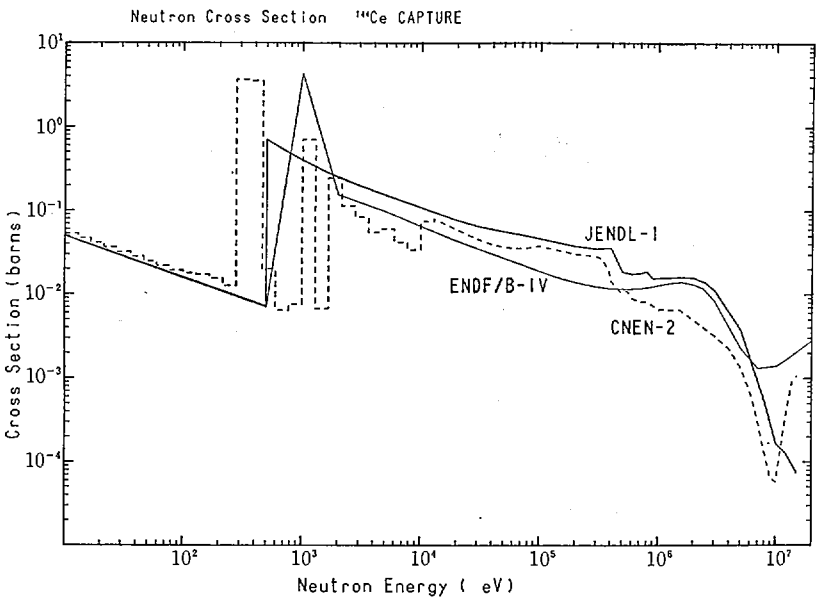

Fig. 3.20.2 Capture cross sections of ^{144}Ce.

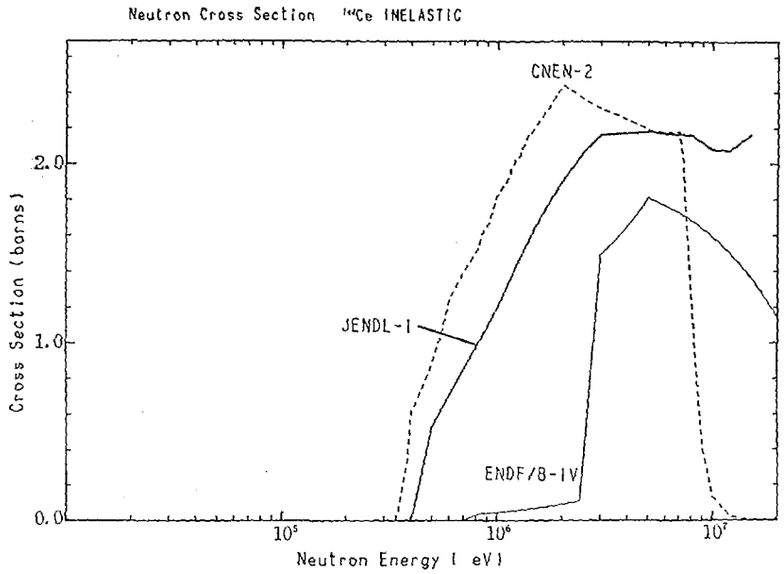

Fig. 3.20.3 Inelastic scattering cross sections of ^{144}Ce.

boring nuclides.

3.20.3 Discussion

The total, capture and inelastic scattering cross sections are shown with those of ENDF/B-IV and CNEN-2 in Figs. 3.20.1~3.20.3, respectively. The CNEN-2 evaluation adopted resolved resonance parameters for 13 levels which are probably hypothetical ones.

The total cross sections of the three evaluations agree fairly well with one another in the energy region above 10 keV.

As to the capture cross section, discrepancies are large among the three evaluations. The difference of the structure above a few hundred keV may be caused by the difference in the inelastic scattering cross section. The capture resonance integral of JENDL-1 is 1.55 barns which is smaller than the measured value by Lantz[187] (2.6±0.26 barns). The CNEN-2 evaluation gives 2.72 barns by introducing hypothetical resonances.

As to the inelastic scattering cross section, even the threshold energies are different among the three. The level of 398 keV in JENDL-1 is based on experiments and that of 800 keV was assumed from the statistical trends. On the other hand, the CNEN-2 evaluation adopted 18 discrete levels for which no experimental evidences were found. The ENDF/B-IV evaluation did not take any discrete level and gives much different energy dependence from those of the other evaluations.

3.21 Neodymium-144

3.21.1 Status of experimental data

The thermal capture cross section has been measured by Pomerance,[53] by Walker and Thode[188] and by Cabell and Wilkins.[174] The experimental values scatter between 0 and 4.8 barns. BNL-325 3rd edition[29] recommends $\sigma_{n,\gamma}{}^{th}=3.6\pm0.3$ barns on the basis of the newest experiment by Cabell and Wilkins. The thermal scattering cross section was measured by Koehler and Wollan[189] and by Vertebny *et al.*[175] Both authors gave 1.0±0.2 barns. No resonance integral has so far been measured.

As for the resonance parameters, the neutron widths were obtained for 20 resonances up to 13.5 keV by Karzhavina *et al.*[177] and for 35 resonances up to 19.4 keV by Tellier.[180] BNL-325 3rd edition recommends the neutron widths for 35 resonances mainly on the basis of the measurements by Tellier, but gives the radiation widths only for two resonances on the basis of the data of Karzhavina *et al.* After the present evaluation Musgrove *et al.*[184] deduced the radiation widths for many levels including p-wave resonances from their capture measurements.

At the time of the present evaluation, no experimental data were available on the capture cross section

above the resonance region. Recently the capture cross section was measured in the energy range from 3 to 70 keV by Musgrove *et al.*[184] and from 5 to 350 keV by Kononov *et al.*[190] The total cross section was measured by Pineo *et al.*[191] between 3 and 650 keV. Some experiments have been reported on the differential elastic and inelastic scattering cross sections in MeV region, but the numerical results are not yet available.

3.21.2 Evaluation

The resonance parameters were taken for 35 levels from BNL-325 3rd edition. For the resonance whose radiation width is not given, Γ_γ=80 meV was assumed by averaging the values of two resonances given by Karzhavina *et al.*[177] With the method described in section 2.3, 20 resonances were assigned as the p-wave ones.

The thermal capture cross section calculated from these parameters is 2.26 barns and is a little lower than 3.6±0.3 barns recommended in BNL-325 3rd edition. The difference was corrected by applying the $1/v$ type background cross section. The effective scattering radius was assumed to be 4.6 fm. As described in section 2.4, the statistical examination suggests that some resonance levels might be missing above 8 keV. The connecting energy was set at 7.73 keV.

The cross sections were calculated with the optical and statistical models in the energy range from 7.73 keV to 15 MeV. Eleven discrete levels were considered in the energy up to 2.37 MeV and the continuum levels were assumed above 2.5 MeV. The γ-ray strength function was determined so that the calculated cross section might join smoothly to the resonance cross section at 7.73 keV.

3.21.3 Discussion

The total, capture and inelastic scattering cross sections of JENDL-1, RCN-2, CNEN-2 and ENDF/B-IV are compared with one another as well as with the experimentlal data in **Figs. 3.21.1~3.21.3**, respectively.

All the evaluated total cross sections are considerably lower than the measured data of Pineo *et al.*[191] The total cross sections of JENDL-1, RCN-2 and CNEN-2, calculated with the present optical potential are a little higher in the energy region above 500 keV than that of ENDF/B-IV.

As to the capture cross section, the values of JENDL-1 agree fairly well with the recently measured data of Musgrove *et al.*[184] and of Kononov *et al.*[190], though the present evaluation was made before publication of these measured data. In contrast with cases of ^{143}Nd and ^{145}Nd, p-wave level missing in Tellier's data[180] little affects the present determination of the γ-ray strength function, because the connecting energy was set as low as 7.73 keV. However, the present p-wave assignment must be in error, as the levels detected by Tellier are s-wave resonances accoding to the analysis of Musgrove *et al.*[184]

The inelastic scattering cross sections of JENDL-1, RCN-2 and CNEN-2 agree fairly well with one another

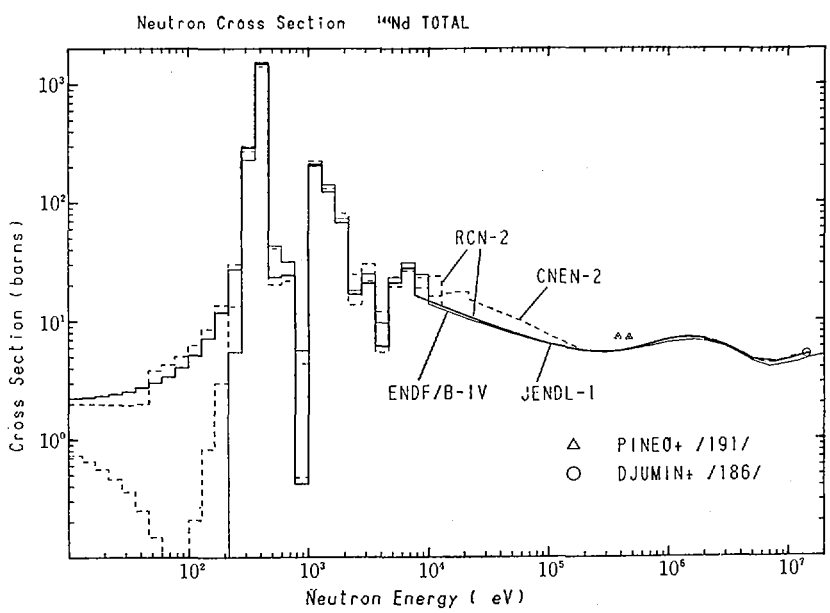

Fig. 3.21.1 Total cross sections of ^{144}Nd.

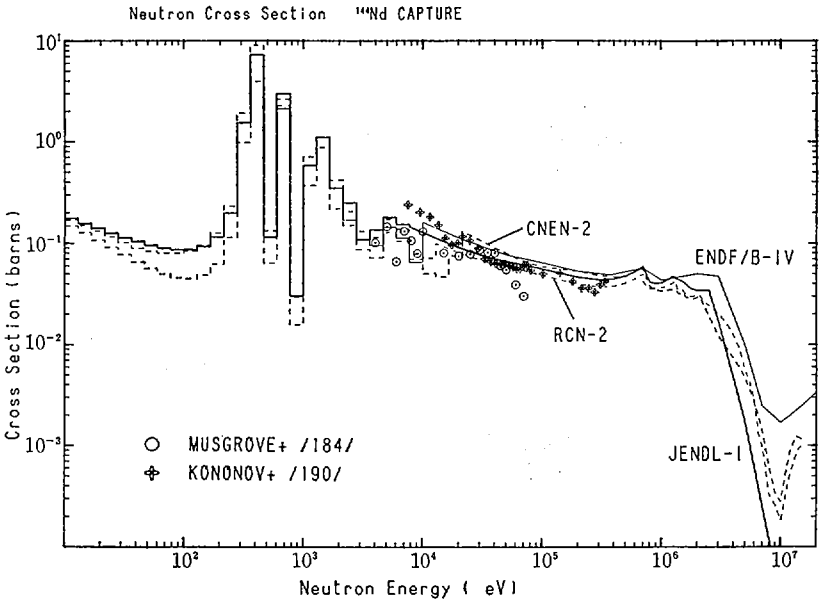

Fig. 3.21.2 Capture cross sections of ^{144}Nd.

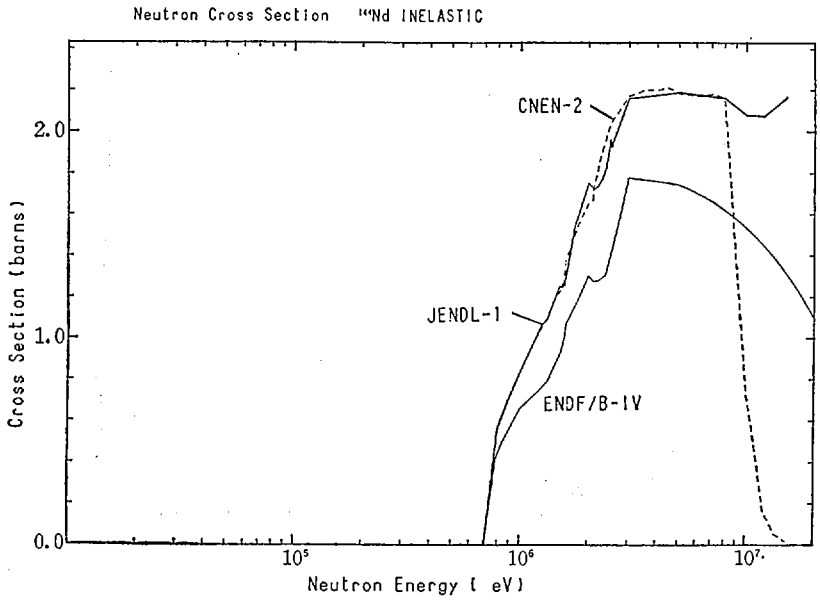

Fig. 3.21.3 Inelastic scattering cross sections of ^{144}Nd.

up to 1.5 MeV, but RCN-2 and CNEN-2 assumed more discrete levels above 2 MeV and gives a little higher values. The values of ENDF/B-IV are much lower probably due to the optical potential parameters, and these lowest values of inelastic scattering cross section are reflected on the capture cross section above 1 MeV as seen in Fig. 3.21.2.

3.22 Neodymium-145

3.22.1 Status of experimental data

Several experiments have been reported on the thermal capture cross section. BNL-325 2nd edition[33] recommended $\sigma_{n,\gamma}{}^{th}=53\pm2$ barns on the basis of the experimental data measured by 1960. After that two experiments have been reported by Cabell and Wilkins[174] and Vertebny *et al.*[175] BNL-325 3rd edition[29] recommends $\sigma_{n,\gamma}{}^{th}=42\pm2$ barns possibly taking account of the low value by Cabell and Wilkins. The thermal scattering cross section was measured by Vertebny *et al.* The total cross section in the thermal neutron energy was measured by Hay and Pattenden[61] and Vertebny *et al.*[175] Some measurements have been reported on the (n, α) reaction cross section in the thermal energy region. The capture resonance integral was reported to be 130 ± 15 barns by Tattersall *et al.*[52] BNL-325 3rd edition recommends 240 ± 35 barns possibly deriving from

the experimental data of Cabell and Wilkins.[174]

The resonance parameters have been reported by more than ten authors. BNL-325 2nd edition recommended the parameters for only 6 levels up to 103.6 eV on the basis of the experiments made by 1963. After that Karzhavina *et al.*[177], Migneco *et al.*[178], Rohr *et al.*[179] and Tellier[180] extended the number of resolved resonances. Particularly Tellier gave the parameters in the energy up to 4.6 keV from his transmission measurements. Works have been made also on J-assignment by Alves *et al.*[181], by Cauvin *et al.*[182] and by Stolovy[183]. On the basis of these new experiments, BNL-325 3rd edition recommends the neutron widths for 191 resonances up to 4,637 keV, but gives the radiation widths for only 34 resonances. Recently Musgrove *et al.*[184] deduced the radiation widths for many resonances beween 2.5 and 4 keV from their capture measurements.

At the time of the present evaluation, no experimental data were available on the smooth cross sections in the energy range above resolved resonances except near 14 MeV. After that the capture cross section was mesured by Musgrove *et al.*[192] from 3 to 500 keV and by Nakajima *et al.*[185] from 5 to 400 keV. The total and capture cross sections were measured by Hockenbury *et al.*[77] below 150 keV.

3.22.2 Evaluation

As to the resonance parameters, the experimental data of Rohr *et al.*[179] and of Tellier[180] were compared with each other and with those recommended in ENDF/B-III. We mainly adopted the neutron widths of Tellier, but added the lowest 4.04 eV level, which was not reported by Tellier nor by Rohr *et al.*, taking account of other experiments. The present parameters agree fairly well with those recommended in BNL-325 3rd edition which was not available at the time of the present work. The s-wave and p-wave assignment was carried out with the method described in section 2.3. The radiation width of 60 meV was assumed for the levels whose value was not experimentally known. The parameters of 177 levels were thus determined up to 4,637 eV, 76 of which were assigned as the s-wave resonances.

The thermal capture cross section calculated from these parameters is 7.85 barns which is much smaller than the experimental values. We adopted the value of 42 barns recommended in BNL-325 3rd edition and the difference was corrected by applying the $1/v$ type background cross section. The elastic scattering cross section was calculated with effective scattering radius of 4.55 fm. The statistical examination mentioned in section 2.4 suggests that some levels may be missing in the energy range above 3.6 keV. The connecting energy was thus set at 3.6 keV.

The cross sections between 3.6 keV and 15 MeV were calculated with the optical and statistical models. Seven discrete levels were considered up to 1.39 MeV and levels were assumed to be overlapping above 1.4 MeV. As no capture data existed at the time of the present calculation, the γ-ray strength function was determined so that the calculated capture cross section might connect smoothly with the resonance cross section.

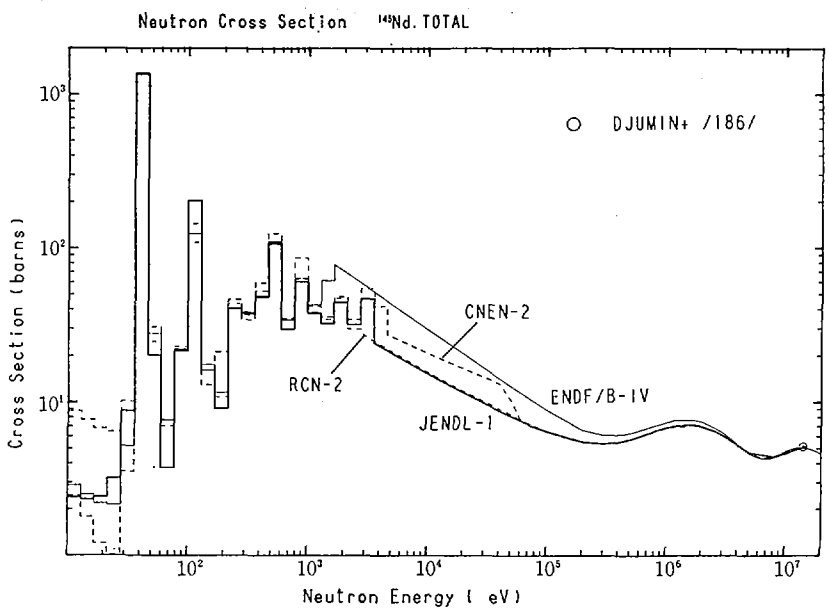

Fig. 3.22.1 Total cross sections of ^{145}Nd.

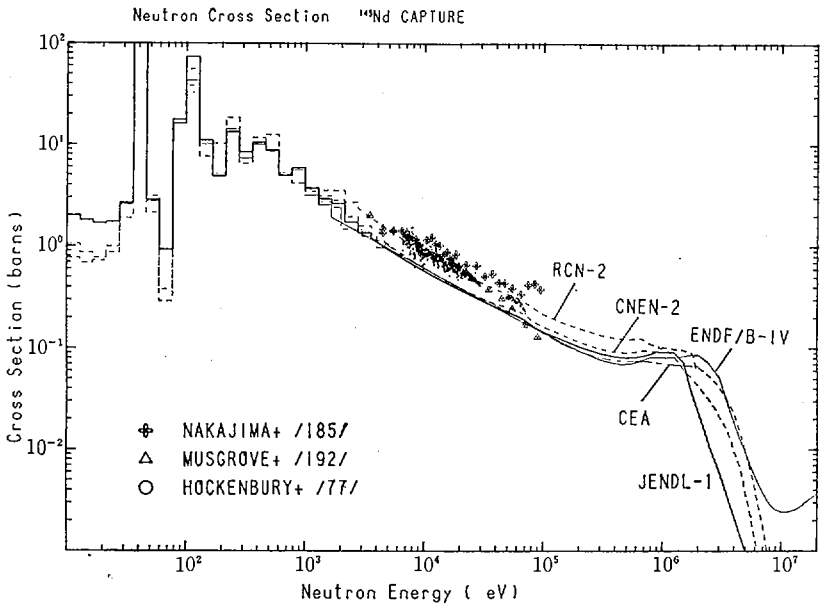

Fig. 3.22.2 Capture cross sections of ^{145}Nd.

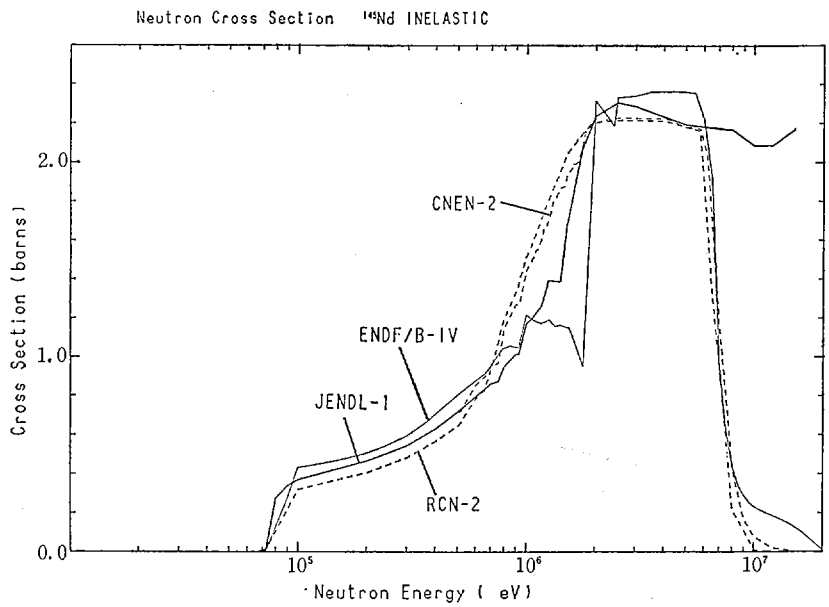

Fig. 3.22.3 Inelastic scattering cross sections of ^{145}Nd.

3.22.3 Discussion

The total, capture and inelastic scattering cross sections are shown with curves of the other evaluations and with the measured data in **Figs. 3.22.1～3.22.3**, respectively.

The total cross section of JENDL-2 is lower than that of ENDF/B-IV, which is calculated with the coupled channel optical model, in the energy range below a few MeV. The present optical potential gives the s-wave strength function $S_0=3.19\times10^{-4}$, which is smaller than the measured values. Therefore the total cross section of JENDL-1 may be too small particularly below 50 keV.

The capture resonance integral calculated from the resonance parameters and the $1/v$ background cross section is 266.3 barns, which is larger than the measured value of Tattersall *et al.*[52] but agrees fairly well with the recommended value in BNL-325 3rd edition. The capture cross sections of all the evaluations except RCN-2 agree with one another in the energy region from 5 keV to 1 MeV but are 30% lower than the recently measured data by Hockenbury *et al.*[77], Musgrove *et al.*[192] and Nakajima *et al.*[185], which agree well with one another. The most recent evaluation of RCN-2[19] took account of these measurements. As in the case of ^{143}Nd, the underestimation of JENDL-1 is caused by its smooth connection to the resonance cross section which is also underestimated by considerable p-wave level missing in the resonance parameters deduced by

Tellier[180] in the energy above 2 keV. The present p-wave assignment must be also in error and all the resonances should be assigned as s-wave ones. The discrepancy of the capture cross section among the evaluations above 1 MeV cannot be explained by the competition with the inelastic scattering, and is probably due to some different models used in the calculation. However, no detailed information is available on the other evaluations.

As to the inelastic scattering cross section, the RCN-2 and CNEN-2 evaluations assumed much more discrete levels than JENDL-1 in the energy range above 500 keV and give higher values. The decrease of ENDF/B-IV cross section above 1 MeV is difficult to be understood, since more discrete levels were assumed than JENDL-1.

3.23 Promethium-147

3.23.1 Status of experimental data

All the measurements on the capture cross section have been made in the thermal neutron energy region. BNL-325 2nd edition[33] recommended on the basis of the measurements by 1962: $\sigma_{n,\gamma}{}^{th}=200\pm50$ barns [$\sigma_{n,\gamma}{}^{th}$ (5.4-day ^{148g}Pm)$=124\pm13$ barns and $\sigma_{n,\gamma}{}^{th}$ (41-day ^{148m}Pm)$=111\pm11$ barns], which are obviously inconsistent with each other. Since then three measurements have been reported by Fenner and Large[193], by Cabell[194] and by Mowatt and Walker.[195] BNL-325 3rd edition[29] recommends $\sigma_{n,\gamma}{}^{th}=181\pm7$ barns [$\sigma_{n,\gamma}{}^{th}$ (^{148g}Pm)$=96.0\pm1.8$ barns and $\sigma_{n,\gamma}{}^{th}$ (^{148m}Pm)$=85\pm5$ barns], possibly based on the absolute value of ^{148g}Pm production cross section by Cabell and the ratio of $\sigma_{n,\gamma}{}^{th}$ (^{148g}Pm)/$\sigma_{n,\gamma}{}^{th}$ (^{148m}Pm) by Fenner and Large. The total cross section in the thermal energy region has been reported by Harvey *et al.*[141], by Codding *et al.*[196], by Kirouac *et al.*[197] and by Belanova *et al.*[198]

The capture resonance integral has been measured by Schuman and Berreth,[199] by Fenner and Large[193] and by Cabell.[194] The data of Schuman and Berreth are more than twice of those of Fenner and Large. BNL-325 3rd edition recommends R. I. (^{148g}Pm)$=1,274\pm66$ barns on the basis of measurements by Cabell and R. I. (^{148m}Pm)$=1,026\pm280$ barns whose experimental basis is not clear.

The resonance parameters were obtained from the total cross section measurements by Harvey *et al.*[141], Codding *et al.*[196], Kirouac *et al.*[197] and Belanova *et al.*[198] No works have so far been made on the spin assignment. BNL-325 3rd edition recommends the neutron widths for 39 resonances up to 317 eV including one negative resonance, but gives the radiation widths for only 5 levels.

The total cross section was measured by Codding *et al.*[196] up to 1 keV and by Foster and Glasgow[70] in MeV region. No other data are available on the cross sections in the energy range above resolved resonances.

3.23.2 Evaluation

The resonance parameters recommended in BNL-325 3rd edition were adopted for 39 levels including a negative resonance. For the levels whose radiation width is not given, the value of 68 meV was assumed by averaging the values of 5 levels given in BNL-325. However, with some careless mistake, the value of 63 meV was actually adopted in the JENDL-1 file.

The thermal capture cross section calculated from these parameters is 182 barns which agrees very well with the value of 181 ± 7 barns recommended in BNL-325 3rd edition. Hence no background correction were required. The elastic scattering cross section was calculated by assuming the effective scattering radius of 4.45 fm.

The statistical examination suggests that some levels may be missing in the energy range above 200 eV. It should be noted, however, that the resonance parameters are the only reliable experimental data for this nuclide in the epithermal energy region, and therefore cannot be ingnored. Taking account of the above situation, the connecting energy was tentatively set at 300 eV.

The cross sections were calculated in the energy range above 300 eV with the optical and statistical models. Six discrete levels were taken into account up to 686 keV and the overlapping levels were assumed above 720 keV. The γ-ray strength function was obtained from the resolved resonance parameters.

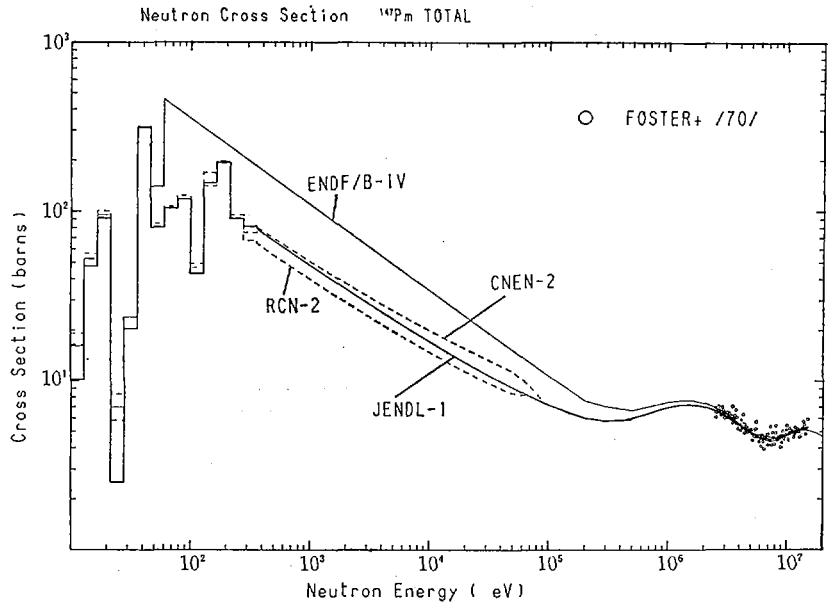

Fig. 3.23.1 Total cross sections of ^{147}Pm.

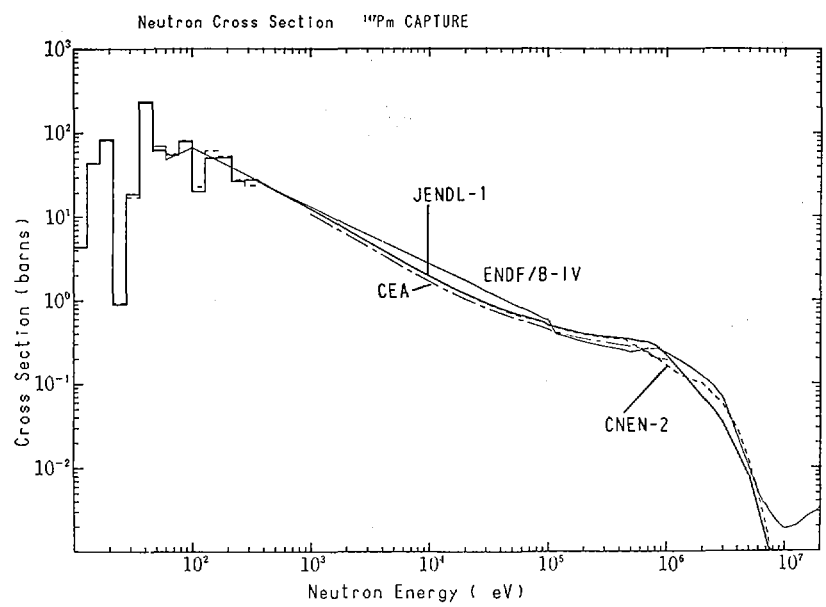

Fig. 3.23.2 Capture cross sections of ^{147}Pm.

3.23.3 Discussion

The total, capture and inelastic scattering cross sections are shown in Figs. 3.23.1~3.23.3 with the measured data as well as data of the other evaluations.

In the mass region of $A=145\sim150$, the s-wave strength function and the effective scattering radius are very sensitive to the nuclear mass, and it was found very difficult to fit these values with a single set of the optical potential parameters. Hence the potential parameters were changed at $A=147$ as seen in Eq. (1) of section 2.2.1. The effective scattering radius was also discontinuously changed at $A=147$ as seen in Fig. 2.7. For ^{147}Pm and ^{147}Sm, the small values are assumed for the effective scattering radius as in the case of lighter nuclides, though the optical potential parameters are those for heavier nuclides. It is probable that the effective scattering radius is underestimated for these nuclides.

The total cross section of JENDL-1 is lower than those of the other evaluations in the resonance region. This might be caused by our adopting much smaller effective scattering radius as mentioned above. The RCN-2 and CNEN-2 evaluations adopted the same optical potential parameters as JENDL-1, while the ENDF/B-IV adopted the coupled channel model and gives higher values below a few MeV, although both potentials reproduce the measured data of Foster and Glasgow[70] in the higher energy region.

The capture resonance integral calculated from the resonance parameters is 2,206 barns which agree well

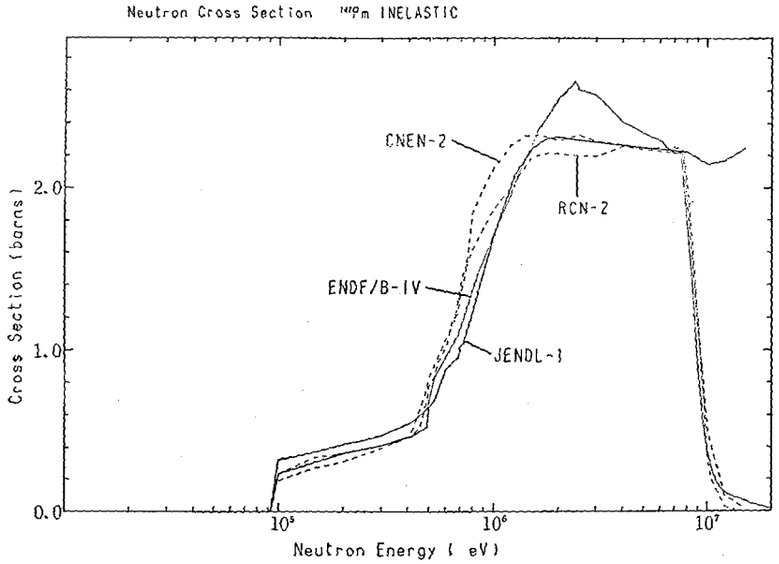

Fig. 2.23.3 Inelastic scattering cross sections of ^{147}Pm.

with the value recommended in BNL-325 3rd edition within the quoted error. In the energy region above resonances, the differences of the capture cross section among the various evaluations are 50% at most.

As to the inelastic scattering cross section, the curves of JENDL-1, RCN-2 and CNEN-2 agree fairly well with one another below 450 keV, while the values of ENDF/B-IV are slightly higher. This difference may be caused by the difference of the optical potential parameters. The total cross section is also higher in ENDF/B-IV. The rapid increase of the RCN-2 and CNEN-2 values above 500 keV can probably attributed to their adopting more discrete levels as seen in TABLE 2.12.23.

3.24 Samarium-147

3.24.1 Status of experimental data

The thermal capture cross section has been measured by several experimenters and the reported values scatter between 50 and 87 barns. BNL-325 2nd edition[33] recommended $\sigma_{n,\gamma}{}^{th}=87\pm60$ barns on the basis of measurements by Tattersall *et al.*[52] However, newer measurements gave lower values than those of Tattersall *et al.*, and BNL-325 recommends $\sigma_{n,\gamma}{}^{th}=64\pm5$ barns in the 3rd edition[29] on the basis of the measurements by Dobrozemsky *et al.*[200] The total cross section was measured by Eiland *et al.*[201] in the energy range between 0.025 eV and 1.2 keV. They gave $\sigma_T{}^{th}=75\pm6$ barns and BNL-325 3rd edition adopts this value. The capture resonance integral was measured by Fenner and Large[193] and by Dobrozemsky *et al.* Their results agree well with each other and lie near 640 barns. However, BNL-325 3rd edition recommends R. I.$=714\pm50$ barns, based on the calculation with the resonance parameters obtained by Eiland *et al.* from their transmission measurements.

The resonance parameters have been deduced from more than ten measurements. BNL-325 2nd edition recommended the parameters for 13 resonances up to 100 eV on the basis of 9 measurements made by 1965. After that several new measurements have been made. Particularly Eiland *et al.*[201] extended the upper limit of the resolved resonances up to 1,161 eV. Resonance spins were assigned by Cauvin *et al.*[182] and by Karzhavina *et al.*[202] up to 400 eV. Taking account of these new measurements, BNL-325 3rd edition recommends the neutron widths for 132 resonances including a negative resonance up to 1,161 eV, but gives the radiation widths for only 6 resonances. Very recently Mizumoto *et al.*[203] obtained the resonance parameters up to 2 keV from their capture and transmission measurements. The α-widths have been reported by several authors.

At the time of the present evaluation, the capture cross section had been measured only by Macklin *et al.*[204] at 30 keV. Recently it was measured by Kononov *et al.*[205] in the energy range from 5.5 to 350 keV and by Mizumoto *et al.*[203] from 3.3 to 300 keV. As is evident from Fig. 3.24.2, the data of Kononov *et al.* are much higher than those of Mizumoto *et al.* and of Macklin *et al.* which agree with each other. Neither

elastic nor inelastic scattering cross sections have so far been measured.

3.24.2 Evaluation

The resonance parameters recommended in BNL-325 3rd edition were adopted except for the negative resonance for which the parameters deduced by Codding *et al.*[196] were adopted. For the levels whose radiation width is not given, the average value of 67 meV was assumed. The s-wave and p-wave assignment was made by considering the magnitude of the neutron widths as described in section 2.3.1. Thus the resonance parameters were determined for 132 levels, 81 of which were assigned as p-wave resonances.

The thermal capture cross section calculated from the resonance parameters is 68.2 barns which lies within the scatter of the experimental data. Therefore no background correction was applied. The thermal elastic scattering cross section was calculated with the effective scattering radius of 4.45 fm. The statistical examination suggests that some levels are missing in the high energy region. The connecting energy was thus set at 750 keV.

The cross sections were calculated with the optical and statistical models in the energy range between 750 keV and 15 MeV. Fourteen discrete levels were taken into account up to 1.18 MeV and levels above 1.2 MeV were assumed to be overlapping. The γ-ray strength function was so adjusted that the calculated capture cross section became 1.0 barns at 30 keV, i.e., agreed with the daum of Macklin *et al.*[204] within the quoted error.

3.24.3 Discussion

The total, capture and inelastic scattering cross sections are shown with the measured and the other evaluated data in Fig. 3.24.1～3.24.3, respectively.

The total cross section of JENDL-1 is the lowest below 1 MeV. The s-wave strength function may be a little underestimated with the present optical potential as seen in TABLE 2.4. The ENDF/B-IV evaluation adopted the coupled channel optical model and gives the largest total cross section.

The present resonance parameters well reproduce the thermal capture cross section. The calculated capture resonance integral is 763.3 barns which agrees with the recommended value in BNL-325 3rd edition within the quoted error but is a little larger than the measured data of Dobrozemsky *et al.*[200] and Fenner and Large[193].

As to the capture cross section above resonance energy region, the datum of Macklin *et al.*[204] was the only available one at the times of all the four evaluations. The values of JENDL-1 and RCN-2 agree with this value within the quoted error but the JENDL-1 gives a little lower values than RCN-2. The values of CNEN-2 are a little lower than those of JENDL-1 in the unresolved resonance region below 70 keV but agree

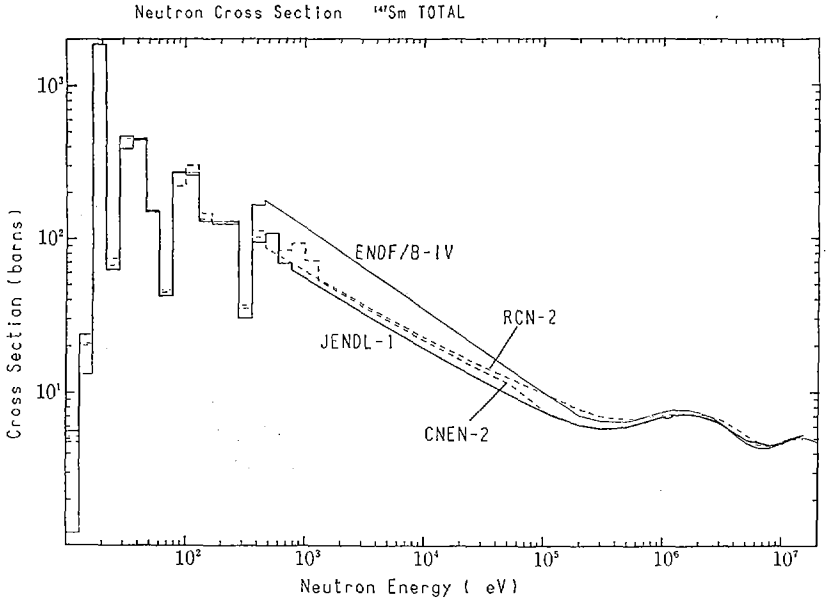

Fig. 3.24.1 Total cross sections of ^{147}Sm.

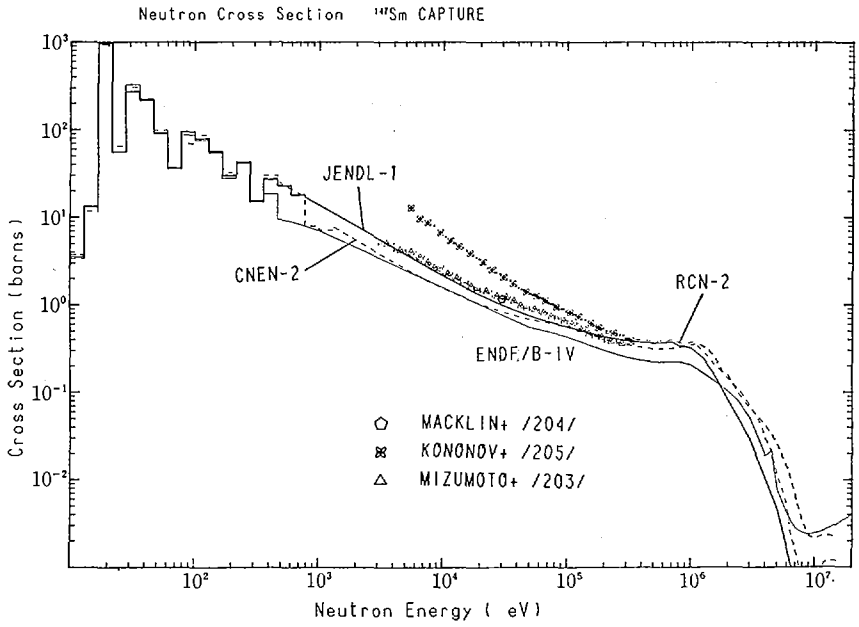

Fig. 3.24.2 Capture cross section of ^{147}Sm.

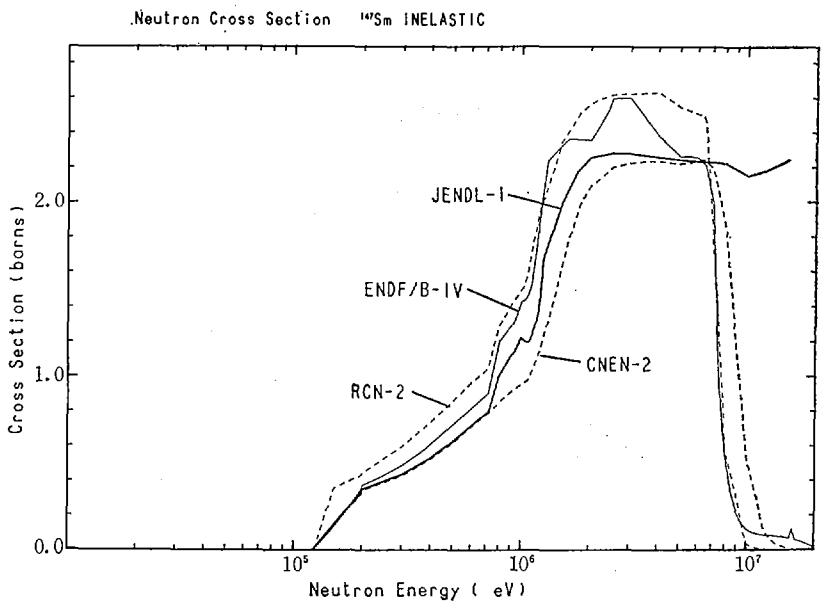

Fig. 3.24.3 Inelastic scattering cross sections of ^{147}Sm.

with the JENDL-1 values between 100 keV and 1 MeV. The ENDF/B-IV evaluation gives the lowest values in the energy range up to 2 MeV. After these works were made, the measured data were reported by Kononov *et al.*[205] and Mizumoto *et al.*[203] The data of Mizumoto *et al.* are a little higher than the values of JENDL-1 and agree well with those of RCN-2 in the energy region below 100 keV. The energy dependence of the data by Kononov *et al.* is very different from those of the data by Mizumoto *et al.* and of the existing evaluated data. It may be quite difficult to reproduce the energy dependence of the data of Kononov *et al.* with the statistical model calculation. Furthermore, the extrapolation of their data gives much larger cross section in the resonance region than that obtained from the resonance parameters. Abandoning the data of Kononov *et al.* on the basis of the arguments above mentioned, we believe that the data of RCN-2 are reasonable and that the JENDL-1 values should be slightly increased below 100 keV.

As seen in TABLE 2.5, the γ-ray strength function of ENDF/B-IV agrees with that obtained from the resolved resonance parameters, but is about one half of those adopted in the other evaluations. The JENDL-1, CNEN-2 and RCN-2 evaluations applied the spherical optical model to very deformed nucleus such as ^{147}Sm and may underestimate the neutron strength function as is suspected from the small total cross section shown

in **Fig. 3.24.1**. The large value of the γ-ray strength function may have been required to compensate the underestimation of the neutron strength function. This problem should be further investigated.

As to the inelastic scattering cross section, the values of RCN-2 and ENDF/B-IV are larger than those of JENDL-1 and CNEN-2. This may be caused by the difference of the optical potential parameters, as the same tendency is observed in the total cross section. It should be noted that an apparent discrepancy between RCN-2 and the others near the threshold energy is not substantial but is caused by the difference of the energy mesh points.

3.25 Samarium-149

3.25.1 Status of experimental data

Much experimental works have been made in the thermal energy region, since this nuclide is a famous poison for thermal reactors. The measured values of the thermal capture cross section scatter between 41,000 barns and 49,000 barns. BNL-325 recommends the lowest value of $\sigma_{n,\gamma}{}^{th}=41,000\pm2,000$ barns in both 2nd[33] and 3rd[29] editions. This recommended value is, however, still higher than the measured values of the total cross section by Pattenden[63] and by Asami *et al.*[206], who gave $\sigma_T{}^{th}=39,900\pm600$ barns and $37,000\pm1,000$ barns, respectively. The resonance integral is very difficult to be measured because of its large resonance near 0.1 eV, and was measured only by Aitken and Cornish[207] who reported R.I.=4,400 barns.

The resonance parameters have been measured by more than 20 experimenters. BNL-325 2nd edition recommended the parameters for 29 resonances up to 99 eV on the basis of measurements by 1965. Since then a lot of measurements have been made. Particularly Karzhavina and Popov[208] deduced the neutron widths for the resonances up to 248 eV. The resonance spins were assigned for 41 resonances up to 185 eV by Cauvin *et al.*[182] and for 84 resonances up to 259 eV by Karzhavina *et al.*[202] The α-widths have also been measured. Based on these measurements, BNL-325 3rd edition recommends the neutron widths for 88 resonances up to 250 eV including a bound state, but gives the radiation widths for only 4 lowlying levels. BNL-325 gives the resonance spins for 41 levels up to 140 eV. Very recently Mizumoto *et al.*[203] deduced the resonance parameters up to 520 eV.

As to the capture cross section above resonance region, the experimental datum of Macklin *et al.*[204] at 30 keV was the only available one at the time of the present evaluation. After that, three sets of measured data have been reported, *i.e.*, the data of Kononov *et al.*[205] between 5.5 and 342.5 keV, of Hockenbury *et al.*[77] below 70 keV and of Mizumoto *et al.*[203] from 3.3 to 300 keV. These three recent data agree fairly well with one another in the energy region above 20 keV but are about 60% larger than the datum of Macklin *et al.* at 30 keV.

The total cross section was measured by Pineo *et al.*[191] in the energy range from 15 to 600 keV, the data being in fair agreement with the measured total cross section of natural Sm element. Recently it was reported that Hockenbury *et al.*[77] measured the total cross section between 20 eV and 150 keV*. No experimental data have so far been reported on the elastic and inelastic scattering cross sections.

3.25.2 Evaluation

We adopted the resonance parameters recommended in BNL-325 3rd edition up to 250 eV with modifying the resonance spins according to the work of Karzhavina *et al.*[202] For the levels whose radiation width was not reported, the average value of 61 meV was assumed. We assigned 34 resonances as the s-wave ones and the remaining 52 resonances as the p-wave ones with the method described in section 2.3.1.

The thermal capture cross section becomes 41,500 barns when calculated with these parameters. The value falls within the scatter of the experimental data, and no background correction was applied. The elastic scattering cross section was calculated with the effective scattering radius of 8.4 fm. The cross section was calculated with these parameters up to 150 eV, above which it was judged that a significant number of levels were missing according to the statistical examination mentioned in section 2.4.

---

* Their numerical data were not published.

Above 150 eV, the cross sections were calculated with the optical and statistical models. Ten discrete levels were adopted up to 640 keV, and the continuum levels were assumed above 650 keV. The calculated capture cross section was normalized to the datum of Macklin *et al.*[204] at 30 keV, by adjusting the γ-ray strength function.

3.25.3 Discussion

The total, capture and inelastic scattering cross sections are shown with the other evaluated data as well as the measured data in Figs. 3.25.1~3.25.3, respectively.

As to the total cross section above a few tens of keV, the values of JENDL-1 and CNEN-2, calculated with the present potential, are considerably lower than those of RCN-2 and ENDF/B-IV and the measured data of Pineo *et al.*[191] below 1 MeV. The present optical potential parameters underpredict the s-wave strength function as seen in TABLE 2.3 : 3.88×10^{-4} compared with the measured value of $(5.1\pm0.9)\times10^{-4}$. The calculated scattering radius is 6 fm, while the value used in the resonance region is 8.4 fm, which was obtained by interpolation of the measured values. These facts suggest that the present global optical potential is not quite appropriate in this mass region. The total cross section must be underestimated below 1 MeV in JENDL-1 and CNEN-2.

The calculated thermal capture cross section agrees with the measured values within the quoted error. The calculated value of resonance capture integral is 3,454 barns, which is a littles lower than 4,400 barns reported by Aitken and Cornish[207].

As to the capture cross section above the resonance energy region, all the evaluated data seem to be normalized to the datum of Macklin *et al.*[204] at 30 keV, and therefore are about 60% lower than the recent by measured data[77,203,205]. In the present evaluation, the average level spacing D_{obs} was adjusted to be 1.63 eV so as to meet with the datum of Macklin *et al.*, while the recommended value in BNL-325 is 2.3 ± 0.3 eV. This disagreement of D_{obs} may be caused by the present optical potential parameters, which give low s-wave strength function as mentioned above, since no such disagreement is observed in the RCN-2 and ENDF/B-IV evaluations as seen in TABLE 2.5. In order to meet with the higher values of the recent data, the radiation width should be also increased. Obvious discrepancies are observed among the evaluated data in the energy range above a few hundred keV. This may reflect the differences in the inelastic scattering cross section as discussed below.

As to the inelastic scattering cross section, the values of JENDL-1 are in fair agreement with those of RCN-2 and CNEN-2 up to about 300 keV, above which the JENDL-1 value becomes much lower than those of the others. This may be caused by the different spin assignment of the second excited level of 277 keV. We assumed $3/2^-$ for this level, while $5/2^-$ is adopted in RCN-2, $7/2^-$ in CNEN-2 and CEA. The inelastic scattering is enhanced for higher spin states since the ground state spin is $7/2^-$. Above 1 MeV, the cross section

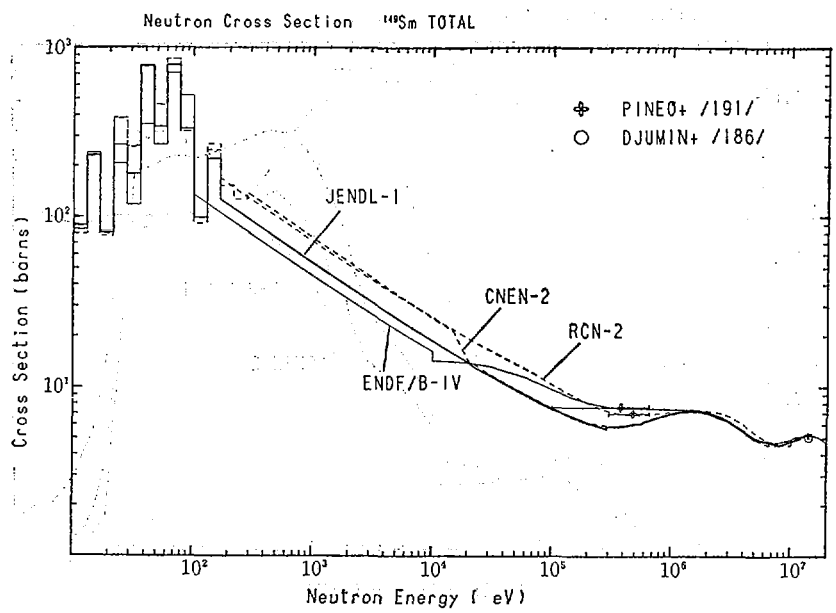

Fig. 3.25.1 Total crros sections of ^{149}Sm.

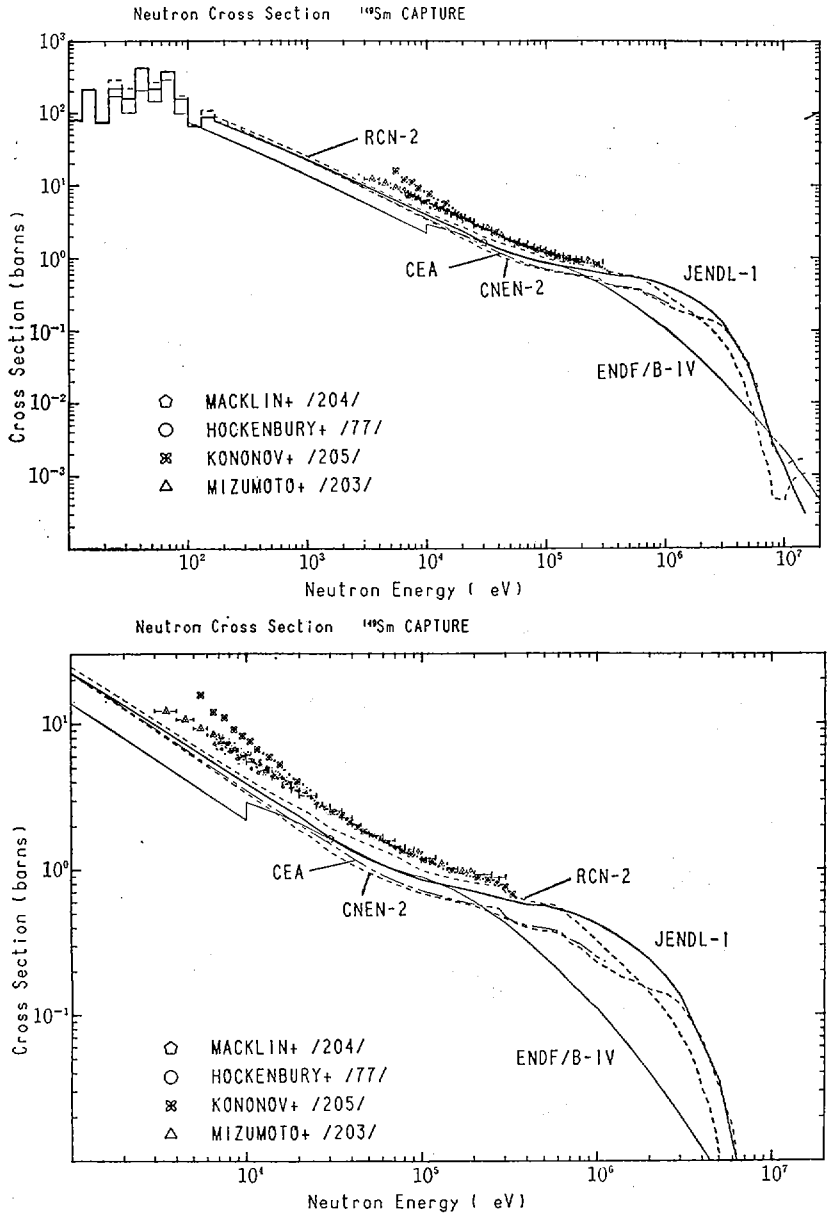

Fig. 3.25.2 Capture cross sections of ^{149}Sm.

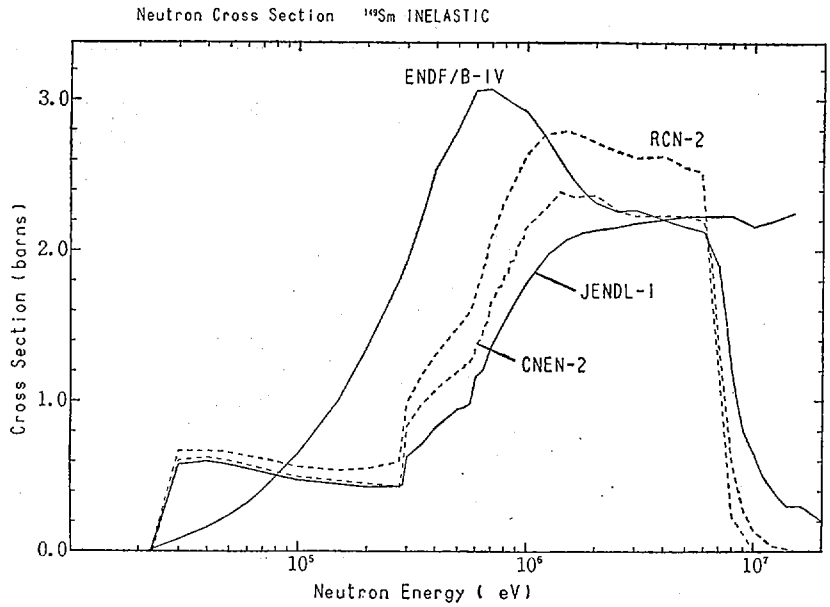

Fig. 3.25.3 Inelastic scattering cross sections of ^{149}Sm.

of JENDL-1 continues to increase, while those of the other evaluations decrease. This may be caused by our adopting a large spin cut-off parameter in this energy range as mentioned in section 2. 2. 3. The energy dependence of ENDF/B-IV is very different from the other evaluations. The reason is not clear, since no precise information is available.

3. 26 Samarium-151

3. 26. 1 Status of experimental data

The experimental data are scarce for this nuclide. The thermal capture cross section was measured by a few experimenters only in 1950's, and the results scatter between 7, 200 and 13, 000 barns. The total cross section in the thermal energy was measured by Pattenden[143], who reported $\sigma_T^{th}=15,000\pm1,800$ barns and R. I. $=3,300\pm700$ barns. BNL-325 recommends the value of Pattenden as the thermal capture cross section in both 2nd[33] and 3rd[29] editions. Recently Kirouac and Eiland[209] measured the total cross section in the energy range between 0. 01 eV and 2. 3 keV. They reported $\sigma_T^{th}=15,200\pm300$ barns and R. I. $=3,520\pm160$ barns which agree with the values of Pattenden within the quoted errors.

The resonance parameters were deduced by Harvey *et al.*[141] up to 6. 3 eV and by Pattenden[143] up to 12. 75 eV. BNL-325 3rd edition recommends $2g\Gamma_n^o$ values for 11 levels including a negative resonance mostly on the basis of the measurements of Pattenden, but gives the radiation widths only for 3 lowlying levels. After that, Kirouac anp Eiland[209] deduced the $2g\Gamma_n$ values for 120 levels up to 300 eV and the radiation widths for 13 lowlying levels from their measurements of the total cross section.

As to the cross sections above resonance region, the total cross section values measured by Kirouac and Eiland[209] are the only experimental data at the present time.

3. 26. 2 Evaluation

The resonance parameters recommended in BNL-325 3rd edition were adopted, since the data of Kirouac and Eiland[209] were not available at the time of the present evaluation. For the levels whose radiation width was not known, the average value of 74. 5 meV was assumed.

The calculated thermal capture cross section from these parameters is 12, 600 barns, which lies within the the scatter of the old experimental data but is lower than the recommended value of 15, 000±1, 8000 barns in BNL-325. The difference was compensated by adding the $1/v$ type background cross section. The elastic scattering cross section was calculated with the effective scattering radius of 8. 35 fm. The upper bound of the resolved resonance region was taken as 13. 4 eV, i. e., $E_{max}+D_{obs}/2$.

Above 13. 4 eV, all the cross sections were calculated with the optical and statistical models. The γ-ray strength function was determined from the resolved resonance parameters. We adopted 12 discrete levels up to 345 keV and assumed continuum levels above 350 keV. It should be noted that the spin of the ground state was assumed to be $5/2^-$ according to the evaluation by Nakasima and Murata[12], while BNL-325 3rd edition recommeds $7/2^-$.

3. 26. 3 Discussion

The total, capture and inelastic scattering cross sections are shown with the other evaluations in **Figs. 3. 26. 1 ~3. 26. 3**, respectively. The JENDL-1 evaluation adopted the resonance parameters up to 13. 4 eV, while the RCN-2 and CNEN-2 evaluations took the parameters of Kirouac and Eiland[209] up to more than one hundred eV.

As is the case of the other Sm isotopes, the total cross section calculated from the present optical potential parameters is considerably lower than that of RCN-2 and ENDF/B-IV in the energy range between 10 keV and 1 MeV. The present optical potential parameters predict the s-wave strength function fairly well: 3. 80 $\times10^{-4}$ compared with the measured value of $(4.0\pm1.8)\times10^{-4}$, but underpredict the effective scattering radius. Though no measured data exist for the total cross section of ^{151}Sm, the calculated total cross section might be too low, if we assume that the total cross section of ^{151}Sm is approximately the same as that of natural samarium.

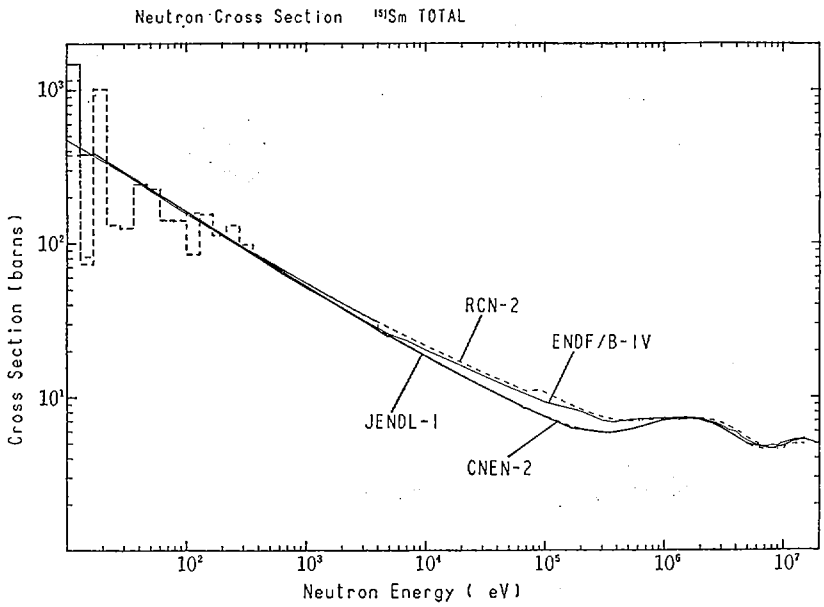

Fig. 3.26.1 Total cross sections of ^{151}Sm.

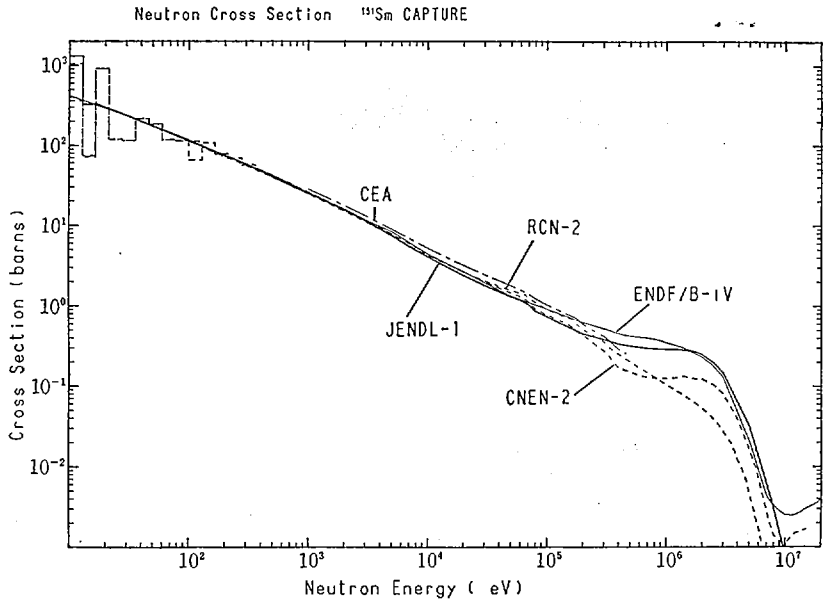

Fig. 3.26.2 Capture cross sections of ^{151}Sm.

The $1/v$ correction was applied for the thermal capture cross section so as to reproduce the 2,200 m/s value of 15,000 barns. With including this background cross section, the calculated capture resonance integral is 4,039 barns which is a little higher than the measured value. Taking it into consideration that the RCN-2 and CNEN-2 evaluations give appropriate values on both the thermal cross section and resonance integral without applying any background cross section, the resonance parameters of Kirouac and Eiland[209] should be taken.

As no experimental data exist in the capture cross section above resonance region, the γ-ray strength function was determined from the resolved resonances. The values of S_γ agree with one another among all the evaluations except CEA which assumes somewhat higher value. Hence the calculated capture cross sections are analogous among all the evaluations except CEA below 100 keV. Above 100 keV, considerable discrepancies appear, probably caused by the differences in the inelastic scattering.

As to the inelastic scattering, ^{151}Sm is a very characteristic nuclide. This nuclide has the first excited state at very low energy (4.8 keV) and has large capture cross section. This makes the calculated inelastic scattering cross section very sensitive to the calculation model. For example, as shown in TABLE 3.2, the effect of the statistical fluctuation of the neutron width is essential: Hauser-Feschbach theory with and without

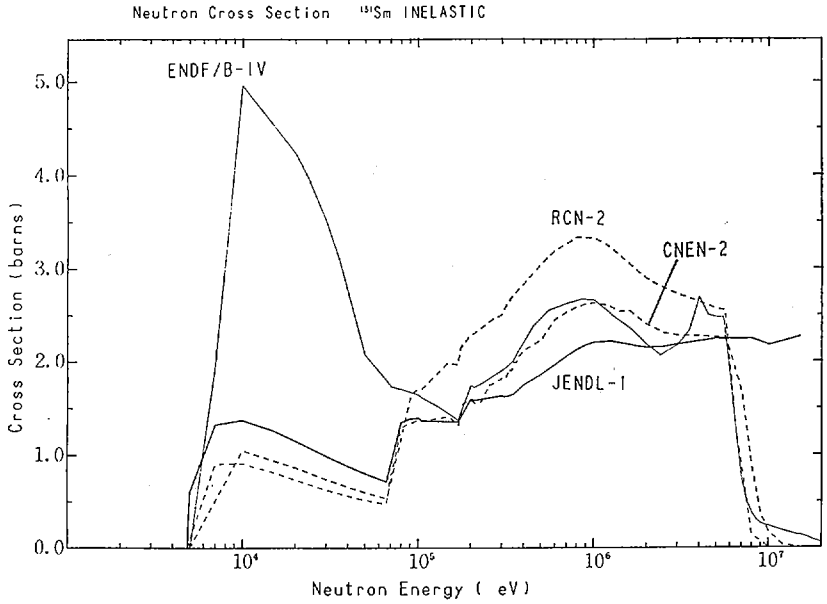

Fig. 3.26.3 Inelastic scattering cross sections of ^{151}Sm.

TABLE 3.2 Effect of calculational method on ^{151}Sm cross sections at 10 keV

	Capture (b)	Compound Elastic (b)	Inelastic (b)
H-F theory without statistical fluctuation	5.2	6.7	2.3
H-F theory with statistical fluctuation	4.1	8.7	1.4

statistical fluctuation gives a difference of a factor 2 at 10 keV. It is also seen from the table that the capture cross section is large compared with the inelastic scattering cross section at this energy, suggesting that the competition due to capture reaction should be treated accurately.

The energy dependence of the inelastic scattering cross section is similar up to 100 keV among JENDL-1, RCN-2 and CNEN-2. Above 100 keV, the RCN-2 and CNEN-2 cross sections increase more rapidly than JENDL-1. This may be attributed to their adopting more discrete levels as seen in TABLE **2.12.26**. The inelastic scattering cross section of ENDF/B-IV is very different from the other evaluations particularly from the threshold energy to 100 keV. The reason of this difference is unclear, as no precise information is available for ENDF/B-IV on this nuclide.

3.27 Europium-153

3.27.1 Status of experimental data

Considerable number of experiments have been reported for this nuclide. The thermal capture cross section has been measured by several experimenters, but the reported values scatter between 274 and 639 barns possibly due to existence of ^{151}Eu which has a large thermal capture cross section of about 9,200 barns. BNL-325 2nd edition[33] recommended $\sigma_{n,\gamma}{}^{th}=390\pm80$ barns, while its 3rd edition[29] gives 390 ± 30 barns which agrees with the recent result of Widder[210] but is a little higher than that of Moxon *et al.*[211] The total and scattering cross sections in the thermal energy range were measured by Vertebny *et al.*[212,213] who gave $\sigma_{el}{}^{th}=8\pm0.3$ barns[212] and $\sigma_T{}^{th}=282\pm10$ barns[213], which are evidently lower than the recommended values in BNL-325. To resolve these uncertainties, Razbudey *et al.*[214] made precise measurements on the total cross section and recommended $\sigma_T{}^{th}=308\pm10$ barns and $\sigma_{n,\gamma}{}^{th}=300\pm15$ barns, which are still lower than those of BNL-325 but agree fairly well with the data of Moxon *et al.* being $\sigma_{n,\gamma}{}^{th}=317\pm15$ barns.

The capture resonance integral has also been measured by several experimenters and the reported values scatter between 1,280 and 3,887 barns. BNL-325 3rd edition recommends R. I. $=1,635\pm200$ barns, probably on the basis of measurements by Rahn *et al.*[215] Two recent measurements by Van der Linden *et al.*[152] and by Kim *et al.*[216], however, gave higher values of 1,829 and 3,414 barns, respectively.

As to the resonance parameters, BNL-325 2nd edition recommended the parameters for 18 levels up to 24.1 eV, while its 3rd edition gives the neutron widths for 76 levels up to 97 eV mainly based on the measurements by Rahn *et al.*[217] but gives the radiation widths for 48 levels. After that, Vertebny *et al.*[218] gave only the resonance energies up to 659 eV.

The experimental data are considerably numerous for the capture cross section in the fast energy region. At the time of the present evaluation, available were data of Konks and Fenin[219], Konks *et al.*[220] and Harlow *et al.*[221] After that, four measurements have been made. The data of Kononov *et al.*[205] are 10% higher than those of Konks and Fenin between 5 and 350 keV. These high values of Kononov *et al.* are supported by the data of Czirr[222] which were deduced from his measurements of natural Europium and ^{151}Eu. On the other hand, the other new data of Moxon *et al.*[211], Hockenbury *et al.*[113] and Mizumoto *et al.*[223] agree with those of Konks and Fenin in the energy region below 10 keV but support the higher value of Kononov *et al.* above 50 keV. Thus three different trends exist in the capture cross section of ^{153}Eu as seen in **Fig. 3.27.2**. No experimental data are available for the total, elastic and inelastic scattering cross sections in the fast energy region.

3.27.2 Evaluation

Resonance parameters were adopted from BNL-325 3rd edition. For levels whose radiation width was not given, the value of 94 meV was assumed on the basis of the measurements by Rahn *et al.*[217]

The thermal capture cross section is calculated from the resonance parameters. The result is 71.7 barns which is in a large underestimation compared with the measured data. Though the uncertainties are still large on the thermal capture cross section, we adopted the value of 390 barns on the basis of the recommendation of BNL-325 3rd edition, and corrected the difference from the calculated value by applying the $1/v$ background cross section. The elastic scattering cross section was calculated with the effective scattering radius of 8.8 fm.

No obvious level missing was found up to 97 eV from the statistical examination and from the staircase plotting of resonances. Hence the connecting energy was determined to be 98 eV, *i.e.*, $E_{max}+D_{obs}/2$.

The cross sections were calculated in the energy region above 98 eV with the optical and statistical models. Twelve discrete levels were adopted up to 706.4 keV and continuum levels were assumed above 710 keV. The γ-ray strength function was adjusted so that the calculated capture cross section might agree with the data of Konks and Fenin[219] at 10 keV. At the final stage of evaluation, the calculated capture cross section was further modified by the eye-guide method to fit the gross structure observed in the data of Konks and Fenin in the energy range from 100 eV to 40 keV as seen in **Fig. 3.27.2**.

3.27.3 Discussion

The total, capture and inelastic scattering cross sections among JENDL-1, CNEN-2 and ENDF/B-IV are compared with one another and with the measured data in **Figs. 3.27.1~3.27.3**, respectively.

The total cross sections of JENDL-1 and CNEN-2 are lower than that of ENDF/B-IV between 100 and 500 keV. No experimental data exist in this energy range even for natural Europium. However, the total cross section is probably underestimated in JENDL-1 and CNEN-2, if we estimate it roughly by interpolation from the data of natural Samarium and Dysprosium. This may be caused by our underestimation of the shape elastic scattering cross section, because the present optical potential parameter set gives the effective scattering radius of 6.5 fm compared with the experimental value of 8.8 fm.

As mentioned in the previous subsection, the measured value of thermal capture cross section cannot be reproduced by calculation from the resonance parameters. Takahashi[224] argued that two resonances should be added at -0.007 and 0.457 eV to those given in BNL-325. The recent measurements by Widder[210] from 0.01 to 9.8 eV denied the existence of 0.457 eV level but seems to suggest the existence of bound levels. The calculated capture resonance integral is 1,529 barns, including the contribution from the added $1/v$ cross section, and is in fair agreement with the experimental value of $1,635\pm200$ barns.

There exist three trends of measured data in the capture cross section above resonance region. The data of all the evaluations reproduce the trend of Konks and Fenin[219] and are lower than the recent measured data in the energy region above 50 keV. The γ-ray strength function adopted in the JENDL-1 evaluation gives

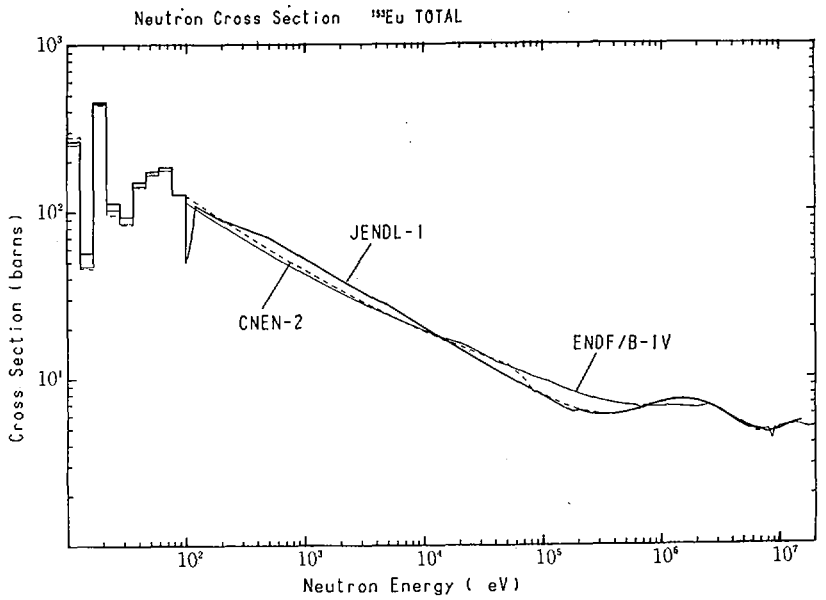

Fig. 3.27.1 Total cross sections of ^{153}Eu.

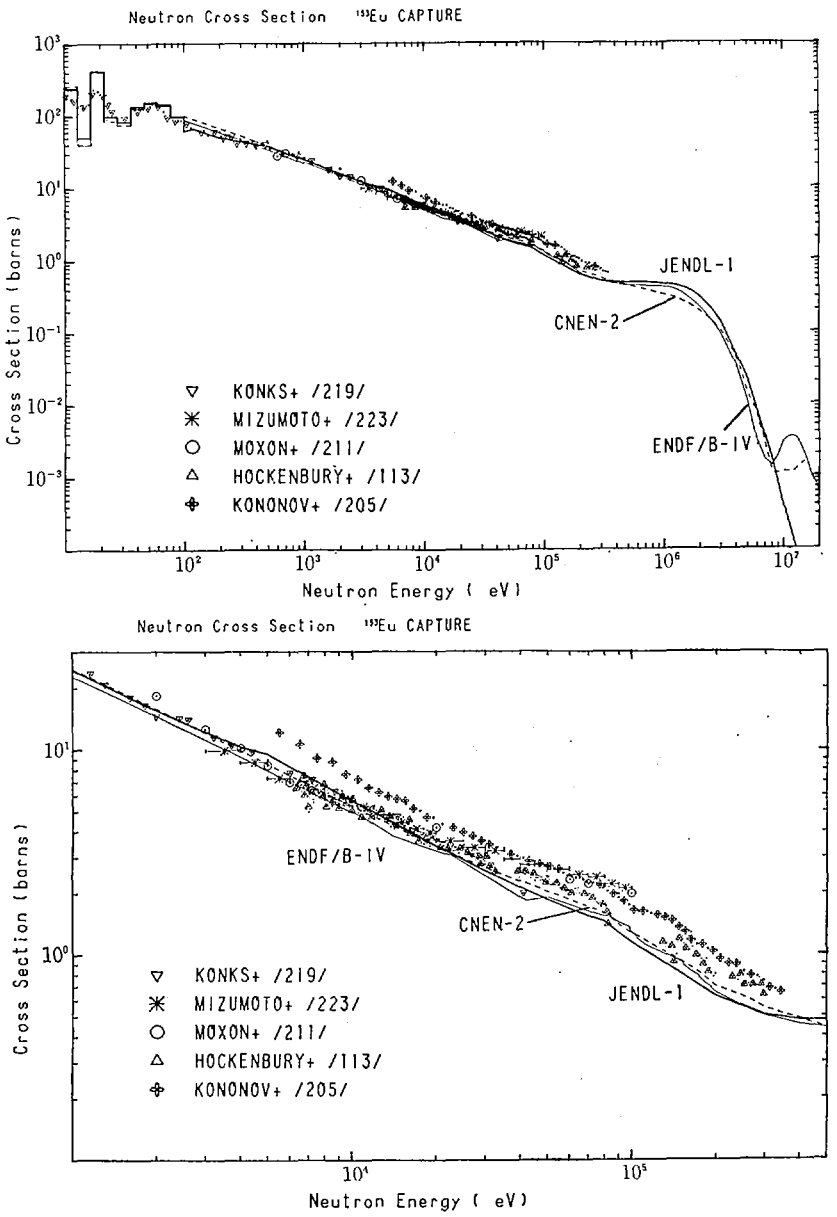

Fig. 3.27.2 Capture cross sections of ^{153}Eu.

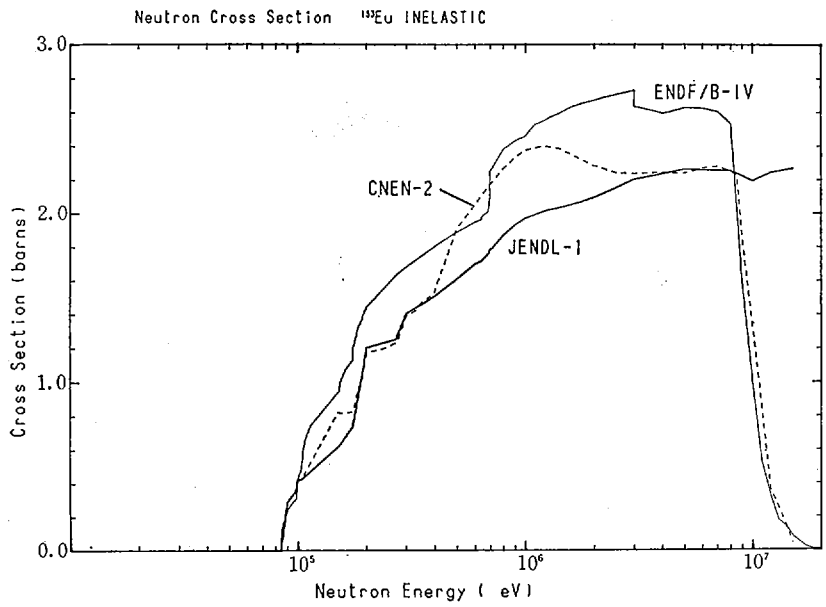

Fig. 3.27.3 Inelastic scattering cross sections of ^{153}Eu.

$D_{obs}=1.46$ eV, assuming $\Gamma_\gamma=94$ meV, which agrees well with the measured value of 1.3 ± 0.2 eV. Furthermore, it is seen that the calculated resonance cross section below 100 eV reproduces the data of Konks and Fenin. Therefore the present evaluation seems to be reasonable below 10 keV. Further work should be required in the energy region above 50 keV.

As to the inelastic scattering cross section, the ENDF/B-IV values are the largest probably due to the optical potential which gives also a large total cross section. The cross sections of JENDL-1 and CNEN-2 agree fairly well up to 400 keV except near 150 keV where an obvious discrepancy exists. In JENDL-1 and ENDF/B-IV no level exists between 270 and 630 keV, while CNEN-2 assumed continuum levels above 400 keV. The discrepancy between JENDL-1 and CNEN-2 near 150 keV cannot be understood, because both of them use the same optical potential and the same level scheme in this energy range.

3.28 Europium-155

3.28.1 Status of experimental data

Experimental data are scarce for this nuclide. The thermal capture cross section was measured in pile spectrum by Hayden *et al.*[225] and by Mowatt.[226] BNL-325 3rd edition[29] recommends $\sigma_{n,\gamma}{}^{th}=4,040\pm125$ barns on the basis of the measurements of Mowatt. No other experimental data are available at the present time.

3.28.2 Evaluation

Since no resonance parameters are available for this nuclide, the average parameters were inferred from those of neighboring nuclides. The average level spacing was assumed to be 2.5 eV, roughly extrapolated from $D_{obs}=0.7\pm0.2$ eV for ^{151}Eu and $D_{obs}=1.3\pm0.2$ eV for ^{153}Eu. Γ_γ was assumed to be 100 meV.

The thermal capture cross section was taken from recommendation in BNL-325 3rd edition, and the $1/v$ behavior was assumed up to 1.25 eV, *i.e.*, $D_{obs}/2$. Above 1.25 eV, all the cross sections were calculated with the optical and statistical models. Adopted level scheme contains 8 discrete levels up to 1.27 MeV and continuum levels above 1.45 MeV.

3.28.3 Discussion

The total, capture and inelastic scattering cross sections are compared with those of CNEN-2 and ENDF/B-IV in **Figs. 3.28.1~3.28.3**, respectively. The CNEN-2 evaluation assumed 5 hypothetical resonances.

The total cross section calculated from the present optical potential parameters shows an energy dependence more enhanced than that of ENDF/B-IV. The present optical model calculation results in the s-wave strength

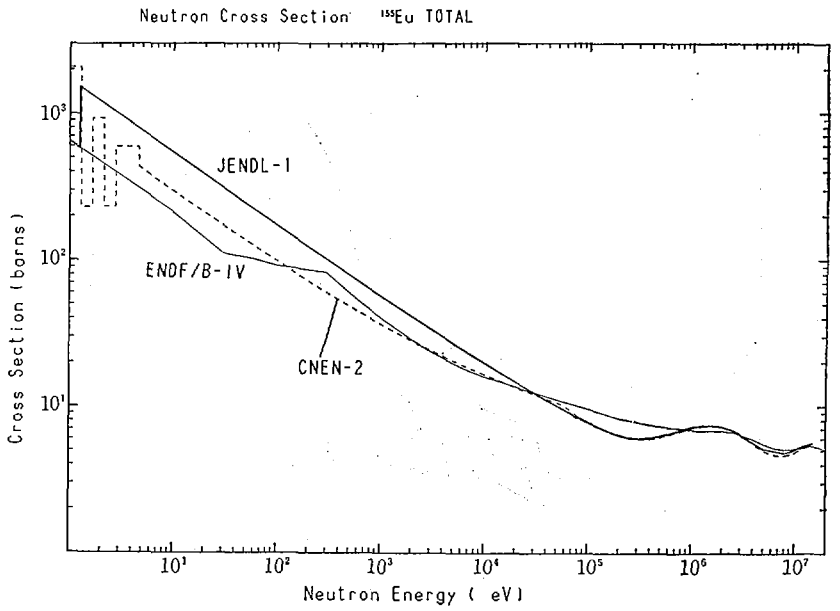

Fig. 3.28.1 Total cross sections of ^{155}Eu.

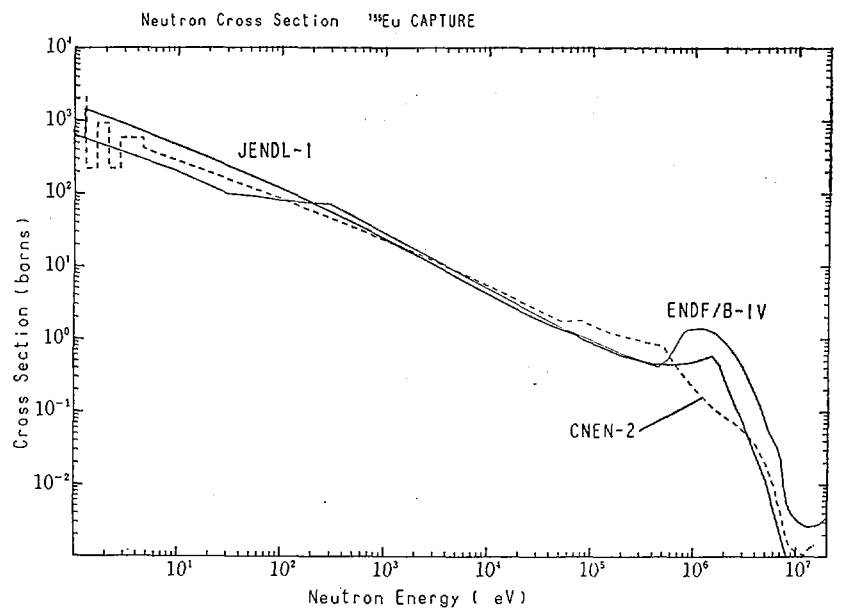

Fig. 3.28.2 Capture cross sections of ^{155}Eu.

function $S_0=4.13\times10^{-4}$ and the effective scattering radius $R=6.1$ fm. The inferred values from the experimental data of the neighboring nuclides are $S_0=2\times10^{-4}$ and $R=8\sim9$ fm. The enhanced energy dependence of the present total cross section may reflect the large S_0 and small R values. It should be noted, however, that careful investigation is required on local systematics of all the parameters, since Europium isotopes are highly deformed nuclei.

The capture cross sections of JENDL-1 and ENDF/B-IV agree fairly well with each other below 500 keV. Cn the other hand, CNEN-2 assumed a small value of D_{obs} and gives a higher capture cross section between 50 and 500 keV. A rapid decrease of CNEN-2 capture cross section above 500 keV is caused by the competition with the inelastic scattering.

Discrepancies are large in the inelastic scattering cross section. The large value of ENDF/B-IV is probably due to its optical potential. As is the case of ^{151}Sm, ^{155}Eu has a large capture cross section and its competition affects the inelastic scattering cross section particularly below a few hundred keV. The smallest value of CNEN-2 below 500 keV is the reflection of its large capture cross section. A rapid increase of the CNEN-2 cross section above 450 keV may be due to its adopting continuum levels, while the JENDL-1 and ENDF/B-IV adopted 4 discrete levels up to 1.27 MeV.

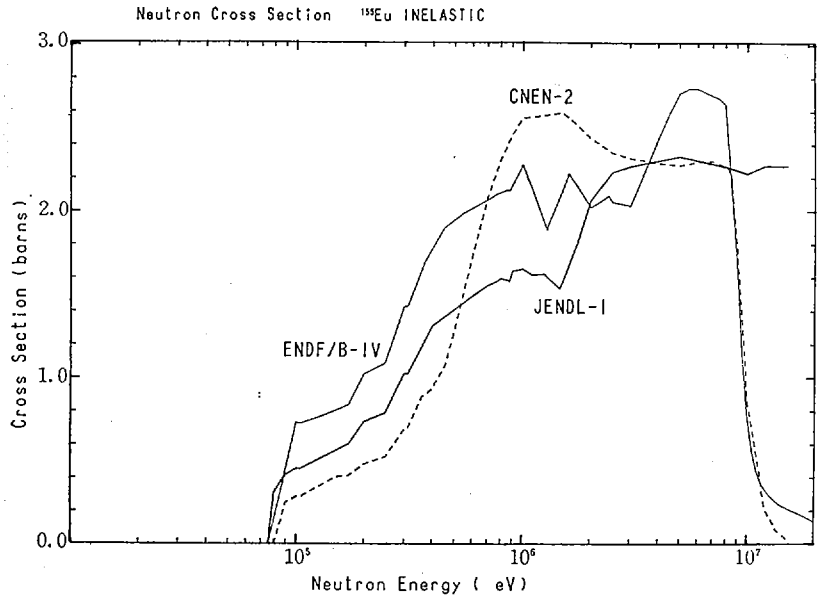

Fig. 3.28.3 Inelastic scattering cross sections of ^{155}Eu.

4. Summary and Discussion

4.1 Discrepancies among the Evaluated Data

Discrepancies among the evaluated data are considerably large as seen in the previous chapter. In order to know how discrepant the evaluted data are, we compare here the evaluated total and capture cross sections at 30 keV and 2 MeV. The values at 30 keV correspond very roughly to the average cross sections over typical neutron spectra in large fast reactors. The values at 2 MeV are chosen to see how strongly the cross sections are dependent on the models and approximations adopted in the calculation. The evaluated inelastic scattering cross sections are compared as the averaged values over a neutron spectrum of a typical large fast reactor and over a fission spectrum.

4.1.1 Total cross section

The total cross sections of the various evaluations at 30 keV and 2 MeV are compared with each other in TABLES 4.1 and 4.2, respectively.

Agreement is satisfactory at 2 MeV. The discrepancies are 9% at maximum and less than 5% in most cases. This means that any set of optical potential parameters produces the very similar total cross section at this energy.

On the other hand, discrepancies become large at 30 keV and reach 80% at maximum. The cross sections

TABLE 4.1 Comparison of total cross sections (barns) at 30 keV among the various evaluations. The value in parenthesis is the ratio to the JENDL-1 value.

Nuclide	ENDF/B-IV	CNEN-2	RCN-2	JENDL-1
^{90}Sr	8.20 (0.98)			8.39
^{93}Zr	8.07 (0.95)	9.57 (1.13)		8.46
^{95}Mo	8.01 (0.94)	8.27 (0.97)	8.53 (1.00)	8.51
^{97}Mo	7.93 (0.93)	9.18 (1.07)	8.43 (0.99)	8.55
^{99}Tc	7.80 (0.91)	8.21 (0.96)	8.79 (1.03)	8.53
^{101}Ru	7.70 (0.91)	9.56 (1.14)	8.46 (1.00)	8.47
^{102}Ru	7.64 (0.91)	7.57 (0.90)	8.41 (1.00)	8.42
^{103}Rh	7.79 (0.95)	7.91 (0.95)	8.71 (1.04)	8.35
^{104}Ru	7.48 (0.90)	7.95 (0.96)	8.27 (1.00)	8.27
^{105}Pd	7.40 (0.90)	8.79 (1.07)	7.79 (0.95)	8.20
^{106}Ru	7.32 (0.90)	8.23 (1.02)		8.10
^{107}Pd	7.23 (0.90)	8.94 (1.11)	7.47 (0.93)	8.02
^{109}Ag	9.12 (1.17)	8.06 (1.03)	8.15 (1.04)	7.80
^{129}I	6.23 (0.92)		5.87 (0.87)	6.78
^{131}Xe	8.71 (1.26)			6.91
^{133}Cs	8.93 (1.25)	6.38 (0.89)	7.03 (0.99)	7.13
^{135}Cs	6.88 (0.94)	7.20 (0.98)		7.34
^{137}Cs	7.25 (0.95)	6.34 (0.83)		7.65
^{143}Nd	13.6 (1.48)	13.8 (1.50)	9.23 (1.00)	9.21
^{144}Ce	9.13 (0.96)	10.7 (1.13)		9.49
^{144}Nd	9.20 (0.97)	13.2 (1.39)	9.54 (1.01)	9.49
^{145}Nd	16.7 (1.69)	14.6 (1.48)	10.1 (1.02)	9.87
^{147}Pm	19.7 (1.79)	13.6 (1.24)	9.85 (0.90)	11.0
^{147}Sm	19.1 (1.58)	14.1 (1.17)	15.0 (1.24)	12.1
^{149}Sm	13.3 (1.13)	12.0 (1.02)	16.6 (1.41)	11.8
^{151}Sm	13.9 (1.19)	11.8 (1.01)	14.6 (1.25)	11.7
^{153}Eu	14.1 (1.12)	13.9 (1.10)		12.6
^{155}Eu	12.5 (1.00)	12.2 (0.98)		12.5

at this energy is sensitive to the local systematics of s- and p-wave neutron strength functions and of the effective scattering radius. Particularly, the values of JENDL-1, calculated from the global optical potential, seem to be lower than the other evaluated values in $A=143\sim149$ region.

4.1.2 Capture cross section

The capture cross sections are compared at 30 keV and 2 MeV in TABLES 4.3 and 4.4, respectively.

Agreement at 30 keV is fairly satisfactory for nuclides whose capture cross sections were measured above 1 keV except for ^{109}Ag and ^{133}Cs where more than one trend exists in the measured data. On the other hand, large discrepancies, a factor of 4 at maximum, are often observed for nuclides for which no measured data are available. It is noted that the ENDF/B-IV values are generally lower than the other evaluations.

Discrepancies at 2 MeV are very large, *i.e.*, one order of magnitude at maximum. The capture cross section is very sensitive to the competing inelastic scattering, and therefore much affected by the level scheme and the level density parameters adopted in each evaluation.

4.1.3 Inelastic scattering cross section

The inelastic scattering cross sections are averaged over a neutron spectrum of a typical large fast reactor[227] and over a fission spectrum, and are given in TABLES 4.5 and 4.6. For both averages, discrepancies lie within 15% in most cases. Generally CNEN-2 gives larger values than JENDL-1. On the other hand, the values of ENDF/B-IV are lower than those of JENDL-1 for lighter FP nuclides but are larger for nuclides whose mass number exceeds 147. RCN-2 gives smaller values than JENDL-1 for neutron spectrum averages but larger ones for fission spectrum averages.

TABLE 4.2 Comparison of total cross sections (barns) at 2 MeV among the various evaluations. The value in parenthesis is the ratio to the JENDL-1 value.

Nuclide	ENDF/B-IV	CNEN-2	RCN-2	JENDL-1
^{90}Sr	4.25 (0.97)			4.38
^{93}Zr	4.41 (0.97)	4.57 (1.00)		4.45
^{95}Mo	4.50 (0.96)	4.69 (1.00)	4.47 (0.96)	4.67
^{97}Mo	4.58 (0.96)	4.80 (1.00)	4.66 (0.97)	4.79
^{99}Tc	5.31 (1.09)	5.07 (1.04)	4.90 (1.00)	4.89
^{101}Ru	4.71 (0.94)	5.15 (1.03)	4.99 (1.00)	4.99
^{102}Ru	4.74 (0.94)	5.19 (1.03)	5.04 (1.00)	5.03
^{103}Rh	5.45 (1.07)	5.22 (1.03)	5.08 (1.00)	5.08
^{104}Ru	4.81 (0.94)	5.25 (1.03)	5.12 (1.00)	5.12
^{105}Pd	4.84 (0.94)	5.27 (1.02)	5.22 (1.01)	5.16
^{106}Ru	4.87 (0.94)	5.20 (1.00)		5.20
^{107}Pd	4.90 (0.94)	5.34 (1.02)	5.28 (1.01)	5.23
^{109}Ag	5.28 (0.99)	5.43 (1.02)	5.67 (1.07)	5.31
^{129}I	5.94 (0.96)		6.17 (1.00)	6.18
^{131}Xe	6.17 (0.98)			6.29
^{133}Cs	6.34 (0.99)	6.41 (1.00)	6.40 (1.00)	6.42
^{135}Cs	6.27 (0.96)	6.52 (1.00)		6.52
^{137}Cs	6.37 (0.96)	6.63 (1.00)		6.63
^{143}Nd	7.34 (1.06)	6.92 (1.00)	6.92 (1.00)	6.92
^{144}Ce	6.66 (0.96)	6.96 (1.00)		6.95
^{144}Nd	6.66 (0.96)	6.96 (1.00)	6.95 (1.00)	6.95
^{145}Nd	7.47 (1.07)	6.99 (1.00)	6.99 (1.00)	6.99
^{147}Pm	7.39 (1.05)	7.05 (1.00)	7.05 (1.00)	7.05
^{147}Sm	7.44 (1.05)	7.08 (1.00)	7.21 (1.02)	7.08
^{149}Sm	7.00 (0.99)	7.11 (1.00)	7.23 (1.02)	7.10
^{151}Sm	7.18 (1.01)	7.14 (1.00)	7.23 (1.01)	7.14
^{153}Eu	6.56 (0.91)	7.18 (1.00)		7.18
^{155}Eu	6.84 (0.95)	7.22 (1.00)		7.23

4.2 Future Work

As described before, discrepancies are large among the existing evaluations, and more efforts are required to improve the neutron data of fission products. Summarizing the discussions in Chapter 3, the future improvement will be directed to the following items. These suggestions were taken into account in the reevaluation work for JENDL-2, which is now in progress.

4.2.1 Adoption of negative resonances

The $1/v$ type background correction was adopted in the present work, when the thermal capture cross section was not reproduced by the calculation from the resonance parameters. This assumes that the difference is caused by the contribution from tails of resonances standing far away where resonance parameters are not given. It is more probable, however, that difference is caused by the contribution from some negative resonances, particularly when the difference is very large, for example, in the cases of ^{95}Mo, ^{97}Mo, ^{102}Ru, ^{104}Ru, ^{105}Pd, ^{145}Nd and ^{153}Eu. Negative resonances should be considered in these cases.

4.2.2 Determination of optical potential parameters

The present evaluation used the global optical potential. Though the present potential reproduces the global trends of σ_T, S_0, S_1 and R very well, it does not reproduce the individual values of these quantities. As seen in TABLE 2.4, the present potential considerably overestimates the s-wave strength function for ^{133}Cs and ^{153}Eu and underestimates it for ^{101}Ru, ^{103}Rh, ^{109}Ag, ^{145}Nd and ^{149}Sm. The discontinuity of the effective scattering radius R at $A=147$ causes some errors in the total and elastic scattering cross sections. To avoid this unrea-

TABLE 4.3 Comparison of capture cross sections (millibarns) at 30 keV among the various evaluations. The value in parenthesis is the ratio to the JENDL-1 value.

Nuclide	ENDF/B-IV		CEA*		CNEN-2		RCN-2		JENDL-1
^{90}Sr	20.5	(1.37)							15
^{93}Zr	73.2	(0.41)			108	(0.61)			177
^{95}Mo	393	(1.02)	386	(1.01)	355	(0.92)	396	(1.03)	384
^{97}Mo	372	(1.04)	389	(1.08)	349	(0.97)	396	(1.10)	359
^{99}Tc	688	(0.90)	745	(0.98)	720	(0.95)	726	(0.95)	761
^{101}Ru	851	(0.78)	1000	(0.91)	1140	(1.04)	970	(0.88)	1097
^{102}Ru	244	(0.78)	255	(0.81)	330	(1.05)	273	(0.87)	314
^{103}Rh	944	(0.96)	890	(0.90)	940	(0.96)	927	(0.94)	984
^{104}Ru	161	(0.91)	207	(1.17)	205	(1.16)	210	(1.19)	177
^{105}Pd	1230	(1.04)	1215	(1.03)	1246	(1.06)	1164	(0.99)	1178
^{106}Ru	77.4	(0.74)			63.0	(0.61)			104
^{107}Pd	895	(0.77)	1384	(1.19)	1199	(1.03)	1416	(1.22)	1165
^{109}Ag	624	(0.51)	854	(0.70)	834	(0.69)	891	(0.73)	1215
^{129}I	460	(0.94)	264	(0.54)			372	(0.76)	490
^{131}Xe	300	(0.71)							424
^{133}Cs	626	(1.21)	616	(1.19)	668	(1.29)	680	(1.31)	518
^{135}Cs	64.5	(0.23)	335	(1.22)	218	(0.79)			275
^{137}Cs	8.30	(0.37)			29.2	(1.32)			22.2
^{143}Nd	277	(1.14)	242	(1.00)	296	(1.22)	307	(1.26)	243
^{144}Ce	35	(0.54)			45.4	(0.70)			65.1
^{144}Nd	95	(1.24)			107	(1.39)	68.9	(0.90)	76.8
^{145}Nd	305	(1.02)	314	(1.05)	317	(1.06)	447	(1.49)	300
^{147}Pm	1300	(1.39)	817	(0.87)	925	(0.99)	905	(0.96)	938
^{147}Sm	776	(0.77)			848	(0.84)	1221	(1.21)	1005
^{149}Sm	1620	(0.98)	1496	(0.91)	1310	(0.80)	1947	(1.18)	1645
^{151}Sm	1967	(1.08)	2457	(1.35)	2011	(1.10)	2062	(1.13)	1825
^{153}Eu	2430	(0.95)			2674	(1.04)			2566
^{155}Eu	2163	(1.15)			2556	(1.36)			1885

* Values are read from figures in CEA-N-1832.

sonableness, CNEN-2 often adopts the unresolved resonance parameter representation below 100 keV and RCN-2 uses the strength function model below a few hundred keV. Recently Delaroche *et al.*[228] developed the SPRT method, which deduces the optical potential parameters from the individual values of S_0, S_1, R and σ_T. This method was found[229] successful when applied to Nd isotopes by some of the present authors. This method should be taken into consideration.

4. 2. 3 Use of recent capture data

At the time of the present evaluation, the capture data above 1 keV were not available for 17 nuclides as shown in TABLE 2. 2. Since then the capture cross sections have been measured extensively for fission product nuclides. Among the seventeen nuclides, the measured capture data are now available for ^{101}Ru, ^{105}Pd, ^{143}Nd, ^{144}Nd and ^{145}Nd. On the other hand, newly measured data show significant discrepancies from the old data, particularly for ^{102}Ru, ^{149}Sm and ^{153}Eu. For these nuclides, reevaluation work is required by taking account of these new measurements.

4. 2. 4 Revision of level schemes

Level schemes adopted in the present work were evaluated by Nakasima and Murata[12] in 1973. After that, Matumoto *et al.*[46] revised the level schemes by using new experimental data. Iijima[22] pointed out that the capture cross section of ^{103}Rh changed by 14% at 1 MeV with the revised level scheme. The calculation should be made with these new level schemes.

4. 2. 5 Determination of level density parameters

The level density parameters were taken from the work of Gilbert and Camern[38]. These parameters

TABLE 4. 4 Comparison of capture cross sections (millibarns) at 2 MeV among the various evaluations. The value in parenthesis is the ratio to the JENDL-1 value.

Nuclide	ENDF/B-IV		CNEN-2		RCN-2		JENDL-1
^{90}Sr	5. 3	(0. 87)					6. 1
^{93}Zr	26. 5	(0. 48)	16. 0	(0. 29)			55. 6
^{95}Mo	28. 4	(0. 87)	19. 0	(0. 58)	24. 7	(0. 76)	32. 7
^{97}Mo	18. 7	(0. 78)	14. 3	(0. 60)	14. 9	(0. 62)	24. 0
^{99}Tc	35. 3	(0. 43)	63. 8	(0. 78)	52. 6	(0. 64)	82. 2
^{101}Ru	24. 9	(0. 37)	40. 4	(0. 60)	37. 6	(0. 56)	67. 1
^{102}Ru	85. 6	(1. 16)	56. 7	(0. 77)	53. 0	(0. 72)	73. 5
^{103}Rh	40. 5	(0. 64)	49. 1	(0. 78)	47. 6	(0. 75)	63. 3
^{104}Ru	31. 9	(0. 85)	48. 1	(1. 28)	44. 4	(1. 18)	37. 5
^{105}Pd	84. 4	(1. 04)	82. 6	(1. 02)	47. 0	(0. 58)	80. 8
^{106}Ru	8. 23	(0. 30)	3. 89	(0. 14)			27. 0
^{107}Pd	64. 7	(0. 83)	71. 2	(0. 91)	75. 3	(0. 96)	78. 1
^{109}Ag	51. 1	(0. 46)	65. 6	(0. 58)	74. 5	(0. 66)	112. 2
^{129}I	44. 2	(0. 78)			21. 2	(0. 37)	56. 7
^{131}Xe	10. 4	(0. 36)					28. 7
^{133}Cs	44. 7	(1. 49)	46. 1	(1. 53)	32. 1	(1. 07)	30. 1
^{135}Cs	2. 73	(0. 15)	14. 7	(0. 81)			18. 1
^{137}Cs	1. 26	(0. 12)	11. 8	(1. 13)			10. 4
^{143}Nd	71. 8	(0. 60)	123. 4	(1. 02)	115. 8	(0. 96)	120. 5
^{144}Ce	13. 1	(0. 84)	4. 96	(0. 32)			15. 6
^{144}Nd	50. 1	(1. 46)	29. 2	(0. 85)	30. 5	(0. 89)	34. 2
^{145}Nd	86. 3	(3. 61)	65. 8	(2. 75)	42. 6	(1. 78)	23. 9
^{147}Pm	124. 6	(1. 76)	102. 8	(1. 45)	88. 7	(1. 25)	70. 7
^{147}Sm	103. 3	(1. 25)	155. 7	(1. 88)	145. 7	(1. 76)	82. 7
^{149}Sm	40. 0	(0. 17)	149. 0	(0. 63)	141. 0	(0. 59)	238. 1
^{151}Sm	233. 1	(0. 94)	124. 5	(0. 50)	53. 7	(0. 22)	249. 1
^{153}Eu	216. 0	(0. 72)	193. 0	(0. 64)			300. 0
^{155}Eu	886. 5	(3. 34)	84. 5	(0. 32)			265. 8

should be updated by using more recent data of average s-wave resonance spacing and level scheme. The spin cut-off parameter σ_M^2 is better calculated with Eq. (12) not with Eq. (6), because Eq. (6) is in error. Further study should be made on the energy dependence of the spin cut-off parameter in the constant temperature model.

4.2.6 Inclusion of direct capture effect

The statistical model calculation was made in the present work, and therefore only the compound capture reaction was taken into account. The present capture cross section must be in considerable underestimation in the energy range above a few MeV, where the direct capture process becomes predominant.

It is now well recognized that the nonstatistical capture process cannot be neglected for some of fission product nuclides such as Sr, Zr, Mo, Ba and Nd. The correlation between the radiation and neutron widths must be treated appropriately for these cases in the capture cross section calculation.

4.2.7 Inclusion of threshold reactions

The threshold reactions except the inelastic scattering were ignored in the present work, since these reactions have minor effects on the fast reactor. However, some nuclides in the fission product mass region are used as the structural or superconductive materials in fusion reactors. The threshold reaction cross sections should be carefully evaluated for these cases.

4.2.8 Feedback from benchmark tests

Thus so far we have discussed solely on the basis of differential data. On the other hand, the present

TABLE 4.5 Comparison of inelastic scattering cross sections (barns) averaged over a typical neutron spectrum of large fast reactor among the various evaluations. The value in parenthesis is the ratio to the JENDL-1 value.

Nuclide	ENDF/B-IV	CNEN-2	RCN-2	JENDL-1
^{90}Sr	1.062 (0.74)			1.427
^{93}Zr	1.072 (0.79)	1.543 (1.14)		1.356
^{95}Mo	1.355 (0.82)	1.643 (0.99)	1.615 (0.98)	1.655
^{97}Mo	1.375 (0.82)	1.601 (0.96)	1.614 (0.97)	1.671
^{99}Tc	1.775 (1.09)	1.973 (1.21)	1.570 (0.97)	1.626
^{101}Ru	1.491 (0.84)	1.987 (1.12)	1.630 (0.92)	1.779
^{102}Ru	1.191 (0.74)	1.824 (1.14)	1.502 (0.94)	1.600
^{103}Rh	2.115 (1.21)	2.034 (1.16)	1.663 (0.95)	1.753
^{104}Ru	1.113 (0.67)	1.906 (1.16)	1.523 (0.92)	1.649
^{105}Pd	1.414 (0.80)	1.962 (1.11)	1.608 (0.91)	1.761
^{106}Ru	1.296 (0.78)	1.643 (0.99)		1.660
^{107}Pd	1.745 (0.97)	1.992 (1.11)	1.521 (0.85)	1.791
^{109}Ag	1.956 (1.13)	2.088 (1.20)	2.035 (1.17)	1.736
^{129}I	1.573 (0.83)		1.768 (0.94)	1.888
^{131}Xe	2.062 (1.05)			1.970
^{133}Cs	2.212 (1.11)	1.992 (1.00)	1.912 (0.96)	1.994
^{135}Cs	1.467 (0.77)	1.958 (1.02)		1.917
^{137}Cs	1.415 (0.87)	1.711 (1.05)		1.632
^{143}Nd	1.341 (0.80)	1.534 (0.92)	1.345 (0.80)	1.673
^{144}Ce	0.142 (0.07)	2.017 (1.04)		1.944
^{144}Nd	1.364 (0.74)	1.869 (1.02)	1.656 (0.90)	1.837
^{145}Nd	1.824 (0.90)	1.748 (0.86)	1.706 (0.84)	2.036
^{147}Pm	2.192 (1.03)	2.127 (1.00)	2.002 (0.94)	2.128
^{147}Sm	2.041 (0.98)	1.930 (0.93)	2.016 (0.97)	2.074
^{149}Sm	2.152 (1.03)	1.956 (0.94)	2.197 (1.05)	2.086
^{151}Sm	2.049 (0.94)	2.112 (0.97)	2.324 (1.07)	2.177
^{153}Eu	2.530 (1.18)	2.232 (1.04)		2.141
^{155}Eu	2.288 (1.08)	2.283 (1.08)		2.121

evaluated data have been tested by using the integral measurements made at STEK[230] and CFRMF[231] in the same working group of JNDC. The sample reactivity worths in various STEK cores and the capture rates in CFRMF were calculated with taking account of the self-shielding effect in small samples and were compared with the measured results. The results of this test were recently published[229].

Satisfactory agreement was observed as a whole between the calculated and measured data. For ^{102}Ru, ^{143}Nd and ^{145}Nd, the integral test suggests that the agreement will be improved if reevaluation is made on the basis of the recent experimental capture data. On the other hand, however, the integral data seem to be inconsistent with the recent differential data for ^{105}Pd and ^{149}Sm. Besides the strong core dependence was observed in the case of ^{103}Rh, indicating that more careful self-shielding corrections are required.

The integral data should be taken into consideration as one of measured data in the evaluation. In fact, the integral data are only available measured data for ^{107}Pd, ^{129}I and ^{131}Xe. However, we will not rely completely on the integral data by mechanically adjusting the cross section data with them.

TABLE 4.6 Comparison of inelastic scattering cross sections (barns) averaged over a fission spectrum among the various evaluations. The value in parenthesis is the ratio to the JENDL-1 value.

Nuclide	ENDF/B-IV	CNEN-2	RCN-2	JENDL-1
^{90}Sr	0.659 (0.74)			0.895
^{93}Zr	0.714 (0.80)	1.039 (1.16)		0.896
^{95}Mo	1.092 (0.84)	1.335 (1.03)	1.380 (1.06)	1.300
^{97}Mo	1.104 (0.86)	1.311 (1.02)	1.436 (1.12)	1.283
^{99}Tc	1.337 (1.05)	1.754 (1.38)	1.288 (1.01)	1.270
^{101}Ru	1.500 (0.92)	1.944 (1.19)	1.678 (1.03)	1.632
^{102}Ru	0.906 (0.77)	1.342 (1.14)	1.129 (0.96)	1.179
^{103}Rh	1.784 (1.20)	1.742 (1.17)	1.479 (1.00)	1.483
^{104}Ru	0.844 (0.66)	1.446 (1.13)	1.212 (0.95)	1.279
^{106}Ru	1.051 (0.80)	1.311 (1.00)		1.312
^{105}Pd	1.311 (0.85)	1.775 (1.15)	1.620 (1.05)	1.541
^{107}Pd	1.626 (1.02)	1.845 (1.16)	1.618 (1.02)	1.593
^{109}Ag	1.576 (1.12)	1.732 (1.23)	1.765 (1.26)	1.405
^{129}I	1.223 (0.85)		1.477 (1.02)	1.441
^{131}Xe	1.761 (1.11)			1.585
^{133}Cs	1.746 (1.09)	1.592 (0.99)	1.776 (1.11)	1.606
^{135}Cs	1.094 (0.80)	1.433 (1.04)		1.373
^{137}Cs	0.962 (1.00)	0.968 (1.01)		0.958
^{143}Nd	0.912 (1.02)	0.966 (1.08)	0.903 (1.01)	0.898
^{144}Ce	0.450 (0.31)	1.797 (1.24)		1.454
^{144}Nd	0.940 (0.77)	1.221 (1.00)	1.197 (0.98)	1.217
^{145}Nd	1.483 (0.93)	1.629 (1.03)	1.641 (1.03)	1.586
^{147}Pm	1.880 (1.06)	1.870 (1.06)	1.777 (1.01)	1.766
^{147}Sm	1.795 (1.10)	1.489 (0.92)	1.902 (1.17)	1.626
^{149}Sm	2.397 (1.35)	1.937 (1.09)	2.294 (1.29)	1.778
^{151}Sm	2.300 (1.10)	2.306 (1.11)	2.833 (1.36)	2.084
^{153}Eu	2.377 (1.23)	2.121 (1.10)		1.934
^{155}Eu	2.036 (1.14)	2.116 (1.19)		1.777

Acknowledgment

The authors wish to thank members of working group on fission product nuclear data of JNDC for their helpful discussion. They are much indebted to Drs. Reffo, Gruppelaar, Prince and Schenter for sending informations concerning CNEN-2, RCN-2 and ENDF/B-IV evaluations. They acknowledge Misses Onozaki, Taniguchi and Saitoh for preparing graphs and tables. Careful typewriting of the manuscript by Misses Hatano, Nakamura and Terakado is much appreciated.

References

1) Bondarenko I. I. (Edited): "Group Constants for Nuclear Reactor Calculations", Consultants Bureau, N. Y. (1964)
2) Benzi V., D'Orazi R., Reffo G. and Vaccari M.: "Fast Neutron Radiative Capture Cross Sections of Stable Nuclei with $29 \leq Z \leq 79$", DOC. CEC (71) 9 (1971)
3) Benzi V., Panini G. C., Reffo G. and Vaccari M.: "An Estimate of (n, n'), (n, 2n) and (n, γ) Excitation Functions for Some Fission Product Nuclei", DOC. CEC (71) 2 (1971)
4) Cook J. L.: "Fission Product Cross Sections", AAEC/TM-549 (1970)
5) Schenter R. E. and Schmittroth F. A.: "Cross Section Evaluations of Twenty Seven Fissisn Product Isotopes for ENDF/B-III, MAT 1201-1231", HEDL-TME-71-143 (1971)
6) Schmittroth F. A. and Schenter R. E.: "Fast Neutron Capture Cross Sections for Fission Product Isotopes", HEDL-TME-73-63 (1973)
7) Lautenbach G.: "Calculated Neutron Absorption Cross Sections of 75 Fission Products", RCN-191 (1973)
8) Tone T.: "Effects of Fission Products on the Physics Parameters of Large Fast Reactors and Uncertainties in the Physics Parameters due to the Fission-Product Nuclear Data Uncertainties", JAERI-M 5449 (1973)
9) Ilberg D., Saphier D. and Yiftah S.: Nucl. Technol., **24**, 111 (1974)
10) Kikuchi Y., Otake I., Tasaka K., Nishimura H., Hasegawa A. and Katsuragi S.: Proc. Int. Symp. Physics of Fast Reactors, Tokyo, 16-19 Oct., 1973, Vol. 2, p. 645 (1973)
11) Kikuchi Y., Hasegawa A., Tasaka K., Nishimura H., Otake I. and Katsuragi S.: "JNDC Fission Product Group Constants —Preliminary Version—", JAERI-M 6001 (1975)
12) Japanese Nuclear Data Committee: "Evaluation of Fission Product Nuclear Data for Fast Reactor (Neutron Cross Sections for 28 Nuclides), JAERI-M 5752 (1974)
13) Iijima S., Nakagawa T., Kikuchi Y., Kawai M., Matsunobu H., Maki K. and Igarasi S.: J. Nucl. Sci. Technol., **14**, 161 (1977)
14) Igarasi, S., Nakagawa T., Kikuchi Y., Asami T. and Narita T.: "Japanese Evaluated Nuclear Data Library, Version-1, JENDL-1", JAERI-1261 (1979)
15) Kikuchi Y., Hasegawa A., Nishimura H. and Tasaka K.: "Fission Product Fast Reactor Constants System of JNDC", JAERI-1248 (1976)
16) Ribon P., Fort E., Krebs J. and Quoc Thuong T.: "Evaluation des Sections Efficaces de Capture et de Diffusion Inélastique de 26 Produits de Fission", CEA-N-1832 (1975)
17) Gruppelaar H.: "Tables of RCN-2 Fission Product Cross Section Evaluation, Volume 1 (24 Nuclides)", ECN-13 (1977)
18) Gruppelaar H.: "Tables of RCN-2 Fission Product Cross Section Evaluation, Volume 2 (13 Nuclides)", ECN-33 (1977)
19) Gruppelaar H.: "Tables of RCN-2 Fission Product Cross Section Evaluation, Volume 3 (Nd ana Pm Isotopes)", ECN-65 (1979)
20) Reffo G.: Private Communication (1978)

21) Gruppelaar H., Janssen A. J. and Dekker J. W. M.: "Intercomparison of Recent Evaluations for the Capture Cross Sections of Some Fission Product Nuclides", ECN-12 (1976)
22) Iijima S.: "Fission Product Nuclear Data (FPND)—1977", Proc. 2nd IAEA Advisory Group Meeting on Fission Product Nuclear Data, Petten, Netherlands, 5-9 Sept. 1977, Vol. 1, p. 279, Review Paper No. 9, IAEA-213 (1978)
23) Reffo G.: Proc. 2nd IAEA Advisory Group Meeting on Fission Product Nuclear Data, Petten, Netherlands, 5-9 Sept. 1977, Annexes and Selected Contributions to the Review Papers, p. 165, INDC(NDS)-87/GO+Sp. (1978).
See also Reffo G.: "Parameter Systematics for Statistical Theory Calculations of Neutron Reaction Cross Sections, CNEN-RT/FI (78) 11 (1978)
24) IAEA: "CINDA 76/77—An Index to the Literature on Microscopic Neutron Data", IAEA, Vienna (1976)
25) Moldauer P. A.: Nucl. Phys., **47**, 65 (1963)
26) Wilmore D. and Hodgson P. E.: Nucl. Phys., **55**, 673 (1964)
27) Becchetti F. D., Jr. and Greenlees G. W.: Phys. Rev., **182**, 1190 (1969)
28) Rosen L., Beery J. G., Goldhaber A. S. and Auerbach E. H.: Ann. Rhys, **34**, 96 (1965)
29) Mughabgab S. F. and Garber D. I.: "Neutron Cross Sections, Vol. 1, Resonance Parameters", BNL-325, 3rd Edition (1973)
30) Moldauer P. A.: Phys, Rev., **123**, 968 (1961)
31) Moldauer P. A.: Phys. Rev., **135**, B642 (1964)
32) Igarasi S.: J. Nucl. Sci. Technol., **12**, 67 (1975)
33) Goldberg M. D., Mughabghab S. F., Purohit S. N., Magurno B. A. and May V. M.: "Neutron Cross Sections, Vol. IIB and Vol. IIC", BNL-325, 2nd Edition, Supplement No. 2 (1966)
34) Baba H. and Baba S.: "Average Level Spacings and the Nuclear Level Density Parameters", JAERI 1183 (1969)
35) Baba H.: Nucl. Phys., **A159**, 625 (1970)
36) Axel P.: Phys. Rev., **126**, 671 (1962)
37) Yoshida T. and Sasaki M.: Private Communication (1976)
38) Gilbert A. and Cameron A. G. W.: Can. J. Phys., **43**, 1446 (1965)
39) Wapstra A. H. and Gove N. B.: Nucl. Data Table, **9**, 267 (1971)
40) Jensen J. H. D. and Luttinger J. M.: Phys. Rev., **86**, 907 (1952)
41) Facchini U. and Saetta-Menichella E.: Energia Nucleare, **15**, 54 (1968)
42) Walker W. H.: "Fission Product Data for Thermal Reactors, Part I—Cross Sections", AECL-3037, Part I (1969)
43) Iijima S., Kobayashi T. and Sakata H.: "Neutron Absorption Cross Section of Fission Product (Report of F. P. Working Group No. 2)", JAERI-1206 (1971) [in Japanese]
44) Kikuchi Y.: "STAT: A Code for Analysis of Statistical Properties of Averaged Resonance Cross Sections", JAERI-M 6248 (1975) [in Japanese]
45) Lederer C. M., Hollander J. M. and Perlman I.: "Table of Isotopes, 6th Edition", John Wiley and Sons, Inc. (1968)
46) Matumoto Z., Murata T. and Nakasima R.: "Level Schemes for Some Fission Product Nuclides —Comparison of Level Schemes Used by JAERI and Petten—", JAERI-M 7734 (1978)
47) Smith A. B., Guenther P. T. and Whalen J. F.: Nucl. Phys., **A244**, 213 (1975)
48) Perey F. and Buck B.: Nucl. Phys, **32**, 353 (1962)
49) Zeisel G.: Acta Phys. Austr., **23**, 223 (1966)
50) Pomerance H.: "Absorption Cross Sections for Long-Lived Fission-Product ^{93}Zr, ^{241}Am and Enriched Stable Platinum Isototopes", ORNL-1879, p. 50 (1955)
51) Block R. C., Jenkins G. L., Parker G. W., Harvey J. A., Slaughter G. G., Lantz P. and Martin W. J.: "Parameters of Neutron Resonances of ^{147}Pm, ^{129}I, ^{93}Zr and ^{237}Np", ORNL-2610, p. 22 (1958)
52) Tattersall R. B., Rose H., Pattenden S. K. and Jowitt D.: J. Nucl. Energy, **A12**, 32 (1960)
53) Pomerance H.: Phys. Rev., **88**, 412 (1952)

54) Weigmann H., Rohr G. and Winter J.: "Neutron Cross Sections and Technology", Proc. Conf. Knoxville, Mar. 15-17, 1971, CONF-710301, p. 749 (1971)
55) Musgrove A. R. de L., Allen B. J., Boldeman J. W. and Macklin R. L.: Nucl. Phys., **A270**, 108 (1976)
56) Kapchigashev S. V. and Popov Yu. P.: Conf. Interaction of Neutrons with Nuclei, Dubna, 1964, JINR-1845, p. 104 (1964)
57) Hockenbury R. W., Gallucci R. H. V. and Yip W.: Bull. Am. Phys. Soc., **21**, 537 (1976)
58) Divadeenam M., Farrell J. A., Kyker G. C. Jr., Bilpuch E. G. and Newson H. W.: Bull. Am. Phys. Soc., **11**, 508 (1966)
59) Shwe H. and Cote R. E., Phys. Rev., **179**, 1148 (1969)
60) Pomerance H.: "Thermal Absorption Cross Section of Tc^{99}", ORNL-1975, p. 31 (1955)
61) Hay H. J. and Pattenden N. J.: NRDC-103, TNCC(UK) 24 (1958)
62) Watanabe T. and Reeder S. D.: Nucl. Sci. Eng., **41**, 188 (1970)
63) Pattenden N. J.: Proc. 2nd UN Int. Conf. Peaceful Uses of Atomic Energy, Geneva, 1958, Vol. 16, p. 44 (1958)
64) Chou J. C. and Werle H.: J. Nucl. Energy, **27**, 811 (1973)
65) Slaughter G. G., Harvey J. A., Block R. C. and Jenkins G. L.: Bull. Am. Phys. Soc., **3**, 364 (1958)
66) Adamchuk Yu. V., Muradyan G. V., Shchepkin Yu. G. and Voskanyan M. A.: "Nuclear Physics Research in the USSR, Collected Abstracts, Issue 18" INDC(CCP)-49/L, p. 14 (1975)
67) Little R. C. and Block R. C.: Trans. Am. Nucl. Soc., **26**, 574 (1977)
68) Harvey J. A.: Appeared in BNL-325 3rd edition, Vol. II[69] as a private communication (1959)
69) Garber D. I. and Kinsey R. R.: "Neutron Cross Sections, Vol. II, Curves", BNL-325, 3rd Edition (1976)
70) Foster D. G., Jr. and Glasgow D. W.: Phys. Rev., **C3**, 576 (1971)
71) Qaim S. M.: J. Inorg. Nucl. Chem., **35**, 3669 (1973)
72) Halperin J., Baldock C. R. and Oliver J. H.: "The Neutron Capture Cross Sections of Ruthenium Nuclides, Mass Number 98 through 101", ORNL-3679, p. 12 (1964)
73) Halperin J., Baldock C. R. and Oliver J. H.: "Neutron Capture Cross Sections of $^{99,100,101}Ru$", ORNL-3832, p. 4 (1965)
74) Coceva C., Corvi F., Giacobbe P. and Carraro G.: Nucl. Phys., **A117**, 586 (1968)
75) Priesmeyer von H. G. and Jung H. H.: Atomkernenergie, **19**, 111 (1972)
76) Macklin R. L. and Halperin J.: Nucl. Sci. Eng., **73**, 174 (1980)
77) Hockenbury R. W., Koste W. R. and Shaw R. A.: Bull. Am. Phys. Soc., **20**, 560 (1975)
78) Priesmeyer von H. G. and Jung H. H.: "Neutron Cross Sections and Technology", Proc. Conf. Knoxville, March 15-17, 1971, CONF-710301, p. 688 (1971)
79) Katcoff S. and Williams D. C.: J. Inorg. Nucl. Chem., **7**, 194 (1958)
80) Lantz P. M.: "Thermal-Neutron Cross Section and Resonance Integral of ^{102}Ru", ORNL-3832, p. 6 (1965)
81) Ishikawa H.: J. Nucl. Sci. Technol., **6**, 587 (1969)
82) Ricabarra M. D., Turjanski R. and Ricabarra G. H.: Can. J. Phys., **47**, 2031 (1969)
83) Van der Linden R., De Corte F., Van der Winkel P. and Hoste J.: J. Radioanal. Chem., **11**, 133 (1972)
84) Bolotin H. H. and Chrien R. E.: Nucl. Phys. **42**, 676 (1963)
85) Macklin R. L., Lazar N. H. and Lyon W. S.: Phys. Rev., **107**, 504 (1957)
86) Murty M. S., Siddappa K. and Rao J. R.: J. Phys. Soc. Jpn., **35**, 8 (1973)
87) Lyon W. S. and Macklin R. L.: Phys. Rev., **114**, 1619 (1959)
88) Dilg W. and Mannhart W.: Z. Phys., **266**, 157 (1974)
89) Walker W. H. and Copley L. A.: Can. J. Phys., **44**, 1985 (1966)
90) Köhler W. and Schneider E.: Nukleonik, **12**, 197 (1969)
91) Hüttel G.: Kernenergie, **14**, 73 (1971)
92) Ribon P., Girard J. and Trochon J.: Nucl. Phys., **A143**, 130 (1970)
93) Carlson A. D. and Fricke M. P.: "Neutron Cross Section Research. Final Report", GULF-RT-A-10739 (1971). See also

Carlson A. D., Fricke M. P. and Friesenhahn S. J.: Trans. Am. Nucl. Soc., **14**, 352 (1971)
94) Haste T. J. and Thomas B. W.: J. Physics, **G1**, 981 (1975)
95) Wilenzick R. M., Seth K. K., Bevington P. R. and Lewis H. W.: Nucl. Phys., **62**, 511 (1965)
96) Zakharova S. M., Stavinsky V. S. and Shubin Yu. N.: "Systematics of Mean Radiation Widths of Neutron Resonances", Nuclear Constants No. 7 (Appendix 2), INDC (CCP)-27/L (1971)
97) Cox S. A.: Phys. Rev. **133B**, 378 (1964)
98) Jain A. P., Chrien R. E., Moore J. A. and Palevsky H.: Phys. Rev., **137B**, 83 (1965)
99) Seth K. K.: Phys. Lett., **16**, 306 (1965)
100) Divadeenam M.: Dissertation Abstracts, Section B, **28**, 3834 (1968)
101) Dilg W. and Vonach H.: "Average Total Neutron Cross Sections of Heavy Elements at 2.7 keV", EANDC (E) 150 "U", Supplement, p. 40 (1972)
102) Pasechnik M. V., Barchuk I. F., Totsky I. A., Strizhak V. I., Korolov A. M., Hofman Y. V., Lovchikova G. N., Koltynin E. A. and Yankov G. B.: Proc. 2nd UN Int. Conf. Peaceful Uses of Atomic Energy, Geneva, 1958, Vol. 15, p. 18 (1958)
103) Diven B. C., Terrell J. and Hemmendinger A.: Phys. Rev., **120**, 556 (1960)
104) Gibbons J. H., Macklin R. L., Miller P. D. and Neiler J. H.: Phys. Rev., **122**, 182 (1961)
105) Popov Yu. P. and Shapiro F. L.: Sov. Phys. JETP, **15**, 683 (1962)
106) Moxon M. C. and Rae E. R.: Nucl. Instrum. Methods, **24**, 445 (1963)
107) Macklin R. L., Gibbons J. H. and Inada T.: Phys. Rev., **129**, 2695 (1963)
108) Csikai J., Petö G., Buczkó M., Miligy Z. and Eissa N. A.: Nucl. Phys., **A95**, 229 (1967)
109) Macklin R. L. and Gibbons J. H.: Phys. Rev., **159**, 1007 (1967)
110) Rigaud F., Irigaray J. L., Petit G. Y., Longo G. and Saporetti F.: Nucl. Phys., **A173**, 551 (1971)
111) Kantele J. and Valkonen M.: Phys. Lett., **39B**, 625 (1972)
112) Rigaud F., Desthuilliers M. G., Petit G. Y., Irigaray J. L., Longo G. and Saporetti F.: Nucl. Sci, Eng., **55**, 17 (1974)
113) Hockenbury R. W., Knox H. R. and Kaushal N. N.: "Nuclear Cross Sections and Technology", Proc. Conf. Washington D. C., March 3-7, 1975, p. 905, NBS Special Publication 425 (1975)
114) Le Rigoleur C., Arnaud A. and Taste J.: "Nuclear Cross Sections and Technology", Proc. Conf. Washington D. C., March 3-7, 1975, p. 953, NBS Special Publication 425 (1975)
115) Seren L., Friedlander H. N. and Turkel S. H.: Phys. Rev., **72**, 888 (1947)
116) Lantz P. M.: "Thermal-Neutron Cross Section and Resonance Integral of ^{104}Ru", ORNL-3679, p. 11, (1964)
117) Chaubey A. K. and Sehgal M. L.: Phys. Rev., **152**, 1055 (1966)
118) Anand R. P., Bhattacharya D., Jhingan M. L. and Kondaiah E.: Proc. Nuclear Physics and Solid State Physics Symp., Bombay, Dec. 27-31, 1974, Vol. 17B, p. 101 (1974)
119) Perkin J. L., O'Connor L. P. and Coleman R. F.: Proc. Phys. Soc. (London), **72**, 505 (1958)
120) Gray P. R., Zander A. R. and Ebrey T. G.: Nucl. Phys., **75**, 215 (1966)
121) Petö G., Miligy Z. and Hunyadi I.: J. Nucl. Energy, **21**, 797 (1967)
122) Yamamuro N., Yokobori H., Aizawa O., Kimura I., Akiyoshi T. and Ebisawa T.: Bull. Tokyo Inst. Technology, **109**, 19 (1972)
123) Wetzel K. J. and Thomas G. E.: Phys. Rev., **C1**, 1501 (1970)
124) Macklin R. L., Halperin J. and Winters R. R.: Nucl. Sci. Eng., **71**, 182 (1979)
125) Werner R. D. and Eastwood T. A.: Nucl. Sci. Eng., **21**, 20 (1965)
126) Halperin J. and Druschel R. E.: "The Thermal—Neutron Capture Cross Section and Recsonance Integral of ^{106}Ru", ORNL-3679, p. 15 (1964)
127) Singh U. N., Block R. C. and Nakagome Y.: Nucl. Sci. Eng., **67**, 54 (1978)
128) Garrison J. D. and Roos B. W.: Nucl. Sci. Eng., **12**, 115 (1962)
129) Pattenden N. J. and Jolly J. E.: "Transmission Measurements of ^{107}Ag and ^{109}Ag", AERE-PR/NP 16, p. 14 (1969)
130) Weston L. W., Seth K. K., Bilpuch E. G. and Newson H. W.: Ann. Phys., **10**, 477 (1960)

131) Kononov V. N. and Stavisskii Yu. Ya.: "Nuclear Data for Reactors", Conf. Proc., Paris, 17-21 Oct. 1966, Vol. 1, p. 496, IAEA (1967)
132) Furr A. K.: "Average Resonance Parameters A=100", Thesis, TID-16059 (1962)
133) Chrien R. E.: Phys. Rev., **141**, 1129 (1966)
134) Dukarevich Yu. V., Dyumin A. N. and Kaminker D. M.: Nucl. Phys., **A92**, 433 (1967)
135) Augustyniak W., Herman M. and Marcinkowski A.: Nucl. Phys., **A247**, 231 (1975)
136) Bhat M. R. and Prince A.: "Evaluated Neutron Cross Sections for ^{107}Ag, ^{109}Ag, and ^{133}Cs", BNL-50383 (1973)
137) Purkayastha B. C. and Martin G. R.: Can. J. Chem., **34**, 293 (1956)
138) Roy J. C. and Wuschke D.: Can. J. Chem., **36**, 1424 (1958)
139) Eastwood T. A., Baerg A. P., Bigham C. B., Brown F., Cabell M. J., Grummitt W. E., Roy J. C., Roy L. P. and Schuman R. P.: Proc. 2nd UN Int. Conf. Peaceful Uses of Atomic Energy, Geneva, 1958, Vol. 16, p. 54 (1958)
140) Wilkey D. D. and Willard J. E.: J. Chem. Phys., **44**, 970 (1966)
141) Harvey J. A., Block R. C., Slaughter G. G., Martin W. J. and Parker G. W.: Proc. 2nd UN Int. Conf. Peaceful Uses of Atomic Energy, Geneva, 1958, Vol. 16, p. 150 (1958)
142) Block R. C., Slaughter G. G. and Harvey J. A.: Nucl. Sci. Eng., **8**, 112 (1960)
143) Pattenden N. J.: Nucl. Sci. Eng., **17**, 371 (1963)
144) Eastwood T. A. and Brown F.: "Neutron Capture Cross Sections for Kr and Xe Isotopes", EANDC(Can)-16/L, p. 6 (1963)
145) MacNamara, J. and Thode H. G.: Phys. Rev., **80**, 296 (1950)
146) Mann D. P., Watson W. W., Chrien R. E., Zimmerman R. L. and Schwartz R. B.: Phys. Rev., **116**, 1516 (1959)
147) Ribon P.: "Etudes de quelques proprités des niveaux excités des noyaux composés par l'interaction de neutrons lents aves ^{103}Rh, Xe, ^{155}Gd, ^{157}Gd, ^{232}Th" CEA-N-1149 (1969)
148) Bhat M. R. and Mughabghab S. F.: "Evaluated Neutron Cross Sections for the Stable Isotopes of Xenon", BNL-50374 (1973)
149) Steinnes E.: J. Inorg. Nucl. Chem., **34**, 2699 (1972)
150) Widder F.: "Neutron Capture Cross Section Measurements in the Energy Region from 0.01 to 10 Electron Volts", EIR-Bericht Nr. 217 (1975)
151) Alian A., Born H. J. and Kim J. I.: J. Radioanal. Chem., **15**, 535 (1973)
152) Van der Linden R., De Corte F. and Hoste J: J. Radioanal. Chem., **20**, 695 (1974)
153) Hickman G. D.: Bull. Am. Phys. Soc., **10**, 12 (1965)
154) Landon H. H. and Sailor V. L.: Phys. Rev., **93**, 1030 (1954)
155) Harvey J. A., Hughes D. J., Carter R. S. and Pilcher V. E.: Phys. Rev., **99**, 10 (1955)
156) Garg J. B., Rainwater J. and Havens W. W. Jr.: Phys. Rev., **137**, B547 (1965)
157) Jung H. H. and Priesmeyer H. G.: Atomkernenergie, **14**, 271 (1969)
158) Thomas B. W., Axmann H. P., Riehs P. and Rae E. R.: "Resonance Capture Gamma-Ray Studies", AERE-PR/NP 18, p. 23 (1972)
159) Riehs P., and Thomas B. W.: "Neutron Capture Gamma-Ray Spectroscopy", Proc. 2nd Int. Symp. on Neutron Capture Gamma-Ray Spectroscopy and Related Topics, Sept. 2-6, 1974, Petten, p. 300 (1974)
160) Kompe D.: Nucl. Phys., **A133**, 513 (1969)
161) Yamamuro N., Doi T., Hayase T., Fujita Y., Kobayashi K. and Block R. C.: "Nuclear Cross Sections and Technology", Proc. Conf., Washington, D. C., March 3-7, 1975, p. 802, NBS Special Publication 425 (1975)
162) Booth R., Ball W. P. and Macgregor M. H.: Phys. Rev., **112**, 226 (1958)
163) Yamamuro N. and Asami A.: "Measurements of Capture Cross Sections in the FP Mass Region", Contributed Paper to NEA Specialists' Meeting on Neutron Cross Sections of Fission Product Nuclei, Bologna, 12-14 Dec. 1979
164) Barnard E., Coetzee N., de Villiers J. A. M., Reitmann D. and Van der Merwe P.: Z. Phys., **271**, 1

(1974)

165) Angeli I. and Hunyadi I.: Acta Phys. Acad. Sci. Hung., **20**, 193 (1966)

166) Angeli I., Csikai J., Nagy J. L., Scharbert T., Sztaricskai T. and Novak D.: Acta Phys. Acad. Sci. Hung., **30**, 115 (1971)

167) Kikuchi S.: Nucl. Phys., **A171**, 480 (1971)

168) Qaim S. M.: J. Inorg. Nucl. Chem., **32**, 1799 (1970)

169) Brzosko J. S., Gierlik E., Soltan A., Jr., Szeflinski Z. and Wilhelmi Z.: Acta Phys. Pol., **B2**, 489 (1971). See also
ibid: "Investigation of the Neutron Capture High Energy Gamma-Rays", INR-1318/I/PL, p. 29 (1971)

170) Rigaud F., Irigaray J. L., Petit G. Y., Longo G. and Saporetti F.: Nucl. Phys., **A176**, 545 (1971)

171) Baerg A. P., Brown F. and Lounsbury M.: Can. J. Phys., **36**, 863 (1958)

172) Jung H. H., Priesmeyer H. G. and Sulitze H.: "Nuclear Data for Reactors", Conf. Proceedings, Helsinki, 15-19 June 1970, Vol. 1, p. 679, IAEA (1970)

173) Stupegia D. C.: J. Nucl. Energy, **A12**, 16 (1960)

174) Cabell M. J. and Wilkins M.: J. Inorg. Nucl. Chem. **30**, 897 (1968)

175) Vertebny V. P., Gnidak N. L. and Pavlenko E. A.: Proc. Conf. on Neutron Phys., Kiev, 28 May-1 June 1973, Vol. 2, p. 104 (1974)

176) Hay H. J.: J. Nucl. Energy, **7**, 199 (1958)

177) Karzhavina E. N., Fong N. N., Popov A. B. and Taskaev A. I.: Sov. J. Nucl. Phys., **8**, 371 (1969)

178) Migneco E., Theobald J. and Weigmann H.: J. Nucl. Energy, **23**, 369 (1969)

179) Rohr G., Weigmann H. and Heske M.: "Neutron Cross Sections and Technology", Prcc. Conf., Knoxville, March 15-17, 1971, p. 743, CONF-710301 (1971)

180) Tellier H.: "Propriétés des niveaux induits par les neutrons de résonance dans les isotopes stables du néodyme", CEA-N 1459 (1971)

181) Alves R. N., de Barros S., Chevillon P. L., Jullien J., Morgenstern J. and Samour C.: Nucl. Phys., **A134**, 118 (1969)

182) Cauvin B., Lottin A., Michaudon A., Newstead C. M., Paya D. and Trochon J.: "Neutron Cross Sections and Technology", Proc. Conf., Knoxville, March 15-17, 1971, p. 785, CONF-710301 (1971)

183) Stolovy A., Namenson A. I., Ritter J. C., Godlove T. F. and Smith G. L.: Phys, Rev., **C5**, 2030 (1972)

184) Musgrove A. R. de L., Allen B. J., Boldeman J. W. and Macklin R. L.: "Non-statistical Effects in the Radiative Capture Cross Sections of the Neodymium Isotopes", AAEC/E 401 (1977)

185) Nakajima Y., Asami A., Kawarasaki Y., Furuta Y., Yamamoto T. and Kanda Y.: "Neutron Physics and Nuclear Data", Proc. Int. Conf., Harwell, September 1978, p. 438, OECD (1978)

186) Djumin A. N., Egorov A. I., Popova G. N. and Smolin V. A.: Izv. Akad. Nauk USSR, Ser. Fiz., **37**, 1019 (1973) [in Russian]

187) Lantz P. M.: Nucl. Sci. Eng., **13**, 289 (1962)

188) Walker W. H. and Thode H. G.: Phys. Rev., **90**, 447 (1953)

189) Koehler W. C. and Wollan E. O.: Phys. Rev., **91**, 597 (1953)

190) Kononov V. N., Yurlov B. D., Poletaev E. D. and Timokhov V. M.: Sov. J. Nucl. Phys., **27**, 5 (1978)

191) Pineo W. F. E., Divadeenam M., Bilpuch E., Seth K. K. and Newson H. W.: Ann. Phys., **84**, 165 (1974)

192) Musgrove A. R. de L., Allen B. J., Boldeman J. W. and Macklin R. L.: "Neutron Physics and Nuclear Data", Proc. Int. Conf., Harwell, September 1878, p. 449, OECD (1978)

193) Fenner N. C. and Large R. S.: J. Inorg. Nucl. Chem., **29**, 2147 (1967)

194) Cabell M. J.: J. Inorg. Nucl. Chem., **32**, 3433 (1970)

195) Mowatt R. S. and Walker W. H.: Can. J. Phys., **49**, 108 (1971)

196) Codding J. W., Jr., Tromp R. L. and Simpson F. B.: Nucl. Sci. Eng., **43**, 58 (1971)

197) Kirouac G. J., Eiland H. M., Conrad C. A., Slovacek R. E. and Seemann K. W.: Nucl. Sci. Eng., **52**, 310 (1973)

198) Belanova T. S., Zamyatnin Yu. S., Kocherygin N. G., Ivanenko V. V., Anufriev V. A., Kolesov A. G., Poruchikov V. A., Kalebin S. M., Ivanov R. N. and Artamonov V. S.: Proc. 3rd All-Union Conf. on

Neutron Physics, Kiev, 9-13 June 1975, Vol. 3, p. 205 (1975) [in Russian]

199) Schuman R. P. and Berreth J. R.: Nucl. Sci. Eng., **12**, 519 (1962)

200) Dobrozemsky R., Pichlmayer F. and Viehböck F. P.: J. Mass Spectrom. Ion Phys., **6**, 415 (1971) [in German], and AEC-tr-7574 [English translation]

201) Eiland H. M., Weinstein S. and Seemann K. W.: Nucl. Sci. Eng., **54**, 286 (1974)

202) Karzhavina E. N., Kim Sek Su and Popov A. B.: "Spins of ^{147}Sm and ^{149}Sm neutron resonances", JINR-P3-6237 (1972) [in Russian]

203) Mizumoto M., Sugimoto M., Nakajima Y., Kawarasaki Y., Furuta Y. and Asami A.: Paper CC6 Presented at Int. Conf. Nuclear Cross Sections for Technology, Knoxville, 22-26 Oct. 1979.

204) Macklin R. L., Gibbons J. H. and Inada T.: Nature, **197**, 369 (1963)

205) Kononov V. N., Yurlov B. D., Poletaev E. D., and Timokhov V. M.: Sov. J. Nucl. Phys., **26**, 500 (1977)

206) Asami T., Okamoto K., Ideno K. and Ohno Y.: J. Phys. Soc. Jpn., **26**, 225 (1969)

207) Aitken K. L. and Cornish F. W.: J. Inorg. Nucl. Chem., **17**, 6 (1961)

208) Karzhavina E. N. and Popov A. B.: "Neutron Resonances of the Isotopes Samarium-147 and 149", INDC(CCP)-30/U, p. 42 (1972)

209) Kirouac G. J. and Eiland H. M.: Phys. Rev., **C11**, 895 (1975)

210) Widder J. F.: Nucl. Sci. Eng., **60**, 53 (1976)

211) Moxon M. C., Endacott D. A. J. and Jolly J. E.: Ann. Nucl. Energy, **3**, 399 (1976)

212) Vertebny V. P., Vlasov M. F., Gnidak N. L., Koloty V. V., Kirilyuk A. L., Pavlenko E. A., Pasechnik M. V., Razbudey V. F. and Fedorova A. F.: "Nuclear Data for Reactors", Conf. Proc., Helsinki, 15-19 June 1970, Vol. 1, p. 651, IAEA, Vienna (1970) [in Russian]

213) Vertebny V. P., Vlasov M. F., Zatserkovsky R. A., Ignatenko A. I., Kirilyuk A. L., Trofimova N. A. and Fedorova A. F.: "Total neutron cross sections of Europium, Gold and Water in the 0.008-0.3 eV energy", INDC(CCP)-30-U, p. 64 (1972)

214) Razbudey V. F., Fedorova A. F. and Muravitsky A. V.: "More accurate values of total neutron cross sections of ^{153}Eu in the 0.008-0.3 eV energy range", INDC(CCP)-100-U, p. 23 (1977)

215) Rahn F., Camarda H. S., Hacken G., Havens W. W. Jr., Liou H. I., Rainwater J., Slagowitz M. and Wynchank S.: Nucl. Sci. Eng., **48**, 219 (1972)

216) Kim J. I., Gryntakis E. M. and Born H. J.: Radiochemica Acta, **22**, 20 (1975)

217) Rahn F., Camarda H. S., Hacken G., Havens W. W. Jr., Liou H. I., Rainwater J., Slagowitz M. and Wynchank S.: Phys. Rev., **C6**, 251 (1972)

218) Vertebny V. P., Vorona P. N., Kalchenko A. I., Koloty V. V., Pasechnik M. V., Pisanko Zh. I., Pshenichny V. A. and Rudishin V. K.: "Resonance of the isotopes Europium-151 and Europium-153", INDC(CCP)-15-U, p. 50 (1971)

219) Konks V. A. and FENIN Yu. I.: Conf. Interaction of Neutrons with Nuclei, Dubna, 1964, JINR-1845, p. 100 (1964)

220) Konks V. A., Popov Yu. P. and Fenin Yu. I.: Sov. J. Nucl. Phys., **7**, 310 (1968)

221) Harlow M. V., Schelberg A. D., Tatro L. D., Warren J. H. and Glass N. W.: "Neutron Cross Sections and Technology", Proc. Conf., Washington, D. C., March 4-7, 1968, NBS Special Publication 299, Vol. 2, p. 837 (1968)

222) Czirr J. B.: "^{165}Ho, ^{151}Eu and natural Europium capture cross section measurement", UCRL-50804 (1970)

223) Mizumoto M., Asami A., Nakajima Y., Kawarasaki Y., Fuketa T. and Takekoshi H.: J. Nucl. Sci. Technol., **16**, 711 (1979)

224) Takahashi H.: "Evaluation of the Neutron and Gamma Ray Production Cross Sections of ^{151}Eu and ^{153}Eu", BNL-19455 (1974)

225) Hayden R. J., Reynolds J. H. and Inghram M. G.: Phys. Rev., **75**, 1500 (1949)

226) Mowatt R. S.: Can. J. Phys., **48**, 1933 (1970)

227) Lesage L. G. (Edited): Proc. NEACRP/IAEA Specialists Meeting on the International Comparison Calculation of a Large Sodium-Cooled Fast Breeder Reactor, Feb. 7-9, 1978, ANL. (to be published)

228) Delaroche J. P., Lagrange C. and Salvy J.: "Nuclear Theory in Neutron Nuclear Data Evaluation", Proc. IAEA Consultants Meeting, Trieste, 8-11 Dec. 1975, Vol. 1, p. 251, IAEA-190 (1976)

229) Iijima S., Watanabe T., Yoshida T., Kikuchi Y. and Nishimura H.: "Fission Product Neutron Cross Section Evaluations for JENDL and the Integral Tests", Proc. Specialists' Meeting on Neutron Cross Sections of Fission Product Nuclei, Bologna, Dec. 12-14, 1979, p. 317, RIT/FIS-LDN (80) 1, NEANDC(E)-209 "L"

230) Veenema J. J. and Janssen A. J.: "Small-sample Reactivity Worths of Fission Product Isotopes and Some Other Materials Measured in STEK", ECN-10 (1976)

231) Harker Y. D., Rogers J. W. and Millsap D. A.: "Fission Product and Reactor Dosimetry Studies at Coupled Fast Reactivity Measurements Facility", ENDF-266 (1978)

232) Livolsi A. Z.: "Neutron Cross Section and Technology", Proc. Conf. Knoxville, March 15-17, 1971, CONF-710301, p. 446 (1971)

Appendix

Tables of cross sections and $\bar{\mu}_L$ averaged over appropriate energy intervals

CROSS SECTION

MATERIAL =1381 SR-90

ENERGY	TOTAL	ELASTIC	CAPTURE	INELA	MU-BAR
1.0000- 5 ~ 1.0000- 2	8.7763+ 0	5.9830+ 0	2.7753+ 0		7.4791- 3
1.0000- 2 ~ 1.5000- 2	7.2779+ 0	5.9830+ 0	1.2869+ 0		7.4791- 3
1.5000- 2 ~ 2.0000- 2	7.0805+ 0	5.9830+ 0	1.0849+ 0		7.4791- 3
2.0000- 2 ~ 3.0000- 2	6.8989+ 0	5.9830+ 0	9.0998- 1		7.4791- 3
3.0000- 2 ~ 4.0000- 2	6.7595+ 0	5.9830+ 0	7.6715- 1		7.4791- 3
4.0000- 2 ~ 5.0000- 2	6.6615+ 0	5.9830+ 0	6.7587- 1		7.4791- 3
5.0000- 2 ~ 6.0000- 2	6.6000+ 0	5.9830+ 0	6.1102- 1		7.4791- 3
6.0000- 2 ~ 8.0000- 2	6.5323+ 0	5.9830+ 0	5.4246- 1		7.4791- 3
8.0000- 2 ~ 1.0000- 1	6.4628+ 0	5.9830+ 0	4.7791- 1		7.4791- 3
1.0000- 1 ~ 1.5000- 1	6.3949+ 0	5.9830+ 0	4.0695- 1		7.4791- 3
1.5000- 1 ~ 2.0000- 1	6.3280+ 0	5.9830+ 0	3.4308- 1		7.4791- 3
2.0000- 1 ~ 3.0000- 1	6.2743+ 0	5.9830+ 0	2.8775- 1		7.4791- 3
3.0000- 1 ~ 4.0000- 1	6.2269+ 0	5.9830+ 0	2.4259- 1		7.4791- 3
4.0000- 1 ~ 5.0000- 1	6.1991+ 0	5.9830+ 0	2.1373- 1		7.4791- 3
5.0000- 1 ~ 6.0000- 1	6.1789+ 0	5.9830+ 0	1.9322- 1		7.4791- 3
6.0000- 1 ~ 8.0000- 1	6.1555+ 0	5.9830+ 0	1.7154- 1		7.4791- 3
8.0000- 1 ~ 1.0000+ 0	6.1358+ 0	5.9830+ 0	1.5113- 1		7.4791- 3
1.0000+ 0 ~ 1.5000+ 0	6.1129+ 0	5.9830+ 0	1.2869- 1		7.4791- 3
1.5000+ 0 ~ 2.0000+ 0	6.0925+ 0	5.9830+ 0	1.0849- 1		7.4791- 3
2.0000+ 0 ~ 3.0000+ 0	6.0749+ 0	5.9830+ 0	9.0997- 2		7.4791- 3
3.0000+ 0 ~ 4.0000+ 0	6.0605+ 0	5.9830+ 0	7.6714- 2		7.4791- 3
4.0000+ 0 ~ 5.0000+ 0	6.0515+ 0	5.9830+ 0	6.7586- 2		7.4791- 3
5.0000+ 0 ~ 6.0000+ 0	6.0444+ 0	5.9830+ 0	6.1100- 2		7.4791- 3
6.0000+ 0 ~ 8.0000+ 0	6.0378+ 0	5.9830+ 0	5.4244- 2		7.4791- 3
8.0000+ 0 ~ 1.0000+ 1	6.0315+ 0	5.9830+ 0	4.7790- 2		7.4790- 3
1.0000+ 1 ~ 1.5000+ 1	6.0240+ 0	5.9830+ 0	4.0695- 2		7.4790- 3
1.5000+ 1 ~ 2.0000+ 1	6.0178+ 0	5.9830+ 0	3.4307- 2		7.4790- 3
2.0000+ 1 ~ 3.0000+ 1	6.0120+ 0	5.9830+ 0	2.8775- 2		7.4789- 3
3.0000+ 1 ~ 4.0000+ 1	6.0076+ 0	5.9830+ 0	2.4259- 2		7.4788- 3
4.0000+ 1 ~ 5.0000+ 1	6.0045+ 0	5.9830+ 0	2.1372- 2		7.4787- 3
5.0000+ 1 ~ 6.0000+ 1	6.0025+ 0	5.9830+ 0	1.9321- 2		7.4786- 3
6.0000+ 1 ~ 8.0000+ 1	6.0004+ 0	5.9830+ 0	1.7154- 2		7.4784- 3
8.0000+ 1 ~ 1.0000+ 2	5.9982+ 0	5.9830+ 0	1.5112- 2		7.4782- 3
1.0000+ 2 ~ 1.5000+ 2	5.9960+ 0	5.9830+ 0	1.2869- 2		7.4778- 3
1.5000+ 2 ~ 2.0000+ 2	5.9939+ 0	5.9830+ 0	1.0849- 2		7.4770- 3
2.0000+ 2 ~ 3.0000+ 2	5.9922+ 0	5.9830+ 0	9.0995- 3		7.4759- 3
3.0000+ 2 ~ 4.0000+ 2	5.9907+ 0	5.9830+ 0	7.6712- 3		7.4746- 3
4.0000+ 2 ~ 5.0000+ 2	5.9898+ 0	5.9830+ 0	6.7585- 3		7.4735- 3
5.0000+ 2 ~ 6.0000+ 2	5.9892+ 0	5.9830+ 0	6.1099- 3		7.4728- 3
6.0000+ 2 ~ 8.0000+ 2	5.9884+ 0	5.9830+ 0	5.4244- 3		7.4726- 3
8.0000+ 2 ~ 1.0000+ 3	5.9878+ 0	5.9830+ 0	4.7789- 3		7.4740- 3
1.0000+ 3 ~ 1.5000+ 3	5.9871+ 0	5.9830+ 0	4.0694- 3		7.4816- 3
1.5000+ 3 ~ 2.0000+ 3	5.9865+ 0	5.9830+ 0	3.4307- 3		7.4998- 3
2.0000+ 3 ~ 3.0000+ 3	5.9859+ 0	5.9830+ 0	2.8775- 3		7.5460- 3
3.0000+ 3 ~ 4.0000+ 3	5.9854+ 0	5.9830+ 0	2.4258- 3		7.6528- 3
4.0000+ 3 ~ 5.0000+ 3	5.9852+ 0	5.9830+ 0	2.1372- 3		7.7681- 3
5.0000+ 3 ~ 6.0000+ 3	5.9849+ 0	5.9830+ 0	1.9321- 3		7.9082- 3
6.0000+ 3 ~ 8.0000+ 3	8.9080+ 0	8.8601+ 0	4.7706- 2		8.1671- 3
8.0000+ 3 ~ 1.0000+ 4	8.7281+ 0	8.6889+ 0	3.8933- 2		8.5828- 3
1.0000+ 4 ~ 1.5000+ 4	8.5615+ 0	8.5312+ 0	2.9982- 2		9.4900- 3
1.5000+ 4 ~ 2.0000+ 4	8.4434+ 0	8.4207+ 0	2.2667- 2		1.0978- 2
2.0000+ 4 ~ 3.0000+ 4	8.3971+ 0	8.3797+ 0	1.7319- 2		1.3877- 2
3.0000+ 4 ~ 4.0000+ 4	8.3988+ 0	8.3851+ 0	1.3655- 2		1.8172- 2
4.0000+ 4 ~ 5.0000+ 4	8.4321+ 0	8.4204+ 0	1.1750- 2		2.3085- 2
5.0000+ 4 ~ 6.0000+ 4	8.4739+ 0	8.4633+ 0	1.0594- 2		2.8468- 2
6.0000+ 4 ~ 8.0000+ 4	8.5361+ 0	8.5262+ 0	9.8607- 3		3.7229- 2
8.0000+ 4 ~ 1.0000+ 5	8.6060+ 0	8.5568+ 0	9.2857- 3		4.9695- 2
1.0000+ 5 ~ 1.5000+ 5	8.6472+ 0	8.6382+ 0	9.0161- 3		7.6714- 2
1.5000+ 5 ~ 2.0000+ 5	8.6668+ 0	8.6579+ 0	8.8977- 3		1.0911- 1
2.0000+ 5 ~ 3.0000+ 5	8.5501+ 0	8.5412+ 0	8.8681- 3		1.5353- 1
3.0000+ 5 ~ 4.0000+ 5	8.2584+ 0	8.2496+ 0	8.8344- 3		2.0590- 1
4.0000+ 5 ~ 5.0000+ 5	7.8927+ 0	7.8840+ 0	8.7446- 3		2.4781- 1
5.0000+ 5 ~ 6.0000+ 5	7.5101+ 0	7.5013+ 0	8.8474- 3		2.8018- 1
6.0000+ 5 ~ 8.0000+ 5	6.9627+ 0	6.9534+ 0	9.2523- 3		3.1335- 1
8.0000+ 5 ~ 1.0000+ 6	6.2876+ 0	6.0203+ 0	6.2576- 3	2.5870- 1	3.5500- 1
1.0000+ 6 ~ 1.5000+ 6	5.4695+ 0	4.6170+ 0	4.6892- 3	8.4241- 1	4.0529- 1
1.5000+ 6 ~ 2.0000+ 6	4.6336+ 0	3.5714+ 0	5.6376- 3	1.0561+ 0	4.1237- 1
2.0000+ 6 ~ 3.0000+ 6	4.0224+ 0	2.6143+ 0	5.0582- 3	1.3995+ 0	4.2961- 1
3.0000+ 6 ~ 4.0000+ 6	3.8274+ 0	2.1540+ 0	2.4617- 3	1.6702+ 0	5.0888- 1
4.0000+ 6 ~ 5.0000+ 6	3.8445+ 0	2.1008+ 0	1.2787- 3	1.7418+ 0	5.9096- 1
5.0000+ 6 ~ 6.0000+ 6	3.9531+ 0	2.1782+ 0	7.5214- 4	1.7700+ 0	6.5843- 1
6.0000+ 6 ~ 8.0000+ 6	4.2230+ 0	2.4533+ 0	4.0145- 4	1.7641+ 0	7.4137- 1
8.0000+ 6 ~ 1.0000+ 7	4.3670+ 0	2.6529+ 0	1.8082- 4	1.7138+ 0	8.1482- 1
1.0000+ 7 ~ 1.5000+ 7	4.1293+ 0	2.4583+ 0	6.2823- 5	1.6694+ 0	8.5724- 1

CROSS SECTION

MATERIAL =1401 ZR-93

ENERGY	TOTAL	ELASTIC	CAPTURE	INELA	MU-BAR
1.0000- 5 ~ 1.0000- 2	9.6521+ 0	5.5217+ 0	4.1303+ 0		7.2376- 3
1.0000- 2 ~ 1.5000- 2	7.4391+ 0	5.5217+ 0	1.9174+ 0		7.2376- 3
1.5000- 2 ~ 2.0000- 2	7.1352+ 0	5.5216+ 0	1.6135+ 0		7.2376- 3
2.0000- 2 ~ 3.0000- 2	6.8777+ 0	5.5216+ 0	1.3561+ 0		7.2376- 3
3.0000- 2 ~ 4.0000- 2	6.6628+ 0	5.5216+ 0	1.1413+ 0		7.2376- 3
4.0000- 2 ~ 5.0000- 2	6.5303+ 0	5.5215+ 0	1.0088+ 0		7.2376- 3
5.0000- 2 ~ 6.0000- 2	6.4314+ 0	5.5215+ 0	9.0994- 1		7.2376- 3
6.0000- 2 ~ 8.0000- 2	6.3289+ 0	5.5214+ 0	8.0752- 1		7.2376- 3
8.0000- 2 ~ 1.0000- 1	6.2352+ 0	5.5213+ 0	7.1389- 1		7.2376- 3
1.0000- 1 ~ 1.5000- 1	6.1278+ 0	5.5212+ 0	6.0662- 1		7.2376- 3
1.5000- 1 ~ 2.0000- 1	6.0338+ 0	5.5210+ 0	5.1287- 1		7.2376- 3
2.0000- 1 ~ 3.0000- 1	5.9505+ 0	5.5206+ 0	4.2991- 1		7.2376- 3
3.0000- 1 ~ 4.0000- 1	5.8840+ 0	5.5202+ 0	3.6380- 1		7.2376- 3
4.0000- 1 ~ 5.0000- 1	5.8404+ 0	5.5197+ 0	3.2065- 1		7.2376- 3
5.0000- 1 ~ 6.0000- 1	5.8094+ 0	5.5193+ 0	2.9009- 1		7.2376- 3
6.0000- 1 ~ 8.0000- 1	5.7775+ 0	5.5187+ 0	2.5888- 1		7.2376- 3
8.0000- 1 ~ 1.0000+ 0	5.7464+ 0	5.5178+ 0	2.2859- 1		7.2376- 3
1.0000+ 0 ~ 1.5000+ 0	5.7121+ 0	5.5162+ 0	1.9587- 1		7.2376- 3
1.5000+ 0 ~ 2.0000+ 0	5.6808+ 0	5.5140+ 0	1.6679- 1		7.2376- 3
2.0000+ 0 ~ 3.0000+ 0	5.6523+ 0	5.5106+ 0	1.4171- 1		7.2376- 3
3.0000+ 0 ~ 4.0000+ 0	5.6278+ 0	5.5060+ 0	1.2182- 1		7.2377- 3
4.0000+ 0 ~ 5.0000+ 0	5.6105+ 0	5.5014+ 0	1.0918- 1		7.2377- 3
5.0000+ 0 ~ 6.0000+ 0	5.5974+ 0	5.4966+ 0	1.0079- 1		7.2378- 3
6.0000+ 0 ~ 8.0000+ 0	5.5814+ 0	5.4894+ 0	9.2050- 2		7.2378- 3
8.0000+ 0 ~ 1.0000+ 1	5.5636+ 0	5.4794+ 0	8.4208- 2		7.2379- 3
1.0000+ 1 ~ 1.5000+ 1	5.5380+ 0	5.4610+ 0	7.6996- 2		7.2380- 3
1.5000+ 1 ~ 2.0000+ 1	5.5049+ 0	5.4328+ 0	7.2067- 2		7.2382- 3
2.0000+ 1 ~ 3.0000+ 1	5.4560+ 0	5.3843+ 0	7.1714- 2		7.2386- 3
3.0000+ 1 ~ 4.0000+ 1	5.3851+ 0	5.3073+ 0	7.7804- 2		7.2392- 3
4.0000+ 1 ~ 5.0000+ 1	5.3013+ 0	5.2098+ 0	9.1408- 2		7.2396- 3
5.0000+ 1 ~ 6.0000+ 1	5.1972+ 0	5.0815+ 0	1.1568- 1		7.2402- 3
6.0000+ 1 ~ 8.0000+ 1	4.9764+ 0	4.7729+ 0	2.0346- 1		7.2414- 3
8.0000+ 1 ~ 1.0000+ 2	4.7323+ 0	3.8428+ 0	8.8951- 1		7.2425- 3
1.0000+ 2 ~ 1.5000+ 2	1.1028+ 2	5.6866+ 1	5.3409+ 1		7.2451- 3
1.5000+ 2 ~ 2.0000+ 2	7.0057+ 0	6.9504+ 0	5.5340- 2		7.2491- 3
2.0000+ 2 ~ 3.0000+ 2	1.0260+ 1	8.9968+ 0	1.2626+ 0		7.2562- 3
3.0000+ 2 ~ 4.0000+ 2	1.4938+ 1	1.2235+ 1	2.6902+ 0		7.2661- 3
4.0000+ 2 ~ 5.0000+ 2	1.3898+ 1	1.1633+ 1	2.2553+ 0		7.2797- 3
5.0000+ 2 ~ 6.0000+ 2	1.3158+ 1	1.1187+ 1	1.9678+ 0		7.2924- 3
6.0000+ 2 ~ 8.0000+ 2	1.2391+ 1	1.0701+ 1	1.6876+ 0		7.3137- 3
8.0000+ 2 ~ 1.0000+ 3	1.1680+ 1	1.0233+ 1	1.4444+ 0		7.3455- 3
1.0000+ 3 ~ 1.5000+ 3	1.0912+ 1	9.7078+ 0	1.2021+ 0		7.4091- 3
1.5000+ 3 ~ 2.0000+ 3	1.0232+ 1	9.2305+ 0	1.0004+ 0		7.5076- 3
2.0000+ 3 ~ 3.0000+ 3	9.6707+ 0	8.8332+ 0	8.3702- 1		7.6794- 3
3.0000+ 3 ~ 4.0000+ 3	9.2549+ 0	8.5481+ 0	7.0391- 1		7.9747- 3
4.0000+ 3 ~ 5.0000+ 3	8.9976+ 0	8.3779+ 0	6.1744- 1		8.2648- 3
5.0000+ 3 ~ 6.0000+ 3	8.8244+ 0	8.2692+ 0	5.5385- 1		8.5802- 3
6.0000+ 3 ~ 8.0000+ 3	8.6665+ 0	8.1918+ 0	4.8351- 1		9.1121- 3
8.0000+ 3 ~ 1.0000+ 4	8.5422+ 0	8.1259+ 0	4.1462- 1		9.8995- 3
1.0000+ 4 ~ 1.5000+ 4	8.4454+ 0	8.1071+ 0	3.3632- 1		1.1463- 2
1.5000+ 4 ~ 2.0000+ 4	8.4001+ 0	8.1338+ 0	2.6531- 1		1.3860- 2
2.0000+ 4 ~ 3.0000+ 4	8.4303+ 0	8.2241+ 0	2.0454- 1		1.8152- 2
3.0000+ 4 ~ 4.0000+ 4	8.5062+ 0	8.3480+ 0	1.5744- 1		2.4188- 2
4.0000+ 4 ~ 5.0000+ 4	8.5946+ 0	8.4649+ 0	1.2928- 1		3.0779- 2
5.0000+ 4 ~ 6.0000+ 4	8.6798+ 0	8.5689+ 0	1.1069- 1		3.7763- 2
6.0000+ 4 ~ 8.0000+ 4	8.7908+ 0	8.6580+ 0	9.2696- 2		4.8756- 2
8.0000+ 4 ~ 1.0000+ 5	8.9079+ 0	8.8304+ 0	7.7428- 2		6.3909- 2
1.0000+ 5 ~ 1.5000+ 5	8.9874+ 0	8.9220+ 0	6.4578- 2		9.4683- 2
1.5000+ 5 ~ 2.0000+ 5	9.0387+ 0	8.9838+ 0	5.4279- 2		1.3104- 1
2.0000+ 5 ~ 3.0000+ 5	8.8845+ 0	8.8195+ 0	4.6876- 2	1.8094- 2	1.8011- 1
3.0000+ 5 ~ 4.0000+ 5	8.6246+ 0	8.3045+ 0	4.2477- 2	2.7449- 1	2.4066- 1
4.0000+ 5 ~ 5.0000+ 5	8.2418+ 0	7.7178+ 0	4.1080- 2	4.8162- 1	2.9120- 1
5.0000+ 5 ~ 6.0000+ 5	7.8457+ 0	7.2401+ 0	4.1041- 2	5.6402- 1	3.2901- 1
6.0000+ 5 ~ 8.0000+ 5	7.2838+ 0	6.6531+ 0	4.1817- 2	5.8862- 1	3.6625- 1
8.0000+ 5 ~ 1.0000+ 6	6.6206+ 0	6.0011+ 0	4.3672- 2	5.7575- 1	3.9398- 1
1.0000+ 6 ~ 1.5000+ 6	5.7184+ 0	5.0709+ 0	4.9211- 2	5.9752- 1	4.0716- 1
1.5000+ 6 ~ 2.0000+ 6	4.8479+ 0	3.8995+ 0	5.4306- 2	8.9265- 1	4.1737- 1
2.0000+ 6 ~ 3.0000+ 6	4.1032+ 0	2.8594+ 0	5.9534- 2	1.1837+ 0	4.2476- 1
3.0000+ 6 ~ 4.0000+ 6	3.8694+ 0	2.2941+ 0	2.8982- 2	1.5293+ 0	4.9334- 1
4.0000+ 6 ~ 5.0000+ 6	3.8528+ 0	2.1108+ 0	8.3384- 3	1.7221+ 0	5.8103- 1
5.0000+ 6 ~ 6.0000+ 6	3.9465+ 0	2.1412+ 0	3.5186- 3	1.7961+ 0	6.5187- 1
6.0000+ 6 ~ 8.0000+ 6	4.2146+ 0	2.4302+ 0	1.6179- 3	1.7758+ 0	7.3730- 1
8.0000+ 6 ~ 1.0000+ 7	4.3756+ 0	2.6552+ 0	6.3887- 4	1.7195+ 0	8.1302- 1
1.0000+ 7 ~ 1.5000+ 7	4.2120+ 0	2.5094+ 0	2.1632- 4	1.7010+ 0	8.5831- 1

CROSS SECTION

MATERIAL =1423 MO-95

ENERGY	TOTAL	ELASTIC	CAPTURE	INELA	MU-BAR
1.0000- 5 ~ 1.0000- 2	4.9218+ 1	4.6172+ 0	4.4606+ 1		7.0851- 3
1.0000- 2 ~ 1.5000- 2	2.5307+ 1	4.6171+ 0	2.0674+ 1		7.0851- 3
1.5000- 2 ~ 2.0000- 2	2.2054+ 1	4.6169+ 0	1.7457+ 1		7.0851- 3
2.0000- 2 ~ 3.0000- 2	1.9250+ 1	4.6168+ 0	1.4622+ 1		7.0851- 3
3.0000- 2 ~ 4.0000- 2	1.6950+ 1	4.6165+ 0	1.2348+ 1		7.0851- 3
4.0000- 2 ~ 5.0000- 2	1.5496+ 1	4.6163+ 0	1.0869+ 1		7.0851- 3
5.0000- 2 ~ 6.0000- 2	1.4439+ 1	4.6161+ 0	9.8168+ 0		7.0851- 3
6.0000- 2 ~ 8.0000- 2	1.3342+ 1	4.6157+ 0	8.7361+ 0		7.0851- 3
8.0000- 2 ~ 1.0000- 1	1.2314+ 1	4.6153+ 0	7.6914+ 0		7.0851- 3
1.0000- 1 ~ 1.5000- 1	1.1164+ 1	4.6145+ 0	6.5503+ 0		7.0851- 3
1.5000- 1 ~ 2.0000- 1	1.0148+ 1	4.6133+ 0	5.5337+ 0		7.0851- 3
2.0000- 1 ~ 3.0000- 1	9.2525+ 0	4.6116+ 0	4.6412+ 0		7.0851- 3
3.0000- 1 ~ 4.0000- 1	8.5339+ 0	4.6092+ 0	3.9242+ 0		7.0851- 3
4.0000- 1 ~ 5.0000- 1	8.0657+ 0	4.6069+ 0	3.4565+ 0		7.0851- 3
5.0000- 1 ~ 6.0000- 1	7.7361+ 0	4.6046+ 0	3.1343+ 0		7.0851- 3
6.0000- 1 ~ 8.0000- 1	7.3924+ 0	4.6010+ 0	2.7911+ 0		7.0851- 3
8.0000- 1 ~ 1.0000+ 0	7.0607+ 0	4.5963+ 0	2.4628+ 0		7.0851- 3
1.0000+ 0 ~ 1.5000+ 0	6.6995+ 0	4.5878+ 0	2.1130+ 0		7.0851- 3
1.5000+ 0 ~ 2.0000+ 0	6.3722+ 0	4.5755+ 0	1.7950+ 0		7.0852- 3
2.0000+ 0 ~ 3.0000+ 0	5.0834+ 0	4.5565+ 0	1.5279+ 0		7.0853- 3
3.0000+ 0 ~ 4.0000+ 0	5.8427+ 0	4.5302+ 0	1.3114+ 0		7.0854- 3
4.0000+ 0 ~ 5.0000+ 0	5.6817+ 0	4.5024+ 0	1.1807+ 0		7.0856- 3
5.0000+ 0 ~ 6.0000+ 0	5.5630+ 0	4.4734+ 0	1.0895+ 0		7.0857- 3
6.0000+ 0 ~ 8.0000+ 0	5.4276+ 0	4.4269+ 0	9.9993- 1		7.0859- 3
8.0000+ 0 ~ 1.0000+ 1	5.2858+ 0	4.3588+ 0	9.2800- 1		7.0861- 3
1.0000+ 1 ~ 1.5000+ 1	5.0965+ 0	4.2205+ 0	8.7559- 1		7.0866- 3
1.5000+ 1 ~ 2.0000+ 1	4.8688+ 0	3.9738+ 0	8.9466- 1		7.0873- 3
2.0000+ 1 ~ 3.0000+ 1	4.6262+ 0	3.4264+ 0	1.1988+ 0		7.0887- 3
3.0000+ 1 ~ 4.0000+ 1	7.1019+ 0	3.0064+ 0	4.0949+ 0		7.0905- 3
4.0000+ 1 ~ 5.0000+ 1	1.0173+ 3	5.6478+ 2	4.5255+ 2		7.0918- 3
5.0000+ 1 ~ 6.0000+ 1	2.0058+ 1	1.6830+ 1	3.2272+ 0		7.0935- 3
6.0000+ 1 ~ 8.0000+ 1	9.6594+ 0	9.0911+ 0	5.6815- 1		7.0966- 3
8.0000+ 1 ~ 1.0000+ 2	7.6143+ 0	7.3644+ 0	2.4996- 1		7.0998- 3
1.0000+ 2 ~ 1.5000+ 2	6.8700+ 0	6.5843+ 0	2.8563- 1		7.1065- 3
1.5000+ 2 ~ 2.0000+ 2	1.0131+ 1	6.5125+ 0	3.5180+ 0		7.1167- 3
2.0000+ 2 ~ 3.0000+ 2	6.3244+ 0	5.9492+ 0	3.7476- 1		7.1334- 3
3.0000+ 2 ~ 4.0000+ 2	2.5708+ 1	1.8960+ 1	6.7470+ 0		7.1601- 3
4.0000+ 2 ~ 5.0000+ 2	6.9371+ 0	6.3124+ 0	6.2458- 1		7.1856- 3
5.0000+ 2 ~ 6.0000+ 2	9.1831+ 0	6.9794+ 0	2.2037+ 0		7.2124- 3
6.0000+ 2 ~ 8.0000+ 2	2.4015+ 1	1.9336+ 1	4.6794+ 0		7.2561- 3
8.0000+ 2 ~ 1.0000+ 3	9.8155+ 0	8.3179+ 0	1.4975+ 0		7.3190- 3
1.0000+ 3 ~ 1.5000+ 3	1.4100+ 1	1.1742+ 1	2.3581+ 0		7.4395- 3
1.5000+ 3 ~ 2.0000+ 3	1.2186+ 1	1.0545+ 1	1.6402+ 0		7.6192- 3
2.0000+ 3 ~ 3.0000+ 3	9.3919+ 0	8.0673+ 0	1.3243+ 0		7.9180- 3
3.0000+ 3 ~ 4.0000+ 3	9.0418+ 0	7.8416+ 0	1.1968+ 0		8.4016- 3
4.0000+ 3 ~ 5.0000+ 3	8.8181+ 0	7.7407+ 0	1.0748+ 0		8.8652- 3
5.0000+ 3 ~ 6.0000+ 3	8.6707+ 0	7.6843+ 0	9.8482- 1		9.3521- 3
6.0000+ 3 ~ 8.0000+ 3	8.5426+ 0	7.6562+ 0	8.8490- 1		1.0147- 2
8.0000+ 3 ~ 1.0000+ 4	8.4491+ 0	7.6631+ 0	7.8399- 1		1.1284- 2
1.0000+ 4 ~ 1.5000+ 4	8.3915+ 0	7.7264+ 0	6.6233- 1		1.3445- 2
1.5000+ 4 ~ 2.0000+ 4	8.3875+ 0	7.8411+ 0	5.4490- 1		1.6642- 2
2.0000+ 4 ~ 3.0000+ 4	8.4607+ 0	8.0220+ 0	4.3571- 1		2.2099- 2
3.0000+ 4 ~ 4.0000+ 4	8.5776+ 0	8.2304+ 0	3.4570- 1		2.9534- 2
4.0000+ 4 ~ 5.0000+ 4	8.6958+ 0	8.4063+ 0	2.8876- 1		3.7415- 2
5.0000+ 4 ~ 6.0000+ 4	8.8036+ 0	8.5536+ 0	2.4958- 1		4.5586- 2
6.0000+ 4 ~ 8.0000+ 4	8.9392+ 0	8.7287+ 0	2.1018- 1		5.8169- 2
8.0000+ 4 ~ 1.0000+ 5	9.0779+ 0	8.9023+ 0	1.7552- 1		7.5156- 2
1.0000+ 5 ~ 1.5000+ 5	9.1702+ 0	9.0240+ 0	1.4402- 1		1.0823- 1
1.5000+ 5 ~ 2.0000+ 5	9.2294+ 0	9.1095+ 0	1.1828- 1		1.4694- 1
2.0000+ 5 ~ 3.0000+ 5	9.1032+ 0	8.8012+ 0	9.6527- 2	2.0245- 1	2.0165- 1
3.0000+ 5 ~ 4.0000+ 5	8.8027+ 0	8.2163+ 0	8.3892- 2	5.0067- 1	2.6567- 1
4.0000+ 5 ~ 5.0000+ 5	8.4139+ 0	7.7171+ 0	8.1675- 2	6.1452- 1	3.1441- 1
5.0000+ 5 ~ 6.0000+ 5	8.0157+ 0	7.2910+ 0	8.2453- 2	6.4203- 1	3.4997- 1
6.0000+ 5 ~ 8.0000+ 5	7.4407+ 0	6.7265+ 0	8.3884- 2	6.3021- 1	3.8539- 1
8.0000+ 5 ~ 1.0000+ 6	6.7757+ 0	5.8186+ 0	7.2113- 2	8.8411- 1	4.3074- 1
1.0000+ 6 ~ 1.5000+ 6	5.8481+ 0	4.4534+ 0	4.8923- 2	1.3444+ 0	4.9139- 1
1.5000+ 6 ~ 2.0000+ 6	4.9830+ 0	3.3188+ 0	3.7355- 2	1.6256+ 0	5.1826- 1
2.0000+ 6 ~ 3.0000+ 6	4.2428+ 0	2.4342+ 0	2.7302- 2	1.7777+ 0	5.2290- 1
3.0000+ 6 ~ 4.0000+ 6	3.8976+ 0	2.0612+ 0	1.7960- 2	1.8174+ 0	5.5316- 1
4.0000+ 6 ~ 5.0000+ 6	3.8567+ 0	2.0270+ 0	1.1765- 2	1.8171+ 0	5.9487- 1
5.0000+ 6 ~ 6.0000+ 6	3.9396+ 0	2.1188+ 0	7.6072- 3	1.8067+ 0	6.4686- 1
6.0000+ 6 ~ 8.0000+ 6	4.2063+ 0	2.4138+ 0	3.9582- 3	1.7805+ 0	7.3409- 1
8.0000+ 6 ~ 1.0000+ 7	4.3808+ 0	2.6539+ 0	1.7239- 3	1.7247+ 0	8.1140- 1
1.0000+ 7 ~ 1.5000+ 7	4.2683+ 0	2.5428+ 0	6.0379- 4	1.7237+ 0	8.5880- 1

CROSS SECTION

MATERIAL =1425 MO-97

ENERGY	TOTAL	ELASTIC	CAPTURE	INELA	MU-BAR
1.0000- 5 ~ 1.0000- 2	1.1865+ 1	5.1129+ 0	6.7522+ 0		6.9388- 3
1.0000- 2 ~ 1.5000- 2	8.2435+ 0	5.1129+ 0	3.1331+ 0		6.9388- 3
1.5000- 2 ~ 2.0000- 2	7.7537+ 0	5.1129+ 0	2.6380+ 0		6.9388- 3
2.0000- 2 ~ 3.0000- 2	7.3266+ 0	5.1129+ 0	2.2154+ 0		6.9388- 3
3.0000- 2 ~ 4.0000- 2	6.9803+ 0	5.1129+ 0	1.8654+ 0		6.9388- 3
4.0000- 2 ~ 5.0000- 2	6.7552+ 0	5.1129+ 0	1.6420+ 0		6.9388- 3
5.0000- 2 ~ 6.0000- 2	6.6014+ 0	5.1129+ 0	1.4913+ 0		6.9388- 3
6.0000- 2 ~ 8.0000- 2	6.4334+ 0	5.1129+ 0	1.3191+ 0		6.9388- 3
8.0000- 2 ~ 1.0000- 1	6.2742+ 0	5.1129+ 0	1.1611+ 0		6.9388- 3
1.0000- 1 ~ 1.5000- 1	6.1039+ 0	5.1129+ 0	9.9140- 1		6.9388- 3
1.5000- 1 ~ 2.0000- 1	5.9470+ 0	5.1129+ 0	8.3362- 1		6.9388- 3
2.0000- 1 ~ 3.0000- 1	5.8137+ 0	5.1128+ 0	7.0115- 1		6.9388- 3
3.0000- 1 ~ 4.0000- 1	5.7028+ 0	5.1128+ 0	5.8960- 1		6.9388- 3
4.0000- 1 ~ 5.0000- 1	5.6340+ 0	5.1128+ 0	5.2163- 1		6.9388- 3
5.0000- 1 ~ 6.0000- 1	5.5831+ 0	5.1128+ 0	4.7030- 1		6.9388- 3
6.0000- 1 ~ 8.0000- 1	5.5301+ 0	5.1127+ 0	4.1712- 1		6.9388- 3
8.0000- 1 ~ 1.0000+ 0	5.4814+ 0	5.1126+ 0	3.6909- 1		6.9388- 3
1.0000+ 0 ~ 1.5000+ 0	5.4260+ 0	5.1125+ 0	3.1336- 1		6.9390- 3
1.5000+ 0 ~ 2.0000+ 0	5.3772+ 0	5.1123+ 0	2.6504- 1		6.9392- 3
2.0000+ 0 ~ 3.0000+ 0	5.3341+ 0	5.1120+ 0	2.2200- 1		6.9394- 3
3.0000+ 0 ~ 4.0000+ 0	5.2995+ 0	5.1116+ 0	1.8793- 1		6.9397- 3
4.0000+ 0 ~ 5.0000+ 0	5.2768+ 0	5.1112+ 0	1.6552- 1		6.9401- 3
5.0000+ 0 ~ 6.0000+ 0	5.2606+ 0	5.1107+ 0	1.4976- 1		6.9403- 3
6.0000+ 0 ~ 8.0000+ 0	5.2437+ 0	5.1100+ 0	1.3376- 1		6.9407- 3
8.0000+ 0 ~ 1.0000+ 1	5.2272+ 0	5.1090+ 0	1.1817- 1		6.9410- 3
1.0000+ 1 ~ 1.5000+ 1	5.2097+ 0	5.1068+ 0	1.0267- 1		6.9419- 3
1.5000+ 1 ~ 2.0000+ 1	5.2532+ 0	5.1030+ 0	1.4993- 1		6.9431- 3
2.0000+ 1 ~ 3.0000+ 1	5.1695+ 0	5.0947+ 0	7.4732- 2		6.9456- 3
3.0000+ 1 ~ 4.0000+ 1	5.1442+ 0	5.0771+ 0	6.6861- 2		6.9488- 3
4.0000+ 1 ~ 5.0000+ 1	5.1122+ 0	5.0436+ 0	6.7892- 2		6.9511- 3
5.0000+ 1 ~ 6.0000+ 1	5.1809+ 0	4.9633+ 0	2.1736- 1		6.9543- 3
6.0000+ 1 ~ 8.0000+ 1	2.6668+ 1	7.6743+ 0	1.8994+ 1		6.9599- 3
8.0000+ 1 ~ 1.0000+ 2	5.3409+ 0	5.2656+ 0	7.5321- 2		6.9657- 3
1.0000+ 2 ~ 1.5000+ 2	5.6545+ 0	5.1242+ 0	5.3029- 1		6.9776- 3
1.5000+ 2 ~ 2.0000+ 2	5.0851+ 0	5.0553+ 0	2.9720- 2		6.9956- 3
2.0000+ 2 ~ 3.0000+ 2	1.0059+ 1	5.7988+ 0	4.2600+ 0		7.0248- 3
3.0000+ 2 ~ 4.0000+ 2	1.1112+ 1	6.6129+ 0	4.4993+ 0		7.0707- 3
4.0000+ 2 ~ 5.0000+ 2	5.0467+ 0	4.9023+ 0	1.4435- 1		7.1141- 3
5.0000+ 2 ~ 6.0000+ 2	3.0490+ 1	2.3142+ 1	7.3479+ 0		7.1593- 3
6.0000+ 2 ~ 8.0000+ 2	1.6901+ 1	1.2578+ 1	4.3231+ 0		7.2322- 3
8.0000+ 2 ~ 1.0000+ 3	6.8127+ 0	6.0368+ 0	7.7588- 1		7.3356- 3
1.0000+ 3 ~ 1.5000+ 3	1.0517+ 1	8.2242+ 0	2.2928+ 0		7.5295- 3
1.5000+ 3 ~ 2.0000+ 3	1.0232+ 1	8.3365+ 0	1.8951+ 0		7.8133- 3
2.0000+ 3 ~ 3.0000+ 3	9.6623+ 0	7.8373+ 0	1.8247+ 0		8.2717- 3
3.0000+ 3 ~ 4.0000+ 3	9.2652+ 0	7.6894+ 0	1.5752+ 0		8.9872- 3
4.0000+ 3 ~ 5.0000+ 3	8.9744+ 0	7.6130+ 0	1.3600+ 0		9.6622- 3
5.0000+ 3 ~ 6.0000+ 3	8.7919+ 0	7.5767+ 0	1.2117+ 0		1.0355- 2
6.0000+ 3 ~ 8.0000+ 3	8.6288+ 0	7.5736+ 0	1.0521+ 0		1.1461- 2
8.0000+ 3 ~ 1.0000+ 4	8.5102+ 0	7.6071+ 0	8.9910- 1		1.3009- 2
1.0000+ 4 ~ 1.5000+ 4	8.4159+ 0	7.7038+ 0	7.0522- 1		1.5860- 2
1.5000+ 4 ~ 2.0000+ 4	8.3861+ 0	7.8526+ 0	5.3076- 1		1.9970- 2
2.0000+ 4 ~ 3.0000+ 4	8.4797+ 0	8.0672+ 0	4.0944- 1		2.6735- 2
3.0000+ 4 ~ 4.0000+ 4	8.6310+ 0	8.3067+ 0	3.2287- 1		3.5718- 2
4.0000+ 4 ~ 5.0000+ 4	8.7732+ 0	8.5037+ 0	2.6875- 1		4.5000- 2
5.0000+ 4 ~ 6.0000+ 4	8.8983+ 0	8.6660+ 0	2.3184- 1		5.4437- 2
6.0000+ 4 ~ 8.0000+ 4	9.0510+ 0	8.8558+ 0	1.9499- 1		6.8677- 2
8.0000+ 4 ~ 1.0000+ 5	9.2034+ 0	9.0404+ 0	1.6283- 1		8.7517- 2
1.0000+ 5 ~ 1.5000+ 5	9.2997+ 0	9.1636+ 0	1.3413- 1		1.2272- 1
1.5000+ 5 ~ 2.0000+ 5	9.3585+ 0	9.2463+ 0	1.1079- 1		1.6349- 1
2.0000+ 5 ~ 3.0000+ 5	9.2418+ 0	9.1453+ 0	9.6436- 2		2.1389- 1
3.0000+ 5 ~ 4.0000+ 5	8.9217+ 0	8.8313+ 0	9.0402- 2		2.6819- 1
4.0000+ 5 ~ 5.0000+ 5	8.5188+ 0	8.4268+ 0	8.9353- 2	2.6058- 3	3.0906- 1
5.0000+ 5 ~ 6.0000+ 5	8.1439+ 0	7.8625+ 0	8.8601- 2	1.6991- 1	3.4508- 1
6.0000+ 5 ~ 8.0000+ 5	7.5524+ 0	6.9203+ 0	7.8154- 2	5.5244- 1	3.9733- 1
8.0000+ 5 ~ 1.0000+ 6	6.9422+ 0	5.6912+ 0	6.3785- 2	1.1855+ 0	4.6374- 1
1.0000+ 6 ~ 1.5000+ 6	5.9974+ 0	4.5282+ 0	4.8647- 2	1.4198+ 0	5.0920- 1
1.5000+ 6 ~ 2.0000+ 6	5.1225+ 0	3.4268+ 0	2.9286- 2	1.6646+ 0	5.3213- 1
2.0000+ 6 ~ 3.0000+ 6	4.3246+ 0	2.4870+ 0	1.8826- 2	1.8150+ 0	5.3995- 1
3.0000+ 6 ~ 4.0000+ 6	3.9282+ 0	2.0727+ 0	1.1790- 2	1.8426+ 0	5.6180- 1
4.0000+ 6 ~ 5.0000+ 6	3.8609+ 0	2.0097+ 0	7.4579- 3	1.8430+ 0	5.9408- 1
5.0000+ 6 ~ 6.0000+ 6	3.9320+ 0	2.0916+ 0	4.4794- 3	1.8288+ 0	6.4247- 1
6.0000+ 6 ~ 8.0000+ 6	4.1963+ 0	2.3932+ 0	1.9974- 3	1.7924+ 0	7.3072- 1
8.0000+ 6 ~ 1.0000+ 7	4.3870+ 0	2.6500+ 0	7.3761- 4	1.7357+ 0	8.0924- 1
1.0000+ 7 ~ 1.5000+ 7	4.3294+ 0	2.5779+ 0	2.4964- 4	1.7503+ 0	8.5915- 1

CROSS SECTION

MATERIAL =1431 TC-99

ENERGY	TOTAL	ELASTIC	CAPTURE	INELA	MU-BAR
1.0000- 5 ~ 1.0000- 2	5.8488+ 1	3.9463+ 0	5.4540+ 1		6.7986- 3
1.0000- 2 ~ 1.5000- 2	2.9298+ 1	3.9480+ 0	2.5350+ 1		6.7989- 3
1.5000- 2 ~ 2.0000- 2	2.5385+ 1	3.9477+ 0	2.1437+ 1		6.7989- 3
2.0000- 2 ~ 3.0000- 2	2.1946+ 1	3.9474+ 0	1.7998+ 1		6.7989- 3
3.0000- 2 ~ 4.0000- 2	1.9192+ 1	3.9470+ 0	1.5245+ 1		6.7989- 3
4.0000- 2 ~ 5.0000- 2	1.7410+ 1	3.9466+ 0	1.3464+ 1		6.7989- 3
5.0000- 2 ~ 6.0000- 2	1.6144+ 1	3.9462+ 0	1.2198+ 1		6.7989- 3
6.0000- 2 ~ 8.0000- 2	1.4850+ 1	3.9455+ 0	1.0904+ 1		6.7989- 3
8.0000- 2 ~ 1.0000- 1	1.3607+ 1	3.9447+ 0	9.6624+ 0		6.7989- 3
1.0000- 1 ~ 1.5000- 1	1.2261+ 1	3.9431+ 0	8.3183+ 0		6.7990- 3
1.5000- 1 ~ 2.0000- 1	1.1082+ 1	3.9409+ 0	7.1411+ 0		6.7990- 3
2.0000- 1 ~ 3.0000- 1	1.0072+ 1	3.9376+ 0	6.1348+ 0		6.7990- 3
3.0000- 1 ~ 4.0000- 1	9.2943+ 0	3.9329+ 0	5.3614+ 0		6.7990- 3
4.0000- 1 ~ 5.0000- 1	8.8140+ 0	3.9280+ 0	4.8860+ 0		6.7990- 3
5.0000- 1 ~ 6.0000- 1	8.5075+ 0	3.9229+ 0	4.5846+ 0		6.7990- 3
6.0000- 1 ~ 8.0000- 1	8.2191+ 0	3.9148+ 0	4.3043+ 0		6.7990- 3
8.0000- 1 ~ 1.0000+ 0	7.9948+ 0	3.9032+ 0	4.0916+ 0		6.7990- 3
1.0000+ 0 ~ 1.5000+ 0	7.9099+ 0	3.8796+ 0	4.0303+ 0		6.7992- 3
1.5000+ 0 ~ 2.0000+ 0	8.1184+ 0	3.8389+ 0	4.2796+ 0		6.7994- 3
2.0000+ 0 ~ 3.0000+ 0	9.2296+ 0	3.7508+ 0	5.4788+ 0		6.7996- 3
3.0000+ 0 ~ 4.0000+ 0	1.3545+ 1	3.5441+ 0	1.0001+ 1		6.8003- 3
4.0000+ 0 ~ 5.0000+ 0	3.8028+ 1	3.0250+ 0	3.5003+ 1		6.8012- 3
5.0000+ 0 ~ 6.0000+ 0	6.7716+ 2	9.0478+ 0	6.6811+ 2		6.8019- 3
6.0000+ 0 ~ 8.0000+ 0	4.1568+ 1	5.8572+ 0	3.5711+ 1		6.8027- 3
8.0000+ 0 ~ 1.0000+ 1	7.5059+ 0	4.5868+ 0	2.9191+ 0		6.8036- 3
1.0000+ 1 ~ 1.5000+ 1	5.3849+ 0	4.2620+ 0	1.1229+ 0		6.8057- 3
1.5000+ 1 ~ 2.0000+ 1	1.7917+ 1	3.5629+ 0	1.4354+ 1		6.8085- 3
2.0000+ 1 ~ 3.0000+ 1	5.3798+ 1	6.0927+ 0	4.7706+ 1		6.8137- 3
3.0000+ 1 ~ 4.0000+ 1	1.0052+ 1	4.4362+ 0	5.6159+ 0		6.8203- 3
4.0000+ 1 ~ 5.0000+ 1	5.2713+ 0	4.5403+ 0	7.3096- 1		6.8251- 3
5.0000+ 1 ~ 6.0000+ 1	1.5273+ 1	4.6415+ 0	1.0632+ 1		6.8314- 3
6.0000+ 1 ~ 8.0000+ 1	4.4002+ 0	4.3567+ 0	4.3508- 2		6.8422- 3
8.0000+ 1 ~ 1.0000+ 2	4.2154+ 0	4.1872+ 0	2.8176- 2		6.8536- 3
1.0000+ 2 ~ 1.5000+ 2	1.0839+ 1	4.7208+ 0	6.1183+ 0		6.8758- 3
1.5000+ 2 ~ 2.0000+ 2	4.5705+ 1	1.8631+ 1	2.6873+ 1		6.9086- 3
2.0000+ 2 ~ 3.0000+ 2	1.1663+ 1	6.8036+ 0	4.8597+ 0		6.9599- 3
3.0000+ 2 ~ 4.0000+ 2	1.5097+ 1	7.7346+ 0	7.3624+ 0		7.0379- 3
4.0000+ 2 ~ 5.0000+ 2	1.4010+ 1	7.6215+ 0	6.3835+ 0		7.1106- 3
5.0000+ 2 ~ 6.0000+ 2	1.2455+ 1	7.5315+ 0	4.9129+ 0		7.1848- 3
6.0000+ 2 ~ 8.0000+ 2	1.1417+ 1	7.4246+ 0	3.9889+ 0		7.3023- 3
8.0000+ 2 ~ 1.0000+ 3	1.0790+ 1	7.3139+ 0	3.4708+ 0		7.4662- 3
1.0000+ 3 ~ 1.5000+ 3	1.0227+ 1	7.1789+ 0	3.0455+ 0		7.7672- 3
1.5000+ 3 ~ 2.0000+ 3	9.6783+ 0	7.0483+ 0	2.6285+ 0		8.2002- 3
2.0000+ 3 ~ 3.0000+ 3	9.0698+ 0	6.9365+ 0	2.1320+ 0		8.8854- 3
3.0000+ 3 ~ 4.0000+ 3	8.6880+ 0	6.8701+ 0	1.8145+ 0		9.9294- 3
4.0000+ 3 ~ 5.0000+ 3	8.5120+ 0	6.8419+ 0	1.6674+ 0		1.0904- 2
5.0000+ 3 ~ 6.0000+ 3	8.4012+ 0	6.8395+ 0	1.5603+ 0		1.1888- 2
6.0000+ 3 ~ 8.0000+ 3	8.3157+ 0	6.8710+ 0	1.4432+ 0		1.3430- 2
8.0000+ 3 ~ 1.0000+ 4	8.2660+ 0	6.9412+ 0	1.3228+ 0		1.5543- 2
1.0000+ 4 ~ 1.5000+ 4	8.2635+ 0	7.0917+ 0	1.1687+ 0		1.9308- 2
1.5000+ 4 ~ 2.0000+ 4	8.3164+ 0	7.3058+ 0	1.0087+ 0		2.4579- 2
2.0000+ 4 ~ 3.0000+ 4	8.4469+ 0	7.5988+ 0	8.4363- 1		3.2884- 2
3.0000+ 4 ~ 4.0000+ 4	8.6163+ 0	7.9175+ 0	6.9650- 1		4.3588- 2
4.0000+ 4 ~ 5.0000+ 4	8.7699+ 0	8.1720+ 0	5.9652- 1		5.4340- 2
5.0000+ 4 ~ 6.0000+ 4	8.9021+ 0	8.3769+ 0	5.2437- 1		6.5048- 2
6.0000+ 4 ~ 8.0000+ 4	9.0604+ 0	8.6113+ 0	4.4862- 1		8.0882- 2
8.0000+ 4 ~ 1.0000+ 5	9.2152+ 0	8.8356+ 0	3.7936- 1		1.0144- 1
1.0000+ 5 ~ 1.5000+ 5	9.1750+ 0	8.8691+ 0	2.9940- 1	5.0573- 3	1.4114- 1
1.5000+ 5 ~ 2.0000+ 5	9.2558+ 0	8.7880+ 0	2.2900- 1	2.3852- 1	1.8786- 1
2.0000+ 5 ~ 3.0000+ 5	9.2444+ 0	8.4231+ 0	1.8034- 1	6.3690- 1	2.4938- 1
3.0000+ 5 ~ 4.0000+ 5	8.9320+ 0	7.9102+ 0	1.5353- 1	8.6745- 1	3.1580- 1
4.0000+ 5 ~ 5.0000+ 5	8.5612+ 0	7.5125+ 0	1.4615- 1	9.0250- 1	3.6228- 1
5.0000+ 5 ~ 6.0000+ 5	8.1822+ 0	7.1545+ 0	1.4436- 1	8.8342- 1	3.9513- 1
6.0000+ 5 ~ 8.0000+ 5	7.6514+ 0	6.6446+ 0	1.4560- 1	8.6128- 1	4.2809- 1
8.0000+ 5 ~ 1.0000+ 6	7.0353+ 0	5.9524+ 0	1.4957- 1	9.3294- 1	4.5975- 1
1.0000+ 6 ~ 1.5000+ 6	6.1570+ 0	4.9744+ 0	1.5436- 1	1.0260+ 0	4.8247- 1
1.5000+ 6 ~ 2.0000+ 6	5.2453+ 0	3.7567+ 0	1.0546- 1	1.3785+ 0	5.0984- 1
2.0000+ 6 ~ 3.0000+ 6	4.3982+ 0	2.6347+ 0	5.9036- 2	1.6985+ 0	5.3533- 1
3.0000+ 6 ~ 4.0000+ 6	3.9611+ 0	2.1208+ 0	3.4611- 2	1.8027+ 0	5.6211- 1
4.0000+ 6 ~ 5.0000+ 6	3.8731+ 0	2.0125+ 0	2.3829- 2	1.8345+ 0	5.9147- 1
5.0000+ 6 ~ 6.0000+ 6	3.9337+ 0	2.0762+ 0	1.4810- 2	1.8337+ 0	6.3892- 1
6.0000+ 6 ~ 8.0000+ 6	4.1926+ 0	2.3782+ 0	6.5438- 3	1.7972+ 0	7.2793- 1
8.0000+ 6 ~ 1.0000+ 7	4.3964+ 0	2.6459+ 0	2.3431- 3	1.7473+ 0	8.0734- 1
1.0000+ 7 ~ 1.5000+ 7	4.3856+ 0	2.6088+ 0	7.5217- 4	1.7752+ 0	8.5937- 1

CROSS SECTION

MATERIAL =1441 RU-101

ENERGY	TOTAL	ELASTIC	CAPTURE	INELA	MU-BAR
1.0000- 5 ~ 1.0000- 2	1.5273+ 1	4.7555+ 0	1.0518+ 1		6.6643- 3
1.0000- 2 ~ 1.5000- 2	9.6407+ 0	4.7555+ 0	4.8853+ 0		6.6644- 3
1.5000- 2 ~ 2.0000- 2	8.8687+ 0	4.7554+ 0	4.1133+ 0		6.6644- 3
2.0000- 2 ~ 3.0000- 2	8.2138+ 0	4.7553+ 0	3.4584+ 0		6.6644- 3
3.0000- 2 ~ 4.0000- 2	7.6685+ 0	4.7552+ 0	2.9132+ 0		6.6645- 3
4.0000- 2 ~ 5.0000- 2	7.3236+ 0	4.7551+ 0	2.5685+ 0		6.6645- 3
5.0000- 2 ~ 6.0000- 2	7.0888+ 0	4.7550+ 0	2.3338+ 0		6.6645- 3
6.0000- 2 ~ 8.0000- 2	6.8215+ 0	4.7548+ 0	2.0667+ 0		6.6645- 3
8.0000- 2 ~ 1.0000- 1	6.5785+ 0	4.7546+ 0	1.8239+ 0		6.6645- 3
1.0000- 1 ~ 1.5000- 1	6.3156+ 0	4.7542+ 0	1.5614+ 0		6.6646- 3
1.5000- 1 ~ 2.0000- 1	6.0730+ 0	4.7537+ 0	1.3194+ 0		6.6646- 3
2.0000- 1 ~ 3.0000- 1	5.8699+ 0	4.7528+ 0	1.1170+ 0		6.6646- 3
3.0000- 1 ~ 4.0000- 1	5.7002+ 0	4.7517+ 0	9.4854- 1		6.6647- 3
4.0000- 1 ~ 5.0000- 1	5.5970+ 0	4.7505+ 0	8.4651- 1		6.6647- 3
5.0000- 1 ~ 6.0000- 1	5.5206+ 0	4.7494+ 0	7.7121- 1		6.6647- 3
6.0000- 1 ~ 8.0000- 1	5.4414+ 0	4.7476+ 0	6.9384- 1		6.6647- 3
8.0000- 1 ~ 1.0000+ 0	5.3706+ 0	4.7451+ 0	6.2551- 1		6.6647- 3
1.0000+ 0 ~ 1.5000+ 0	5.2908+ 0	4.7407+ 0	5.5014- 1		6.6651- 3
1.5000+ 0 ~ 2.0000+ 0	5.2240+ 0	4.7339+ 0	4.9008- 1		6.6657- 3
2.0000+ 0 ~ 3.0000+ 0	5.1686+ 0	4.7228+ 0	4.4581- 1		6.6663- 3
3.0000+ 0 ~ 4.0000+ 0	5.1314+ 0	4.7057+ 0	4.2563- 1		6.6674- 3
4.0000+ 0 ~ 5.0000+ 0	5.1145+ 0	4.6859+ 0	4.2861- 1		6.6686- 3
5.0000+ 0 ~ 6.0000+ 0	5.1125+ 0	4.6623+ 0	4.5024- 1		6.6695- 3
6.0000+ 0 ~ 8.0000+ 0	5.1386+ 0	4.6164+ 0	5.2226- 1		6.6706- 3
8.0000+ 0 ~ 1.0000+ 1	5.2508+ 0	4.5273+ 0	7.2326- 1		6.6718- 3
1.0000+ 1 ~ 1.5000+ 1	8.5864+ 0	4.0108+ 0	4.5756+ 0		6.6752- 3
1.5000+ 1 ~ 2.0000+ 1	1.4648+ 2	9.6583+ 0	1.3682+ 2		6.6796- 3
2.0000+ 1 ~ 3.0000+ 1	5.4499+ 0	4.9756+ 0	4.7433- 1		6.6879- 3
3.0000+ 1 ~ 4.0000+ 1	5.2516+ 0	4.2981+ 0	9.5348- 1		6.6981- 3
4.0000+ 1 ~ 5.0000+ 1	7.8796+ 1	9.9070+ 0	6.8889+ 1		6.7057- 3
5.0000+ 1 ~ 6.0000+ 1	1.2216+ 1	4.7602+ 0	7.4555+ 0		6.7153- 3
6.0000+ 1 ~ 8.0000+ 1	7.0206+ 1	1.8121+ 1	5.2085+ 1		6.7317- 3
8.0000+ 1 ~ 1.0000+ 2	6.0536+ 0	5.2522+ 0	8.0138- 1		6.7490- 3
1.0000+ 2 ~ 1.5000+ 2	1.3459+ 1	5.8204+ 0	7.6382+ 0		6.7823- 3
1.5000+ 2 ~ 2.0000+ 2	2.0438+ 1	8.1886+ 0	1.2250+ 1		6.8310- 3
2.0000+ 2 ~ 3.0000+ 2	8.1603+ 0	5.5013+ 0	2.6590+ 0		6.9063- 3
3.0000+ 2 ~ 4.0000+ 2	3.6114+ 1	2.0539+ 1	1.5575+ 1		7.0186- 3
4.0000+ 2 ~ 5.0000+ 2	2.2830+ 1	1.3911+ 1	8.9196+ 0		7.1228- 3
5.0000+ 2 ~ 6.0000+ 2	1.1933+ 1	8.6437+ 0	3.2897+ 0		7.2281- 3
6.0000+ 2 ~ 8.0000+ 2	1.4013+ 1	9.3942+ 0	4.6168+ 0		7.3933- 3
8.0000+ 2 ~ 1.0000+ 3	1.0363+ 1	6.6415+ 0	3.7156+ 0		7.6214- 3
1.0000+ 3 ~ 1.5000+ 3	9.7673+ 0	6.5675+ 0	3.1946+ 0		8.0353- 3
1.5000+ 3 ~ 2.0000+ 3	9.2489+ 0	6.4941+ 0	2.7529+ 0		8.6251- 3
2.0000+ 3 ~ 3.0000+ 3	8.8373+ 0	6.4299+ 0	2.4067+ 0		9.5468- 3
3.0000+ 3 ~ 4.0000+ 3	8.5533+ 0	6.3944+ 0	2.1558+ 0		1.0933- 2
4.0000+ 3 ~ 5.0000+ 3	8.3878+ 0	6.3826+ 0	2.0028+ 0		1.2219- 2
5.0000+ 3 ~ 6.0000+ 3	8.2850+ 0	6.3891+ 0	1.8949+ 0		1.3507- 2
6.0000+ 3 ~ 8.0000+ 3	8.2084+ 0	6.4247+ 0	1.7825+ 0		1.5509- 2
8.0000+ 3 ~ 1.0000+ 4	8.1678+ 0	6.4964+ 0	1.6699+ 0		1.8222- 2
1.0000+ 4 ~ 1.5000+ 4	8.1763+ 0	6.6496+ 0	1.5243+ 0		2.2965- 2
1.5000+ 4 ~ 2.0000+ 4	8.2398+ 0	6.8715+ 0	1.3666+ 0		2.9476- 2
2.0000+ 4 ~ 3.0000+ 4	8.3794+ 0	7.1856+ 0	1.1895+ 0		3.9402- 2
3.0000+ 4 ~ 4.0000+ 4	8.5558+ 0	7.5337+ 0	1.0195+ 0		5.1884- 2
4.0000+ 4 ~ 5.0000+ 4	8.7124+ 0	7.8154+ 0	8.9550- 1		6.4112- 2
5.0000+ 4 ~ 6.0000+ 4	8.8455+ 0	8.0432+ 0	8.0137- 1		7.6068- 2
6.0000+ 4 ~ 8.0000+ 4	9.0028+ 0	8.3042+ 0	6.9802- 1		9.3427- 2
8.0000+ 4 ~ 1.0000+ 5	9.1542+ 0	8.5543+ 0	5.9952- 1		1.1558- 1
1.0000+ 5 ~ 1.5000+ 5	9.1327+ 0	8.6159+ 0	4.8152- 1	3.3483- 2	1.5717- 1
1.5000+ 5 ~ 2.0000+ 5	9.2383+ 0	8.5627+ 0	3.7555- 1	2.9693- 1	2.0584- 1
2.0000+ 5 ~ 3.0000+ 5	9.1770+ 0	8.3266+ 0	3.0396- 1	5.4429- 1	2.6528- 1
3.0000+ 5 ~ 4.0000+ 5	8.8206+ 0	7.6571+ 0	2.2457- 1	9.3511- 1	3.4082- 1
4.0000+ 5 ~ 5.0000+ 5	8.5186+ 0	6.9173+ 0	1.6883- 1	1.4310+ 0	4.0705- 1
5.0000+ 5 ~ 6.0000+ 5	8.1596+ 0	6.4147+ 0	1.4105- 1	1.6037+ 0	4.5368- 1
6.0000+ 5 ~ 8.0000+ 5	7.6795+ 0	5.8465+ 0	1.1103- 1	1.7215+ 0	4.9966- 1
8.0000+ 5 ~ 1.0000+ 6	7.0885+ 0	5.2385+ 0	9.3339- 2	1.7566+ 0	5.3647- 1
1.0000+ 6 ~ 1.5000+ 6	6.2522+ 0	4.4158+ 0	7.4644- 2	1.7606+ 0	5.6055- 1
1.5000+ 6 ~ 2.0000+ 6	5.3486+ 0	3.5044+ 0	6.8212- 2	1.7746+ 0	5.6822- 1
2.0000+ 6 ~ 3.0000+ 6	4.4664+ 0	2.5998+ 0	6.2054- 2	1.8017+ 0	5.6550- 1
3.0000+ 6 ~ 4.0000+ 6	3.9931+ 0	2.1241+ 0	4.3947- 2	1.8206+ 0	5.7368- 1
4.0000+ 6 ~ 5.0000+ 6	3.8876+ 0	2.0015+ 0	2.8321- 2	1.8544+ 0	5.9342- 1
5.0000+ 6 ~ 6.0000+ 6	3.9382+ 0	2.0595+ 0	1.6730- 2	1.8521+ 0	6.3665- 1
6.0000+ 6 ~ 8.0000+ 6	4.1896+ 0	2.3617+ 0	6.9796- 3	1.8093+ 0	7.2535- 1
8.0000+ 6 ~ 1.0000+ 7	4.4058+ 0	2.6400+ 0	2.4391- 3	1.7625+ 0	8.0512- 1
1.0000+ 7 ~ 1.5000+ 7	4.4377+ 0	2.6371+ 0	8.8474- 4	1.7990+ 0	8.5944- 1

MATERIAL =1442 CROSS SECTION RU-102

ENERGY	TOTAL	ELASTIC	CAPTURE	INELA	MU-BAR
1.0000- 5 ~ 1.0000- 2	9.4733+ 0	5.4184+ 0	4.0559+ 0		6.5992- 3
1.0000- 2 ~ 1.5000- 2	7.3010+ 0	5.4184+ 0	1.8787+ 0		6.5992- 3
1.5000- 2 ~ 2.0000- 2	7.0014+ 0	5.4184+ 0	1.5879+ 0		6.5992- 3
2.0000- 2 ~ 3.0000- 2	6.7496+ 0	5.4184+ 0	1.3285+ 0		6.5992- 3
3.0000- 2 ~ 4.0000- 2	6.5377+ 0	5.4184+ 0	1.1228+ 0		6.5992- 3
4.0000- 2 ~ 5.0000- 2	6.4085+ 0	5.4184+ 0	9.8717- 1		6.5992- 3
5.0000- 2 ~ 6.0000- 2	6.3109+ 0	5.4184+ 0	8.9154- 1		6.5992- 3
6.0000- 2 ~ 8.0000- 2	6.2099+ 0	5.4184+ 0	7.9393- 1		6.5993- 3
8.0000- 2 ~ 1.0000- 1	6.1185+ 0	5.4184+ 0	6.9803- 1		6.5993- 3
1.0000- 1 ~ 1.5000- 1	6.0125+ 0	5.4184+ 0	5.9493- 1		6.5993- 3
1.5000- 1 ~ 2.0000- 1	5.9205+ 0	5.4184+ 0	5.0121- 1		6.5993- 3
2.0000- 1 ~ 3.0000- 1	5.8385+ 0	5.4184+ 0	4.2068- 1		6.5993- 3
3.0000- 1 ~ 4.0000- 1	5.7734+ 0	5.4184+ 0	3.5441- 1		6.5993- 3
4.0000- 1 ~ 5.0000- 1	5.7306+ 0	5.4184+ 0	3.1178- 1		6.5993- 3
5.0000- 1 ~ 6.0000- 1	5.7003+ 0	5.4184+ 0	2.8315- 1		6.5993- 3
6.0000- 1 ~ 8.0000- 1	5.6695+ 0	5.4184+ 0	2.5061- 1		6.5993- 3
8.0000- 1 ~ 1.0000+ 0	5.6392+ 0	5.4184+ 0	2.2047- 1		6.5993- 3
1.0000+ 0 ~ 1.5000+ 0	5.6066+ 0	5.4184+ 0	1.8827- 1		6.5995- 3
1.5000+ 0 ~ 2.0000+ 0	5.5770+ 0	5.4185+ 0	1.5831- 1		6.5997- 3
2.0000+ 0 ~ 3.0000+ 0	5.5515+ 0	5.4185+ 0	1.3313- 1		6.5999- 3
3.0000+ 0 ~ 4.0000+ 0	5.5306+ 0	5.4185+ 0	1.1195- 1		6.6004- 3
4.0000+ 0 ~ 5.0000+ 0	5.5172+ 0	5.4186+ 0	9.9029- 2		6.6010- 3
5.0000+ 0 ~ 6.0000+ 0	5.5082+ 0	5.4186+ 0	8.9258- 2		6.6014- 3
6.0000+ 0 ~ 8.0000+ 0	5.4980+ 0	5.4187+ 0	7.9165- 2		6.6020- 3
8.0000+ 0 ~ 1.0000+ 1	5.4885+ 0	5.4188+ 0	7.0033- 2		6.6026- 3
1.0000+ 1 ~ 1.5000+ 1	5.4785+ 0	5.4190+ 0	5.9435- 2		6.6044- 3
1.5000+ 1 ~ 2.0000+ 1	5.4693+ 0	5.4192+ 0	5.0235- 2		6.6068- 3
2.0000+ 1 ~ 3.0000+ 1	5.4616+ 0	5.4195+ 0	4.2044- 2		6.6116- 3
3.0000+ 1 ~ 4.0000+ 1	5.4554+ 0	5.4199+ 0	3.5544- 2		6.6178- 3
4.0000+ 1 ~ 5.0000+ 1	5.4517+ 0	5.4203+ 0	3.1270- 2		6.6223- 3
5.0000+ 1 ~ 6.0000+ 1	5.4489+ 0	5.4206+ 0	2.8255- 2		6.6286- 3
6.0000+ 1 ~ 8.0000+ 1	5.4462+ 0	5.4211+ 0	2.5090- 2		6.6398- 3
8.0000+ 1 ~ 1.0000+ 2	5.4437+ 0	5.4214+ 0	2.2141- 2		6.6516- 3
1.0000+ 2 ~ 1.5000+ 2	5.4394+ 0	5.4200+ 0	1.9200- 2		6.6757- 3
1.5000+ 2 ~ 2.0000+ 2	5.7460+ 0	5.4298+ 0	3.1610- 1		6.7125- 3
2.0000+ 2 ~ 3.0000+ 2	5.4415+ 0	5.4279+ 0	1.3490- 2		6.7721- 3
3.0000+ 2 ~ 4.0000+ 2	5.4141+ 0	5.4012+ 0	1.2830- 2		6.8659- 3
4.0000+ 2 ~ 5.0000+ 2	6.6976+ 0	5.5294+ 0	1.1681+ 0		6.9546- 3
5.0000+ 2 ~ 6.0000+ 2	5.4135+ 0	5.4043+ 0	9.1633- 3		7.0463- 3
6.0000+ 2 ~ 8.0000+ 2	5.3793+ 0	5.3712+ 0	8.0748- 3		7.1935- 3
8.0000+ 2 ~ 1.0000+ 3	5.3180+ 0	5.3107+ 0	7.3269- 3		7.4005- 3
1.0000+ 3 ~ 1.5000+ 3	9.6242+ 0	8.6612+ 0	9.6296- 1		7.7831- 3
1.5000+ 3 ~ 2.0000+ 3	9.1839+ 0	8.0100+ 0	1.1734+ 0		8.3342- 3
2.0000+ 3 ~ 3.0000+ 3	8.7765+ 0	7.7407+ 0	1.0356+ 0		9.2016- 3
3.0000+ 3 ~ 4.0000+ 3	8.4960+ 0	7.5729+ 0	9.2134- 1		1.0505- 2
4.0000+ 3 ~ 5.0000+ 3	8.3330+ 0	7.4881+ 0	8.4346- 1		1.1713- 2
5.0000+ 3 ~ 6.0000+ 3	8.2319+ 0	7.4483+ 0	7.8251- 1		1.2923- 2
6.0000+ 3 ~ 8.0000+ 3	8.1570+ 0	7.4457+ 0	7.1009- 1		1.4802- 2
8.0000+ 3 ~ 1.0000+ 4	8.1181+ 0	7.4830+ 0	6.3360- 1		1.7357- 2
1.0000+ 4 ~ 1.5000+ 4	8.1283+ 0	7.5879+ 0	5.3808- 1		2.1874- 2
1.5000+ 4 ~ 2.0000+ 4	8.1932+ 0	7.7477+ 0	4.4419- 1		2.8149- 2
2.0000+ 4 ~ 3.0000+ 4	8.3333+ 0	7.9746+ 0	3.5621- 1		3.7904- 2
3.0000+ 4 ~ 4.0000+ 4	8.5092+ 0	8.2242+ 0	2.8375- 1		5.0321- 2
4.0000+ 4 ~ 5.0000+ 4	8.6645+ 0	8.4258+ 0	2.3815- 1		6.2601- 2
5.0000+ 4 ~ 6.0000+ 4	8.7960+ 0	8.5885+ 0	2.0716- 1		7.4662- 2
6.0000+ 4 ~ 8.0000+ 4	8.9507+ 0	8.7740+ 0	1.7648- 1		9.2211- 2
8.0000+ 4 ~ 1.0000+ 5	9.0990+ 0	8.9488+ 0	1.5011- 1		1.1460- 1
1.0000+ 5 ~ 1.5000+ 5	9.1842+ 0	9.0538+ 0	1.2950- 1		1.5343- 1
1.5000+ 5 ~ 2.0000+ 5	9.2309+ 0	9.1168+ 0	1.1348- 1		1.9758- 1
2.0000+ 5 ~ 3.0000+ 5	9.1210+ 0	9.0132+ 0	1.0788- 1		2.4932- 1
3.0000+ 5 ~ 4.0000+ 5	8.8371+ 0	8.7242+ 0	1.1283- 1		3.0240- 1
4.0000+ 5 ~ 5.0000+ 5	8.4428+ 0	8.3193+ 0	1.0862- 1	1.4870- 2	3.4265- 1
5.0000+ 5 ~ 6.0000+ 5	8.1687+ 0	7.6709+ 0	8.7976- 2	4.0316- 1	3.8445- 1
6.0000+ 5 ~ 8.0000+ 5	7.6931+ 0	6.8046+ 0	7.4344- 2	8.1272- 1	4.3417- 1
8.0000+ 5 ~ 1.0000+ 6	7.1113+ 0	6.0877+ 0	7.7317- 2	9.4606- 1	4.6698- 1
1.0000+ 6 ~ 1.5000+ 6	6.2518+ 0	4.9909+ 0	7.1453- 2	1.1873+ 0	5.0350- 1
1.5000+ 6 ~ 2.0000+ 6	5.3613+ 0	3.8559+ 0	7.1001- 2	1.4339+ 0	5.2595- 1
2.0000+ 6 ~ 3.0000+ 6	4.4651+ 0	2.7913+ 0	6.8803- 2	1.6031+ 0	5.3784- 1
3.0000+ 6 ~ 4.0000+ 6	4.0089+ 0	2.1984+ 0	4.6220- 2	1.7559+ 0	5.6108- 1
4.0000+ 6 ~ 5.0000+ 6	3.8967+ 0	2.0215+ 0	2.7319- 2	1.8414+ 0	5.8854- 1
5.0000+ 6 ~ 6.0000+ 6	3.9429+ 0	2.0575+ 0	1.5121- 2	1.8603+ 0	6.3514- 1
6.0000+ 6 ~ 8.0000+ 6	4.1899+ 0	2.3566+ 0	5.8746- 3	1.8159+ 0	7.2405- 1
8.0000+ 6 ~ 1.0000+ 7	4.4110+ 0	2.6373+ 0	1.9245- 3	1.7709+ 0	8.0417- 1
1.0000+ 7 ~ 1.5000+ 7	4.4603+ 0	2.6492+ 0	7.6639- 4	1.8098+ 0	8.5946- 1

MATERIAL =1451 CROSS SECTION RH-103

ENERGY	TOTAL	ELASTIC	CAPTURE	INELA	MU-BAR
1.0000- 5 ~ 1.0000- 2	4.4069+ 2	3.8099+ 0	4.3688+ 2		6.5349- 3
1.0000- 2 ~ 1.5000- 2	2.0908+ 2	3.8057+ 0	2.0527+ 2		6.5350- 3
1.5000- 2 ~ 2.0000- 2	1.7867+ 2	3.8028+ 0	1.7487+ 2		6.5351- 3
2.0000- 2 ~ 3.0000- 2	1.5186+ 2	3.7984+ 0	1.4806+ 2		6.5351- 3
3.0000- 2 ~ 4.0000- 2	1.3095+ 2	3.7924+ 0	1.2716+ 2		6.5352- 3
4.0000- 2 ~ 5.0000- 2	1.1744+ 2	3.7864+ 0	1.1366+ 2		6.5352- 3
5.0000- 2 ~ 6.0000- 2	1.0815+ 2	3.7802+ 0	1.0437+ 2		6.5352- 3
6.0000- 2 ~ 8.0000- 2	9.8989+ 1	3.7707+ 0	9.5218+ 1		6.5352- 3
8.0000- 2 ~ 1.0000- 1	9.0373+ 1	3.7576+ 0	8.6616+ 1		6.5353- 3
1.0000- 1 ~ 1.5000- 1	8.2106+ 1	3.7333+ 0	7.8372+ 1		6.5353- 3
1.5000- 1 ~ 2.0000- 1	7.5902+ 1	3.6960+ 0	7.2206+ 1		6.5353- 3
2.0000- 1 ~ 3.0000- 1	7.3575+ 1	3.6313+ 0	6.9944+ 1		6.5354- 3
3.0000- 1 ~ 4.0000- 1	7.6134+ 1	3.5296+ 0	7.2605+ 1		6.5354- 3
4.0000- 1 ~ 5.0000- 1	8.4165+ 1	3.4028+ 0	8.0762+ 1		6.5354- 3
5.0000- 1 ~ 6.0000- 1	9.8344+ 1	3.2428+ 0	9.5101+ 1		6.5355- 3
6.0000- 1 ~ 8.0000- 1	1.4024+ 2	2.9068+ 0	1.3734+ 2		6.5355- 3
8.0000- 1 ~ 1.0000+ 0	3.0080+ 2	2.2543+ 0	2.9855+ 2		6.5355- 3
1.0000+ 0 ~ 1.5000+ 0	2.0748+ 3	1.1385+ 1	2.0634+ 3		6.5358- 3
1.5000+ 0 ~ 2.0000+ 0	1.5349+ 2	7.8087+ 0	1.4568+ 2		6.5364- 3
2.0000+ 0 ~ 3.0000+ 0	2.3594+ 1	5.7575+ 0	1.7837+ 1		6.5369- 3
3.0000+ 0 ~ 4.0000+ 0	9.2748+ 0	5.2349+ 0	4.0400+ 0		6.5380- 3
4.0000+ 0 ~ 5.0000+ 0	6.7466+ 0	5.0789+ 0	1.6677+ 0		6.5394- 3
5.0000+ 0 ~ 6.0000+ 0	5.8611+ 0	4.9815+ 0	8.7960- 1		6.5404- 3
6.0000+ 0 ~ 8.0000+ 0	5.3466+ 0	4.8999+ 0	4.4666- 1		6.5418- 3
8.0000+ 0 ~ 1.0000+ 1	5.0607+ 0	4.8384+ 0	2.2226- 1		6.5431- 3
1.0000+ 1 ~ 1.5000+ 1	4.8855+ 0	4.7859+ 0	1.0359- 1		6.5467- 3
1.5000+ 1 ~ 2.0000+ 1	4.7975+ 0	4.7474+ 0	5.0108- 2		6.5515- 3
2.0000+ 1 ~ 3.0000+ 1	4.7485+ 0	4.7181+ 0	3.0359- 2		6.5606- 3
3.0000+ 1 ~ 4.0000+ 1	4.8595+ 0	4.6878+ 0	1.7178- 1		6.5718- 3
4.0000+ 1 ~ 5.0000+ 1	8.0930+ 0	4.6779+ 0	3.4151+ 0		6.5802- 3
5.0000+ 1 ~ 6.0000+ 1	4.6636+ 0	4.6195+ 0	4.4086- 2		6.5910- 3
6.0000+ 1 ~ 8.0000+ 1	5.0487+ 0	4.5724+ 0	4.7631- 1		6.6095- 3
8.0000+ 1 ~ 1.0000+ 2	8.3941+ 0	4.6103+ 0	3.7838+ 0		6.6291- 3
1.0000+ 2 ~ 1.5000+ 2	7.9484+ 0	4.2998+ 0	3.6486+ 0		6.6672- 3
1.5000+ 2 ~ 2.0000+ 2	3.6068+ 1	1.6207+ 1	1.9861+ 1		6.7232- 3
2.0000+ 2 ~ 3.0000+ 2	1.8079+ 1	7.5808+ 0	1.0498+ 1		6.8104- 3
3.0000+ 2 ~ 4.0000+ 2	1.4417+ 1	8.2245+ 0	6.1921+ 0		6.9418- 3
4.0000+ 2 ~ 5.0000+ 2	2.1149+ 1	1.2109+ 1	9.0399+ 0		7.0639- 3
5.0000+ 2 ~ 6.0000+ 2	1.0152+ 1	6.6324+ 0	3.5197+ 0		7.1877- 3
6.0000+ 2 ~ 8.0000+ 2	1.6415+ 1	1.0587+ 1	5.8283+ 0		7.3827- 3
8.0000+ 2 ~ 1.0000+ 3	1.0557+ 1	7.4397+ 0	3.1175+ 0		7.6524- 3
1.0000+ 3 ~ 1.5000+ 3	1.0939+ 1	7.9322+ 0	3.0066+ 0		8.1425- 3
1.5000+ 3 ~ 2.0000+ 3	1.2100+ 1	8.9951+ 0	3.1052+ 0		8.8409- 3
2.0000+ 3 ~ 3.0000+ 3	9.7856+ 0	7.6714+ 0	2.1142+ 0		9.9306- 3
3.0000+ 3 ~ 4.0000+ 3	9.6499+ 0	7.6734+ 0	1.9764+ 0		1.1560- 2
4.0000+ 3 ~ 5.0000+ 3	8.2650+ 0	6.5083+ 0	1.7559+ 0		1.3069- 2
5.0000+ 3 ~ 6.0000+ 3	8.1653+ 0	6.4969+ 0	1.6676+ 0		1.4572- 2
6.0000+ 3 ~ 8.0000+ 3	8.0906+ 0	6.5146+ 0	1.5753+ 0		1.6895- 2
8.0000+ 3 ~ 1.0000+ 4	8.0518+ 0	6.5694+ 0	1.4813+ 0		2.0023- 2
1.0000+ 4 ~ 1.5000+ 4	8.0617+ 0	6.7026+ 0	1.3571+ 0		2.5443- 2
1.5000+ 4 ~ 2.0000+ 4	8.1255+ 0	6.9036+ 0	1.2205+ 0		3.2821- 2
2.0000+ 4 ~ 3.0000+ 4	8.2632+ 0	7.1942+ 0	1.0653+ 0		4.3916- 2
3.0000+ 4 ~ 4.0000+ 4	8.4357+ 0	7.5178+ 0	9.1575- 1		5.7712- 2
4.0000+ 4 ~ 5.0000+ 4	8.5874+ 0	7.7798+ 0	8.0620- 1	1.9426- 4	7.1064- 2
5.0000+ 4 ~ 6.0000+ 4	8.7157+ 0	7.9913+ 0	7.2268- 1	8.1383- 4	8.3988- 2
6.0000+ 4 ~ 8.0000+ 4	8.8658+ 0	8.2325+ 0	6.3048- 1	2.2262- 3	1.0255- 1
8.0000+ 4 ~ 1.0000+ 5	9.0088+ 0	8.4620+ 0	5.4210- 1	4.6224- 3	1.2596- 1
1.0000+ 5 ~ 1.5000+ 5	9.0909+ 0	8.6229+ 0	4.4775- 1	1.3067- 2	1.6584- 1
1.5000+ 5 ~ 2.0000+ 5	9.1356+ 0	8.7403+ 0	3.6597- 1	2.4079- 2	2.1099- 1
2.0000+ 5 ~ 3.0000+ 5	9.0323+ 0	8.6813+ 0	3.0455- 1	4.5576- 2	2.6359- 1
3.0000+ 5 ~ 4.0000+ 5	8.7110+ 0	8.0873+ 0	2.2163- 1	3.9867- 1	3.3171- 1
4.0000+ 5 ~ 5.0000+ 5	8.4521+ 0	7.2958+ 0	1.5476- 1	9.9641- 1	3.9491- 1
5.0000+ 5 ~ 6.0000+ 5	8.1239+ 0	6.7585+ 0	1.2472- 1	1.2404+ 0	4.3944- 1
6.0000+ 5 ~ 8.0000+ 5	7.6837+ 0	6.2377+ 0	1.0735- 1	1.3386+ 0	4.7750- 1
8.0000+ 5 ~ 1.0000+ 6	7.1219+ 0	5.6357+ 0	9.7095- 2	1.3888+ 0	5.0962- 1
1.0000+ 6 ~ 1.5000+ 6	6.3221+ 0	4.6768+ 0	8.4281- 2	1.5600+ 0	5.4444- 1
1.5000+ 6 ~ 2.0000+ 6	5.4432+ 0	3.6500+ 0	7.2941- 2	1.7181+ 0	5.6683- 1
2.0000+ 6 ~ 3.0000+ 6	4.5335+ 0	2.6607+ 0	4.5529- 2	1.8234+ 0	5.7680- 1
3.0000+ 6 ~ 4.0000+ 6	4.0303+ 0	2.1434+ 0	2.5967- 2	1.8569+ 0	5.8285- 1
4.0000+ 6 ~ 5.0000+ 6	3.9097+ 0	1.9981+ 0	1.6539- 2	1.8918+ 0	5.9606- 1
5.0000+ 6 ~ 6.0000+ 6	3.9503+ 0	2.0465+ 0	9.5087- 3	1.8850+ 0	6.3598- 1
6.0000+ 6 ~ 8.0000+ 6	4.1909+ 0	2.3465+ 0	3.7402- 3	1.8298+ 0	7.2332- 1
8.0000+ 6 ~ 1.0000+ 7	4.4182+ 0	2.6336+ 0	1.4159- 3	1.7824+ 0	8.0285- 1
1.0000+ 7 ~ 1.5000+ 7	4.4888+ 0	2.6644+ 0	4.8327- 4	1.8236+ 0	8.5945- 1

CROSS SECTION

MATERIAL =1443 RU-104

ENERGY	TOTAL	ELASTIC	CAPTURE	INELA	MU-BAR
1.0000- 5 ~ 1.0000- 2	6.5630+ 0	5.2907+ 0	1.2724+ 0		6.4716- 3
1.0000- 2 ~ 1.5000- 2	5.8812+ 0	5.2907+ 0	5.9045- 1		6.4716- 3
1.5000- 2 ~ 2.0000- 2	5.7877+ 0	5.2907+ 0	4.9709- 1		6.4716- 3
2.0000- 2 ~ 3.0000- 2	5.7083+ 0	5.2907+ 0	4.1753- 1		6.4716- 3
3.0000- 2 ~ 4.0000- 2	5.6421+ 0	5.2907+ 0	3.5151- 1		6.4716- 3
4.0000- 2 ~ 5.0000- 2	5.6011+ 0	5.2907+ 0	3.1033- 1		6.4716- 3
5.0000- 2 ~ 6.0000- 2	5.5708+ 0	5.2907+ 0	2.8017- 1		6.4716- 3
6.0000- 2 ~ 8.0000- 2	5.5392+ 0	5.2907+ 0	2.4857- 1		6.4716- 3
8.0000- 2 ~ 1.0000- 1	5.5102+ 0	5.2906+ 0	2.1946- 1		6.4715- 3
1.0000- 1 ~ 1.5000- 1	5.4772+ 0	5.2906+ 0	1.8655- 1		6.4716- 3
1.5000- 1 ~ 2.0000- 1	5.4482+ 0	5.2905+ 0	1.5749- 1		6.4717- 3
2.0000- 1 ~ 3.0000- 1	5.4225+ 0	5.2905+ 0	1.3193- 1		6.4717- 3
3.0000- 1 ~ 4.0000- 1	5.4020+ 0	5.2906+ 0	1.1139- 1		6.4717- 3
4.0000- 1 ~ 5.0000- 1	5.3886+ 0	5.2905+ 0	9.8072- 2		6.4717- 3
5.0000- 1 ~ 6.0000- 1	5.3791+ 0	5.2905+ 0	8.8572- 2		6.4717- 3
6.0000- 1 ~ 8.0000- 1	5.3693+ 0	5.2905+ 0	7.8803- 2		6.4717- 3
8.0000- 1 ~ 1.0000+ 0	5.3598+ 0	5.2904+ 0	6.9391- 2		6.4717- 3
1.0000+ 0 ~ 1.5000+ 0	5.3494+ 0	5.2903+ 0	5.9081- 2		6.4718- 3
1.5000+ 0 ~ 2.0000+ 0	5.3400+ 0	5.2901+ 0	4.9914- 2		6.4720- 3
2.0000+ 0 ~ 3.0000+ 0	5.3317+ 0	5.2899+ 0	4.1849- 2		6.4721- 3
3.0000+ 0 ~ 4.0000+ 0	5.3249+ 0	5.2895+ 0	3.5381- 2		6.4726- 3
4.0000+ 0 ~ 5.0000+ 0	5.3204+ 0	5.2892+ 0	3.1157- 2		6.4732- 3
5.0000+ 0 ~ 6.0000+ 0	5.3171+ 0	5.2889+ 0	2.8237- 2		6.4736- 3
6.0000+ 0 ~ 8.0000+ 0	5.3135+ 0	5.2864+ 0	2.5144- 2		6.4742- 3
8.0000+ 0 ~ 1.0000+ 1	5.3099+ 0	5.2877+ 0	2.2176- 2		6.4748- 3
1.0000+ 1 ~ 1.5000+ 1	5.3055+ 0	5.2864+ 0	1.9011- 2		6.4766- 3
1.5000+ 1 ~ 2.0000+ 1	5.3009+ 0	5.2846+ 0	1.6135- 2		6.4789- 3
2.0000+ 1 ~ 3.0000+ 1	5.2954+ 0	5.2816+ 0	1.3718- 2		6.4841- 3
3.0000+ 1 ~ 4.0000+ 1	5.2892+ 0	5.2773+ 0	1.1764- 2		6.4908- 3
4.0000+ 1 ~ 5.0000+ 1	5.2831+ 0	5.2725+ 0	1.0591- 2		6.4958- 3
5.0000+ 1 ~ 6.0000+ 1	5.2771+ 0	5.2673+ 0	9.7889- 3		6.5027- 3
6.0000+ 1 ~ 8.0000+ 1	5.2672+ 0	5.2580+ 0	9.0314- 3		6.5152- 3
8.0000+ 1 ~ 1.0000+ 2	5.2518+ 0	5.2432+ 0	8.4900- 3		6.5284- 3
1.0000+ 2 ~ 1.5000+ 2	5.2121+ 0	5.2032+ 0	8.7589- 3		6.5558- 3
1.5000+ 2 ~ 2.0000+ 2	5.0822+ 0	5.0658+ 0	1.6300- 2		6.5982- 3
2.0000+ 2 ~ 3.0000+ 2	1.2581+ 1	6.6530+ 0	5.9283+ 0		6.6678- 3
3.0000+ 2 ~ 4.0000+ 2	9.6511+ 0	5.9978+ 0	3.6533+ 0		6.7783- 3
4.0000+ 2 ~ 5.0000+ 2	4.9753+ 0	4.9666+ 0	8.7087- 3		6.8833- 3
5.0000+ 2 ~ 6.0000+ 2	4.1236+ 0	4.0879+ 0	3.5684- 2		6.9920- 3
6.0000+ 2 ~ 8.0000+ 2	2.9245+ 1	2.4845+ 1	4.4013+ 0		7.1671- 3
8.0000+ 2 ~ 1.0000+ 3	6.3065+ 0	5.2969+ 0	9.5672- 3		7.4134- 3
1.0000+ 3 ~ 1.5000+ 3	1.3909+ 1	1.2449+ 1	1.4602+ 0		7.8675- 3
1.5000+ 3 ~ 2.0000+ 3	9.0539+ 0	8.2345+ 0	8.2897- 1		8.5196- 3
2.0000+ 3 ~ 3.0000+ 3	8.6554+ 0	7.9303+ 0	7.2489- 1		9.5403- 3
3.0000+ 3 ~ 4.0000+ 3	8.3735+ 0	7.7405+ 0	6.3109- 1		1.1063- 2
4.0000+ 3 ~ 5.0000+ 3	8.2092+ 0	7.6419+ 0	5.6574- 1		1.2471- 2
5.0000+ 3 ~ 6.0000+ 3	8.1071+ 0	7.5907+ 0	5.1518- 1		1.3874- 2
6.0000+ 3 ~ 8.0000+ 3	8.0305+ 0	7.5733+ 0	4.5819- 1		1.6048- 2
8.0000+ 3 ~ 1.0000+ 4	7.9896+ 0	7.5910+ 0	3.9531- 1		1.8991- 2
1.0000+ 4 ~ 1.5000+ 4	7.8963+ 0	7.6664+ 0	3.2594- 1		2.4162- 2
1.5000+ 4 ~ 2.0000+ 4	8.0564+ 0	7.7948+ 0	2.6057- 1		3.1299- 2
2.0000+ 4 ~ 3.0000+ 4	8.1291+ 0	7.9839+ 0	2.0352- 1		4.2258- 2
3.0000+ 4 ~ 4.0000+ 4	8.3560+ 0	8.1965+ 0	1.5884- 1		5.6055- 2
4.0000+ 4 ~ 5.0000+ 4	8.5030+ 0	8.3705+ 0	1.3206- 1		5.9534- 2
5.0000+ 4 ~ 6.0000+ 4	8.6268+ 0	8.5120+ 0	1.1458- 1		8.2631- 2
6.0000+ 4 ~ 8.0000+ 4	8.7712+ 0	8.6732+ 0	9.7999- 2		1.0146- 1
8.0000+ 4 ~ 1.0000+ 5	8.9089+ 0	8.8245+ 0	8.4380- 2		1.2520- 1
1.0000+ 5 ~ 1.5000+ 5	8.9870+ 0	8.9119+ 0	7.5442- 2		1.6523- 1
1.5000+ 5 ~ 2.0000+ 5	9.0309+ 0	8.9616+ 0	6.9118- 2		2.1041- 1
2.0000+ 5 ~ 3.0000+ 5	8.9353+ 0	8.8665+ 0	6.8739- 2		2.6214- 1
3.0000+ 5 ~ 4.0000+ 5	8.5815+ 0	8.4629+ 0	5.7621- 2	6.0655- 2	3.1982- 1
4.0000+ 5 ~ 5.0000+ 5	8.3934+ 0	7.8043+ 0	4.2588- 2	5.4149- 1	3.7284- 1
5.0000+ 5 ~ 6.0000+ 5	8.0959+ 0	7.2223+ 0	3.7754- 2	8.3544- 1	4.1484- 1
6.0000+ 5 ~ 8.0000+ 5	7.6717+ 0	6.6792+ 0	3.8088- 2	9.5404- 1	4.4983- 1
8.0000+ 5 ~ 1.0000+ 6	7.1459+ 0	6.0931+ 0	3.8533- 2	1.0237+ 0	4.7665- 1
1.0000+ 6 ~ 1.5000+ 6	6.3701+ 0	5.0117+ 0	3.2171- 2	1.3242+ 0	5.1525- 1
1.5000+ 6 ~ 2.0000+ 6	5.4911+ 0	3.9453+ 0	3.5442- 2	1.5084+ 0	5.3469- 1
2.0000+ 6 ~ 3.0000+ 6	4.5680+ 0	2.8505+ 0	3.8281- 2	1.6553+ 0	5.4706- 1
3.0000+ 6 ~ 4.0000+ 6	4.0501+ 0	2.2341+ 0	2.8313- 2	1.7793+ 0	5.5726- 1
4.0000+ 6 ~ 5.0000+ 6	3.9217+ 0	2.0251+ 0	1.7253- 2	1.8728+ 0	5.8931- 1
5.0000+ 6 ~ 6.0000+ 6	3.9567+ 0	2.0471+ 0	9.3225- 3	1.8910+ 0	6.3322- 1
6.0000+ 6 ~ 8.0000+ 6	4.1909+ 0	2.3405+ 0	3.2714- 3	1.8363+ 0	7.2112- 1
8.0000+ 6 ~ 1.0000+ 7	4.4242+ 0	2.6288+ 0	9.4170- 4	1.7936+ 0	8.0136- 1
1.0000+ 7 ~ 1.5000+ 7	4.5142+ 0	2.6780+ 0	3.2357- 4	1.8356+ 0	8.5938- 1

CROSS SECTION

MATERIAL =1461 PO-105

ENERGY	TOTAL	ELASTIC	CAPTURE	INELA	MU-BAR
1.0000- 5 ~ 1.0000- 2	4.8037+ 1	4.7495+ 0	4.3287+ 1		6.4106- 3
1.0000- 2 ~ 1.5000- 2	2.4826+ 1	4.7494+ 0	2.0077+ 1		6.4108- 3
1.5000- 2 ~ 2.0000- 2	2.1679+ 1	4.7493+ 0	1.6930+ 1		6.4108- 3
2.0000- 2 ~ 3.0000- 2	1.8950+ 1	4.7493+ 0	1.4200+ 1		6.4109- 3
3.0000- 2 ~ 4.0000- 2	1.6725+ 1	4.7492+ 0	1.1976+ 1		6.4109- 3
4.0000- 2 ~ 5.0000- 2	1.5307+ 1	4.7490+ 0	1.0558+ 1		6.4109- 3
5.0000- 2 ~ 6.0000- 2	1.4284+ 1	4.7489+ 0	9.5348+ 0		6.4110- 3
6.0000- 2 ~ 8.0000- 2	1.3223+ 1	4.7488+ 0	8.4745+ 0		6.4110- 3
8.0000- 2 ~ 1.0000- 1	1.2221+ 1	4.7486+ 0	7.4728+ 0		6.4110- 3
1.0000- 1 ~ 1.5000- 1	1.1107+ 1	4.7482+ 0	6.3590+ 0		6.4111- 3
1.5000- 1 ~ 2.0000- 1	1.0125+ 1	4.7476+ 0	5.3775+ 0		6.4111- 3
2.0000- 1 ~ 3.0000- 1	9.2554+ 0	4.7468+ 0	4.5086+ 0		6.4112- 3
3.0000- 1 ~ 4.0000- 1	8.5627+ 0	4.7457+ 0	3.8170+ 0		6.4112- 3
4.0000- 1 ~ 5.0000- 1	8.1085+ 0	4.7445+ 0	3.3639+ 0		6.4113- 3
5.0000- 1 ~ 6.0000- 1	7.7912+ 0	4.7434+ 0	3.0479+ 0		6.4113- 3
6.0000- 1 ~ 8.0000- 1	7.4625+ 0	4.7416+ 0	2.7209+ 0		6.4114- 3
8.0000- 1 ~ 1.0000+ 0	7.1435+ 0	4.7392+ 0	2.4043+ 0		6.4114- 3
1.0000+ 0 ~ 1.5000+ 0	6.8032+ 0	4.7348+ 0	2.0684+ 0		6.4119- 3
1.5000+ 0 ~ 2.0000+ 0	6.4944+ 0	4.7281+ 0	1.7663+ 0		6.4126- 3
2.0000+ 0 ~ 3.0000+ 0	6.2366+ 0	4.7167+ 0	1.5199+ 0		6.4133- 3
3.0000+ 0 ~ 4.0000+ 0	6.0314+ 0	4.6993+ 0	1.3321+ 0		6.4150- 3
4.0000+ 0 ~ 5.0000+ 0	5.9144+ 0	4.6781+ 0	1.2349+ 0		6.4170- 3
5.0000+ 0 ~ 6.0000+ 0	5.8497+ 0	4.6520+ 0	1.1944+ 0		6.4186- 3
6.0000+ 0 ~ 8.0000+ 0	5.8407+ 0	4.5985+ 0	1.2426+ 0		6.4206- 3
8.0000+ 0 ~ 1.0000+ 1	6.1342+ 0	4.4647+ 0	1.6674+ 0		6.4226- 3
1.0000+ 1 ~ 1.5000+ 1	9.5306+ 1	6.1591+ 0	8.9146+ 1		6.4279- 3
1.5000+ 1 ~ 2.0000+ 1	6.5627+ 0	5.0487+ 0	1.5114+ 0		6.4349- 3
2.0000+ 1 ~ 3.0000+ 1	3.8321+ 1	5.6506+ 0	3.2669+ 1		6.4478- 3
3.0000+ 1 ~ 4.0000+ 1	9.0921+ 0	5.0129+ 0	4.0783+ 0		6.4638- 3
4.0000+ 1 ~ 5.0000+ 1	5.2128+ 0	4.7530+ 0	4.5833- 1		6.4756- 3
5.0000+ 1 ~ 6.0000+ 1	3.6077+ 1	6.1506+ 0	2.9926+ 1		6.4906- 3
6.0000+ 1 ~ 8.0000+ 1	2.9726+ 1	6.9370+ 0	2.2789+ 1		6.5159- 3
8.0000+ 1 ~ 1.0000+ 2	3.4375+ 1	7.9347+ 0	2.6440+ 1		6.5427- 3
1.0000+ 2 ~ 1.5000+ 2	9.3398+ 0	5.0586+ 0	4.2807+ 0		6.5941- 3
1.5000+ 2 ~ 2.0000+ 2	1.5658+ 1	6.6053+ 0	9.0455+ 0		6.6690- 3
2.0000+ 2 ~ 3.0000+ 2	1.4032+ 1	6.5490+ 0	7.4795+ 0		6.7838- 3
3.0000+ 2 ~ 4.0000+ 2	1.2737+ 1	6.4901+ 0	6.2284+ 0		6.9541- 3
4.0000+ 2 ~ 5.0000+ 2	1.1903+ 1	6.4445+ 0	5.4439+ 0		7.1115- 3
5.0000+ 2 ~ 6.0000+ 2	1.1312+ 1	6.4071+ 0	4.8981+ 0		7.2697- 3
5.0000+ 2 ~ 8.0000+ 2	1.0703+ 1	6.3612+ 0	4.3367+ 0		7.5167- 3
8.0000+ 2 ~ 1.0000+ 3	1.0144+ 1	6.3121+ 0	3.8259+ 0		7.8557- 3
1.0000+ 3 ~ 1.5000+ 3	9.5484+ 0	6.2499+ 0	3.2932+ 0		8.4651- 3
1.5000+ 3 ~ 2.0000+ 3	9.0295+ 0	6.1872+ 0	2.8403+ 0		9.3263- 3
2.0000+ 3 ~ 3.0000+ 3	8.6169+ 0	6.1318+ 0	2.4844+ 0		1.0657- 2
3.0000+ 3 ~ 4.0000+ 3	8.3311+ 0	6.1009+ 0	2.2272+ 0		1.2625- 2
4.0000+ 3 ~ 5.0000+ 3	8.1640+ 0	6.0905+ 0	2.0711+ 0		1.4439- 2
5.0000+ 3 ~ 6.0000+ 3	8.0596+ 0	6.0965+ 0	1.9621+ 0		1.6237- 2
6.0000+ 3 ~ 8.0000+ 3	7.9802+ 0	6.1288+ 0	1.8504+ 0		1.8998- 2
8.0000+ 3 ~ 1.0000+ 4	7.9361+ 0	6.1948+ 0	1.7400+ 0		2.2688- 2
1.0000+ 4 ~ 1.5000+ 4	7.9385+ 0	6.3378+ 0	1.5985+ 0		2.9004- 2
1.5000+ 4 ~ 2.0000+ 4	7.9936+ 0	6.5471+ 0	1.4450+ 0		3.7496- 2
2.0000+ 4 ~ 3.0000+ 4	8.1203+ 0	6.8463+ 0	1.2699+ 0		5.0004- 2
3.0000+ 4 ~ 4.0000+ 4	8.2809+ 0	7.1793+ 0	1.0990+ 0		6.5314- 2
4.0000+ 4 ~ 5.0000+ 4	8.4224+ 0	7.4487+ 0	9.7213- 1		7.9891- 2
5.0000+ 4 ~ 6.0000+ 4	8.5417+ 0	7.6660+ 0	8.7466- 1		9.3826- 2
6.0000+ 4 ~ 8.0000+ 4	8.6808+ 0	7.9137+ 0	7.6646- 1		1.1359- 1
8.0000+ 4 ~ 1.0000+ 5	8.8132+ 0	8.1504+ 0	6.6254- 1		1.3820- 1
1.0000+ 5 ~ 1.5000+ 5	8.8896+ 0	8.3280+ 0	5.5379- 1		1.7904- 1
1.5000+ 5 ~ 2.0000+ 5	8.9322+ 0	8.4668+ 0	4.5960- 1		2.2494- 1
2.0000+ 5 ~ 3.0000+ 5	8.8154+ 0	8.4227+ 0	3.8688- 1	5.3057- 3	2.7813- 1
3.0000+ 5 ~ 4.0000+ 5	8.5290+ 0	7.7572+ 0	2.8250- 1	4.8695- 1	3.5194- 1
4.0000+ 5 ~ 5.0000+ 5	8.3007+ 0	6.9270+ 0	2.0002- 1	1.1729+ 0	4.2113- 1
5.0000+ 5 ~ 6.0000+ 5	8.0439+ 0	6.4280+ 0	1.6025- 1	1.4553+ 0	4.6724- 1
6.0000+ 5 ~ 8.0000+ 5	7.6318+ 0	5.9218+ 0	1.2478- 1	1.5851+ 0	5.0890- 1
8.0000+ 5 ~ 1.0000+ 6	7.1514+ 0	5.3757+ 0	1.0062- 1	1.6750+ 0	5.4166- 1
1.0000+ 6 ~ 1.5000+ 6	6.3915+ 0	4.6286+ 0	9.6726- 2	1.6653+ 0	5.6179- 1
1.5000+ 6 ~ 2.0000+ 6	5.5264+ 0	3.7228+ 0	8.6321- 2	1.7158+ 0	5.7415- 1
2.0000+ 6 ~ 3.0000+ 6	4.5959+ 0	2.7541+ 0	6.9574- 2	1.7687+ 0	5.7958- 1
3.0000+ 6 ~ 4.0000+ 6	4.0684+ 0	2.1904+ 0	4.5892- 2	1.8247+ 0	5.8460- 1
4.0000+ 6 ~ 5.0000+ 6	3.9339+ 0	2.0078+ 0	2.8898- 2	1.8914+ 0	5.9582- 1
5.0000+ 6 ~ 6.0000+ 6	3.9544+ 0	2.0398+ 0	1.6238- 2	1.8977+ 0	6.3447- 1
6.0000+ 6 ~ 8.0000+ 6	4.1929+ 0	2.3331+ 0	6.0888- 3	1.8415+ 0	7.2072- 1
8.0000+ 6 ~ 1.0000+ 7	4.4304+ 0	2.6255+ 0	1.9092- 3	1.8020+ 0	8.0029- 1
1.0000+ 7 ~ 1.5000+ 7	4.5343+ 0	2.6886+ 0	6.4413- 4	1.8449+ 0	8.5934- 1

CROSS SECTION

MATERIAL =1444 RU-106

ENERGY	TOTAL	ELASTIC	CAPTURE	INELA	MU-BAR
1.0000- 5 ~ 1.0000- 2	5.6011+ 0	5.1470+ 0	4.5029- 1		6.3493- 3
1.0000- 2 ~ 1.5000- 2	5.3581+ 0	5.1470+ 0	2.0881- 1		6.3493- 3
1.5000- 2 ~ 2.0000- 2	5.3244+ 0	5.1470+ 0	1.7604- 1		6.3493- 3
2.0000- 2 ~ 3.0000- 2	5.2963+ 0	5.1470+ 0	1.4765- 1		6.3493- 3
3.0000- 2 ~ 4.0000- 2	5.2724+ 0	5.1470+ 0	1.2448- 1		6.3493- 3
4.0000- 2 ~ 5.0000- 2	5.2582+ 0	5.1470+ 0	1.0967- 1		6.3493- 3
5.0000- 2 ~ 6.0000- 2	5.2469+ 0	5.1470+ 0	9.9145- 2		6.3493- 3
6.0000- 2 ~ 8.0000- 2	5.2357+ 0	5.1470+ 0	8.8020- 2		6.3493- 3
8.0000- 2 ~ 1.0000- 1	5.2257+ 0	5.1470+ 0	7.7548- 2		6.3493- 3
1.0000- 1 ~ 1.5000- 1	5.2135+ 0	5.1470+ 0	6.6035- 2		6.3493- 3
1.5000- 1 ~ 2.0000- 1	5.2034+ 0	5.1470+ 0	5.5670- 2		6.3493- 3
2.0000- 1 ~ 3.0000- 1	5.1940+ 0	5.1470+ 0	4.6694- 2		6.3493- 3
3.0000- 1 ~ 4.0000- 1	5.1869+ 0	5.1470+ 0	3.9365- 2		6.3493- 3
4.0000- 1 ~ 5.0000- 1	5.1819+ 0	5.1470+ 0	3.4682- 2		6.3493- 3
5.0000- 1 ~ 6.0000- 1	5.1786+ 0	5.1470+ 0	3.1354- 2		6.3493- 3
6.0000- 1 ~ 8.0000- 1	5.1752+ 0	5.1470+ 0	2.7836- 2		6.3493- 3
8.0000- 1 ~ 1.0000+ 0	5.1717+ 0	5.1470+ 0	2.4524- 2		6.3493- 3
1.0000+ 0 ~ 1.5000+ 0	5.1681+ 0	5.1470+ 0	2.0883- 2		6.3494- 3
1.5000+ 0 ~ 2.0000+ 0	5.1647+ 0	5.1470+ 0	1.7605- 2		6.3497- 3
2.0000+ 0 ~ 3.0000+ 0	5.1619+ 0	5.1470+ 0	1.4767- 2		6.3499- 3
3.0000+ 0 ~ 4.0000+ 0	5.1595+ 0	5.1470+ 0	1.2449- 2		6.3503- 3
4.0000+ 0 ~ 5.0000+ 0	5.1581+ 0	5.1470+ 0	1.0968- 2		6.3509- 3
5.0000+ 0 ~ 6.0000+ 0	5.1571+ 0	5.1470+ 0	9.9155- 3		6.3513- 3
6.0000+ 0 ~ 8.0000+ 0	5.1559+ 0	5.1470+ 0	8.8029- 3		6.3518- 3
8.0000+ 0 ~ 1.0000+ 1	5.1548+ 0	5.1470+ 0	7.7556- 3		6.3524- 3
1.0000+ 1 ~ 1.5000+ 1	5.1537+ 0	5.1470+ 0	6.6041- 3		6.3541- 3
1.5000+ 1 ~ 2.0000+ 1	5.1526+ 0	5.1470+ 0	5.5676- 3		6.3565- 3
2.0000+ 1 ~ 3.0000+ 1	5.1517+ 0	5.1470+ 0	4.6699- 3		6.3618- 3
3.0000+ 1 ~ 4.0000+ 1	5.1510+ 0	5.1470+ 0	3.9369- 3		6.3686- 3
4.0000+ 1 ~ 5.0000+ 1	5.1505+ 0	5.1470+ 0	3.4685- 3		6.3737- 3
5.0000+ 1 ~ 6.0000+ 1	5.1502+ 0	5.1470+ 0	3.1357- 3		6.3811- 3
6.0000+ 1 ~ 8.0000+ 1	5.1498+ 0	5.1470+ 0	2.7839- 3		6.3944- 3
8.0000+ 1 ~ 1.0000+ 2	5.1495+ 0	5.1470+ 0	2.4527- 3		6.4084- 3
1.0000+ 2 ~ 1.5000+ 2	5.1491+ 0	5.1470+ 0	2.0885- 3		6.4381- 3
1.5000+ 2 ~ 2.0000+ 2	5.1488+ 0	5.1470+ 0	1.7607- 3		6.4843- 3
2.0000+ 2 ~ 3.0000+ 2	5.1485+ 0	5.1470+ 0	1.4768- 3		6.5608- 3
3.0000+ 2 ~ 4.0000+ 2	5.1483+ 0	5.1470+ 0	1.2450- 3		6.6832- 3
4.0000+ 2 ~ 5.0000+ 2	5.1481+ 0	5.1470+ 0	1.0969- 3		6.7999- 3
5.0000+ 2 ~ 6.0000+ 2	1.1326+ 1	1.0343+ 1	9.8204- 1		6.9211- 3
6.0000+ 2 ~ 8.0000+ 2	1.0707+ 1	9.8356+ 0	8.7112- 1		7.1163- 3
8.0000+ 2 ~ 1.0000+ 3	1.0139+ 1	9.3630+ 0	7.7507- 1		7.3912- 3
1.0000+ 3 ~ 1.5000+ 3	9.5326+ 0	8.8567+ 0	6.7533- 1		7.8982- 3
1.5000+ 3 ~ 2.0000+ 3	9.0037+ 0	8.4173+ 0	5.8615- 1		8.6257- 3
2.0000+ 3 ~ 3.0000+ 3	8.5818+ 0	8.0776+ 0	5.0404- 1		9.7634- 3
3.0000+ 3 ~ 4.0000+ 3	8.2877+ 0	7.8575+ 0	4.2828- 1		1.1459- 2
4.0000+ 3 ~ 5.0000+ 3	8.1148+ 0	7.7371+ 0	3.7611- 1		1.3026- 2
5.0000+ 3 ~ 6.0000+ 3	8.0058+ 0	7.6680+ 0	3.3680- 1		1.4587- 2
6.0000+ 3 ~ 8.0000+ 3	7.9210+ 0	7.6278+ 0	2.9228- 1		1.7003- 2
8.0000+ 3 ~ 1.0000+ 4	7.8713+ 0	7.6213+ 0	2.4878- 1		2.0269- 2
1.0000+ 4 ~ 1.5000+ 4	7.8660+ 0	7.6647+ 0	1.9991- 1		2.5984- 2
1.5000+ 4 ~ 2.0000+ 4	7.9127+ 0	7.7557+ 0	1.5636- 1		3.3839- 2
2.0000+ 4 ~ 3.0000+ 4	8.0300+ 0	7.9087+ 0	1.2021- 1		4.5796- 2
3.0000+ 4 ~ 4.0000+ 4	8.1807+ 0	8.0873+ 0	9.2920- 2		6.0733- 2
4.0000+ 4 ~ 5.0000+ 4	8.3145+ 0	8.2372+ 0	7.7166- 2		7.5191- 2
5.0000+ 4 ~ 6.0000+ 4	8.4274+ 0	8.3600+ 0	6.7288- 2		8.9132- 2
6.0000+ 4 ~ 8.0000+ 4	8.5593+ 0	8.5009+ 0	5.8311- 2		1.0900- 1
8.0000+ 4 ~ 1.0000+ 5	8.6847+ 0	8.6333+ 0	5.1304- 2		1.3381- 1
1.0000+ 5 ~ 1.5000+ 5	8.7581+ 0	8.7105+ 0	4.7554- 2		1.7475- 1
1.5000+ 5 ~ 2.0000+ 5	8.8002+ 0	8.7549+ 0	4.5315- 2		2.2069- 1
2.0000+ 5 ~ 3.0000+ 5	8.6194+ 0	8.5484+ 0	3.4997- 2	3.5554- 2	2.7675- 1
3.0000+ 5 ~ 4.0000+ 5	8.5093+ 0	7.9518+ 0	2.4013- 2	5.2789- 1	3.4421- 1
4.0000+ 5 ~ 5.0000+ 5	8.2576+ 0	7.3780+ 0	2.0266- 2	8.5803- 1	3.9675- 1
5.0000+ 5 ~ 6.0000+ 5	7.9999+ 0	7.0207+ 0	1.9876- 2	9.5889- 1	4.2960- 1
6.0000+ 5 ~ 8.0000+ 5	7.6209+ 0	6.6064+ 0	2.0035- 2	9.9226- 1	4.5827- 1
8.0000+ 5 ~ 1.0000+ 6	7.1541+ 0	6.0079+ 0	1.6754- 2	1.1287+ 0	4.8825- 1
1.0000+ 6 ~ 1.5000+ 6	6.4297+ 0	5.0696+ 0	1.7673- 2	1.3399+ 0	5.1891- 1
1.5000+ 6 ~ 2.0000+ 6	5.5483+ 0	4.0898+ 0	2.4082- 2	1.4336+ 0	5.3194- 1
2.0000+ 6 ~ 3.0000+ 6	4.6297+ 0	2.9718+ 0	2.7248- 2	1.6250+ 0	5.4958- 1
3.0000+ 6 ~ 4.0000+ 6	4.0908+ 0	2.2780+ 0	1.8168- 2	1.7838+ 0	5.7050- 1
4.0000+ 6 ~ 5.0000+ 6	3.9485+ 0	2.0329+ 0	9.6997- 3	1.8975+ 0	5.9066- 1
5.0000+ 6 ~ 6.0000+ 6	3.9731+ 0	2.0394+ 0	4.6256- 3	1.9205+ 0	6.3298- 1
6.0000+ 6 ~ 8.0000+ 6	4.1941+ 0	2.3264+ 0	1.3580- 3	1.8562+ 0	7.1891- 1
8.0000+ 6 ~ 1.0000+ 7	4.4370+ 0	2.6202+ 0	3.2532- 4	1.8158+ 0	7.9873- 1
1.0000+ 7 ~ 1.5000+ 7	4.5574+ 0	2.7009+ 0	9.7927- 5	1.8563+ 0	8.5923- 1

CROSS SECTION

MATERIAL =1462 PD-107

ENERGY	TOTAL	ELASTIC	CAPTURE	INELA	MU-BAR
1.0000- 5 ~ 1.0000- 2	3.5971+ 1	5.0670+ 0	3.0837+ 1		6.2903- 3
1.0000- 2 ~ 1.5000- 2	1.9411+ 1	5.0670+ 0	1.4299+ 1		6.2904- 3
1.5000- 2 ~ 2.0000- 2	1.7148+ 1	5.0670+ 0	1.2055+ 1		6.2905- 3
2.0000- 2 ~ 3.0000- 2	1.5218+ 1	5.0670+ 0	1.0111+ 1		6.2905- 3
3.0000- 2 ~ 4.0000- 2	1.3615+ 1	5.0670+ 0	8.5238+ 0		6.2905- 3
4.0000- 2 ~ 5.0000- 2	1.2604+ 1	5.0670+ 0	7.5096+ 0		6.2906- 3
5.0000- 2 ~ 6.0000- 2	1.1899+ 1	5.0670+ 0	6.7890+ 0		6.2906- 3
6.0000- 2 ~ 8.0000- 2	1.1115+ 1	5.0670+ 0	6.0272+ 0		6.2906- 3
8.0000- 2 ~ 1.0000- 1	1.0401+ 1	5.0670+ 0	5.3101+ 0		6.2906- 3
1.0000- 1 ~ 1.5000- 1	9.6167+ 0	5.0670+ 0	4.5216+ 0		6.2907- 3
1.5000- 1 ~ 2.0000- 1	8.8950+ 0	5.0670+ 0	3.8119+ 0		6.2907- 3
2.0000- 1 ~ 3.0000- 1	8.2874+ 0	5.0670+ 0	3.1973+ 0		6.2907- 3
3.0000- 1 ~ 4.0000- 1	7.7753+ 0	5.0670+ 0	2.6954+ 0		6.2908- 3
4.0000- 1 ~ 5.0000- 1	7.4652+ 0	5.0670+ 0	2.3747+ 0		6.2908- 3
5.0000- 1 ~ 6.0000- 1	7.2275+ 0	5.0670+ 0	2.1468+ 0		6.2908- 3
6.0000- 1 ~ 8.0000- 1	6.9830+ 0	5.0670+ 0	1.9059+ 0		6.2908- 3
8.0000- 1 ~ 1.0000+ 0	6.7645+ 0	5.0670+ 0	1.6792+ 0		6.2908- 3
1.0000+ 0 ~ 1.5000+ 0	6.5047+ 0	5.0670+ 0	1.4299+ 0		6.2916- 3
1.5000+ 0 ~ 2.0000+ 0	6.2861+ 0	5.0670+ 0	1.2054+ 0		6.2927- 3
2.0000+ 0 ~ 3.0000+ 0	6.0840+ 0	5.0670+ 0	1.0110+ 0		6.2938- 3
3.0000+ 0 ~ 4.0000+ 0	5.9296+ 0	5.0670+ 0	8.5236- 1		6.2958- 3
4.0000+ 0 ~ 5.0000+ 0	5.8231+ 0	5.0670+ 0	7.5094- 1		6.2982- 3
5.0000+ 0 ~ 6.0000+ 0	6.4588+ 1	5.9070+ 0	5.7636+ 1		6.3000- 3
6.0000+ 0 ~ 8.0000+ 0	5.7975+ 1	5.8954+ 0	5.0990+ 1		6.3023- 3
8.0000+ 0 ~ 1.0000+ 1	5.1681+ 1	5.8832+ 0	4.4755+ 1		6.3046- 3
1.0000+ 1 ~ 1.5000+ 1	4.4805+ 1	5.8625+ 0	3.7874+ 1		6.3106- 3
1.5000+ 1 ~ 2.0000+ 1	3.8576+ 1	5.8383+ 0	3.1689+ 1		6.3185- 3
2.0000+ 1 ~ 3.0000+ 1	3.3242+ 1	5.8075+ 0	2.6332+ 1		6.3332- 3
3.0000+ 1 ~ 4.0000+ 1	2.8879+ 1	5.7747+ 0	2.1973+ 1		6.3513- 3
4.0000+ 1 ~ 5.0000+ 1	2.6015+ 1	5.7504+ 0	1.9212+ 1		6.3648- 3
5.0000+ 1 ~ 6.0000+ 1	2.4016+ 1	5.7280+ 0	1.7251+ 1		6.3819- 3
6.0000+ 1 ~ 8.0000+ 1	2.1947+ 1	5.6976+ 0	1.5178+ 1		6.4107- 3
8.0000+ 1 ~ 1.0000+ 2	1.9943+ 1	5.6656+ 0	1.3243+ 1		6.4412- 3
1.0000+ 2 ~ 1.5000+ 2	1.7765+ 1	5.6200+ 0	1.1130+ 1		6.4997- 3
1.5000+ 2 ~ 2.0000+ 2	1.5820+ 1	5.5674+ 0	9.2450+ 0		6.5849- 3
2.0000+ 2 ~ 3.0000+ 2	1.4148+ 1	5.5076+ 0	7.6371+ 0		6.7155- 3
3.0000+ 2 ~ 4.0000+ 2	1.2816+ 1	5.4453+ 0	6.3514+ 0		6.9091- 3
4.0000+ 2 ~ 5.0000+ 2	1.1957+ 1	5.3970+ 0	5.5452+ 0		7.0877- 3
5.0000+ 2 ~ 6.0000+ 2	1.1348+ 1	5.3574+ 0	4.9842+ 0		7.2671- 3
6.0000+ 2 ~ 8.0000+ 2	1.0721+ 1	5.3087+ 0	4.4066+ 0		7.5470- 3
8.0000+ 2 ~ 1.0000+ 3	1.0143+ 1	5.2567+ 0	3.8603+ 0		7.9309- 3
1.0000+ 3 ~ 1.5000+ 3	9.5266+ 0	5.1904+ 0	3.3307+ 0		8.6198- 3
1.5000+ 3 ~ 2.0000+ 3	8.9880+ 0	5.1233+ 0	2.8627+ 0		9.5918- 3
2.0000+ 3 ~ 3.0000+ 3	8.5568+ 0	5.0625+ 0	2.4935+ 0		1.1089- 2
3.0000+ 3 ~ 4.0000+ 3	8.2542+ 0	5.0251+ 0	2.2260+ 0		1.3297- 2
4.0000+ 3 ~ 5.0000+ 3	8.0753+ 0	5.0092+ 0	2.0636+ 0		1.5328- 2
5.0000+ 3 ~ 6.0000+ 3	7.9616+ 0	5.0099+ 0	1.9506+ 0		1.7336- 2
6.0000+ 3 ~ 8.0000+ 3	7.8712+ 0	5.0349+ 0	1.8354+ 0		2.0411- 2
8.0000+ 3 ~ 1.0000+ 4	7.8155+ 0	5.0915+ 0	1.7227+ 0		2.4507- 2
1.0000+ 4 ~ 1.5000+ 4	7.8023+ 0	5.2197+ 0	1.5804+ 0		3.1484- 2
1.5000+ 4 ~ 2.0000+ 4	7.8402+ 0	5.4110+ 0	1.4277+ 0		4.0813- 2
2.0000+ 4 ~ 3.0000+ 4	7.9476+ 0	5.6882+ 0	1.2555+ 0		5.4423- 2
3.0000+ 4 ~ 4.0000+ 4	8.0882+ 0	5.9980+ 0	1.0878+ 0		7.0946- 2
4.0000+ 4 ~ 5.0000+ 4	8.2142+ 0	7.2491+ 0	9.6359- 1		8.6534- 2
5.0000+ 4 ~ 6.0000+ 4	8.3210+ 0	7.4519+ 0	8.6816- 1		1.0132- 1
6.0000+ 4 ~ 8.0000+ 4	8.4459+ 0	7.6831+ 0	7.6228- 1		1.2211- 1
8.0000+ 4 ~ 1.0000+ 5	8.5649+ 0	7.9041+ 0	6.6055- 1		1.4777- 1
1.0000+ 5 ~ 1.5000+ 5	8.6092+ 0	8.0250+ 0	5.4762- 1	2.8469- 2	1.9102- 1
1.5000+ 5 ~ 2.0000+ 5	8.6679+ 0	8.0826+ 0	4.4746- 1	1.3187- 1	2.4006- 1
2.0000+ 5 ~ 3.0000+ 5	8.6068+ 0	8.0172+ 0	3.7088- 1	2.1765- 1	2.9520- 1
3.0000+ 5 ~ 4.0000+ 5	8.3069+ 0	7.4651+ 0	2.6008- 1	5.7784- 1	3.6724- 1
4.0000+ 5 ~ 5.0000+ 5	8.1654+ 0	6.6787+ 0	1.6319- 1	1.3207+ 0	4.3868- 1
5.0000+ 5 ~ 6.0000+ 5	7.9321+ 0	6.1691+ 0	1.2081- 1	1.6416+ 0	4.8841- 1
6.0000+ 5 ~ 8.0000+ 5	7.5843+ 0	5.7600+ 0	9.9627- 2	1.7247+ 0	5.2558- 1
8.0000+ 5 ~ 1.0000+ 6	7.1483+ 0	5.3242+ 0	8.5371- 2	1.7387+ 0	5.5159- 1
1.0000+ 6 ~ 1.5000+ 6	6.4419+ 0	4.6569+ 0	8.8926- 2	1.6952+ 0	5.6805- 1
1.5000+ 6 ~ 2.0000+ 6	5.6014+ 0	3.7845+ 0	8.3371- 2	1.7322+ 0	5.8190- 1
2.0000+ 6 ~ 3.0000+ 6	4.6603+ 0	2.8114+ 0	6.6331- 2	1.7791+ 0	5.9003- 1
3.0000+ 6 ~ 4.0000+ 6	4.1142+ 0	2.2210+ 0	4.0401- 2	1.8432+ 0	5.9247- 1
4.0000+ 6 ~ 5.0000+ 6	3.9652+ 0	2.0143+ 0	2.2683- 2	1.9209+ 0	5.9941- 1
5.0000+ 6 ~ 6.0000+ 6	3.9847+ 0	2.0347+ 0	1.1578- 2	1.9283+ 0	6.3523- 1
6.0000+ 6 ~ 8.0000+ 6	4.1990+ 0	2.3205+ 0	3.8468- 3	1.8630+ 0	7.1892- 1
8.0000+ 6 ~ 1.0000+ 7	4.4457+ 0	2.6175+ 0	1.2514- 3	1.8261+ 0	7.9772- 1
1.0000+ 7 ~ 1.5000+ 7	4.5777+ 0	2.7114+ 0	3.5329- 4	1.8659+ 0	8.5919- 1

MATERIAL =1471 CROSS SECTION AG-109

ENERGY	TOTAL	ELASTIC	CAPTURE	INELA	MU-BAR
1.0000- 5 ~ 1.0000- 2	2.7970+ 2	1.9319+ 0	2.7777+ 2		6.1743- 3
1.0000- 2 ~ 1.5000- 2	1.3103+ 2	1.9300+ 0	1.2910+ 2		6.1743- 3
1.5000- 2 ~ 2.0000- 2	1.1125+ 2	1.9287+ 0	1.0932+ 2		6.1743- 3
2.0000- 2 ~ 3.0000- 2	9.3646+ 1	1.9268+ 0	9.1719+ 1		6.1743- 3
3.0000- 2 ~ 4.0000- 2	7.9736+ 1	1.9242+ 0	7.7812+ 1		6.1743- 3
4.0000- 2 ~ 5.0000- 2	7.0600+ 1	1.9216+ 0	6.8678+ 1		6.1743- 3
5.0000- 2 ~ 6.0000- 2	6.4183+ 1	1.9191+ 0	6.2264+ 1		6.1743- 3
6.0000- 2 ~ 8.0000- 2	5.7672+ 1	1.9152+ 0	5.5757+ 1		6.1743- 3
8.0000- 2 ~ 1.0000- 1	5.1314+ 1	1.9100+ 0	4.9404+ 1		6.1743- 3
1.0000- 1 ~ 1.5000- 1	4.4568+ 1	1.9007+ 0	4.2667+ 1		6.1743- 3
1.5000- 1 ~ 2.0000- 1	3.8545+ 1	1.8874+ 0	3.6657+ 1		6.1743- 3
2.0000- 1 ~ 3.0000- 1	3.3543+ 1	1.8668+ 0	3.1677+ 1		6.1743- 3
3.0000- 1 ~ 4.0000- 1	2.9627+ 1	1.8387+ 0	2.7788+ 1		6.1743- 3
4.0000- 1 ~ 5.0000- 1	2.7289+ 1	1.8095+ 0	2.5479+ 1		6.1743- 3
5.0000- 1 ~ 6.0000- 1	2.5891+ 1	1.7791+ 0	2.4112+ 1		6.1743- 3
6.0000- 1 ~ 8.0000- 1	2.4506+ 1	1.7318+ 0	2.2775+ 1		6.1743- 3
8.0000- 1 ~ 1.0000+ 0	2.3600+ 1	1.6650+ 0	2.1935+ 1		6.1743- 3
1.0000+ 0 ~ 1.5000+ 0	2.3708+ 1	1.5389+ 0	2.2170+ 1		6.1752- 3
1.5000+ 0 ~ 2.0000+ 0	2.5842+ 1	1.3660+ 0	2.4476+ 1		6.1766- 3
2.0000+ 0 ~ 3.0000+ 0	3.5282+ 1	1.1359+ 0	3.4146+ 1		6.1781- 3
3.0000+ 0 ~ 4.0000+ 0	7.8209+ 1	1.7626+ 0	7.6447+ 1		6.1803- 3
4.0000+ 0 ~ 5.0000+ 0	7.6948+ 2	4.5296+ 1	7.2419+ 2		6.1827- 3
5.0000+ 0 ~ 6.0000+ 0	6.5179+ 3	5.7846+ 2	5.9395+ 3		6.1845- 3
6.0000+ 0 ~ 8.0000+ 0	8.3491+ 1	1.8771+ 1	6.4720+ 1		6.1868- 3
8.0000+ 0 ~ 1.0000+ 1	1.8031+ 1	8.4560+ 0	9.5750+ 0		6.1892- 3
1.0000+ 1 ~ 1.5000+ 1	8.3931+ 0	5.9082+ 0	2.4849+ 0		6.1953- 3
1.5000+ 1 ~ 2.0000+ 1	5.5961+ 0	4.7612+ 0	8.3484- 1		6.2033- 3
2.0000+ 1 ~ 3.0000+ 1	7.7135+ 0	3.5816+ 0	4.1318+ 0		6.2185- 3
3.0000+ 1 ~ 4.0000+ 1	8.2912+ 1	8.3739+ 0	7.4538+ 1		6.2374- 3
4.0000+ 1 ~ 5.0000+ 1	3.6684+ 1	6.0321+ 0	3.0652+ 1		6.2514- 3
5.0000+ 1 ~ 6.0000+ 1	7.2954+ 1	1.8468+ 1	5.4486+ 1		6.2692- 3
6.0000+ 1 ~ 8.0000+ 1	6.3292+ 1	1.5200+ 1	4.8092+ 1		6.2995- 3
8.0000+ 1 ~ 1.0000+ 2	1.6015+ 1	5.2278+ 0	1.0787+ 1		6.3314- 3
1.0000+ 2 ~ 1.5000+ 2	4.2355+ 1	1.9155+ 1	2.3199+ 1		6.3932- 3
1.5000+ 2 ~ 2.0000+ 2	2.2310+ 1	9.2762+ 0	1.3034+ 1		6.4835- 3
2.0000+ 2 ~ 3.0000+ 2	1.1068+ 1	5.3107+ 0	5.7569+ 0		6.6226- 3
3.0000+ 2 ~ 4.0000+ 2	2.6698+ 1	1.4737+ 1	1.1960+ 1		6.8299- 3
4.0000+ 2 ~ 5.0000+ 2	1.4984+ 1	9.2819+ 0	5.7017+ 0		7.0218- 3
5.0000+ 2 ~ 6.0000+ 2	2.9083+ 1	1.8711+ 1	1.0372+ 1		7.2149- 3
6.0000+ 2 ~ 8.0000+ 2	1.5680+ 1	1.0781+ 1	4.8995+ 0		7.5171- 3
8.0000+ 2 ~ 1.0000+ 3	1.0943+ 1	7.6623+ 0	3.2809+ 0		7.9323- 3
1.0000+ 3 ~ 1.5000+ 3	9.5829+ 0	6.3350+ 0	3.2425+ 0		8.6797- 3
1.5000+ 3 ~ 2.0000+ 3	9.0063+ 0	6.2324+ 0	2.7719+ 0		9.7362- 3
2.0000+ 3 ~ 3.0000+ 3	8.5399+ 0	6.1354+ 0	2.4039+ 0		1.1368- 2
3.0000+ 3 ~ 4.0000+ 3	8.2068+ 0	6.0622+ 0	2.1419+ 0		1.3782- 2
4.0000+ 3 ~ 5.0000+ 3	8.0065+ 0	6.0187+ 0	1.9856+ 0		1.6007- 2
5.0000+ 3 ~ 6.0000+ 3	7.8764+ 0	5.9962+ 0	1.8794+ 0		1.8210- 2
6.0000+ 3 ~ 8.0000+ 3	7.7673+ 0	5.9910+ 0	1.7756+ 0		2.1594- 2
8.0000+ 3 ~ 1.0000+ 4	7.6919+ 0	6.0125+ 0	1.6785+ 0		2.6115- 2
1.0000+ 4 ~ 1.5000+ 4	7.6536+ 0	6.0916+ 0	1.5607+ 0		3.3832- 2
1.5000+ 4 ~ 2.0000+ 4	7.6651+ 0	6.2284+ 0	1.4358+ 0		4.4152- 2
2.0000+ 4 ~ 3.0000+ 4	7.7441+ 0	6.4494+ 0	1.2920+ 0		5.9137- 2
3.0000+ 4 ~ 4.0000+ 4	7.8566+ 0	6.7081+ 0	1.1468+ 0		7.7200- 2
4.0000+ 4 ~ 5.0000+ 4	7.9617+ 0	6.9259+ 0	1.0346+ 0		9.4074- 2
5.0000+ 4 ~ 6.0000+ 4	8.0522+ 0	7.1057+ 0	9.4560- 1		1.0994- 1
6.0000+ 4 ~ 8.0000+ 4	8.1591+ 0	7.3148+ 0	8.4383- 1		1.3201- 1
8.0000+ 4 ~ 1.0000+ 5	8.2619+ 0	7.5183+ 0	7.4305- 1	2.9170- 4	1.5898- 1
1.0000+ 5 ~ 1.5000+ 5	8.3202+ 0	7.6830+ 0	6.2886- 1	6.8770- 3	2.0193- 1
1.5000+ 5 ~ 2.0000+ 5	8.3659+ 0	7.8194+ 0	5.2658- 1	1.7476- 2	2.4968- 1
2.0000+ 5 ~ 3.0000+ 5	8.3229+ 0	7.8353+ 0	4.4774- 1	3.8776- 2	3.0244- 1
3.0000+ 5 ~ 4.0000+ 5	8.1319+ 0	7.5209+ 0	3.5423- 1	2.5369- 1	3.6299- 1
4.0000+ 5 ~ 5.0000+ 5	7.9724+ 0	7.0156+ 0	2.6958- 1	6.8528- 1	4.1620- 1
5.0000+ 5 ~ 6.0000+ 5	7.8002+ 0	6.6171+ 0	2.2566- 1	9.5634- 1	4.5467- 1
6.0000+ 5 ~ 8.0000+ 5	7.4956+ 0	6.2026+ 0	2.0316- 1	1.0895+ 0	4.8859- 1
8.0000+ 5 ~ 1.0000+ 6	7.1137+ 0	5.6445+ 0	1.6104- 1	1.3080+ 0	5.2317- 1
1.0000+ 6 ~ 1.5000+ 6	6.4886+ 0	4.8438+ 0	1.2866- 1	1.5138+ 0	5.5475- 1
1.5000+ 6 ~ 2.0000+ 6	5.6732+ 0	3.9053+ 0	1.1861- 1	1.6476+ 0	5.8074- 1
2.0000+ 6 ~ 3.0000+ 6	4.7297+ 0	2.8881+ 0	9.1255- 2	1.7462+ 0	5.9771- 1
3.0000+ 6 ~ 4.0000+ 6	4.1670+ 0	2.2567+ 0	5.2636- 2	1.8455+ 0	6.0032- 1
4.0000+ 6 ~ 5.0000+ 6	4.0001+ 0	2.0229+ 0	3.0042- 2	1.9378+ 0	6.0313- 1
5.0000+ 6 ~ 6.0000+ 6	4.0063+ 0	2.0297+ 0	1.5518- 2	1.9502+ 0	6.3595- 1
6.0000+ 6 ~ 8.0000+ 6	4.2043+ 0	2.3051+ 0	5.2182- 3	1.8818+ 0	7.1646- 1
8.0000+ 6 ~ 1.0000+ 7	4.4604+ 0	2.6058+ 0	1.8076- 3	1.8520+ 0	7.9442- 1
1.0000+ 7 ~ 1.5000+ 7	4.6172+ 0	2.7328+ 0	5.4416- 4	1.8839+ 0	8.5887- 1

MATERIAL =1531 CROSS SECTION I -129

ENERGY	TOTAL	ELASTIC	CAPTURE	INELA	MU-BAR
1.0000- 5 ~ 1.0000- 2	8.7871+ 1	3.8920+ 0	8.3974+ 1		5.2127- 3
1.0000- 2 ~ 1.5000- 2	4.2813+ 1	3.8920+ 0	3.8918+ 1		5.2127- 3
1.5000- 2 ~ 2.0000- 2	3.6745+ 1	3.8920+ 0	3.2856+ 1		5.2127- 3
2.0000- 2 ~ 3.0000- 2	3.1414+ 1	3.8920+ 0	2.7519+ 1		5.2127- 3
3.0000- 2 ~ 4.0000- 2	2.7123+ 1	3.8920+ 0	2.3233+ 1		5.2127- 3
4.0000- 2 ~ 5.0000- 2	2.4320+ 1	3.8920+ 0	2.0429+ 1		5.2127- 3
5.0000- 2 ~ 6.0000- 2	2.2386+ 1	3.8920+ 0	1.8489+ 1		5.2127- 3
6.0000- 2 ~ 8.0000- 2	2.0319+ 1	3.8920+ 0	1.6428+ 1		5.2127- 3
8.0000- 2 ~ 1.0000- 1	1.8337+ 1	3.8920+ 0	1.4446+ 1		5.2127- 3
1.0000- 1 ~ 1.5000- 1	1.6213+ 1	3.8920+ 0	1.2321+ 1		5.2127- 3
1.5000- 1 ~ 2.0000- 1	1.4266+ 1	3.8919+ 0	1.0374+ 1		5.2127- 3
2.0000- 1 ~ 3.0000- 1	1.2604+ 1	3.8919+ 0	8.7120+ 0		5.2127- 3
3.0000- 1 ~ 4.0000- 1	1.1227+ 1	3.8918+ 0	7.3357+ 0		5.2127- 3
4.0000- 1 ~ 5.0000- 1	1.0365+ 1	3.8917+ 0	6.4724+ 0		5.2127- 3
5.0000- 1 ~ 6.0000- 1	9.7391+ 0	3.8917+ 0	5.8486+ 0		5.2127- 3
6.0000- 1 ~ 8.0000- 1	9.0787+ 0	3.8916+ 0	5.1873+ 0		5.2127- 3
8.0000- 1 ~ 1.0000+ 0	8.4693+ 0	3.8914+ 0	4.5769+ 0		5.2127- 3
1.0000+ 0 ~ 1.5000+ 0	7.7841+ 0	3.8912+ 0	3.8933+ 0		5.2127- 3
1.5000+ 0 ~ 2.0000+ 0	7.1763+ 0	3.8909+ 0	3.2849+ 0		5.2127- 3
2.0000+ 0 ~ 3.0000+ 0	6.6434+ 0	3.8903+ 0	2.7534+ 0		5.2127- 3
3.0000+ 0 ~ 4.0000+ 0	6.2132+ 0	3.8896+ 0	2.3232+ 0		5.2131- 3
4.0000+ 0 ~ 5.0000+ 0	5.9353+ 0	3.8888+ 0	2.0467+ 0		5.2138- 3
5.0000+ 0 ~ 6.0000+ 0	5.7361+ 0	3.8881+ 0	1.8483+ 0		5.2144- 3
6.0000+ 0 ~ 8.0000+ 0	5.5305+ 0	3.8868+ 0	1.6434+ 0		5.2151- 3
8.0000+ 0 ~ 1.0000+ 1	5.3330+ 0	3.8851+ 0	1.4480+ 0		5.2157- 3
1.0000+ 1 ~ 1.5000+ 1	5.1143+ 0	3.8818+ 0	1.2324+ 0		5.2173- 3
1.5000+ 1 ~ 2.0000+ 1	4.9180+ 0	3.8763+ 0	1.0417+ 0		5.2193- 3
2.0000+ 1 ~ 3.0000+ 1	4.7398+ 0	3.8660+ 0	8.7325- 1		5.2236- 3
3.0000+ 1 ~ 4.0000+ 1	4.5873+ 0	3.8465+ 0	7.3825- 1		5.2290- 3
4.0000+ 1 ~ 5.0000+ 1	4.4719+ 0	3.8149+ 0	6.5536- 1		5.2331- 3
5.0000+ 1 ~ 6.0000+ 1	4.3617+ 0	3.7515+ 0	6.0833- 1		5.2389- 3
6.0000+ 1 ~ 8.0000+ 1	2.2962+ 1	5.9829+ 0	1.6977+ 1		5.2491- 3
8.0000+ 1 ~ 1.0000+ 2	5.6154+ 0	3.9668+ 0	1.6473+ 0		5.2600- 3
1.0000+ 2 ~ 1.5000+ 2	2.4161+ 1	1.1141+ 1	1.3020+ 1		5.2829- 3
1.5000+ 2 ~ 2.0000+ 2	3.1783+ 1	1.7285+ 1	1.4494+ 1		5.3184- 3
2.0000+ 2 ~ 3.0000+ 2	3.1716+ 1	1.9924+ 1	1.1787+ 1		5.3779- 3
3.0000+ 2 ~ 4.0000+ 2	2.7351+ 1	1.8170+ 1	9.1491+ 0		5.4751- 3
4.0000+ 2 ~ 5.0000+ 2	2.4547+ 1	1.6951+ 1	7.5717+ 0		5.5687- 3
5.0000+ 2 ~ 6.0000+ 2	2.2553+ 1	1.6033+ 1	6.5098+ 0		5.6678- 3
6.0000+ 2 ~ 8.0000+ 2	2.0453+ 1	1.5001+ 1	5.4452+ 0		5.8310- 3
8.0000+ 2 ~ 1.0000+ 3	1.8484+ 1	1.3974+ 1	4.5005+ 0		6.0666- 3
1.0000+ 3 ~ 1.5000+ 3	1.6323+ 1	1.2769+ 1	3.5455+ 0		6.5197- 3
1.5000+ 3 ~ 2.0000+ 3	1.4376+ 1	1.1615+ 1	2.7581+ 0		7.1960- 3
2.0000+ 3 ~ 3.0000+ 3	1.2701+ 1	1.0549+ 1	2.1511+ 0		8.3154- 3
3.0000+ 3 ~ 4.0000+ 3	1.1361+ 1	9.6437+ 0	1.7123+ 0		1.0106- 2
4.0000+ 3 ~ 5.0000+ 3	1.0498+ 1	9.0381+ 0	1.4562+ 0		1.1812- 2
5.0000+ 3 ~ 6.0000+ 3	9.8856+ 0	8.5976+ 0	1.2867+ 0		1.3576- 2
6.0000+ 3 ~ 8.0000+ 3	9.2502+ 0	8.1281+ 0	1.1213+ 0		1.6407- 2
8.0000+ 3 ~ 1.0000+ 4	8.6621+ 0	7.6865+ 0	9.7449- 1		2.0360- 2
1.0000+ 4 ~ 1.5000+ 4	8.0278+ 0	7.2062+ 0	8.2037- 1		2.7521- 2
1.5000+ 4 ~ 2.0000+ 4	7.4655+ 0	6.7805+ 0	6.8439- 1		3.7580- 2
2.0000+ 4 ~ 3.0000+ 4	6.9506+ 0	6.3827+ 0	5.5475- 1	1.2265- 2	5.3666- 2
3.0000+ 4 ~ 4.0000+ 4	6.6390+ 0	6.0291+ 0	4.3937- 1	1.6874- 1	7.4313- 2
4.0000+ 4 ~ 5.0000+ 4	6.4185+ 0	5.8192+ 0	3.6551- 1	2.3311- 1	9.4320- 2
5.0000+ 4 ~ 6.0000+ 4	6.2704+ 0	5.6877+ 0	3.1710- 1	2.6525- 1	1.1335- 1
6.0000+ 4 ~ 8.0000+ 4	6.1252+ 0	5.5595+ 0	2.7036- 1	2.9511- 1	1.4006- 1
8.0000+ 4 ~ 1.0000+ 5	6.0020+ 0	5.4501+ 0	2.3068- 1	3.2116- 1	1.7264- 1
1.0000+ 5 ~ 1.5000+ 5	5.9224+ 0	5.3785+ 0	1.9589- 1	3.4623- 1	2.2201- 1
1.5000+ 5 ~ 2.0000+ 5	5.8659+ 0	5.3274+ 0	1.6706- 1	3.7012- 1	2.7588- 1
2.0000+ 5 ~ 3.0000+ 5	5.8661+ 0	5.3315+ 0	1.4540- 1	3.8908- 1	3.3039- 1
3.0000+ 5 ~ 4.0000+ 5	5.9957+ 0	5.3839+ 0	1.3016- 1	4.8169- 1	3.7814- 1
4.0000+ 5 ~ 5.0000+ 5	6.1303+ 0	5.4594+ 0	1.2270- 1	5.4824- 1	4.0578- 1
5.0000+ 5 ~ 6.0000+ 5	6.2691+ 0	5.5440+ 0	1.2001- 1	6.0523- 1	4.2173- 1
6.0000+ 5 ~ 8.0000+ 5	6.4283+ 0	5.6046+ 0	1.1335- 1	7.1045- 1	4.3903- 1
8.0000+ 5 ~ 1.0000+ 6	6.5953+ 0	5.4564+ 0	8.5590- 2	1.0532+ 0	4.7152- 1
1.0000+ 5 ~ 1.5000+ 6	6.6165+ 0	5.1731+ 0	7.7559- 2	1.3658+ 0	5.2105- 1
1.5000+ 6 ~ 2.0000+ 6	6.3798+ 0	4.6308+ 0	6.6987- 2	1.6806+ 0	5.8910- 1
2.0000+ 6 ~ 3.0000+ 6	5.7307+ 0	3.7062+ 0	3.9736- 2	1.9797+ 0	6.5850- 1
3.0000+ 6 ~ 4.0000+ 6	4.9944+ 0	2.8370+ 0	1.8943- 2	2.1192+ 0	6.7268- 1
4.0000+ 6 ~ 5.0000+ 6	4.4858+ 0	2.3346+ 0	9.9531- 3	2.1267+ 0	5.5680- 1
5.0000+ 6 ~ 6.0000+ 6	4.3070+ 0	2.1798+ 0	5.0320- 3	2.1203+ 0	6.6490- 1
6.0000+ 6 ~ 8.0000+ 6	4.3650+ 0	2.2655+ 0	1.7674- 3	2.0958+ 0	7.0271- 1
8.0000+ 6 ~ 1.0000+ 7	4.5520+ 0	2.4919+ 0	5.2394- 4	2.0571+ 0	7.6547- 1
1.0000+ 7 ~ 1.5000+ 7	4.8026+ 0	2.8227+ 0	1.0269- 4	1.9793+ 0	8.5336- 1

MATERIAL =1541 CROSS SECTION XE-131

ENERGY	TOTAL	ELASTIC	CAPTURE	INELA	MU-BAR
1.0000- 5 ~ 1.0000- 2	2.7498+ 2	3.1326+ 0	2.7184+ 2		5.1332- 3
1.0000- 2 ~ 1.5000- 2	1.2935+ 2	3.1366+ 0	1.2625+ 2		5.1332- 3
1.5000- 2 ~ 2.0000- 2	1.0955+ 2	3.1393+ 0	1.0636+ 2		5.1332- 3
2.0000- 2 ~ 3.0000- 2	9.2505+ 1	3.1433+ 0	8.9390+ 1		5.1332- 3
3.0000- 2 ~ 4.0000- 2	7.8530+ 1	3.1487+ 0	7.5345+ 1		5.1332- 3
4.0000- 2 ~ 5.0000- 2	6.9691+ 1	3.1541+ 0	6.6556+ 1		5.1332- 3
5.0000- 2 ~ 6.0000- 2	6.3328+ 1	3.1595+ 0	6.0191+ 1		5.1332- 3
6.0000- 2 ~ 8.0000- 2	5.6666+ 1	3.1676+ 0	5.3473+ 1		5.1332- 3
8.0000- 2 ~ 1.0000- 1	5.0451+ 1	3.1784+ 0	4.7286+ 1		5.1332- 3
1.0000- 1 ~ 1.5000- 1	4.3562+ 1	3.1975+ 0	4.0362+ 1		5.1332- 3
1.5000- 1 ~ 2.0000- 1	3.7463+ 1	3.2251+ 0	3.4240+ 1		5.1332- 3
2.0000- 1 ~ 3.0000- 1	3.2190+ 1	3.2670+ 0	2.8922+ 1		5.1332- 3
3.0000- 1 ~ 4.0000- 1	2.7992+ 1	3.3239+ 0	2.4670+ 1		5.1332- 3
4.0000- 1 ~ 5.0000- 1	2.5340+ 1	3.3820+ 0	2.1967+ 1		5.1332- 3
5.0000- 1 ~ 6.0000- 1	2.3509+ 1	3.4414+ 0	2.0057+ 1		5.1332- 3
6.0000- 1 ~ 8.0000- 1	2.1675+ 1	3.5335+ 0	1.8130+ 1		5.1332- 3
8.0000- 1 ~ 1.0000+ 0	2.0025+ 1	3.6607+ 0	1.6338+ 1		5.1332- 3
1.0000+ 0 ~ 1.5000+ 0	1.8383+ 1	3.8998+ 0	1.4476+ 1		5.1332- 3
1.5000+ 0 ~ 2.0000+ 0	1.7296+ 1	4.2778+ 0	1.3000+ 1		5.1332- 3
2.0000+ 0 ~ 3.0000+ 0	1.6971+ 1	4.9529+ 0	1.2011+ 1		5.1332- 3
3.0000+ 0 ~ 4.0000+ 0	1.7904+ 1	6.1504+ 0	1.1718+ 1		5.1332- 3
4.0000+ 0 ~ 5.0000+ 0	1.9975+ 1	7.7871+ 0	1.2178+ 1		5.1332- 3
5.0000+ 0 ~ 6.0000+ 0	2.3419+ 1	1.0127+ 1	1.3286+ 1		5.1332- 3
6.0000+ 0 ~ 8.0000+ 0	3.2842+ 1	1.6192+ 1	1.6648+ 1		5.1332- 3
8.0000+ 0 ~ 1.0000+ 1	6.1701+ 1	3.4732+ 1	2.6969+ 1		5.1332- 3
1.0000+ 1 ~ 1.5000+ 1	7.0583+ 3	4.9180+ 3	2.1403+ 3		5.1348- 3
1.5000+ 1 ~ 2.0000+ 1	5.8803+ 2	4.2729+ 2	1.6074+ 2		5.1373- 3
2.0000+ 1 ~ 3.0000+ 1	3.1473+ 1	2.5510+ 1	5.9628+ 0		5.1409- 3
3.0000+ 1 ~ 4.0000+ 1	1.0567+ 1	8.8847+ 0	1.6817+ 0		5.1449- 3
4.0000+ 1 ~ 5.0000+ 1	6.8044+ 1	1.2628+ 1	5.5415+ 1		5.1480- 3
5.0000+ 1 ~ 6.0000+ 1	5.8555+ 0	4.9479+ 0	9.0701- 1		5.1523- 3
6.0000+ 1 ~ 8.0000+ 1	2.1579+ 1	4.5683+ 0	1.7010+ 1		5.1603- 3
8.0000+ 1 ~ 1.0000+ 2	2.7339+ 0	1.8515+ 0	8.8226- 1		5.1687- 3
1.0000+ 2 ~ 1.5000+ 2	2.2598+ 2	1.8422+ 2	4.1765+ 1		5.1866- 3
1.5000+ 2 ~ 2.0000+ 2	1.2299+ 1	6.7159+ 0	5.5830+ 0		5.2149- 3
2.0000+ 2 ~ 3.0000+ 2	3.2684+ 1	2.1628+ 1	1.1056+ 1		5.2629- 3
3.0000+ 2 ~ 4.0000+ 2	5.0902+ 0	3.8969+ 0	1.1931+ 0		5.3427- 3
4.0000+ 2 ~ 5.0000+ 2	5.9810+ 1	5.0525+ 1	9.2851+ 0		5.4202- 3
5.0000+ 2 ~ 6.0000+ 2	9.6863+ 0	7.0789+ 0	2.6073+ 0		5.5030- 3
6.0000+ 2 ~ 8.0000+ 2	1.8582+ 1	1.4192+ 1	4.3896+ 0		5.6405- 3
8.0000+ 2 ~ 1.0000+ 3	2.0407+ 1	1.6452+ 1	3.9508+ 0		5.8408- 3
1.0000+ 3 ~ 1.5000+ 3	1.7937+ 1	1.4842+ 1	3.0873+ 0		6.2307- 3
1.5000+ 3 ~ 2.0000+ 3	1.5707+ 1	1.3322+ 1	2.3823+ 0		6.8182- 3
2.0000+ 3 ~ 3.0000+ 3	1.3785+ 1	1.1940+ 1	1.8448+ 0		7.8028- 3
3.0000+ 3 ~ 4.0000+ 3	1.2243+ 1	1.0779+ 1	1.4595+ 0		9.4002- 3
4.0000+ 3 ~ 5.0000+ 3	1.1250+ 1	1.0010+ 1	1.2362+ 0		1.0931- 2
5.0000+ 3 ~ 6.0000+ 3	1.0544+ 1	9.4536+ 0	1.0890+ 0		1.2527- 2
6.0000+ 3 ~ 8.0000+ 3	9.8082+ 0	8.8615+ 0	9.4589- 1		1.5106- 2
8.0000+ 3 ~ 1.0000+ 4	9.1248+ 0	8.3047+ 0	8.1928- 1		1.8738- 2
1.0000+ 4 ~ 1.5000+ 4	8.3838+ 0	7.6958+ 0	6.8715- 1		2.5393- 2
1.5000+ 4 ~ 2.0000+ 4	7.7232+ 0	7.1515+ 0	5.7136- 1		3.4831- 2
2.0000+ 4 ~ 3.0000+ 4	7.1748+ 0	6.7025+ 0	4.7140- 1		4.9661- 2
3.0000+ 4 ~ 4.0000+ 4	6.7346+ 0	6.3445+ 0	3.8965- 1		6.8395- 2
4.0000+ 4 ~ 5.0000+ 4	6.4655+ 0	6.1276+ 0	3.3765- 1		8.6577- 2
5.0000+ 4 ~ 6.0000+ 4	6.2823+ 0	5.9806+ 0	3.0150- 1		1.0401- 1
6.0000+ 4 ~ 8.0000+ 4	6.0997+ 0	5.8345+ 0	2.6510- 1		1.2852- 1
8.0000+ 4 ~ 1.0000+ 5	5.9397+ 0	5.6335+ 0	2.2638- 1	7.9593- 2	1.6057- 1
1.0000+ 5 ~ 1.5000+ 5	5.8276+ 0	5.4675+ 0	1.9093- 1	1.6798- 1	2.0996- 1
1.5000+ 5 ~ 2.0000+ 5	5.7416+ 0	5.3501+ 0	1.6316- 1	2.2813- 1	2.6345- 1
2.0000+ 5 ~ 3.0000+ 5	5.7512+ 0	5.3254+ 0	1.4115- 1	2.8444- 1	3.1664- 1
3.0000+ 5 ~ 4.0000+ 5	5.7868+ 0	5.2740+ 0	1.1164- 1	4.0117- 1	3.7014- 1
4.0000+ 5 ~ 5.0000+ 5	6.0131+ 0	5.2038+ 0	8.6909- 2	7.2253- 1	4.0851- 1
5.0000+ 5 ~ 6.0000+ 5	6.1651+ 0	5.1942+ 0	7.2523- 2	8.9845- 1	4.3301- 1
6.0000+ 5 ~ 8.0000+ 5	6.3635+ 0	5.2013+ 0	5.8908- 2	1.1035+ 0	4.5763- 1
8.0000+ 5 ~ 1.0000+ 6	6.5815+ 0	5.1883+ 0	4.6743- 2	1.3466+ 0	4.8459- 1
1.0000+ 6 ~ 1.5000+ 6	6.6765+ 0	5.0177+ 0	3.8890- 2	1.6194+ 0	5.3491- 1
1.5000+ 6 ~ 2.0000+ 6	6.4737+ 0	4.5676+ 0	3.1815- 2	1.8733+ 0	6.0651- 1
2.0000+ 6 ~ 3.0000+ 6	5.8464+ 0	3.7411+ 0	2.2724- 2	2.0789+ 0	6.7215- 1
3.0000+ 6 ~ 4.0000+ 6	5.0837+ 0	2.8928+ 0	1.2528- 2	2.1611+ 0	6.8193- 1
4.0000+ 6 ~ 5.0000+ 6	4.5426+ 0	2.3762+ 0	6.8123- 3	2.1465+ 0	6.6301- 1
5.0000+ 6 ~ 6.0000+ 6	4.3439+ 0	2.2076+ 0	3.4883- 3	2.1316+ 0	6.6830- 1
6.0000+ 6 ~ 8.0000+ 6	4.3818+ 0	2.2700+ 0	1.2157- 3	2.1094+ 0	7.0224- 1
8.0000+ 6 ~ 1.0000+ 7	4.5497+ 0	2.4814+ 0	3.6928- 4	2.0654+ 0	7.6329- 1
1.0000+ 7 ~ 1.5000+ 7	4.8172+ 0	2.8251+ 0	7.2706- 5	1.9917+ 0	8.5266- 1

MATERIAL =1551 CROSS SECTION CS-133

ENERGY	TOTAL	ELASTIC	CAPTURE	INELA	MU-BAR
1.0000- 5 ~ 1.0000- 2	9.1437+ 1	2.0233+ 0	8.9418+ 1		5.0560- 3
1.0000- 2 ~ 1.5000- 2	4.3570+ 1	2.0229+ 0	4.1532+ 1		5.0560- 3
1.5000- 2 ~ 2.0000- 2	3.7053+ 1	2.0226+ 0	3.5050+ 1		5.0560- 3
2.0000- 2 ~ 3.0000- 2	3.1467+ 1	2.0221+ 0	2.9434+ 1		5.0560- 3
3.0000- 2 ~ 4.0000- 2	2.6872+ 1	2.0216+ 0	2.4864+ 1		5.0560- 3
4.0000- 2 ~ 5.0000- 2	2.3987+ 1	2.0210+ 0	2.1956+ 1		5.0560- 3
5.0000- 2 ~ 6.0000- 2	2.1887+ 1	2.0204+ 0	1.9861+ 1		5.0560- 3
6.0000- 2 ~ 8.0000- 2	1.9795+ 1	2.0195+ 0	1.7695+ 1		5.0560- 3
8.0000- 2 ~ 1.0000- 1	1.7681+ 1	2.0183+ 0	1.5655+ 1		5.0560- 3
1.0000- 1 ~ 1.5000- 1	1.5414+ 1	2.0162+ 0	1.3399+ 1		5.0560- 3
1.5000- 1 ~ 2.0000- 1	1.3441+ 1	2.0131+ 0	1.1427+ 1		5.0560- 3
2.0000- 1 ~ 3.0000- 1	1.1713+ 1	2.0083+ 0	9.7050+ 0		5.0560- 3
3.0000- 1 ~ 4.0000- 1	1.0367+ 1	2.0017+ 0	8.3640+ 0		5.0560- 3
4.0000- 1 ~ 5.0000- 1	9.5057+ 0	1.9949+ 0	7.5102+ 0		5.0560- 3
5.0000- 1 ~ 6.0000- 1	8.9227+ 0	1.9878+ 0	6.9366+ 0		5.0560- 3
6.0000- 1 ~ 8.0000- 1	8.3558+ 0	1.9764+ 0	6.3788+ 0		5.0560- 3
8.0000- 1 ~ 1.0000+ 0	7.8453+ 0	1.9602+ 0	5.8847+ 0		5.0560- 3
1.0000+ 0 ~ 1.5000+ 0	7.4276+ 0	1.9276+ 0	5.4997+ 0		5.0560- 3
1.5000+ 0 ~ 2.0000+ 0	7.2797+ 0	1.8723+ 0	5.4075+ 0		5.0560- 3
2.0000+ 0 ~ 3.0000+ 0	7.9009+ 0	1.7588+ 0	6.1385+ 0		5.0560- 3
3.0000+ 0 ~ 4.0000+ 0	1.0937+ 1	1.5562+ 0	9.3751+ 0		5.0560- 3
4.0000+ 0 ~ 5.0000+ 0	2.5568+ 1	1.3670+ 0	2.4200+ 1		5.0560- 3
5.0000+ 0 ~ 6.0000+ 0	1.5411+ 3	7.5121+ 1	1.4660+ 3		5.0560- 3
6.0000+ 0 ~ 8.0000+ 0	1.6084+ 2	1.4584+ 1	1.4625+ 2		5.0560- 3
8.0000+ 0 ~ 1.0000+ 1	7.6577+ 0	3.5177+ 0	4.1388+ 0		5.0560- 3
1.0000+ 1 ~ 1.5000+ 1	4.2234+ 0	2.7958+ 0	1.4262+ 0		5.0575- 3
1.5000+ 1 ~ 2.0000+ 1	3.6695+ 0	2.3405+ 0	1.3266+ 0		5.0598- 3
2.0000+ 1 ~ 3.0000+ 1	6.2883+ 1	6.2241+ 0	5.6658+ 1		5.0631- 3
3.0000+ 1 ~ 4.0000+ 1	3.0484+ 0	2.4554+ 0	5.9222- 1		5.0668- 3
4.0000+ 1 ~ 5.0000+ 1	8.3782+ 1	1.3006+ 1	7.0776+ 1		5.0696- 3
5.0000+ 1 ~ 6.0000+ 1	4.2394+ 0	3.2783+ 0	9.6002- 1		5.0735- 3
6.0000+ 1 ~ 8.0000+ 1	2.8708+ 0	2.4905+ 0	3.7968- 1		5.0807- 3
8.0000+ 1 ~ 1.0000+ 2	3.4436+ 1	6.2448+ 0	2.8191+ 1		5.0882- 3
1.0000+ 2 ~ 1.5000+ 2	4.9034+ 1	2.0469+ 1	2.8564+ 1		5.1043- 3
1.5000+ 2 ~ 2.0000+ 2	3.5544+ 0	2.5867+ 0	9.6751- 1		5.1297- 3
2.0000+ 2 ~ 3.0000+ 2	5.4983+ 1	3.6102+ 1	1.8882+ 1		5.1725- 3
3.0000+ 2 ~ 4.0000+ 2	5.9686+ 0	3.7706+ 0	2.1979+ 0		5.2437- 3
4.0000+ 2 ~ 5.0000+ 2	2.7664+ 1	1.6986+ 1	1.0678+ 1		5.3126- 3
5.0000+ 2 ~ 6.0000+ 2	2.2669+ 1	1.3085+ 1	9.5841+ 0		5.3863- 3
6.0000+ 2 ~ 8.0000+ 2	1.0978+ 1	7.6359+ 0	3.3424+ 0		5.5087- 3
8.0000+ 2 ~ 1.0000+ 3	8.9508+ 0	6.0387+ 0	2.9120+ 0		5.6873- 3
1.0000+ 3 ~ 1.5000+ 3	1.5312+ 1	1.1495+ 1	3.8171+ 0		6.0353- 3
1.5000+ 3 ~ 2.0000+ 3	1.7552+ 1	1.4436+ 1	3.1124+ 0		6.5606- 3
2.0000+ 3 ~ 3.0000+ 3	1.5297+ 1	1.2905+ 1	2.3913+ 0		7.4445- 3
3.0000+ 3 ~ 4.0000+ 3	1.3478+ 1	1.1602+ 1	1.8707+ 0		8.8891- 3
4.0000+ 3 ~ 5.0000+ 3	1.2307+ 1	1.0734+ 1	1.5693+ 0		1.0278- 2
5.0000+ 3 ~ 6.0000+ 3	1.1475+ 1	1.0102+ 1	1.3716+ 0		1.1733- 2
6.0000+ 3 ~ 8.0000+ 3	1.0605+ 1	9.4237+ 0	1.1804+ 0		1.4100- 2
8.0000+ 3 ~ 1.0000+ 4	9.7936+ 0	8.7788+ 0	1.0137+ 0		1.7455- 2
1.0000+ 4 ~ 1.5000+ 4	8.9092+ 0	8.0645+ 0	8.4369- 1		2.3665- 2
1.5000+ 4 ~ 2.0000+ 4	8.1170+ 0	7.4184+ 0	6.9821- 1		3.2551- 2
2.0000+ 4 ~ 3.0000+ 4	7.4515+ 0	6.8747+ 0	5.7600- 1		4.6688- 2
3.0000+ 4 ~ 4.0000+ 4	6.9132+ 0	6.4358+ 0	4.7705- 1		6.4700- 2
4.0000+ 4 ~ 5.0000+ 4	6.5799+ 0	6.1654+ 0	4.1426- 1		8.2323- 2
5.0000+ 4 ~ 6.0000+ 4	6.3505+ 0	5.9799+ 0	3.7044- 1		9.9314- 2
6.0000+ 4 ~ 8.0000+ 4	6.1187+ 0	5.7928+ 0	3.2577- 1		1.2333- 1
8.0000+ 4 ~ 1.0000+ 5	5.9096+ 0	5.5383+ 0	2.7330- 1	9.7706- 2	1.5530- 1
1.0000+ 5 ~ 1.5000+ 5	5.7201+ 0	5.2986+ 0	2.2154- 1	1.9813- 1	2.0622- 1
1.5000+ 5 ~ 2.0000+ 5	5.5849+ 0	5.1051+ 0	1.8133- 1	2.9802- 1	2.6198- 1
2.0000+ 5 ~ 3.0000+ 5	5.6185+ 0	5.0171+ 0	1.5268- 1	4.4846- 1	3.1825- 1
3.0000+ 5 ~ 4.0000+ 5	5.7208+ 0	5.0565+ 0	1.3442- 1	5.2987- 1	3.6531- 1
4.0000+ 5 ~ 5.0000+ 5	5.8897+ 0	5.1621+ 0	1.2587- 1	6.0179- 1	3.9110- 1
5.0000+ 5 ~ 6.0000+ 5	6.0693+ 0	5.2792+ 0	1.2237- 1	6.6797- 1	4.0622- 1
6.0000+ 5 ~ 8.0000+ 5	6.2857+ 0	5.3026+ 0	9.3932- 2	8.8921- 1	4.3151- 1
8.0000+ 5 ~ 1.0000+ 6	6.5571+ 0	5.1778+ 0	6.6935- 2	1.3123+ 0	4.7271- 1
1.0000+ 6 ~ 1.5000+ 6	6.7324+ 0	4.9857+ 0	4.9445- 2	1.6968+ 0	5.3628- 1
1.5000+ 6 ~ 2.0000+ 6	6.5865+ 0	4.5784+ 0	3.5142- 2	1.9721+ 0	6.1639- 1
2.0000+ 6 ~ 3.0000+ 6	5.9793+ 0	3.8117+ 0	2.2389- 2	2.1421+ 0	6.8265- 1
3.0000+ 6 ~ 4.0000+ 6	5.1863+ 0	2.9688+ 0	1.1679- 2	2.1890+ 0	6.9007- 1
4.0000+ 6 ~ 5.0000+ 6	4.6112+ 0	2.4311+ 0	6.3901- 3	2.1610+ 0	6.6911- 1
5.0000+ 6 ~ 6.0000+ 6	4.3895+ 0	2.2440+ 0	3.2619- 3	2.1413+ 0	6.7191- 1
6.0000+ 6 ~ 8.0000+ 6	4.4009+ 0	2.2773+ 0	1.1187- 3	2.1216+ 0	7.0176- 1
8.0000+ 6 ~ 1.0000+ 7	4.5462+ 0	2.4695+ 0	3.3068- 4	2.0737+ 0	7.6091- 1
1.0000+ 7 ~ 1.5000+ 7	4.8356+ 0	2.8272+ 0	6.3678- 5	2.0080+ 0	8.5178- 1

CROSS SECTION

MATERIAL =1552 CS-135

ENERGY	TOTAL	ELASTIC	CAPTURE	INELA	MU-BAR
1.0000- 5 ~ 1.0000- 2	3.0286+ 1	3.3980+ 0	2.6826+ 1		4.9811- 3
1.0000- 2 ~ 1.5000- 2	1.5862+ 1	3.3980+ 0	1.2439+ 1		4.9811- 3
1.5000- 2 ~ 2.0000- 2	1.3912+ 1	3.3980+ 0	1.0487+ 1		4.9811- 3
2.0000- 2 ~ 3.0000- 2	1.2216+ 1	3.3980+ 0	8.7957+ 0		4.9811- 3
3.0000- 2 ~ 4.0000- 2	1.0838+ 1	3.3980+ 0	7.4150+ 0		4.9811- 3
4.0000- 2 ~ 5.0000- 2	9.9612+ 0	3.3980+ 0	6.5328+ 0		4.9811- 3
5.0000- 2 ~ 6.0000- 2	9.3147+ 0	3.3980+ 0	5.9059+ 0		4.9811- 3
6.0000- 2 ~ 8.0000- 2	8.6628+ 0	3.3980+ 0	5.2432+ 0		4.9811- 3
8.0000- 2 ~ 1.0000- 1	8.0441+ 0	3.3980+ 0	4.6193+ 0		4.9811- 3
1.0000- 1 ~ 1.5000- 1	7.3450+ 0	3.3980+ 0	3.9335+ 0		4.9811- 3
1.5000- 1 ~ 2.0000- 1	6.7373+ 0	3.3980+ 0	3.3160+ 0		4.9811- 3
2.0000- 1 ~ 3.0000- 1	6.1906+ 0	3.3980+ 0	2.7814+ 0		4.9811- 3
3.0000- 1 ~ 4.0000- 1	5.7621+ 0	3.3980+ 0	2.3448+ 0		4.9811- 3
4.0000- 1 ~ 5.0000- 1	5.4700+ 0	3.3980+ 0	2.0658+ 0		4.9811- 3
5.0000- 1 ~ 6.0000- 1	5.2777+ 0	3.3980+ 0	1.8675+ 0		4.9811- 3
6.0000- 1 ~ 8.0000- 1	5.0715+ 0	3.3980+ 0	1.6580+ 0		4.9811- 3
8.0000- 1 ~ 1.0000+ 0	4.8637+ 0	3.3980+ 0	1.4607+ 0		4.9811- 3
1.0000+ 0 ~ 1.5000+ 0	4.6533+ 0	3.3980+ 0	1.2438+ 0		4.9811- 3
1.5000+ 0 ~ 2.0000+ 0	4.4517+ 0	3.3980+ 0	1.0486+ 0		4.9811- 3
2.0000+ 0 ~ 3.0000+ 0	4.2863+ 0	3.3980+ 0	8.7951- 1		4.9811- 3
3.0000+ 0 ~ 4.0000+ 0	4.1434+ 0	3.3980+ 0	7.4146- 1		4.9811- 3
4.0000+ 0 ~ 5.0000+ 0	4.0570+ 0	3.3980+ 0	6.5324- 1		4.9811- 3
5.0000+ 0 ~ 6.0000+ 0	3.9959+ 0	3.3980+ 0	5.9055- 1		4.9811- 3
6.0000+ 0 ~ 8.0000+ 0	3.9253+ 0	3.3980+ 0	5.2429- 1		4.9811- 3
8.0000+ 0 ~ 1.0000+ 1	3.8642+ 0	3.3980+ 0	4.6190- 1		4.9811- 3
1.0000+ 1 ~ 1.5000+ 1	3.7951+ 0	3.3980+ 0	3.9332- 1		4.9819- 3
1.5000+ 1 ~ 2.0000+ 1	3.7322+ 0	3.3980+ 0	3.3158- 1		4.9832- 3
2.0000+ 1 ~ 3.0000+ 1	3.6789+ 0	3.3980+ 0	2.7812- 1		4.9853- 3
3.0000+ 1 ~ 4.0000+ 1	1.1554+ 2	7.4366+ 1	4.1057+ 1		4.9876- 3
4.0000+ 1 ~ 5.0000+ 1	1.0236+ 2	6.8417+ 1	3.3856+ 1		4.9894- 3
5.0000+ 1 ~ 6.0000+ 1	9.2928+ 1	6.3873+ 1	2.8961+ 1		4.9921- 3
6.0000+ 1 ~ 8.0000+ 1	8.2887+ 1	5.8699+ 1	2.4006+ 1		4.9969- 3
8.0000+ 1 ~ 1.0000+ 2	7.3392+ 1	5.3662+ 1	1.9646+ 1		5.0021- 3
1.0000+ 2 ~ 1.5000+ 2	6.2966+ 1	4.7736+ 1	1.5199+ 1		5.0135- 3
1.5000+ 2 ~ 2.0000+ 2	5.3585+ 1	4.2065+ 1	1.1507+ 1		5.0317- 3
2.0000+ 2 ~ 3.0000+ 2	4.5465+ 1	3.6835+ 1	8.6257+ 0		5.0634- 3
3.0000+ 2 ~ 4.0000+ 2	3.8856+ 1	3.2339+ 1	6.4924+ 0		5.1176- 3
4.0000+ 2 ~ 5.0000+ 2	3.4622+ 1	2.9347+ 1	5.2561+ 0		5.1708- 3
5.0000+ 2 ~ 6.0000+ 2	3.1609+ 1	2.7159+ 1	4.4430+ 0		5.2284- 3
6.0000+ 2 ~ 8.0000+ 2	2.8429+ 1	2.4776+ 1	3.6472+ 0		5.3254- 3
8.0000+ 2 ~ 1.0000+ 3	2.5442+ 1	2.2478+ 1	2.9573+ 0		5.4688- 3
1.0000+ 3 ~ 1.5000+ 3	2.2160+ 1	1.9875+ 1	2.2796+ 0		5.7532- 3
1.5000+ 3 ~ 2.0000+ 3	1.9203+ 1	1.7465+ 1	1.7357+ 0		6.1884- 3
2.0000+ 3 ~ 3.0000+ 3	1.6649+ 1	1.5320+ 1	1.3290+ 0		6.9330- 3
3.0000+ 3 ~ 4.0000+ 3	1.4584+ 1	1.3540+ 1	1.0414+ 0		8.1716- 3
4.0000+ 3 ~ 5.0000+ 3	1.3255+ 1	1.2378+ 1	8.7607- 1		9.3704- 3
5.0000+ 3 ~ 6.0000+ 3	1.2311+ 1	1.1543+ 1	7.6736- 1		1.0638- 2
6.0000+ 3 ~ 8.0000+ 3	1.1321+ 1	1.0659+ 1	6.6169- 1		1.2716- 2
8.0000+ 3 ~ 1.0000+ 4	1.0396+ 1	9.8275+ 0	5.6766- 1		1.5685- 2
1.0000+ 4 ~ 1.5000+ 4	9.3845+ 0	8.9149+ 0	4.6904- 1		2.1241- 2
1.5000+ 4 ~ 2.0000+ 4	8.4766+ 0	8.0935+ 0	3.8281- 1		2.9266- 2
2.0000+ 4 ~ 3.0000+ 4	7.7086+ 0	7.3985+ 0	3.0949- 1		4.2229- 2
3.0000+ 4 ~ 4.0000+ 4	7.0846+ 0	6.8332+ 0	2.5116- 1		5.8936- 2
4.0000+ 4 ~ 5.0000+ 4	6.6956+ 0	6.4801+ 0	2.1537- 1		7.5472- 2
5.0000+ 4 ~ 6.0000+ 4	6.4263+ 0	6.2350+ 0	1.9121- 1		9.1559- 2
6.0000+ 4 ~ 8.0000+ 4	6.1520+ 0	5.9846+ 0	1.6739- 1		1.1448- 1
8.0000+ 4 ~ 1.0000+ 5	5.9086+ 0	5.7619+ 0	1.4679- 1		1.4282- 1
1.0000+ 5 ~ 1.5000+ 5	5.7162+ 0	5.5884+ 0	1.2706- 1		1.8633- 1
1.5000+ 5 ~ 2.0000+ 5	5.5580+ 0	5.4477+ 0	1.0985- 1		2.3395- 1
2.0000+ 5 ~ 3.0000+ 5	5.4752+ 0	5.3448+ 0	9.2049- 2	3.8172- 2	2.8512- 1
3.0000+ 5 ~ 4.0000+ 5	5.6220+ 0	5.3403+ 0	7.7757- 2	2.0410- 1	3.3010- 1
4.0000+ 5 ~ 5.0000+ 5	5.7944+ 0	5.4294+ 0	7.0666- 2	2.9454- 1	3.5547- 1
5.0000+ 5 ~ 6.0000+ 5	5.9925+ 0	5.5498+ 0	6.7368- 2	3.7566- 1	3.7056- 1
6.0000+ 5 ~ 8.0000+ 5	6.2531+ 0	5.6741+ 0	6.4378- 2	5.1478- 1	3.8937- 1
8.0000+ 5 ~ 1.0000+ 6	6.5643+ 0	5.7040+ 0	5.4026- 2	8.0639- 1	4.1931- 1
1.0000+ 6 ~ 1.5000+ 6	6.7733+ 0	5.5576+ 0	4.6217- 2	1.1685+ 0	4.7995- 1
1.5000+ 6 ~ 2.0000+ 6	6.6780+ 0	4.9012+ 0	2.5896- 2	1.7484+ 0	5.8526- 1
2.0000+ 6 ~ 3.0000+ 6	6.0830+ 0	3.9446+ 0	1.1414- 2	2.1229+ 0	6.7804- 1
3.0000+ 6 ~ 4.0000+ 6	5.2656+ 0	3.0460+ 0	5.4846- 3	2.1969+ 0	6.9242- 1
4.0000+ 6 ~ 5.0000+ 6	4.6650+ 0	2.4808+ 0	3.2614- 3	2.1678+ 0	6.7217- 1
5.0000+ 6 ~ 6.0000+ 6	4.4244+ 0	2.2744+ 0	1.8782- 3	2.1479+ 0	6.7407- 1
6.0000+ 6 ~ 8.0000+ 6	4.4120+ 0	2.2823+ 0	8.0585- 4	2.1286+ 0	7.0082- 1
8.0000+ 6 ~ 1.0000+ 7	4.5391+ 0	2.4580+ 0	2.8700- 4	2.0782+ 0	7.5854- 1
1.0000+ 7 ~ 1.5000+ 7	4.8482+ 0	2.8269+ 0	7.7365- 5	2.0210+ 0	8.5080- 1

CROSS SECTION

MATERIAL =1553 CS-137

ENERGY	TOTAL	ELASTIC	CAPTURE	INELA	MU-BAR
1.0000- 5 ~ 1.0000- 2	3.5470+ 0	3.2050+ 0	3.3922- 1		4.9083- 3
1.0000- 2 ~ 1.5000- 2	3.3643+ 0	3.2050+ 0	1.5730- 1		4.9083- 3
1.5000- 2 ~ 2.0000- 2	3.3383+ 0	3.2050+ 0	1.3261- 1		4.9083- 3
2.0000- 2 ~ 3.0000- 2	3.3177+ 0	3.2050+ 0	1.1123- 1		4.9083- 3
3.0000- 2 ~ 4.0000- 2	3.2993+ 0	3.2050+ 0	9.3767- 2		4.9083- 3
4.0000- 2 ~ 5.0000- 2	3.2887+ 0	3.2050+ 0	8.2611- 2		4.9083- 3
5.0000- 2 ~ 6.0000- 2	3.2806+ 0	3.2050+ 0	7.4684- 2		4.9083- 3
6.0000- 2 ~ 8.0000- 2	3.2717+ 0	3.2050+ 0	6.6304- 2		4.9083- 3
8.0000- 2 ~ 1.0000- 1	3.2642+ 0	3.2050+ 0	5.8415- 2		4.9083- 3
1.0000- 1 ~ 1.5000- 1	3.2551+ 0	3.2050+ 0	4.9742- 2		4.9083- 3
1.5000- 1 ~ 2.0000- 1	3.2475+ 0	3.2050+ 0	4.1934- 2		4.9083- 3
2.0000- 1 ~ 3.0000- 1	3.2404+ 0	3.2050+ 0	3.5173- 2		4.9083- 3
3.0000- 1 ~ 4.0000- 1	3.2350+ 0	3.2050+ 0	2.9652- 2		4.9083- 3
4.0000- 1 ~ 5.0000- 1	3.2314+ 0	3.2050+ 0	2.6124- 2		4.9083- 3
5.0000- 1 ~ 6.0000- 1	3.2287+ 0	3.2050+ 0	2.3617- 2		4.9083- 3
6.0000- 1 ~ 8.0000- 1	3.2262+ 0	3.2050+ 0	2.0967- 2		4.9083- 3
8.0000- 1 ~ 1.0000+ 0	3.2237+ 0	3.2050+ 0	1.8472- 2		4.9083- 3
1.0000+ 0 ~ 1.5000+ 0	3.2209+ 0	3.2050+ 0	1.5730- 2		4.9083- 3
1.5000+ 0 ~ 2.0000+ 0	3.2184+ 0	3.2050+ 0	1.3261- 2		4.9083- 3
2.0000+ 0 ~ 3.0000+ 0	3.2162+ 0	3.2050+ 0	1.1123- 2		4.9083- 3
3.0000+ 0 ~ 4.0000+ 0	3.2145+ 0	3.2050+ 0	9.3768- 3		4.9083- 3
4.0000+ 0 ~ 5.0000+ 0	3.2133+ 0	3.2050+ 0	8.2611- 3		4.9083- 3
5.0000+ 0 ~ 6.0000+ 0	3.2126+ 0	3.2050+ 0	7.4684- 3		4.9083- 3
6.0000+ 0 ~ 8.0000+ 0	3.2117+ 0	3.2050+ 0	6.6304- 3		4.9083- 3
8.0000+ 0 ~ 1.0000+ 1	3.2109+ 0	3.2050+ 0	5.8415- 3		4.9083- 3
1.0000+ 1 ~ 1.5000+ 1	3.2100+ 0	3.2050+ 0	4.9742- 3		4.9083- 3
1.5000+ 1 ~ 2.0000+ 1	3.2092+ 0	3.2050+ 0	4.1935- 3		4.9083- 3
2.0000+ 1 ~ 3.0000+ 1	3.2086+ 0	3.2050+ 0	3.5173- 3		4.9096- 3
3.0000+ 1 ~ 4.0000+ 1	3.2080+ 0	3.2050+ 0	2.9652- 3		4.9116- 3
4.0000+ 1 ~ 5.0000+ 1	3.2076+ 0	3.2050+ 0	2.6124- 3		4.9131- 3
5.0000+ 1 ~ 6.0000+ 1	3.2074+ 0	3.2050+ 0	2.3617- 3		4.9151- 3
6.0000+ 1 ~ 8.0000+ 1	3.2071+ 0	3.2050+ 0	2.0967- 3		4.9184- 3
8.0000+ 1 ~ 1.0000+ 2	3.2069+ 0	3.2050+ 0	1.8473- 3		4.9220- 3
1.0000+ 2 ~ 1.5000+ 2	3.2066+ 0	3.2050+ 0	1.5730- 3		4.9300- 3
1.5000+ 2 ~ 2.0000+ 2	3.2063+ 0	3.2050+ 0	1.3261- 3		4.9433- 3
2.0000+ 2 ~ 3.0000+ 2	3.2061+ 0	3.2050+ 0	1.1123- 3		4.9670- 3
3.0000+ 2 ~ 4.0000+ 2	3.2060+ 0	3.2050+ 0	9.3769- 4		5.0086- 3
4.0000+ 2 ~ 5.0000+ 2	3.2058+ 0	3.2050+ 0	8.2612- 4		5.0498- 3
5.0000+ 2 ~ 6.0000+ 2	1.8971+ 1	1.8791+ 1	1.7997- 1		5.0951- 3
6.0000+ 2 ~ 8.0000+ 2	3.1838+ 1	3.1527+ 1	3.1146- 1		5.1723- 3
8.0000+ 2 ~ 1.0000+ 3	2.8424+ 1	2.8164+ 1	2.5984- 1		5.2878- 3
1.0000+ 3 ~ 1.5000+ 3	2.4672+ 1	2.4463+ 1	2.0860- 1		5.5201- 3
1.5000+ 3 ~ 2.0000+ 3	2.1291+ 1	2.1125+ 1	1.6590- 1		5.8795- 3
2.0000+ 3 ~ 3.0000+ 3	1.8368+ 1	1.8237+ 1	1.3116- 1		6.5024- 3
3.0000+ 3 ~ 4.0000+ 3	1.6001+ 1	1.5897+ 1	1.0347- 1		7.5525- 3
4.0000+ 3 ~ 5.0000+ 3	1.4478+ 1	1.4392+ 1	8.6350- 2		8.5744- 3
5.0000+ 3 ~ 6.0000+ 3	1.3395+ 1	1.3321+ 1	7.4726- 2		9.6633- 3
6.0000+ 3 ~ 8.0000+ 3	1.2258+ 1	1.2195+ 1	6.2907- 2		1.1461- 2
8.0000+ 3 ~ 1.0000+ 4	1.1193+ 1	1.1141+ 1	5.2036- 2		1.4052- 2
1.0000+ 4 ~ 1.5000+ 4	1.0027+ 1	9.9860+ 0	4.0966- 2		1.8957- 2
1.5000+ 4 ~ 2.0000+ 4	8.9777+ 0	8.9458+ 0	3.1926- 2		2.6121- 2
2.0000+ 4 ~ 3.0000+ 4	8.0846+ 0	8.0594+ 0	2.5167- 2		3.7888- 2
3.0000+ 4 ~ 4.0000+ 4	7.3566+ 0	7.3364+ 0	2.0208- 2		5.3237- 2
4.0000+ 4 ~ 5.0000+ 4	6.9000+ 0	6.8827+ 0	1.7276- 2		6.6605- 2
5.0000+ 4 ~ 6.0000+ 4	6.5821+ 0	6.5668+ 0	1.5250- 2		8.3684- 2
6.0000+ 4 ~ 8.0000+ 4	6.2560+ 0	6.2429+ 0	1.3126- 2		1.0535- 1
8.0000+ 4 ~ 1.0000+ 5	5.9641+ 0	5.9528+ 0	1.1256- 2		1.3232- 1
1.0000+ 5 ~ 1.5000+ 5	5.7241+ 0	5.7147+ 0	9.3909- 3		1.7427- 1
1.5000+ 5 ~ 2.0000+ 5	5.5227+ 0	5.5148+ 0	7.7924- 3		2.2033- 1
2.0000+ 5 ~ 3.0000+ 5	5.4550+ 0	5.4483+ 0	6.7544- 3		2.6578- 1
3.0000+ 5 ~ 4.0000+ 5	5.5476+ 0	5.5414+ 0	6.2472- 3		3.0267- 1
4.0000+ 5 ~ 5.0000+ 5	5.6931+ 0	5.6619+ 0	6.0391- 3	2.5245- 2	3.2513- 1
5.0000+ 5 ~ 6.0000+ 5	5.9396+ 0	5.7683+ 0	5.9674- 3	1.6572- 1	3.4126- 1
6.0000+ 5 ~ 8.0000+ 5	6.2452+ 0	5.9716+ 0	6.2096- 3	2.6765- 1	3.5704- 1
8.0000+ 5 ~ 1.0000+ 6	6.5663+ 0	6.1763+ 0	6.7247- 3	3.8331- 1	3.7876- 1
1.0000+ 6 ~ 1.5000+ 6	6.8389+ 0	6.1761+ 0	7.9487- 3	6.5484- 1	4.3084- 1
1.5000+ 6 ~ 2.0000+ 6	6.7597+ 0	5.8469+ 0	9.9537- 3	9.0249- 1	4.9794- 1
2.0000+ 6 ~ 3.0000+ 6	6.1260+ 0	4.6686+ 0	5.8341- 3	1.4433+ 0	5.9209- 1
3.0000+ 6 ~ 4.0000+ 6	5.3475+ 0	3.2890+ 0	1.7578- 3	2.0202+ 0	6.6104- 1
4.0000+ 6 ~ 5.0000+ 6	4.7249+ 0	2.5837+ 0	8.6382- 4	2.1126+ 0	6.6324- 1
5.0000+ 6 ~ 6.0000+ 6	4.4664+ 0	2.3191+ 0	4.9088- 4	2.1468+ 0	6.7421- 1
6.0000+ 6 ~ 8.0000+ 6	4.4292+ 0	2.2950+ 0	2.5572- 4	2.1340+ 0	6.9974- 1
8.0000+ 6 ~ 1.0000+ 7	4.5374+ 0	2.4492+ 0	1.1580- 4	2.0855+ 0	7.5684- 1
1.0000+ 7 ~ 1.5000+ 7	4.8654+ 0	2.8278+ 0	4.0635- 5	2.0373+ 0	8.5000- 1

MATERIAL =1601 CROSS SECTION NO-143

ENERGY	TOTAL	ELASTIC	CAPTURE	INELA	MU-BAR
1.0000- 5 ~ 1.0000- 2	1.0497+ 3	3.6804+ 1	1.0130+ 3		4.7024- 3
1.0000- 2 ~ 1.5000- 2	5.0546+ 2	3.6709+ 1	4.6883+ 2		4.7024- 3
1.5000- 2 ~ 2.0000- 2	4.3057+ 2	3.6646+ 1	3.9392+ 2		4.7024- 3
2.0000- 2 ~ 3.0000- 2	3.6675+ 2	3.6551+ 1	3.3025+ 2		4.7024- 3
3.0000- 2 ~ 4.0000- 2	3.1345+ 2	3.6426+ 1	2.7705+ 2		4.7024- 3
4.0000- 2 ~ 5.0000- 2	2.8028+ 2	3.6302+ 1	2.4405+ 2		4.7024- 3
5.0000- 2 ~ 6.0000- 2	2.5561+ 2	3.6178+ 1	2.1946+ 2		4.7024- 3
6.0000- 2 ~ 8.0000- 2	2.2979+ 2	3.5994+ 1	1.9382+ 2		4.7024- 3
8.0000- 2 ~ 1.0000- 1	2.0592+ 2	3.5751+ 1	1.7023+ 2		4.7024- 3
1.0000- 1 ~ 1.5000- 1	1.7838+ 2	3.5331+ 1	1.4308+ 2		4.7024- 3
1.5000- 1 ~ 2.0000- 1	1.5377+ 2	3.4745+ 1	1.1905+ 2		4.7024- 3
2.0000- 1 ~ 3.0000- 1	1.3138+ 2	3.3894+ 1	9.7493+ 1		4.7024- 3
3.0000- 1 ~ 4.0000- 1	1.1278+ 2	3.2810+ 1	7.9985+ 1		4.7024- 3
4.0000- 1 ~ 5.0000- 1	1.0015+ 2	3.1776+ 1	6.8365+ 1		4.7024- 3
5.0000- 1 ~ 6.0000- 1	9.0800+ 1	3.0793+ 1	6.0003+ 1		4.7024- 3
6.0000- 1 ~ 8.0000- 1	8.0500+ 1	2.9413+ 1	5.1083+ 1		4.7024- 3
8.0000- 1 ~ 1.0000+ 0	7.0457+ 1	2.7725+ 1	4.2723+ 1		4.7024- 3
1.0000+ 0 ~ 1.5000+ 0	5.8492+ 1	2.5152+ 1	3.3317+ 1		4.7024- 3
1.5000+ 0 ~ 2.0000+ 0	4.7051+ 1	2.2112+ 1	2.4931+ 1		4.7024- 3
2.0000+ 0 ~ 3.0000+ 0	3.6370+ 1	1.8499+ 1	1.7848+ 1		4.7024- 3
3.0000+ 0 ~ 4.0000+ 0	2.7143+ 1	1.4744+ 1	1.2387+ 1		4.7024- 3
4.0000+ 0 ~ 5.0000+ 0	2.1384+ 1	1.2146+ 1	9.2295+ 0		4.7024- 3
5.0000+ 0 ~ 6.0000+ 0	1.7360+ 1	1.0131+ 1	7.2286+ 0		4.7024- 3
6.0000+ 0 ~ 8.0000+ 0	1.3328+ 1	7.9689+ 0	5.3429+ 0		4.7024- 3
8.0000+ 0 ~ 1.0000+ 1	9.8360+ 0	5.9996+ 0	3.8305+ 0		4.7024- 3
1.0000+ 1 ~ 1.5000+ 1	6.5402+ 0	4.0022+ 0	2.5345+ 0		4.7024- 3
1.5000+ 1 ~ 2.0000+ 1	4.1222+ 0	2.4607+ 0	1.6605+ 0		4.7024- 3
2.0000+ 1 ~ 3.0000+ 1	2.5687+ 0	1.4249+ 0	1.1428+ 0		4.7034- 3
3.0000+ 1 ~ 4.0000+ 1	1.6890+ 0	8.1637- 1	8.6786- 1		4.7049- 3
4.0000+ 1 ~ 5.0000+ 1	1.6154+ 0	6.9711- 1	9.1825- 1		4.7060- 3
5.0000+ 1 ~ 6.0000+ 1	1.5440+ 2	5.0475+ 1	1.0393+ 2		4.7074- 3
6.0000+ 1 ~ 8.0000+ 1	9.6589- 1	2.8258- 1	6.8325- 1		4.7098- 3
8.0000+ 1 ~ 1.0000+ 2	1.2643+ 0	7.1648- 1	5.4784- 1		4.7123- 3
1.0000+ 2 ~ 1.5000+ 2	1.3424+ 2	1.0870+ 2	2.5540+ 1		4.7179- 3
1.5000+ 2 ~ 2.0000+ 2	7.8154+ 2	7.2784+ 2	5.3701+ 1		4.7270- 3
2.0000+ 2 ~ 3.0000+ 2	6.5182+ 0	5.9578+ 0	5.6038- 1		4.7430- 3
3.0000+ 2 ~ 4.0000+ 2	1.9932+ 2	1.8305+ 2	1.6271+ 1		4.7710- 3
4.0000+ 2 ~ 5.0000+ 2	1.7221+ 2	1.6205+ 2	1.0160+ 1		4.7987- 3
5.0000+ 2 ~ 6.0000+ 2	1.6078+ 1	1.1335+ 1	4.7432+ 0		4.8291- 3
6.0000+ 2 ~ 8.0000+ 2	3.1587+ 1	2.8648+ 1	2.9332+ 0		4.8808- 3
8.0000+ 2 ~ 1.0000+ 3	2.0026+ 1	1.7409+ 1	2.6163+ 0		4.9581- 3
1.0000+ 3 ~ 1.5000+ 3	4.7495+ 1	4.4946+ 1	2.5498+ 0		5.1141- 3
1.5000+ 3 ~ 2.0000+ 3	3.4130+ 1	3.2217+ 1	1.9132+ 0		5.3566- 3
2.0000+ 3 ~ 3.0000+ 3	3.4572+ 1	3.3507+ 1	1.0657+ 0		5.7802- 3
3.0000+ 3 ~ 4.0000+ 3	1.9161+ 1	1.8234+ 1	9.2751- 1		6.5048- 3
4.0000+ 3 ~ 5.0000+ 3	2.1876+ 1	2.0997+ 1	8.7827- 1		7.2146- 3
5.0000+ 3 ~ 6.0000+ 3	1.8220+ 1	1.7523+ 1	6.9657- 1		7.9795- 3
6.0000+ 3 ~ 8.0000+ 3	1.6454+ 1	1.5861+ 1	5.9300- 1		9.2567- 3
8.0000+ 3 ~ 1.0000+ 4	1.4794+ 1	1.4290+ 1	5.0299- 1		1.1122- 2
1.0000+ 4 ~ 1.5000+ 4	1.2967+ 1	1.2555+ 1	4.1190- 1		1.4723- 2
1.5000+ 4 ~ 2.0000+ 4	1.1318+ 1	1.0983+ 1	3.3492- 1		2.0078- 2
2.0000+ 4 ~ 3.0000+ 4	9.8972+ 0	9.6247+ 0	2.7235- 1		2.9127- 2
3.0000+ 4 ~ 4.0000+ 4	8.7343+ 0	8.5103+ 0	2.2389- 1		4.1188- 2
4.0000+ 4 ~ 5.0000+ 4	7.9959+ 0	7.8009+ 0	1.9494- 1		5.3555- 2
5.0000+ 4 ~ 6.0000+ 4	7.4760+ 0	7.3003+ 0	1.7567- 1		6.5931- 2
6.0000+ 4 ~ 8.0000+ 4	6.9349+ 0	6.7782+ 0	1.5673- 1		8.4092- 2
8.0000+ 4 ~ 1.0000+ 5	6.4414+ 0	6.3013+ 0	1.4008- 1		1.0718- 1
1.0000+ 5 ~ 1.5000+ 5	5.9973+ 0	5.8737+ 0	1.2346- 1		1.4438- 1
1.5000+ 5 ~ 2.0000+ 5	5.6119+ 0	5.5031+ 0	1.0857- 1		1.8560- 1
2.0000+ 5 ~ 3.0000+ 5	5.4147+ 0	5.3179+ 0	9.6760- 2		2.2669- 1
3.0000+ 5 ~ 4.0000+ 5	5.4456+ 0	5.3564+ 0	8.9186- 2		2.6039- 1
4.0000+ 5 ~ 5.0000+ 5	5.6318+ 0	5.5447+ 0	8.6996- 2		2.7842- 1
5.0000+ 5 ~ 6.0000+ 5	5.8771+ 0	5.7891+ 0	8.8062- 2		2.8992- 1
6.0000+ 5 ~ 8.0000+ 5	6.2478+ 0	6.1460+ 0	9.3265- 2	8.6673- 3	3.0640- 1
8.0000+ 5 ~ 1.0000+ 6	6.6793+ 0	6.4750+ 0	1.0262- 1	1.0180- 1	3.3602- 1
1.0000+ 6 ~ 1.5000+ 6	7.0173+ 0	6.5860+ 0	1.2146- 1	3.0984- 1	4.0279- 1
1.5000+ 6 ~ 2.0000+ 6	7.0247+ 0	6.0239+ 0	1.2050- 1	8.7972- 1	5.0655- 1
2.0000+ 6 ~ 3.0000+ 6	6.4436+ 0	4.7565+ 0	9.1899- 2	1.5814+ 0	6.2741- 1
3.0000+ 6 ~ 4.0000+ 6	5.6026+ 0	3.3915+ 0	1.2846- 2	2.1680+ 0	7.0018- 1
4.0000+ 6 ~ 5.0000+ 6	4.9228+ 0	2.7168+ 0	3.1162- 3	2.1810+ 0	6.8762- 1
5.0000+ 6 ~ 6.0000+ 6	4.6099+ 0	2.4277+ 0	1.0185- 3	2.1805+ 0	6.8790- 1
6.0000+ 6 ~ 8.0000+ 6	4.4907+ 0	2.3244+ 0	2.9307- 4	2.1653+ 0	7.0220- 1
8.0000+ 6 ~ 1.0000+ 7	4.5373+ 0	2.4211+ 0	7.4721- 5	2.1139+ 0	7.5189- 1
1.0000+ 7 ~ 1.5000+ 7	4.9210+ 0	2.8261+ 0	1.4416- 5	2.0947+ 0	8.4681- 1

MATERIAL =1581 CROSS SECTION CE-144

ENERGY	TOTAL	ELASTIC	CAPTURE	INELA	MU-BAR
1.0000- 5 ~ 1.0000- 2	5.7562+ 0	2.6590+ 0	3.0837+ 0		4.6697- 3
1.0000- 2 ~ 1.5000- 2	4.0992+ 0	2.6590+ 0	1.4299+ 0		4.6697- 3
1.5000- 2 ~ 2.0000- 2	3.8713+ 0	2.6590+ 0	1.2055+ 0		4.6697- 3
2.0000- 2 ~ 3.0000- 2	3.6783+ 0	2.6590+ 0	1.0111+ 0		4.6697- 3
3.0000- 2 ~ 4.0000- 2	3.5167+ 0	2.6590+ 0	8.5239- 1		4.6697- 3
4.0000- 2 ~ 5.0000- 2	3.4184+ 0	2.6590+ 0	7.5097- 1		4.6697- 3
5.0000- 2 ~ 6.0000- 2	3.3421+ 0	2.6590+ 0	6.7890- 1		4.6697- 3
6.0000- 2 ~ 8.0000- 2	3.2657+ 0	2.6590+ 0	6.0273- 1		4.6697- 3
8.0000- 2 ~ 1.0000- 1	3.1964+ 0	2.6590+ 0	5.3101- 1		4.6697- 3
1.0000- 1 ~ 1.5000- 1	3.1139+ 0	2.6590+ 0	4.5217- 1		4.6697- 3
1.5000- 1 ~ 2.0000- 1	3.0449+ 0	2.6590+ 0	3.8120- 1		4.6697- 3
2.0000- 1 ~ 3.0000- 1	2.9808+ 0	2.6590+ 0	3.1973- 1		4.6697- 3
3.0000- 1 ~ 4.0000- 1	2.9320+ 0	2.6590+ 0	2.6955- 1		4.6697- 3
4.0000- 1 ~ 5.0000- 1	2.8979+ 0	2.6590+ 0	2.3747- 1		4.6697- 3
5.0000- 1 ~ 6.0000- 1	2.8752+ 0	2.6590+ 0	2.1469- 1		4.6697- 3
6.0000- 1 ~ 8.0000- 1	2.8521+ 0	2.6590+ 0	1.9060- 1		4.6697- 3
8.0000- 1 ~ 1.0000+ 0	2.8280+ 0	2.6590+ 0	1.6792- 1		4.6697- 3
1.0000+ 0 ~ 1.5000+ 0	2.8035+ 0	2.6590+ 0	1.4299- 1		4.6697- 3
1.5000+ 0 ~ 2.0000+ 0	2.7805+ 0	2.6590+ 0	1.2054- 1		4.6697- 3
2.0000+ 0 ~ 3.0000+ 0	2.7612+ 0	2.6590+ 0	1.0111- 1		4.6697- 3
3.0000+ 0 ~ 4.0000+ 0	2.7449+ 0	2.6590+ 0	8.5237- 2		4.6697- 3
4.0000+ 0 ~ 5.0000+ 0	2.7347+ 0	2.6590+ 0	7.5095- 2		4.6697- 3
5.0000+ 0 ~ 6.0000+ 0	2.7279+ 0	2.6590+ 0	6.7889- 2		4.6697- 3
6.0000+ 0 ~ 8.0000+ 0	2.7197+ 0	2.6590+ 0	6.0272- 2		4.6697- 3
8.0000+ 0 ~ 1.0000+ 1	2.7125+ 0	2.6590+ 0	5.3100- 2		4.6697- 3
1.0000+ 1 ~ 1.5000+ 1	2.7048+ 0	2.6590+ 0	4.5216- 2		4.6697- 3
1.5000+ 1 ~ 2.0000+ 1	2.6974+ 0	2.6590+ 0	3.8119- 2		4.6697- 3
2.0000+ 1 ~ 3.0000+ 1	2.6914+ 0	2.6590+ 0	3.1973- 2		4.6705- 3
3.0000+ 1 ~ 4.0000+ 1	2.6861+ 0	2.6590+ 0	2.6954- 2		4.6717- 3
4.0000+ 1 ~ 5.0000+ 1	2.6831+ 0	2.6590+ 0	2.3747- 2		4.6726- 3
5.0000+ 1 ~ 6.0000+ 1	2.6807+ 0	2.6590+ 0	2.1468- 2		4.6737- 3
6.0000+ 1 ~ 8.0000+ 1	2.6782+ 0	2.6590+ 0	1.9059- 2		4.6756- 3
8.0000+ 1 ~ 1.0000+ 2	2.6760+ 0	2.6590+ 0	1.6792- 2		4.6777- 3
1.0000+ 2 ~ 1.5000+ 2	2.6734+ 0	2.6590+ 0	1.4299- 2		4.6824- 3
1.5000+ 2 ~ 2.0000+ 2	2.6712+ 0	2.6590+ 0	1.2054- 2		4.6902- 3
2.0000+ 2 ~ 3.0000+ 2	2.6692+ 0	2.6590+ 0	1.0111- 2		4.7042- 3
3.0000+ 2 ~ 4.0000+ 2	2.6676+ 0	2.6590+ 0	8.5236- 3		4.7290- 3
4.0000+ 2 ~ 5.0000+ 2	2.6666+ 0	2.6590+ 0	7.5094- 3		4.7536- 3
5.0000+ 2 ~ 6.0000+ 2	5.4869+ 1	5.4221+ 1	6.4737- 1		4.7808- 3
6.0000+ 2 ~ 8.0000+ 2	4.8985+ 1	4.8453+ 1	5.3155- 1		4.8273- 3
8.0000+ 2 ~ 1.0000+ 3	4.3447+ 1	4.3012+ 1	4.3502- 1		4.8974- 3
1.0000+ 3 ~ 1.5000+ 3	3.7358+ 1	3.7014+ 1	3.4424- 1		5.0397- 3
1.5000+ 3 ~ 2.0000+ 3	3.1873+ 1	3.1599+ 1	2.7347- 1		5.2620- 3
2.0000+ 3 ~ 3.0000+ 3	2.7120+ 1	2.6899+ 1	2.2163- 1		5.6525- 3
3.0000+ 3 ~ 4.0000+ 3	2.3254+ 1	2.3070+ 1	1.8397- 1		6.3241- 3
4.0000+ 3 ~ 5.0000+ 3	2.0771+ 1	2.0610+ 1	1.6110- 1		6.9833- 3
5.0000+ 3 ~ 6.0000+ 3	1.9006+ 1	1.8860+ 1	1.4552- 1		7.6953- 3
6.0000+ 3 ~ 8.0000+ 3	1.7142+ 1	1.7013+ 1	1.2966- 1		8.8868- 3
8.0000+ 3 ~ 1.0000+ 4	1.5390+ 1	1.5276+ 1	1.1411- 1		1.0630- 2
1.0000+ 4 ~ 1.5000+ 4	1.3462+ 1	1.3365+ 1	9.6934- 2		1.4008- 2
1.5000+ 4 ~ 2.0000+ 4	1.1720+ 1	1.1638+ 1	8.1887- 2		1.9046- 2
2.0000+ 4 ~ 3.0000+ 4	1.0218+ 1	1.0148+ 1	7.0304- 2		2.7601- 2
3.0000+ 4 ~ 4.0000+ 4	8.9880+ 0	8.9259+ 0	6.2055- 2		3.9050- 2
4.0000+ 4 ~ 5.0000+ 4	8.2061+ 0	8.1485+ 0	5.7607- 2		5.0836- 2
5.0000+ 4 ~ 6.0000+ 4	7.6549+ 0	7.6002+ 0	5.4651- 2		6.2664- 2
6.0000+ 4 ~ 8.0000+ 4	7.0805+ 0	7.0291+ 0	5.1357- 2		8.0073- 2
8.0000+ 4 ~ 1.0000+ 5	6.5555+ 0	6.5077+ 0	4.7791- 2		1.0226- 1
1.0000+ 5 ~ 1.5000+ 5	6.0784+ 0	6.0351+ 0	4.3288- 2		1.3825- 1
1.5000+ 5 ~ 2.0000+ 5	5.6632+ 0	5.6242+ 0	3.8998- 2		1.7819- 1
2.0000+ 5 ~ 3.0000+ 5	5.4439+ 0	5.4079+ 0	3.6067- 2		2.1828- 1
3.0000+ 5 ~ 4.0000+ 5	5.4617+ 0	5.4265+ 0	3.5270- 2		2.5147- 1
4.0000+ 5 ~ 5.0000+ 5	5.6434+ 0	5.3423+ 0	2.5731- 2	2.7399- 1	2.8346- 1
5.0000+ 5 ~ 6.0000+ 5	5.8902+ 0	5.2534+ 0	1.7921- 2	6.1970- 1	3.1326- 1
6.0000+ 5 ~ 8.0000+ 5	6.2720+ 0	5.4084+ 0	1.7845- 2	8.4630- 1	3.4296- 1
8.0000+ 5 ~ 1.0000+ 6	6.6989+ 0	5.5910+ 0	1.6166- 2	1.0920+ 0	3.8577- 1
1.0000+ 6 ~ 1.5000+ 6	7.0626+ 0	5.6054+ 0	1.5626- 2	1.4418+ 0	4.7236- 1
1.5000+ 6 ~ 2.0000+ 6	7.0735+ 0	5.2743+ 0	1.5751- 2	1.7827+ 0	5.7943- 1
2.0000+ 6 ~ 3.0000+ 6	6.5164+ 0	4.4467+ 0	1.3476- 2	2.0526+ 0	6.7160- 1
3.0000+ 6 ~ 4.0000+ 6	5.6336+ 0	3.4307+ 0	8.2199- 3	2.1694+ 0	6.9928- 1
4.0000+ 6 ~ 5.0000+ 6	4.9495+ 0	2.7474+ 0	4.8146- 3	2.1781+ 0	6.8757- 1
5.0000+ 6 ~ 6.0000+ 6	4.6310+ 0	2.4496+ 0	2.6282- 3	2.1776+ 0	6.8821- 1
6.0000+ 6 ~ 8.0000+ 6	4.5021+ 0	2.3327+ 0	9.9475- 4	2.1672+ 0	7.0250- 1
8.0000+ 6 ~ 1.0000+ 7	4.5413+ 0	2.4197+ 0	3.0580- 4	2.1190+ 0	7.5183- 1
1.0000+ 7 ~ 1.5000+ 7	4.9305+ 0	2.8269+ 0	1.1776- 4	2.1033+ 0	8.4656- 1

CROSS SECTION

MATERIAL =1602 NO-144

ENERGY	TOTAL	ELASTIC	CAPTURE	INELA	MU-BAR
1.0000- 5 ~ 1.0000- 2	1.2886+ 1	1.8703+ 0	1.0994+ 1		4.6697- 3
1.0000- 2 ~ 1.5000- 2	6.9765+ 0	1.8704+ 0	5.0901+ 0		4.6697- 3
1.5000- 2 ~ 2.0000- 2	6.1797+ 0	1.8705+ 0	4.2944+ 0		4.6697- 3
2.0000- 2 ~ 3.0000- 2	5.5269+ 0	1.8706+ 0	3.6064+ 0		4.6697- 3
3.0000- 2 ~ 4.0000- 2	4.9298+ 0	1.8708+ 0	3.0456+ 0		4.6697- 3
4.0000- 2 ~ 5.0000- 2	4.5889+ 0	1.8709+ 0	2.6836+ 0		4.6697- 3
5.0000- 2 ~ 6.0000- 2	4.3282+ 0	1.8711+ 0	2.4232+ 0		4.6697- 3
6.0000- 2 ~ 8.0000- 2	4.0346+ 0	1.8714+ 0	2.1538+ 0		4.6697- 3
8.0000- 2 ~ 1.0000- 1	3.7939+ 0	1.8717+ 0	1.8979+ 0		4.6697- 3
1.0000- 1 ~ 1.5000- 1	3.4999+ 0	1.8723+ 0	1.6143+ 0		4.6697- 3
1.5000- 1 ~ 2.0000- 1	3.2522+ 0	1.8731+ 0	1.3637+ 0		4.6697- 3
2.0000- 1 ~ 3.0000- 1	3.0257+ 0	1.8743+ 0	1.1419+ 0		4.6697- 3
3.0000- 1 ~ 4.0000- 1	2.8517+ 0	1.8760+ 0	9.6483- 1		4.6697- 3
4.0000- 1 ~ 5.0000- 1	2.7374+ 0	1.8777+ 0	8.4863- 1		4.6697- 3
5.0000- 1 ~ 6.0000- 1	2.6491+ 0	1.8793+ 0	7.6754- 1		4.6697- 3
6.0000- 1 ~ 8.0000- 1	2.5724+ 0	1.8818+ 0	6.8297- 1		4.6697- 3
8.0000- 1 ~ 1.0000+ 0	2.4939+ 0	1.8851+ 0	6.0091- 1		4.6697- 3
1.0000+ 0 ~ 1.5000+ 0	2.4075+ 0	1.8909+ 0	5.1296- 1		4.6697- 3
1.5000+ 0 ~ 2.0000+ 0	2.3376+ 0	1.8992+ 0	4.3257- 1		4.6697- 3
2.0000+ 0 ~ 3.0000+ 0	2.2784+ 0	1.9117+ 0	3.6413- 1		4.6697- 3
3.0000+ 0 ~ 4.0000+ 0	2.2401+ 0	1.9284+ 0	3.0755- 1		4.6697- 3
4.0000+ 0 ~ 5.0000+ 0	2.2181+ 0	1.9452+ 0	2.7203- 1		4.6697- 3
5.0000+ 0 ~ 6.0000+ 0	2.2117+ 0	1.9620+ 0	2.4697- 1		4.6697- 3
6.0000+ 0 ~ 8.0000+ 0	2.2102+ 0	1.9874+ 0	2.1989- 1		4.6697- 3
8.0000+ 0 ~ 1.0000+ 1	2.2172+ 0	2.0214+ 0	1.9513- 1		4.6697- 3
1.0000+ 1 ~ 1.5000+ 1	2.2519+ 0	2.0817+ 0	1.6804- 1		4.6697- 3
1.5000+ 1 ~ 2.0000+ 1	2.3139+ 0	2.1692+ 0	1.4401- 1		4.6697- 3
2.0000+ 1 ~ 3.0000+ 1	2.4297+ 0	2.3042+ 0	1.2394- 1		4.6705- 3
3.0000+ 1 ~ 4.0000+ 1	2.6049+ 0	2.4961+ 0	1.0828- 1		4.6717- 3
4.0000+ 1 ~ 5.0000+ 1	2.8256+ 0	2.7254+ 0	9.9155- 2		4.6726- 3
5.0000+ 1 ~ 6.0000+ 1	3.0647+ 0	2.9704+ 0	9.3172- 2		4.6737- 3
6.0000+ 1 ~ 8.0000+ 1	3.4672+ 0	3.3788+ 0	8.8178- 2		4.6757- 3
8.0000+ 1 ~ 1.0000+ 2	4.1303+ 0	4.0449+ 0	8.5370- 2		4.6778- 3
1.0000+ 2 ~ 1.5000+ 2	5.7905+ 0	5.7025+ 0	8.7931- 2		4.6825- 3
1.5000+ 2 ~ 2.0000+ 2	9.8809+ 0	9.7752+ 0	1.0574- 1		4.6903- 3
2.0000+ 2 ~ 3.0000+ 2	3.3427+ 1	3.3197+ 1	2.3038- 1		4.7044- 3
3.0000+ 2 ~ 4.0000+ 2	1.5626+ 3	1.5549+ 3	7.7285+ 0		4.7292- 3
4.0000+ 2 ~ 5.0000+ 2	1.3762+ 2	1.3698+ 2	6.4020- 1		4.7539- 3
5.0000+ 2 ~ 6.0000+ 2	1.5739+ 1	1.5657+ 1	8.1820- 2		4.7811- 3
6.0000+ 2 ~ 8.0000+ 2	2.2518+ 1	1.9730+ 1	2.7882+ 0		4.8277- 3
8.0000+ 2 ~ 1.0000+ 3	2.9730- 1	2.6879- 1	2.8511- 2		4.8979- 3
1.0000+ 3 ~ 1.5000+ 3	1.9856+ 2	1.9805+ 2	5.1039- 1		5.0404- 3
1.5000+ 3 ~ 2.0000+ 3	7.9839+ 1	7.8790+ 1	1.0489+ 0		5.2630- 3
2.0000+ 3 ~ 3.0000+ 3	1.8239+ 1	1.8044+ 1	1.9481- 1		5.6541- 3
3.0000+ 3 ~ 4.0000+ 3	2.2331+ 1	2.2112+ 1	2.1887- 1		6.3266- 3
4.0000+ 3 ~ 5.0000+ 3	2.0145+ 1	2.0004+ 1	1.4047- 1		6.9866- 3
5.0000+ 3 ~ 6.0000+ 3	7.8330+ 0	7.7405+ 0	9.2467- 2		7.6996- 3
6.0000+ 3 ~ 8.0000+ 3	2.6007+ 1	2.5856+ 1	1.5193- 1		8.8928- 3
8.0000+ 3 ~ 1.0000+ 4	1.5390+ 1	1.5256+ 1	1.3420- 1		1.0639- 2
1.0000+ 4 ~ 1.5000+ 4	1.3462+ 1	1.3347+ 1	1.1440- 1		1.4021- 2
1.5000+ 4 ~ 2.0000+ 4	1.1720+ 1	1.1623+ 1	9.6893- 2		1.9065- 2
2.0000+ 4 ~ 3.0000+ 4	1.0218+ 1	1.0135+ 1	8.3131- 2		2.7630- 2
3.0000+ 4 ~ 4.0000+ 4	8.9879+ 0	8.9147+ 0	7.3241- 2		3.9094- 2
4.0000+ 4 ~ 5.0000+ 4	8.2061+ 0	8.1381+ 0	6.7981- 2		5.0896- 2
5.0000+ 4 ~ 6.0000+ 4	7.6549+ 0	7.5902+ 0	6.4630- 2		6.2741- 2
6.0000+ 4 ~ 8.0000+ 4	7.0805+ 0	7.0194+ 0	6.1093- 2		8.0179- 2
8.0000+ 4 ~ 1.0000+ 5	6.5555+ 0	6.4981+ 0	5.7383- 2		1.0241- 1
1.0000+ 5 ~ 1.5000+ 5	6.0784+ 0	6.0257+ 0	5.2667- 2		1.3846- 1
1.5000+ 5 ~ 2.0000+ 5	5.6632+ 0	5.6151+ 0	4.8099- 2		1.7848- 1
2.0000+ 5 ~ 3.0000+ 5	5.4439+ 0	5.3990+ 0	4.4940- 2		2.1863- 1
3.0000+ 5 ~ 4.0000+ 5	5.4617+ 0	5.4175+ 0	4.4192- 2		2.5188- 1
4.0000+ 5 ~ 5.0000+ 5	5.6443+ 0	5.5980+ 0	4.6255- 2		2.7007- 1
5.0000+ 5 ~ 6.0000+ 5	5.8902+ 0	5.8400+ 0	5.0231- 2		2.8209- 1
6.0000+ 5 ~ 8.0000+ 5	6.2701+ 0	6.0750+ 0	5.2474- 2	1.4201- 1	3.0612- 1
8.0000+ 5 ~ 1.0000+ 6	6.6993+ 0	5.9530+ 0	4.0605- 2	7.0602- 1	3.5261- 1
1.0000+ 6 ~ 1.5000+ 6	7.0565+ 0	5.9634+ 0	4.3954- 2	1.0495+ 0	4.4419- 1
1.5000+ 6 ~ 2.0000+ 6	7.0511+ 0	5.5085+ 0	3.6975- 2	1.5048+ 0	5.5570- 1
2.0000+ 6 ~ 3.0000+ 6	6.4668+ 0	4.5185+ 0	2.9322- 2	1.9159+ 0	6.6177- 1
3.0000+ 6 ~ 4.0000+ 6	5.6336+ 0	3.4275+ 0	9.4053- 3	2.1686+ 0	6.9995- 1
4.0000+ 6 ~ 5.0000+ 6	4.9495+ 0	2.7428+ 0	2.9966- 3	2.1828+ 0	6.8873- 1
5.0000+ 6 ~ 6.0000+ 6	4.6310+ 0	2.4456+ 0	1.0933- 3	2.1834+ 0	6.8930- 1
6.0000+ 6 ~ 8.0000+ 6	4.5021+ 0	2.3313+ 0	2.9696- 4	2.1696+ 0	7.0290- 1
8.0000+ 6 ~ 1.0000+ 7	4.5413+ 0	2.4197+ 0	7.1889- 5	2.1193+ 0	7.5183- 1
1.0000+ 7 ~ 1.5000+ 7	4.9305+ 0	2.8269+ 0	1.5173- 5	2.1033+ 0	8.4656- 1

CROSS SECTION

MATERIAL =1603 NO-145

ENERGY	TOTAL	ELASTIC	CAPTURE	INELA	MU-BAR
1.0000- 5 ~ 1.0000- 2	1.2971+ 2	3.5426- 1	1.2936+ 2		4.6375- 3
1.0000- 2 ~ 1.5000- 2	6.0411+ 1	3.5450- 1	6.0056+ 1		4.6375- 3
1.5000- 2 ~ 2.0000- 2	5.0922+ 1	3.5467- 1	5.0568+ 1		4.6375- 3
2.0000- 2 ~ 3.0000- 2	4.2848+ 1	3.5491- 1	4.2494+ 1		4.6375- 3
3.0000- 2 ~ 4.0000- 2	3.6144+ 1	3.5524- 1	3.5789+ 1		4.6375- 3
4.0000- 2 ~ 5.0000- 2	3.1884+ 1	3.5556- 1	3.1528+ 1		4.6375- 3
5.0000- 2 ~ 6.0000- 2	2.9001+ 1	3.5588- 1	2.8645+ 1		4.6375- 3
6.0000- 2 ~ 8.0000- 2	2.5709+ 1	3.5636- 1	2.5353+ 1		4.6375- 3
8.0000- 2 ~ 1.0000- 1	2.2702+ 1	3.5699- 1	2.2340+ 1		4.6375- 3
1.0000- 1 ~ 1.5000- 1	1.9461+ 1	3.5807- 1	1.9065+ 1		4.6375- 3
1.5000- 1 ~ 2.0000- 1	1.6474+ 1	3.5956- 1	1.6111+ 1		4.6375- 3
2.0000- 1 ~ 3.0000- 1	1.3966+ 1	3.6168- 1	1.3578+ 1		4.6375- 3
3.0000- 1 ~ 4.0000- 1	1.1880+ 1	3.6429- 1	1.1513+ 1		4.6375- 3
4.0000- 1 ~ 5.0000- 1	1.0610+ 1	3.6662- 1	1.0206+ 1		4.6375- 3
5.0000- 1 ~ 6.0000- 1	9.6801+ 0	3.6862- 1	9.3114+ 0		4.6375- 3
6.0000- 1 ~ 8.0000- 1	8.7248+ 0	3.7103- 1	8.3521+ 0		4.6375- 3
8.0000- 1 ~ 1.0000+ 0	7.8889+ 0	3.7297- 1	7.4895+ 0		4.6375- 3
1.0000+ 0 ~ 1.5000+ 0	7.0446+ 0	3.8595- 1	6.6353+ 0		4.6375- 3
1.5000+ 0 ~ 2.0000+ 0	6.5127+ 0	4.0420- 1	6.0984+ 0		4.6375- 3
2.0000+ 0 ~ 3.0000+ 0	7.3826+ 0	4.7670- 1	6.9032+ 0		4.6375- 3
3.0000+ 0 ~ 4.0000+ 0	1.2735+ 2	3.9778+ 0	1.2337+ 2		4.6375- 3
4.0000+ 0 ~ 5.0000+ 0	4.9889+ 2	1.3224+ 1	4.8567+ 2		4.6375- 3
5.0000+ 0 ~ 6.0000+ 0	5.2995+ 0	3.1297- 1	4.9863+ 0		4.6375- 3
6.0000+ 0 ~ 8.0000+ 0	3.1968+ 0	3.1745- 1	2.8784+ 0		4.6375- 3
8.0000+ 0 ~ 1.0000+ 1	2.6191+ 0	3.4757- 1	2.2672+ 0		4.6375- 3
1.0000+ 1 ~ 1.5000+ 1	2.3578+ 0	4.2931- 1	1.9143+ 0		4.6375- 3
1.5000+ 1 ~ 2.0000+ 1	2.3457+ 0	6.3501- 1	1.7045+ 0		4.6375- 3
2.0000+ 1 ~ 3.0000+ 1	3.4855+ 0	1.7030+ 0	1.7822+ 0		4.6375- 3
3.0000+ 1 ~ 4.0000+ 1	2.9076+ 1	2.3185+ 1	5.8916+ 0		4.6375- 3
4.0000+ 1 ~ 5.0000+ 1	1.4787+ 3	1.2678+ 3	2.1082+ 2		4.6375- 3
5.0000+ 1 ~ 6.0000+ 1	1.1374+ 1	9.6114+ 0	1.7623+ 0		4.6389- 3
6.0000+ 1 ~ 8.0000+ 1	3.4518+ 0	2.5393+ 0	9.1221- 1		4.6423- 3
8.0000+ 1 ~ 1.0000+ 2	2.4056+ 1	4.0652+ 0	1.9989+ 1		4.6459- 3
1.0000+ 2 ~ 1.5000+ 2	1.1355+ 2	7.0362+ 1	4.3181+ 1		4.6515- 3
1.5000+ 2 ~ 2.0000+ 2	1.3155+ 1	5.0536+ 0	8.1034+ 0		4.6596- 3
2.0000+ 2 ~ 3.0000+ 2	2.7566+ 1	1.8662+ 1	8.9041+ 0		4.6739- 3
3.0000+ 2 ~ 4.0000+ 2	3.4792+ 1	2.4998+ 1	9.7932+ 0		4.6989- 3
4.0000+ 2 ~ 5.0000+ 2	8.6488+ 1	7.3856+ 1	1.2633+ 1		4.7235- 3
5.0000+ 2 ~ 6.0000+ 2	1.0485+ 2	9.7977+ 1	6.8751+ 0		4.7505- 3
6.0000+ 2 ~ 8.0000+ 2	2.7199+ 1	2.2721+ 1	4.4782+ 0		4.7966- 3
8.0000+ 2 ~ 1.0000+ 3	6.8437+ 1	6.1823+ 1	6.6141+ 0		4.8654- 3
1.0000+ 3 ~ 1.5000+ 3	3.2437+ 1	2.9289+ 1	3.1484+ 0		5.0043- 3
1.5000+ 3 ~ 2.0000+ 3	4.6750+ 1	4.3601+ 1	3.1489+ 0		5.2202- 3
2.0000+ 3 ~ 3.0000+ 3	4.3029+ 1	4.1352+ 1	1.6762+ 0		5.5979- 3
3.0000+ 3 ~ 4.0000+ 3	2.8602+ 1	2.7376+ 1	1.2258+ 0		6.2451- 3
4.0000+ 3 ~ 5.0000+ 3	2.1980+ 1	2.0963+ 1	1.0155+ 0		6.8797- 3
5.0000+ 3 ~ 6.0000+ 3	2.0087+ 1	1.9213+ 1	8.7284- 1		7.5649- 3
6.0000+ 3 ~ 8.0000+ 3	1.8086+ 1	1.7348+ 1	7.3740- 1		8.7115- 3
8.0000+ 3 ~ 1.0000+ 4	1.6202+ 1	1.5580+ 1	6.2115- 1		1.0390- 2
1.0000+ 4 ~ 1.5000+ 4	1.4130+ 1	1.3623+ 1	5.0594- 1		1.3646- 2
1.5000+ 4 ~ 2.0000+ 4	1.2259+ 1	1.1849+ 1	4.1050- 1		1.8504- 2
2.0000+ 4 ~ 3.0000+ 4	1.0644+ 1	1.0309+ 1	3.3469- 1		2.6767- 2
3.0000+ 4 ~ 4.0000+ 4	9.3201+ 0	9.0436+ 0	2.7640- 1		3.7843- 2
4.0000+ 4 ~ 5.0000+ 4	8.4774+ 0	8.2357+ 0	2.4162- 1		4.9267- 2
5.0000+ 4 ~ 6.0000+ 4	7.8829+ 0	7.6644+ 0	2.1844- 1		6.0750- 2
6.0000+ 4 ~ 8.0000+ 4	7.2438+ 0	6.9982+ 0	1.8940- 1	5.5537- 2	7.8567- 2
8.0000+ 4 ~ 1.0000+ 5	6.6949+ 0	6.2088+ 0	1.5621- 1	3.2960- 1	1.0416- 1
1.0000+ 5 ~ 1.5000+ 5	6.1733+ 0	5.6384+ 0	1.3178- 1	3.9857- 1	1.4397- 1
1.5000+ 5 ~ 2.0000+ 5	5.7183+ 0	5.1576+ 0	1.1174- 1	4.4565- 1	1.8824- 1
2.0000+ 5 ~ 3.0000+ 5	5.4702+ 0	4.8671+ 0	9.6329- 2	5.0616- 1	2.3418- 1
3.0000+ 5 ~ 4.0000+ 5	5.4720+ 0	4.7985+ 0	8.6142- 2	5.8750- 1	2.7431- 1
4.0000+ 5 ~ 5.0000+ 5	5.6515+ 0	4.8971+ 0	8.2134- 2	6.7264- 1	2.9829- 1
5.0000+ 5 ~ 6.0000+ 5	5.9002+ 0	5.0647+ 0	8.1679- 2	7.5428- 1	3.1545- 1
6.0000+ 5 ~ 8.0000+ 5	6.2800+ 0	5.3377+ 0	8.5200- 2	8.5739- 1	3.4007- 1
8.0000+ 5 ~ 1.0000+ 6	6.7136+ 0	5.5956+ 0	9.1716- 2	1.0266+ 0	3.8115- 1
1.0000+ 6 ~ 1.5000+ 6	7.0317+ 0	5.5979+ 0	8.6952- 2	1.3470+ 0	4.7294- 1
1.5000+ 6 ~ 2.0000+ 6	7.1109+ 0	5.0503+ 0	4.1550- 2	2.0156+ 0	6.0983- 1
2.0000+ 6 ~ 3.0000+ 6	6.5598+ 0	4.2613+ 0	1.2026- 2	2.2844+ 0	7.0715- 1
3.0000+ 6 ~ 4.0000+ 6	5.6743+ 0	3.3939+ 0	3.6940- 3	2.2589+ 0	7.1624- 1
4.0000+ 6 ~ 5.0000+ 6	4.9819+ 0	2.7548+ 0	1.4814- 3	2.2124+ 0	6.9537- 1
5.0000+ 6 ~ 6.0000+ 6	4.6549+ 0	2.4660+ 0	6.0007- 4	2.1875+ 0	6.9122- 1
6.0000+ 6 ~ 8.0000+ 6	4.5127+ 0	2.3372+ 0	1.6140- 4	2.1743+ 0	7.0325- 1
8.0000+ 6 ~ 1.0000+ 7	4.5419+ 0	2.4149+ 0	3.3974- 5	2.1248+ 0	7.5094- 1
1.0000+ 7 ~ 1.5000+ 7	4.9385+ 0	2.8253+ 0	4.5027- 6	2.1129+ 0	8.4587- 1

MATERIAL =1621 CROSS SECTION SM-147

ENERGY	TOTAL	ELASTIC	CAPTURE	INELA	MU-BAR
1.0000- 5 ~ 1.0000- 2	2.2152+ 2	1.3680- 1	2.2138+ 2		4.5744- 3
1.0000- 2 ~ 1.5000- 2	1.0086+ 2	1.3618- 1	1.0072+ 2		4.5744- 3
1.5000- 2 ~ 2.0000- 2	8.3941+ 1	1.3582- 1	8.3805+ 1		4.5744- 3
2.0000- 2 ~ 3.0000- 2	6.9472+ 1	1.3537- 1	6.9337+ 1		4.5744- 3
3.0000- 2 ~ 4.0000- 2	5.7243+ 1	1.3491- 1	5.7108+ 1		4.5744- 3
4.0000- 2 ~ 5.0000- 2	4.9615+ 1	1.3463- 1	4.9480+ 1		4.5744- 3
5.0000- 2 ~ 6.0000- 2	4.3859+ 1	1.3448- 1	4.3725+ 1		4.5744- 3
6.0000- 2 ~ 8.0000- 2	3.7839+ 1	1.3455- 1	3.7705+ 1		4.5744- 3
8.0000- 2 ~ 1.0000- 1	3.2116+ 1	1.3405- 1	3.1981+ 1		4.5744- 3
1.0000- 1 ~ 1.5000- 1	2.5890+ 1	1.3262- 1	2.5758+ 1		4.5744- 3
1.5000- 1 ~ 2.0000- 1	2.0239+ 1	1.3240- 1	2.0107+ 1		4.5744- 3
2.0000- 1 ~ 3.0000- 1	1.5551+ 1	1.3118- 1	1.5420+ 1		4.5744- 3
3.0000- 1 ~ 4.0000- 1	1.1891+ 1	1.3110- 1	1.1759+ 1		4.5744- 3
4.0000- 1 ~ 5.0000- 1	9.7620+ 0	1.3057- 1	9.6314+ 0		4.5744- 3
5.0000- 1 ~ 6.0000- 1	8.4201+ 0	1.3001- 1	8.2901+ 0		4.5744- 3
6.0000- 1 ~ 8.0000- 1	7.1749+ 0	1.3029- 1	7.0446+ 0		4.5744- 3
8.0000- 1 ~ 1.0000+ 0	6.2265+ 0	1.3006- 1	6.0964+ 0		4.5744- 3
1.0000+ 0 ~ 1.5000+ 0	5.6797+ 0	1.3159- 1	5.5481+ 0		4.5744- 3
1.5000+ 0 ~ 2.0000+ 0	6.1866+ 0	1.3277- 1	6.0539+ 0		4.5744- 3
2.0000+ 0 ~ 3.0000+ 0	1.6002+ 1	1.9268- 1	1.5810+ 1		4.5744- 3
3.0000+ 0 ~ 4.0000+ 0	6.6903+ 2	1.3404+ 1	6.5563+ 2		4.5744- 3
4.0000+ 0 ~ 5.0000+ 0	9.5433+ 0	7.7653- 1	8.7668+ 0		4.5744- 3
5.0000+ 0 ~ 6.0000+ 0	3.6976+ 0	5.9712- 1	3.1005+ 0		4.5744- 3
6.0000+ 0 ~ 8.0000+ 0	2.9485+ 0	6.8939- 1	2.2591+ 0		4.5744- 3
8.0000+ 0 ~ 1.0000+ 1	3.4233+ 0	1.0313+ 0	2.3920+ 0		4.5744- 3
1.0000+ 1 ~ 1.5000+ 1	8.8527+ 0	3.5890+ 0	5.2637+ 0		4.5744- 3
1.5000+ 1 ~ 2.0000+ 1	1.7550+ 3	8.3068+ 2	9.2427+ 2		4.5744- 3
2.0000+ 1 ~ 3.0000+ 1	8.4352+ 1	1.0012+ 1	7.4341+ 1		4.5744- 3
3.0000+ 1 ~ 4.0000+ 1	6.7877+ 2	2.9683+ 2	3.8194+ 2		4.5744- 3
4.0000+ 1 ~ 5.0000+ 1	1.2670+ 2	3.6091+ 1	9.2606+ 1		4.5744- 3
5.0000+ 1 ~ 6.0000+ 1	1.3786+ 2	7.1078+ 1	6.6779+ 1		4.5763- 3
6.0000+ 1 ~ 8.0000+ 1	4.1137+ 1	5.8304+ 0	3.5307+ 1		4.5809- 3
8.0000+ 1 ~ 1.0000+ 2	3.3000+ 2	2.1970+ 2	1.1029+ 2		4.5858- 3
1.0000+ 2 ~ 1.5000+ 2	1.7106+ 2	1.1459+ 2	5.6474+ 1		4.5927- 3
1.5000+ 2 ~ 2.0000+ 2	1.5922+ 2	1.0866+ 2	5.0560+ 1		4.6024- 3
2.0000+ 2 ~ 3.0000+ 2	1.0479+ 2	6.8988+ 1	3.5801+ 1		4.6188- 3
3.0000+ 2 ~ 4.0000+ 2	7.6526+ 1	5.3257+ 1	2.3273+ 1		4.6464- 3
4.0000+ 2 ~ 5.0000+ 2	6.5002+ 1	4.2384+ 1	2.2618+ 1		4.6732- 3
5.0000+ 2 ~ 6.0000+ 2	1.2370+ 2	9.9934+ 1	2.3768+ 1		4.7020- 3
6.0000+ 2 ~ 8.0000+ 2	6.7191+ 1	4.9606+ 1	1.7582+ 1		4.7502- 3
8.0000+ 2 ~ 1.0000+ 3	5.8384+ 1	4.3048+ 1	1.5319+ 1		4.8212- 3
1.0000+ 3 ~ 1.5000+ 3	5.0130+ 1	3.8259+ 1	1.1847+ 1		4.9611- 3
1.5000+ 3 ~ 2.0000+ 3	4.2684+ 1	3.3698+ 1	8.9765+ 0		5.1749- 3
2.0000+ 3 ~ 3.0000+ 3	3.6230+ 1	2.9487+ 1	6.7404+ 0		5.5412- 3
3.0000+ 3 ~ 4.0000+ 3	3.0964+ 1	2.5855+ 1	5.0907+ 0		6.1555- 3
4.0000+ 3 ~ 5.0000+ 3	2.7584+ 1	2.3435+ 1	4.1355+ 0		6.7528- 3
5.0000+ 3 ~ 6.0000+ 3	2.5177+ 1	2.1603+ 1	3.5091+ 0		7.3912- 3
6.0000+ 3 ~ 8.0000+ 3	2.2631+ 1	1.9728+ 1	2.8989+ 0		8.4495- 3
8.0000+ 3 ~ 1.0000+ 4	2.0231+ 1	1.7856+ 1	2.3717+ 0		9.9859- 3
1.0000+ 4 ~ 1.5000+ 4	1.7581+ 1	1.5721+ 1	1.8563+ 0		1.2940- 2
1.5000+ 4 ~ 2.0000+ 4	1.5179+ 1	1.3734+ 1	1.4440+ 0		1.7323- 2
2.0000+ 4 ~ 3.0000+ 4	1.3089+ 1	1.1948+ 1	1.1400+ 0		2.4744- 2
3.0000+ 4 ~ 4.0000+ 4	1.1365+ 1	1.0443+ 1	9.2186- 1		3.4678- 2
4.0000+ 4 ~ 5.0000+ 4	1.0257+ 1	9.4568+ 0	8.0027- 1		4.4925- 2
5.0000+ 4 ~ 6.0000+ 4	9.4685+ 0	8.7458+ 0	7.2267- 1		5.5244- 2
6.0000+ 4 ~ 8.0000+ 4	8.6362+ 0	7.9866+ 0	6.4960- 1		7.0518- 2
8.0000+ 4 ~ 1.0000+ 5	7.8619+ 0	7.2726+ 0	5.8931- 1		9.0160- 2
1.0000+ 5 ~ 1.5000+ 5	7.0262+ 0	6.4586+ 0	5.2200- 1	4.0743- 2	1.2574- 1
1.5000+ 5 ~ 2.0000+ 5	6.3949+ 0	5.6861+ 0	4.5605- 1	2.4386- 1	1.6685- 1
2.0000+ 5 ~ 3.0000+ 5	6.0037+ 0	5.1965+ 0	4.1044- 1	3.9565- 1	2.0975- 1
3.0000+ 5 ~ 4.0000+ 5	5.8520+ 0	4.9934+ 0	3.8376- 1	4.8475- 1	2.4890- 1
4.0000+ 5 ~ 5.0000+ 5	5.9558+ 0	5.0038+ 0	3.7314- 1	5.7912- 1	2.7565- 1
5.0000+ 5 ~ 6.0000+ 5	6.1440+ 0	5.1020+ 0	3.7154- 1	6.7085- 1	2.9813- 1
6.0000+ 5 ~ 8.0000+ 5	6.4546+ 0	5.2685+ 0	3.6863- 1	8.1773- 1	3.3417- 1
8.0000+ 5 ~ 1.0000+ 6	6.8232+ 0	5.3743+ 0	3.3435- 1	1.1147+ 0	3.9253- 1
1.0000+ 6 ~ 1.5000+ 6	7.0714+ 0	5.2454+ 0	2.4612- 1	1.5785+ 0	5.0780- 1
1.5000+ 6 ~ 2.0000+ 6	7.1726+ 0	4.8974+ 0	1.2119- 1	2.1522+ 0	6.3701- 1
2.0000+ 6 ~ 3.0000+ 6	6.7107+ 0	4.3843+ 0	5.0024- 2	2.2745+ 0	7.1100- 1
3.0000+ 6 ~ 4.0000+ 6	5.8896+ 0	3.5811+ 0	1.7921- 2	2.2688+ 0	7.2281- 1
4.0000+ 6 ~ 5.0000+ 6	5.2106+ 0	2.9362+ 0	7.0818- 3	2.2512+ 0	7.1057- 1
5.0000+ 6 ~ 6.0000+ 6	4.8607+ 0	2.6155+ 0	2.8409- 3	2.2397+ 0	7.0802- 1
6.0000+ 6 ~ 8.0000+ 6	4.6534+ 0	2.4206+ 0	7.5815- 4	2.2292+ 0	7.1831- 1
8.0000+ 6 ~ 1.0000+ 7	4.6319+ 0	2.4442+ 0	1.4404- 4	2.1859+ 0	7.5900- 1
1.0000+ 7 ~ 1.5000+ 7	5.0453+ 0	2.8517+ 0	1.6170- 5	2.1932+ 0	8.4647- 1

MATERIAL =1611 CROSS SECTION PM-147

ENERGY	TOTAL	ELASTIC	CAPTURE	INELA	MU-BAR
1.0000- 5 ~ 1.0000- 2	5.7065+ 2	1.4925+ 0	5.6916+ 2		4.5744- 3
1.0000- 2 ~ 1.5000- 2	2.6415+ 2	1.4927+ 0	2.6266+ 2		4.5744- 3
1.5000- 2 ~ 2.0000- 2	2.2298+ 2	1.4928+ 0	2.2148+ 2		4.5744- 3
2.0000- 2 ~ 3.0000- 2	1.8626+ 2	1.4931+ 0	1.8477+ 2		4.5744- 3
3.0000- 2 ~ 4.0000- 2	1.5700+ 2	1.4937+ 0	1.5550+ 2		4.5744- 3
4.0000- 2 ~ 5.0000- 2	1.3770+ 2	1.4944+ 0	1.3621+ 2		4.5744- 3
5.0000- 2 ~ 6.0000- 2	1.2402+ 2	1.4953+ 0	1.2253+ 2		4.5744- 3
6.0000- 2 ~ 8.0000- 2	1.0999+ 2	1.4970+ 0	1.0849+ 2		4.5744- 3
8.0000- 2 ~ 1.0000- 1	9.6210+ 1	1.4998+ 0	9.4711+ 1		4.5744- 3
1.0000- 1 ~ 1.5000- 1	8.1256+ 1	1.5065+ 0	7.9749+ 1		4.5744- 3
1.5000- 1 ~ 2.0000- 1	6.7738+ 1	1.5189+ 0	6.6219+ 1		4.5744- 3
2.0000- 1 ~ 3.0000- 1	5.6026+ 1	1.5449+ 0	5.4481+ 1		4.5744- 3
3.0000- 1 ~ 4.0000- 1	4.6619+ 1	1.5904+ 0	4.5029+ 1		4.5744- 3
4.0000- 1 ~ 5.0000- 1	4.0697+ 1	1.6477+ 0	3.9050+ 1		4.5744- 3
5.0000- 1 ~ 6.0000- 1	3.6898+ 1	1.7154+ 0	3.5182+ 1		4.5744- 3
6.0000- 1 ~ 8.0000- 1	3.2979+ 1	1.8303+ 0	3.1148+ 1		4.5744- 3
8.0000- 1 ~ 1.0000+ 0	2.9798+ 1	2.0178+ 0	2.7780+ 1		4.5744- 3
1.0000+ 0 ~ 1.5000+ 0	2.7708+ 1	2.4596+ 0	2.5248+ 1		4.5744- 3
1.5000+ 0 ~ 2.0000+ 0	2.8412+ 1	3.3757+ 0	2.5037+ 1		4.5744- 3
2.0000+ 0 ~ 3.0000+ 0	3.7416+ 1	6.2623+ 0	3.1153+ 1		4.5744- 3
3.0000+ 0 ~ 4.0000+ 0	7.8825+ 1	1.8332+ 1	6.0492+ 1		4.5744- 3
4.0000+ 0 ~ 5.0000+ 0	4.6697+ 2	1.4021+ 2	3.2677+ 2		4.5744- 3
5.0000+ 0 ~ 6.0000+ 0	1.2394+ 4	4.1126+ 3	8.2816+ 3		4.5744- 3
6.0000+ 0 ~ 8.0000+ 0	1.0814+ 3	1.0267+ 2	9.7870+ 2		4.5744- 3
8.0000+ 0 ~ 1.0000+ 1	2.8434+ 1	1.3496+ 1	1.4938+ 1		4.5744- 3
1.0000+ 1 ~ 1.5000+ 1	1.0744+ 1	4.6114+ 0	6.1325+ 0		4.5744- 3
1.5000+ 1 ~ 2.0000+ 1	1.2051+ 2	8.3892+ 0	1.1213+ 2		4.5744- 3
2.0000+ 1 ~ 3.0000+ 1	1.4983+ 1	2.0107+ 0	1.2972+ 1		4.5744- 3
3.0000+ 1 ~ 4.0000+ 1	2.0864+ 2	5.2082+ 1	1.5656+ 2		4.5744- 3
4.0000+ 1 ~ 5.0000+ 1	2.0371+ 2	5.4054+ 1	1.4965+ 2		4.5744- 3
5.0000+ 1 ~ 6.0000+ 1	1.7365+ 1	2.6476+ 0	1.4717+ 1		4.5766- 3
6.0000+ 1 ~ 8.0000+ 1	8.7849+ 1	4.1524+ 1	4.6325+ 1		4.5821- 3
8.0000+ 1 ~ 1.0000+ 2	1.3613+ 2	4.4809+ 1	9.1317+ 1		4.5879- 3
1.0000+ 2 ~ 1.5000+ 2	1.1349+ 2	7.2984+ 1	4.0503+ 1		4.5962- 3
1.5000+ 2 ~ 2.0000+ 2	1.4888+ 2	1.0776+ 2	4.1119+ 1		4.6077- 3
2.0000+ 2 ~ 3.0000+ 2	1.0065+ 2	6.9955+ 1	3.0699+ 1		4.6271- 3
3.0000+ 2 ~ 4.0000+ 2	8.0058+ 1	5.1767+ 1	2.8210+ 1		4.6597- 3
4.0000+ 2 ~ 5.0000+ 2	7.0885+ 1	4.7601+ 1	2.3224+ 1		4.6915- 3
5.0000+ 2 ~ 6.0000+ 2	6.4360+ 1	4.4470+ 1	1.9867+ 1		4.7253- 3
6.0000+ 2 ~ 8.0000+ 2	5.7465+ 1	4.0950+ 1	1.6495+ 1		4.7821- 3
8.0000+ 2 ~ 1.0000+ 3	5.0979+ 1	3.7461+ 1	1.3496+ 1		4.8656- 3
1.0000+ 3 ~ 1.5000+ 3	4.3844+ 1	3.3372+ 1	1.0451+ 1		5.0300- 3
1.5000+ 3 ~ 2.0000+ 3	3.7414+ 1	2.9473+ 1	7.9318+ 0		5.2810- 3
2.0000+ 3 ~ 3.0000+ 3	3.1841+ 1	2.5869+ 1	5.9693+ 0		5.7100- 3
3.0000+ 3 ~ 4.0000+ 3	2.7299+ 1	2.2760+ 1	4.5223+ 0		6.4280- 3
4.0000+ 3 ~ 5.0000+ 3	2.4381+ 1	2.0685+ 1	3.6840+ 0		7.1254- 3
5.0000+ 3 ~ 6.0000+ 3	2.2304+ 1	1.9165+ 1	3.1343+ 0		7.8696- 3
6.0000+ 3 ~ 8.0000+ 3	2.0109+ 1	1.7506+ 1	2.5995+ 0		9.1016- 3
8.0000+ 3 ~ 1.0000+ 4	1.8040+ 1	1.5899+ 1	2.1378+ 0		1.0887- 2
1.0000+ 4 ~ 1.5000+ 4	1.5758+ 1	1.4069+ 1	1.6865+ 0		1.4311- 2
1.5000+ 4 ~ 2.0000+ 4	1.3690+ 1	1.2365+ 1	1.3249+ 0		1.9379- 2
2.0000+ 4 ~ 3.0000+ 4	1.1895+ 1	1.0837+ 1	1.0570+ 0		2.7917- 2
3.0000+ 4 ~ 4.0000+ 4	1.0415+ 1	9.5517+ 0	8.6283- 1		3.9298- 2
4.0000+ 4 ~ 5.0000+ 4	9.4657+ 0	8.7127+ 0	7.5294- 1		5.0977- 2
5.0000+ 4 ~ 6.0000+ 4	8.7916+ 0	8.1098+ 0	6.8171- 1		6.2680- 2
6.0000+ 4 ~ 8.0000+ 4	8.0824+ 0	7.4689+ 0	6.1343- 1		7.9903- 2
8.0000+ 4 ~ 1.0000+ 5	7.4145+ 0	6.8170+ 0	5.4794- 1	4.8952- 2	1.0276- 1
1.0000+ 5 ~ 1.5000+ 5	6.7981+ 0	6.0514+ 0	4.6833- 1	2.7288- 1	1.4361- 1
1.5000+ 5 ~ 2.0000+ 5	6.2429+ 0	5.4877+ 0	4.1600- 1	3.3507- 1	1.8736- 1
2.0000+ 5 ~ 3.0000+ 5	5.9049+ 0	5.1395+ 0	3.8023- 1	3.8475- 1	2.3225- 1
3.0000+ 5 ~ 4.0000+ 5	5.8296+ 0	5.0334+ 0	3.6041- 1	4.3573- 1	2.7153- 1
4.0000+ 5 ~ 5.0000+ 5	5.8984+ 0	5.0531+ 0	3.4694- 1	4 9847- 1	2.9932- 1
5.0000+ 5 ~ 6.0000+ 5	6.1420+ 0	5.0666+ 0	3.2982- 1	7.4590- 1	3.2649- 1
6.0000+ 5 ~ 8.0000+ 5	6.4701+ 0	5.1434+ 0	3.0951- 1	1.0174+ 0	3.6583- 1
8.0000+ 5 ~ 1.0000+ 6	6.8580+ 0	5.1342+ 0	2.5314- 1	1.4705+ 0	4.3008- 1
1.0000+ 6 ~ 1.5000+ 6	7.1657+ 0	4.9773+ 0	1.5798- 1	2.0291+ 0	5.4544- 1
1.5000+ 6 ~ 2.0000+ 6	7.1641+ 0	4.7824+ 0	9.0364- 2	2.2908+ 0	6.5305- 1
2.0000+ 6 ~ 3.0000+ 6	6.6494+ 0	4.3006+ 0	5.0293- 2	2.2973+ 0	7.1260- 1
3.0000+ 6 ~ 4.0000+ 6	5.8079+ 0	3.4900+ 0	2.3227- 2	2.2734+ 0	7.1887- 1
4.0000+ 6 ~ 5.0000+ 6	5.1401+ 0	2.8573+ 0	1.1148- 2	2.2558+ 0	7.0352- 1
5.0000+ 6 ~ 6.0000+ 6	4.8152+ 0	2.5644+ 0	5.1445- 3	2.2434+ 0	7.0312- 1
6.0000+ 6 ~ 8.0000+ 6	4.6581+ 0	2.4233+ 0	1.5765- 3	2.2311+ 0	7.1872- 1
8.0000+ 6 ~ 1.0000+ 7	4.6762+ 0	2.4893+ 0	4.6477- 4	2.1846+ 0	7.6445- 1
1.0000+ 7 ~ 1.5000+ 7	5.0812+ 0	2.8939+ 0	1.2793- 4	2.1870+ 0	8.5085- 1

CROSS SECTION

MATERIAL =1622 SM-149

ENERGY	TOTAL	ELASTIC	CAPTURE	INELA	MU-BAR
1.0000- 5 ~ 1.0000- 2	8.5110+ 4	1.3487+ 2	8.4975+ 4		4.5130- 3
1.0000- 2 ~ 1.5000- 2	4.6184+ 4	1.5242+ 2	4.6032+ 4		4.5130- 3
1.5000- 2 ~ 2.0000- 2	4.2812+ 4	1.6659+ 2	4.2646+ 4		4.5130- 3
2.0000- 2 ~ 3.0000- 2	4.2021+ 4	1.9304+ 2	4.1828+ 4		4.5130- 3
3.0000- 2 ~ 4.0000- 2	4.4598+ 4	2.3954+ 2	4.4359+ 4		4.5130- 3
4.0000- 2 ~ 5.0000- 2	5.0945+ 4	3.0648+ 2	5.0638+ 4		4.5130- 3
5.0000- 2 ~ 6.0000- 2	6.1527+ 4	4.0565+ 2	6.1122+ 4		4.5130- 3
6.0000- 2 ~ 8.0000- 2	8.7937+ 4	6.5523+ 2	8.7281+ 4		4.5130- 3
8.0000- 2 ~ 1.0000- 1	1.2656+ 5	1.0665+ 3	1.2549+ 5		4.5130- 3
1.0000- 1 ~ 1.5000- 1	7.1551+ 4	7.0068+ 2	7.0850+ 4		4.5130- 3
1.5000- 1 ~ 2.0000- 1	1.5151+ 4	1.8613+ 2	1.4965+ 4		4.5130- 3
2.0000- 1 ~ 3.0000- 1	4.0290+ 3	6.3234+ 1	3.9638+ 3		4.5130- 3
3.0000- 1 ~ 4.0000- 1	1.3521+ 3	2.7153+ 1	1.3249+ 3		4.5130- 3
4.0000- 1 ~ 5.0000- 1	7.4014+ 2	1.6126+ 1	7.2402+ 2		4.5130- 3
5.0000- 1 ~ 6.0000- 1	5.7393+ 2	1.0638+ 1	5.6330+ 2		4.5130- 3
6.0000- 1 ~ 8.0000- 1	1.1669+ 3	9.2956+ 0	1.1576+ 3		4.5130- 3
8.0000- 1 ~ 1.0000+ 0	8.0280+ 3	1.1276+ 2	7.9153+ 3		4.5130- 3
1.0000+ 0 ~ 1.5000+ 0	2.6510+ 2	1.5863+ 1	2.4924+ 2		4.5130- 3
1.5000+ 0 ~ 2.0000+ 0	4.8647+ 1	7.7179+ 0	4.0929+ 1		4.5130- 3
2.0000+ 0 ~ 3.0000+ 0	2.2410+ 1	5.2450+ 0	1.7165+ 1		4.5130- 3
3.0000+ 0 ~ 4.0000+ 0	1.7636+ 1	3.6365+ 0	1.4000+ 1		4.5130- 3
4.0000+ 0 ~ 5.0000+ 0	8.4125+ 2	2.6899+ 1	8.1435+ 2		4.5130- 3
5.0000+ 0 ~ 6.0000+ 0	2.0131+ 2	1.2079+ 1	1.8923+ 2		4.5130- 3
6.0000+ 0 ~ 8.0000+ 0	1.1453+ 2	4.3250+ 0	1.1021+ 2		4.5130- 3
8.0000+ 0 ~ 1.0000+ 1	1.0717+ 3	1.3328+ 2	9.3843+ 2		4.5130- 3
1.0000+ 1 ~ 1.5000+ 1	2.0264+ 2	1.6247+ 1	1.8639+ 2		4.5130- 3
1.5000+ 1 ~ 2.0000+ 1	9.7027+ 1	8.4598+ 0	8.8558+ 1		4.5130- 3
2.0000+ 1 ~ 3.0000+ 1	2.0781+ 2	3.3602+ 1	1.7420+ 2		4.5130- 3
3.0000+ 1 ~ 4.0000+ 1	1.2163+ 2	1.6173+ 1	1.0546+ 2		4.5130- 3
4.0000+ 1 ~ 5.0000+ 1	8.9237+ 2	4.0154+ 2	4.9083+ 2		4.5130- 3
5.0000+ 1 ~ 6.0000+ 1	5.2156+ 2	2.1419+ 2	3.0737+ 2		4.5160- 3
6.0000+ 1 ~ 8.0000+ 1	6.4818+ 2	3.4328+ 2	3.0490+ 2		4.5237- 3
8.0000+ 1 ~ 1.0000+ 2	3.8989+ 2	2.0420+ 2	1.8569+ 2		4.5317- 3
1.0000+ 2 ~ 1.5000+ 2	1.7583+ 2	9.9013+ 1	7.6813+ 1		4.5425- 3
1.5000+ 2 ~ 2.0000+ 2	1.2453+ 2	4.8680+ 1	7.5811+ 1		4.5568- 3
2.0000+ 2 ~ 3.0000+ 2	1.0493+ 2	4.4960+ 1	5.9948+ 1		4.5804- 3
3.0000+ 2 ~ 4.0000+ 2	8.8923+ 1	4.1393+ 1	4.7428+ 1		4.5185- 3
4.0000+ 2 ~ 5.0000+ 2	7.8685+ 1	3.8836+ 1	3.9772+ 1		4.6552- 3
5.0000+ 2 ~ 6.0000+ 2	7.1407+ 1	3.6855+ 1	3.4520+ 1		4.6938- 3
6.0000+ 2 ~ 8.0000+ 2	6.3718+ 1	3.4550+ 1	2.9141+ 1		4.7574- 3
8.0000+ 2 ~ 1.0000+ 3	5.6479+ 1	3.2186+ 1	2.4261+ 1		4.8493- 3
1.0000+ 3 ~ 1.5000+ 3	4.8515+ 1	2.9305+ 1	1.9180+ 1		5.0268- 3
1.5000+ 3 ~ 2.0000+ 3	4.1339+ 1	2.6455+ 1	1.4870+ 1		5.2932- 3
2.0000+ 3 ~ 3.0000+ 3	3.5117+ 1	2.3703+ 1	1.1409+ 1		5.7402- 3
3.0000+ 3 ~ 4.0000+ 3	3.0043+ 1	2.1234+ 1	8.7813+ 0		6.4729- 3
4.0000+ 3 ~ 5.0000+ 3	2.6785+ 1	1.9540+ 1	7.2247+ 0		7.1790- 3
5.0000+ 3 ~ 6.0000+ 3	2.4465+ 1	1.8271+ 1	6.1854+ 0		7.9252- 3
6.0000+ 3 ~ 8.0000+ 3	2.2012+ 1	1.5853+ 1	5.1527+ 0		9.1498- 3
8.0000+ 3 ~ 1.0000+ 4	1.9699+ 1	1.5449+ 1	4.2432+ 0		1.0910- 2
1.0000+ 4 ~ 1.5000+ 4	1.7145+ 1	1.3805+ 1	3.3335+ 0		1.4256- 2
1.5000+ 4 ~ 2.0000+ 4	1.4830+ 1	1.2237+ 1	2.5912+ 0		1.9178- 2
2.0000+ 4 ~ 3.0000+ 4	1.2718+ 1	1.0535+ 1	1.9504+ 0	2.2201- 1	2.8109- 2
3.0000+ 4 ~ 4.0000+ 4	1.1156+ 1	9.0758+ 0	1.4892+ 0	5.8871- 1	4.0124- 2
4.0000+ 4 ~ 5.0000+ 4	1.0089+ 1	8.2346+ 0	1.2662+ 0	5.8749- 1	5.2188- 2
5.0000+ 4 ~ 6.0000+ 4	9.3292+ 0	7.6394+ 0	1.1267+ 0	5.6315- 1	6.4239- 2
6.0000+ 4 ~ 8.0000+ 4	8.5283+ 0	7.0056+ 0	9.9558- 1	5.2715- 1	8.1991- 2
8.0000+ 4 ~ 1.0000+ 5	7.7839+ 0	6.4074+ 0	8.8664- 1	4.9995- 1	1.0475- 1
1.0000+ 5 ~ 1.5000+ 5	7.0618+ 0	5.8003+ 0	8.0037- 1	4.6109- 1	1.4283- 1
1.5000+ 5 ~ 2.0000+ 5	6.4209+ 0	5.2523+ 0	7.3013- 1	4.3854- 1	1.8556- 1
2.0000+ 5 ~ 3.0000+ 5	5.9225+ 0	4.8186+ 0	6.5885- 1	4.4480- 1	2.3413- 1
3.0000+ 5 ~ 4.0000+ 5	5.8853+ 0	4.5678+ 0	5.9656- 1	7.2077- 1	2.8165- 1
4.0000+ 5 ~ 5.0000+ 5	5.9994+ 0	4.5449+ 0	5.6091- 1	8.8499- 1	3.1381- 1
5.0000+ 5 ~ 6.0000+ 5	6.1354+ 0	4.5918+ 0	5.4800- 1	9.9578- 1	3.4200- 1
6.0000+ 5 ~ 8.0000+ 5	6.5060+ 0	4.6618+ 0	5.0415- 1	1.3403+ 0	3.8826- 1
8.0000+ 5 ~ 1.0000+ 6	6.8828+ 0	4.7708+ 0	4.4718- 1	1.6649+ 0	4.5217- 1
1.0000+ 6 ~ 1.5000+ 6	7.1928+ 0	4.8708+ 0	3.6190- 1	1.9596+ 0	5.5346- 1
1.5000+ 6 ~ 2.0000+ 6	7.2074+ 0	4.8210+ 0	2.7226- 1	2.1137+ 0	6.5204- 1
2.0000+ 6 ~ 3.0000+ 6	6.7229+ 0	4.3808+ 0	1.8079- 1	2.1594+ 0	7.1194- 1
3.0000+ 6 ~ 4.0000+ 6	5.8902+ 0	3.5709+ 0	9.2280- 2	2.1966+ 0	7.2127- 1
4.0000+ 6 ~ 5.0000+ 6	5.2119+ 0	2.9240+ 0	4.7146- 2	2.2184+ 0	7.0845- 1
5.0000+ 6 ~ 6.0000+ 6	4.8702+ 0	2.6117+ 0	2.2065- 2	2.2285+ 0	7.0780- 1
6.0000+ 6 ~ 8.0000+ 6	4.6823+ 0	2.4378+ 0	6.4995- 3	2.2307+ 0	7.2002- 1
8.0000+ 6 ~ 1.0000+ 7	4.5784+ 0	2.4788+ 0	1.9512- 3	2.1958+ 0	7.6269- 1
1.0000+ 7 ~ 1.5000+ 7	5.0951+ 0	2.8878+ 0	6.2796- 4	2.2063+ 0	8.4914- 1

CROSS SECTION

MATERIAL =1623 SM-151

ENERGY	TOTAL	ELASTIC	CAPTURE	INELA	MU-BAR
1.0000- 5 ~ 1.0000- 2	6.0717+ 4	1.2988+ 1	6.0704+ 4		4.4533- 3
1.0000- 2 ~ 1.5000- 2	2.5950+ 4	1.3205+ 1	2.5937+ 4		4.4533- 3
1.5000- 2 ~ 2.0000- 2	2.0743+ 4	1.3181+ 1	2.0730+ 4		4.4533- 3
2.0000- 2 ~ 3.0000- 2	1.5908+ 4	1.2957+ 1	1.5890+ 4		4.4533- 3
3.0000- 2 ~ 4.0000- 2	1.1822+ 4	1.2462+ 1	1.1802+ 4		4.4533- 3
4.0000- 2 ~ 5.0000- 2	9.2049+ 3	1.1977+ 1	9.1934+ 3		4.4533- 3
5.0000- 2 ~ 6.0000- 2	7.3852+ 3	1.1454+ 1	7.3662+ 3		4.4533- 3
6.0000- 2 ~ 8.0000- 2	5.5773+ 3	1.0671+ 1	5.5632+ 3		4.4533- 3
8.0000- 2 ~ 1.0000- 1	4.0708+ 3	9.7335+ 0	4.0589+ 3		4.4533- 3
1.0000- 1 ~ 1.5000- 1	2.7543+ 3	8.5098+ 0	2.7405+ 3		4.4533- 3
1.5000- 1 ~ 2.0000- 1	1.8635+ 3	7.3374+ 0	1.8499+ 3		4.4533- 3
2.0000- 1 ~ 3.0000- 1	1.3270+ 3	6.3229+ 0	1.3180+ 3		4.4533- 3
3.0000- 1 ~ 4.0000- 1	1.0134+ 3	5.5329+ 0	1.0069+ 3		4.4533- 3
4.0000- 1 ~ 5.0000- 1	8.6460+ 2	4.9705+ 0	8.5839+ 2		4.4533- 3
5.0000- 1 ~ 6.0000- 1	7.8395+ 2	4.4661+ 0	7.7776+ 2		4.4533- 3
6.0000- 1 ~ 8.0000- 1	7.4799+ 2	3.6672+ 0	7.4291+ 2		4.4533- 3
8.0000- 1 ~ 1.0000+ 0	1.0652+ 3	3.3410+ 0	1.0618+ 3		4.4533- 3
1.0000+ 0 ~ 1.5000+ 0	2.6440+ 3	2.6320+ 1	2.6173+ 3		4.4533- 3
1.5000+ 0 ~ 2.0000+ 0	1.2576+ 3	9.5267+ 0	1.2480+ 3		4.4533- 3
2.0000+ 0 ~ 3.0000+ 0	7.4706+ 2	1.2945+ 1	7.3346+ 2		4.4533- 3
3.0000+ 0 ~ 4.0000+ 0	3.1459+ 2	5.1695+ 0	3.0921+ 2		4.4533- 3
4.0000+ 0 ~ 5.0000+ 0	6.9456+ 2	1.0509+ 1	6.8389+ 2		4.4533- 3
5.0000+ 0 ~ 6.0000+ 0	4.1600+ 2	5.8453+ 0	4.1014+ 2		4.4533- 3
6.0000+ 0 ~ 8.0000+ 0	9.5642+ 2	5.6356+ 1	8.9987+ 2		4.4533- 3
8.0000+ 0 ~ 1.0000+ 1	1.9803+ 2	6.0793+ 0	1.9163+ 2		4.4533- 3
1.0000+ 1 ~ 1.5000+ 1	9.8396+ 2	1.1236+ 2	8.7156+ 2		4.4533- 3
1.5000+ 1 ~ 2.0000+ 1	3.7995+ 2	5.5083+ 1	3.2472+ 2		4.4533- 3
2.0000+ 1 ~ 3.0000+ 1	3.1937+ 2	5.3068+ 1	2.6563+ 2		4.4533- 3
3.0000+ 1 ~ 4.0000+ 1	2.6974+ 2	5.1010+ 1	2.1788+ 2		4.4533- 3
4.0000+ 1 ~ 5.0000+ 1	2.3797+ 2	4.9532+ 1	1.8810+ 2		4.4533- 3
5.0000+ 1 ~ 6.0000+ 1	2.1542+ 2	4.8246+ 1	1.6697+ 2		4.4570- 3
6.0000+ 1 ~ 8.0000+ 1	1.9162+ 2	4.6578+ 1	1.4462+ 2		4.4667- 3
8.0000+ 1 ~ 1.0000+ 2	1.6917+ 2	4.4875+ 1	1.2409+ 2		4.4768- 3
1.0000+ 2 ~ 1.5000+ 2	1.4449+ 2	4.2581+ 1	1.0182+ 2		4.4901- 3
1.5000+ 2 ~ 2.0000+ 2	1.2228+ 2	4.0102+ 1	8.2141+ 1		4.5073- 3
2.0000+ 2 ~ 3.0000+ 2	1.0304+ 2	3.7473+ 1	6.5555+ 1		4.5355- 3
3.0000+ 2 ~ 4.0000+ 2	8.7349+ 1	3.4896+ 1	5.2353+ 1		4.5804- 3
4.0000+ 2 ~ 5.0000+ 2	7.7306+ 1	3.3018+ 1	4.4212+ 1		4.6233- 3
5.0000+ 2 ~ 6.0000+ 2	7.0166+ 1	3.1545+ 1	3.8589+ 1		4.6682- 3
6.0000+ 2 ~ 8.0000+ 2	6.2623+ 1	2.9805+ 1	3.2791+ 1		4.7415- 3
8.0000+ 2 ~ 1.0000+ 3	5.5522+ 1	2.7996+ 1	2.7494+ 1		4.8467- 3
1.0000+ 3 ~ 1.5000+ 3	4.7711+ 1	2.5753+ 1	2.1926+ 1		5.0480- 3
1.5000+ 3 ~ 2.0000+ 3	4.0671+ 1	2.3498+ 1	1.7159+ 1		5.3478- 3
2.0000+ 3 ~ 3.0000+ 3	3.4567+ 1	2.1276+ 1	1.3286+ 1		5.8456- 3
3.0000+ 3 ~ 4.0000+ 3	2.9385+ 1	1.9147+ 1	1.0206+ 1		6.6706- 3
4.0000+ 3 ~ 5.0000+ 3	2.5941+ 1	1.7585+ 1	8.2942+ 0	4.4093- 2	7.4749- 3
5.0000+ 3 ~ 6.0000+ 3	2.4121+ 1	1.6329+ 1	6.9563+ 0	7.9787- 1	8.3559- 3
6.0000+ 3 ~ 8.0000+ 3	2.1714+ 1	1.4853+ 1	5.5909+ 0	1.2480+ 0	9.8261- 3
8.0000+ 3 ~ 1.0000+ 4	1.9445+ 1	1.3557+ 1	4.5164+ 0	1.3581+ 0	1.1893- 2
1.0000+ 4 ~ 1.5000+ 4	1.6940+ 1	1.2119+ 1	3.4998+ 0	1.3139+ 0	1.5778- 2
1.5000+ 4 ~ 2.0000+ 4	1.4670+ 1	1.0772+ 1	2.6912+ 0	1.2050+ 0	2.1458- 2
2.0000+ 4 ~ 3.0000+ 4	1.2695+ 1	9.5375+ 0	2.0910+ 0	1.0654+ 0	3.0893- 2
3.0000+ 4 ~ 4.0000+ 4	1.1066+ 1	8.4751+ 0	1.6589+ 0	9.3192- 1	4.3378- 2
4.0000+ 4 ~ 5.0000+ 4	1.0019+ 1	7.7637+ 0	1.4166+ 0	8.3931- 1	5.6121- 2
5.0000+ 4 ~ 6.0000+ 4	9.2749+ 0	7.2421+ 0	1.2610+ 0	7.7192- 1	6.8862- 2
6.0000+ 4 ~ 8.0000+ 4	8.4523+ 0	6.4623+ 0	1.0415+ 0	9.4514- 1	9.0752- 2
8.0000+ 4 ~ 1.0000+ 5	7.7601+ 0	5.5740+ 0	8.0561- 1	1.3802+ 0	1.2244- 1
1.0000+ 5 ~ 1.5000+ 5	6.9455+ 0	4.9355+ 0	6.4227- 1	1.3634+ 0	1.7219- 1
1.5000+ 5 ~ 2.0000+ 5	6.2947+ 0	4.3584+ 0	5.0226- 1	1.4321+ 0	2.2895- 1
2.0000+ 5 ~ 3.0000+ 5	6.0342+ 0	4.0081+ 0	4.1773- 1	1.6075+ 0	2.8697- 1
3.0000+ 5 ~ 4.0000+ 5	5.9080+ 0	3.8774+ 0	3.6193- 1	1.6687+ 0	3.3901- 1
4.0000+ 5 ~ 5.0000+ 5	6.0492+ 0	3.9109+ 0	3.2987- 1	1.8086+ 0	3.7283- 1
5.0000+ 5 ~ 6.0000+ 5	6.2493+ 0	4.0199+ 0	3.1472- 1	1.9149+ 0	3.9915- 1
6.0000+ 5 ~ 8.0000+ 5	6.5768+ 0	4.2207+ 0	3.0204- 1	2.0542+ 0	4.3751- 1
8.0000+ 5 ~ 1.0000+ 6	6.9423+ 0	4.4750+ 0	2.9423- 1	2.1732+ 0	4.9072- 1
1.0000+ 6 ~ 1.5000+ 6	7.2463+ 0	4.7486+ 0	2.8927- 1	2.2082+ 0	5.7503- 1
1.5000+ 6 ~ 2.0000+ 6	7.2479+ 0	4.8115+ 0	2.6803- 1	2.1683+ 0	6.5896- 1
2.0000+ 6 ~ 3.0000+ 6	6.7446+ 0	4.3844+ 0	1.9554- 1	2.1628+ 0	7.1329- 1
3.0000+ 6 ~ 4.0000+ 6	5.9015+ 0	3.5669+ 0	9.6579- 2	2.2034+ 0	7.2095- 1
4.0000+ 6 ~ 5.0000+ 6	5.2219+ 0	2.9194+ 0	4.4858- 2	2.2326+ 0	7.0730- 1
5.0000+ 6 ~ 6.0000+ 6	4.8860+ 0	2.6141+ 0	2.0734- 2	2.2447+ 0	7.0720- 1
6.0000+ 6 ~ 8.0000+ 6	4.7134+ 0	2.4566+ 0	6.6509- 3	2.2441+ 0	7.2174- 1
8.0000+ 6 ~ 1.0000+ 7	4.7240+ 0	2.5113+ 0	1.6723- 3	2.2089+ 0	7.6585- 1
1.0000+ 7 ~ 1.5000+ 7	5.1446+ 0	2.9217+ 0	3.3977- 4	2.2223+ 0	8.5138- 1

CROSS SECTION

MATERIAL =1631 EU-153

ENERGY	TOTAL	ELASTIC	CAPTURE	INELA	MU-BAR
1.0000- 5 ~ 1.0000- 2	4.3329+ 2	5.8817+ 0	4.2675+ 2		4.3950- 3
1.0000- 2 ~ 1.5000- 2	2.3436+ 2	5.8771+ 0	2.2843+ 2		4.3950- 3
1.5000- 2 ~ 2.0000- 2	2.0494+ 2	5.8740+ 0	1.9836+ 2		4.3950- 3
2.0000- 2 ~ 3.0000- 2	1.7806+ 2	5.8692+ 0	1.7214+ 2		4.3950- 3
3.0000- 2 ~ 4.0000- 2	1.5650+ 2	5.8628+ 0	1.5008+ 2		4.3950- 3
4.0000- 2 ~ 5.0000- 2	1.4196+ 2	5.8563+ 0	1.3605+ 2		4.3950- 3
5.0000- 2 ~ 6.0000- 2	1.3178+ 2	5.8496+ 0	1.2591+ 2		4.3950- 3
6.0000- 2 ~ 8.0000- 2	1.2136+ 2	5.8393+ 0	1.1509+ 2		4.3950- 3
8.0000- 2 ~ 1.0000- 1	1.1107+ 2	5.8250+ 0	1.0521+ 2		4.3950- 3
1.0000- 1 ~ 1.5000- 1	1.0068+ 2	5.7980+ 0	9.4646+ 1		4.3950- 3
1.5000- 1 ~ 2.0000- 1	9.2313+ 1	5.7548+ 0	8.6424+ 1		4.3950- 3
2.0000- 1 ~ 3.0000- 1	9.1092+ 1	5.6716+ 0	8.5164+ 1		4.3950- 3
3.0000- 1 ~ 4.0000- 1	1.2527+ 2	5.4988+ 0	1.1963+ 2		4.3950- 3
4.0000- 1 ~ 5.0000- 1	2.8290+ 2	5.6534+ 0	2.7718+ 2		4.3950- 3
5.0000- 1 ~ 6.0000- 1	1.2204+ 2	5.8307+ 0	1.1611+ 2		4.3950- 3
6.0000- 1 ~ 8.0000- 1	6.4645+ 1	5.5742+ 0	5.8952+ 1		4.3950- 3
8.0000- 1 ~ 1.0000+ 0	5.5562+ 1	5.3511+ 0	5.0148+ 1		4.3950- 3
1.0000+ 0 ~ 1.5000+ 0	6.0564+ 1	4.8412+ 0	5.5610+ 1		4.3950- 3
1.5000+ 0 ~ 2.0000+ 0	1.9875+ 2	4.1065+ 0	1.9463+ 2		4.3950- 3
2.0000+ 0 ~ 3.0000+ 0	1.0890+ 3	1.7208+ 1	1.0718+ 3		4.3950- 3
3.0000+ 0 ~ 4.0000+ 0	1.0205+ 3	1.6148+ 1	1.0043+ 3		4.3950- 3
4.0000+ 0 ~ 5.0000+ 0	1.8383+ 2	1.3391+ 1	1.7041+ 2		4.3950- 3
5.0000+ 0 ~ 6.0000+ 0	5.4925+ 1	7.3039+ 0	4.7571+ 1		4.3950- 3
6.0000+ 0 ~ 8.0000+ 0	1.2990+ 2	7.7809+ 0	1.2211+ 2		4.3950- 3
8.0000+ 0 ~ 1.0000+ 1	4.4383+ 2	2.2262+ 1	4.2157+ 2		4.3950- 3
1.0000+ 1 ~ 1.5000+ 1	1.7653+ 2	1.3849+ 1	1.6268+ 2		4.3950- 3
1.5000+ 1 ~ 2.0000+ 1	3.3161+ 2	1.8346+ 1	3.1326+ 2		4.3950- 3
2.0000+ 1 ~ 3.0000+ 1	1.5251+ 2	1.9952+ 1	1.3255+ 2		4.3950- 3
3.0000+ 1 ~ 4.0000+ 1	1.4473+ 2	1.4660+ 1	1.3007+ 2		4.3950- 3
4.0000+ 1 ~ 5.0000+ 1	1.1594+ 2	1.2801+ 1	1.0313+ 2		4.3950- 3
5.0000+ 1 ~ 6.0000+ 1	1.7999+ 2	2.2162+ 1	1.5783+ 2		4.3950- 3
6.0000+ 1 ~ 8.0000+ 1	1.5612+ 2	3.5338+ 1	1.2078+ 2		4.3950- 3
8.0000+ 1 ~ 1.0000+ 2	1.4377+ 2	3.7631+ 1	1.1165+ 2		4.3950- 3
1.0000+ 2 ~ 1.5000+ 2	8.9945+ 1	4.1976+ 1	6.2678+ 1		4.4192- 3
1.5000+ 2 ~ 2.0000+ 2	9.3687+ 1	3.9746+ 1	5.3918+ 1		4.4498- 3
2.0000+ 2 ~ 3.0000+ 2	8.4021+ 1	3.7352+ 1	4.6668+ 1		4.4777- 3
3.0000+ 2 ~ 4.0000+ 2	7.6794+ 1	3.4974+ 1	4.1818+ 1		4.5220- 3
4.0000+ 2 ~ 5.0000+ 2	7.1916+ 1	3.3225+ 1	3.8690+ 1		4.5642- 3
5.0000+ 2 ~ 6.0000+ 2	6.7286+ 1	3.1843+ 1	3.5416+ 1		4.6082- 3
6.0000+ 2 ~ 8.0000+ 2	6.0821+ 1	3.0198+ 1	3.0603+ 1		4.6797- 3
8.0000+ 2 ~ 1.0000+ 3	5.4687+ 1	2.8474+ 1	2.6191+ 1		4.7820- 3
1.0000+ 3 ~ 1.5000+ 3	4.7641+ 1	2.6314+ 1	2.1300+ 1		4.9766- 3
1.5000+ 3 ~ 2.0000+ 3	4.1127+ 1	2.4123+ 1	1.6992+ 1		5.2654- 3
2.0000+ 3 ~ 3.0000+ 3	3.5618+ 1	2.1939+ 1	1.3676+ 1		5.7425- 3
3.0000+ 3 ~ 4.0000+ 3	3.1106+ 1	1.9922+ 1	1.1180+ 1		6.5116- 3
4.0000+ 3 ~ 5.0000+ 3	2.8390+ 1	1.8510+ 1	9.8798+ 0		7.2478- 3
5.0000+ 3 ~ 6.0000+ 3	2.6295+ 1	1.7435+ 1	8.8486+ 0		8.0195- 3
6.0000+ 3 ~ 8.0000+ 3	2.3634+ 1	1.6210+ 1	7.4148+ 0		9.2757- 3
8.0000+ 3 ~ 1.0000+ 4	2.1123+ 1	1.4977+ 1	6.1371+ 0		1.1069- 2
1.0000+ 4 ~ 1.5000+ 4	1.8350+ 1	1.3502+ 1	4.8392+ 0		1.4444- 2
1.5000+ 4 ~ 2.0000+ 4	1.5835+ 1	1.2067+ 1	3.7649+ 0		1.9375- 2
2.0000+ 4 ~ 3.0000+ 4	1.3643+ 1	1.0703+ 1	2.9369+ 0		2.7566- 2
3.0000+ 4 ~ 4.0000+ 4	1.1835+ 1	9.5050+ 0	2.3291+ 0		3.8412- 2
4.0000+ 4 ~ 5.0000+ 4	1.0672+ 1	8.6877+ 0	1.9838+ 0		4.9508- 2
5.0000+ 4 ~ 6.0000+ 4	9.8424+ 0	8.0805+ 0	1.7617+ 0		6.0631- 2
6.0000+ 4 ~ 8.0000+ 4	8.9659+ 0	7.4141+ 0	1.5517+ 0		7.7058- 2
8.0000+ 4 ~ 1.0000+ 5	8.1081+ 0	6.6106+ 0	1.2854+ 0	2.1137- 1	1.0059- 1
1.0000+ 5 ~ 1.5000+ 5	7.1577+ 0	5.6719+ 0	9.5837- 1	5.1862- 1	1.4577- 1
1.5000+ 5 ~ 2.0000+ 5	6.3765+ 0	4.8393+ 0	7.1079- 1	8.2534- 1	1.9806- 1
2.0000+ 5 ~ 3.0000+ 5	6.1238+ 0	4.3018+ 0	5.6128- 1	1.2596+ 0	2.5429- 1
3.0000+ 5 ~ 4.0000+ 5	6.0210+ 0	4.0684+ 0	4.9180- 1	1.4606+ 0	3.0565- 1
4.0000+ 5 ~ 5.0000+ 5	6.1096+ 0	4.0714+ 0	4.7690- 1	1.5616+ 0	3.3962- 1
5.0000+ 5 ~ 6.0000+ 5	6.2953+ 0	4.1633+ 0	4.7664- 1	1.6557+ 0	3.6780- 1
6.0000+ 5 ~ 8.0000+ 5	6.6010+ 0	4.3475+ 0	4.7559- 1	1.7781+ 0	4.1043- 1
8.0000+ 5 ~ 1.0000+ 6	6.9634+ 0	4.5734+ 0	4.6418- 1	1.9259+ 0	4.7068- 1
1.0000+ 6 ~ 1.5000+ 6	7.2636+ 0	4.8171+ 0	4.3298- 1	2.0133+ 0	5.6381- 1
1.5000+ 6 ~ 2.0000+ 6	7.2804+ 0	4.8609+ 0	3.5052- 1	2.0684+ 0	6.5547- 1
2.0000+ 6 ~ 3.0000+ 6	6.8123+ 0	4.4496+ 0	2.0779- 1	2.1516+ 0	7.1386- 1
3.0000+ 6 ~ 4.0000+ 6	5.9821+ 0	3.6407+ 0	8.2953- 2	2.2207+ 0	7.2409- 1
4.0000+ 6 ~ 5.0000+ 6	5.2938+ 0	2.9842+ 0	3.2793- 2	2.2500+ 0	7.1244- 1
5.0000+ 6 ~ 6.0000+ 6	4.9418+ 0	2.6614+ 0	1.3655- 2	2.2611+ 0	7.1187- 1
6.0000+ 6 ~ 8.0000+ 6	4.7385+ 0	2.4715+ 0	4.0360- 3	2.2576+ 0	7.2304- 1
8.0000+ 6 ~ 1.0000+ 7	4.7278+ 0	2.5013+ 0	8.9829- 4	2.2239+ 0	7.6407- 1
1.0000+ 7 ~ 1.5000+ 7	5.1569+ 0	2.9149+ 0	1.4545- 4	2.2415+ 0	8.4966- 1

CROSS SECTION

MATERIAL =1632 EU-155

ENERGY	TOTAL	ELASTIC	CAPTURE	INELA	MU-BAR
1.0000- 5 ~ 1.0000- 2	1.2537+ 4	8.3470+ 0	1.2458+ 4		4.3384- 3
1.0000- 2 ~ 1.5000- 2	5.8278+ 3	8.3470+ 0	5.7770+ 3		4.3384- 3
1.5000- 2 ~ 2.0000- 2	4.9152+ 3	8.3470+ 0	4.8703+ 3		4.3384- 3
2.0000- 2 ~ 3.0000- 2	4.1244+ 3	8.3470+ 0	4.0850+ 3		4.3384- 3
3.0000- 2 ~ 4.0000- 2	3.4785+ 3	8.3470+ 0	3.4438+ 3		4.3384- 3
4.0000- 2 ~ 5.0000- 2	3.0656+ 3	8.3470+ 0	3.0341+ 3		4.3384- 3
5.0000- 2 ~ 6.0000- 2	2.7721+ 3	8.3470+ 0	2.7429+ 3		4.3384- 3
6.0000- 2 ~ 8.0000- 2	2.4618+ 3	8.3470+ 0	2.4352+ 3		4.3384- 3
8.0000- 2 ~ 1.0000- 1	2.1696+ 3	8.3470+ 0	2.1454+ 3		4.3384- 3
1.0000- 1 ~ 1.5000- 1	1.8482+ 3	8.3470+ 0	1.8269+ 3		4.3384- 3
1.5000- 1 ~ 2.0000- 1	1.5587+ 3	8.3470+ 0	1.5401+ 3		4.3384- 3
2.0000- 1 ~ 3.0000- 1	1.3080+ 3	8.3470+ 0	1.2918+ 3		4.3384- 3
3.0000- 1 ~ 4.0000- 1	1.1031+ 3	8.3470+ 0	1.0891+ 3		4.3384- 3
4.0000- 1 ~ 5.0000- 1	9.7219+ 2	8.3470+ 0	9.5948+ 2		4.3384- 3
5.0000- 1 ~ 6.0000- 1	8.7912+ 2	8.3470+ 0	8.6741+ 2		4.3384- 3
6.0000- 1 ~ 8.0000- 1	7.8070+ 2	8.3470+ 0	7.7008+ 2		4.3384- 3
8.0000- 1 ~ 1.0000+ 0	6.8803+ 2	8.3470+ 0	6.7846+ 2		4.3384- 3
1.0000+ 0 ~ 1.5000+ 0	1.0372+ 3	5.0284+ 1	9.8636+ 2		4.3384- 3
1.5000+ 0 ~ 2.0000+ 0	1.2960+ 3	9.1081+ 1	1.2032+ 3		4.3384- 3
2.0000+ 0 ~ 3.0000+ 0	1.0881+ 3	8.9422+ 1	9.9763+ 2		4.3384- 3
3.0000+ 0 ~ 4.0000+ 0	9.1811+ 2	8.7470+ 1	8.2915+ 2		4.3384- 3
4.0000+ 0 ~ 5.0000+ 0	8.0931+ 2	8.5694+ 1	7.2073+ 2		4.3384- 3
5.0000+ 0 ~ 6.0000+ 0	7.3198+ 2	8.4304+ 1	6.4468+ 2		4.3384- 3
6.0000+ 0 ~ 8.0000+ 0	6.5018+ 2	8.2685+ 1	5.6522+ 2		4.3384- 3
8.0000+ 0 ~ 1.0000+ 1	5.7314+ 2	8.1006+ 1	4.9131+ 2		4.3384- 3
1.0000+ 1 ~ 1.5000+ 1	4.8851+ 2	7.8382+ 1	4.0949+ 2		4.3384- 3
1.5000+ 1 ~ 2.0000+ 1	4.1232+ 2	7.5446+ 1	3.3642+ 2		4.3384- 3
2.0000+ 1 ~ 3.0000+ 1	3.4636+ 2	7.2029+ 1	2.7350+ 2		4.3384- 3
3.0000+ 1 ~ 4.0000+ 1	2.9250+ 2	6.8593+ 1	2.2287+ 2		4.3384- 3
4.0000+ 1 ~ 5.0000+ 1	2.5802+ 2	6.6146+ 1	1.9147+ 2		4.3384- 3
5.0000+ 1 ~ 6.0000+ 1	2.3356+ 2	6.4056+ 1	1.6925+ 2		4.3384- 3
6.0000+ 1 ~ 8.0000+ 1	2.0772+ 2	6.1399+ 1	1.4583+ 2		4.3384- 3
8.0000+ 1 ~ 1.0000+ 2	1.8335+ 2	5.8704+ 1	1.2442+ 2		4.3384- 3
1.0000+ 2 ~ 1.5000+ 2	1.5658+ 2	5.5145+ 1	1.0134+ 2		4.3572- 3
1.5000+ 2 ~ 2.0000+ 2	1.3250+ 2	5.1371+ 1	8.1079+ 1		4.3813- 3
2.0000+ 2 ~ 3.0000+ 2	1.1162+ 2	4.7457+ 1	6.4146+ 1		4.4044- 3
3.0000+ 2 ~ 4.0000+ 2	9.4593+ 1	4.3707+ 1	5.0778+ 1		4.4418- 3
4.0000+ 2 ~ 5.0000+ 2	8.3691+ 1	4.1012+ 1	4.2597+ 1		4.4776- 3
5.0000+ 2 ~ 6.0000+ 2	7.5941+ 1	3.8925+ 1	3.6982+ 1		4.5155- 3
6.0000+ 2 ~ 8.0000+ 2	6.7753+ 1	3.6495+ 1	3.1229+ 1		4.5776- 3
8.0000+ 2 ~ 1.0000+ 3	6.0047+ 1	3.4004+ 1	2.6009+ 1		4.6674- 3
1.0000+ 3 ~ 1.5000+ 3	5.1569+ 1	3.0966+ 1	2.0570+ 1		4.8408- 3
1.5000+ 3 ~ 2.0000+ 3	4.3926+ 1	2.7959+ 1	1.5953+ 1		5.1009- 3
2.0000+ 3 ~ 3.0000+ 3	3.7298+ 1	2.5051+ 1	1.2242+ 1		5.5369- 3
3.0000+ 3 ~ 4.0000+ 3	3.1893+ 1	2.2442+ 1	9.4210+ 0		6.2505- 3
4.0000+ 3 ~ 5.0000+ 3	2.8422+ 1	2.0650+ 1	7.7495+ 0		6.9378- 3
5.0000+ 3 ~ 6.0000+ 3	2.5950+ 1	1.9308+ 1	6.6325+ 0		7.6636- 3
6.0000+ 3 ~ 8.0000+ 3	2.3334+ 1	1.7806+ 1	5.5214+ 0		8.8537- 3
8.0000+ 3 ~ 1.0000+ 4	2.0867+ 1	1.6317+ 1	4.5419+ 0		1.0564- 2
1.0000+ 4 ~ 1.5000+ 4	1.8141+ 1	1.4573+ 1	3.5609+ 0		1.3808- 2
1.5000+ 4 ~ 2.0000+ 4	1.5669+ 1	1.2907+ 1	2.7602+ 0		1.8577- 2
2.0000+ 4 ~ 3.0000+ 4	1.3515+ 1	1.1358+ 1	2.1545+ 0		2.6553- 2
3.0000+ 4 ~ 4.0000+ 4	1.1739+ 1	1.0022+ 1	1.7159+ 0		3.7154- 2
4.0000+ 4 ~ 5.0000+ 4	1.0597+ 1	9.1259+ 0	1.4704+ 0		4.8028- 2
5.0000+ 4 ~ 6.0000+ 4	9.7826+ 0	8.4681+ 0	1.3145+ 0		5.8943- 2
6.0000+ 4 ~ 8.0000+ 4	8.8780+ 0	7.6952+ 0	1.1471+ 0	3.5319- 2	7.5723- 2
8.0000+ 4 ~ 1.0000+ 5	8.1252+ 0	6.7787+ 0	9.4456- 1	4.0127- 1	9.9802- 2
1.0000+ 5 ~ 1.5000+ 5	7.3067+ 0	6.0067+ 0	7.8508- 1	5.0769- 1	1.3880- 1
1.5000+ 5 ~ 2.0000+ 5	6.6128+ 0	5.3321+ 0	6.4220- 1	6.3532- 1	1.8266- 1
2.0000+ 5 ~ 3.0000+ 5	6.1878+ 0	4.8016+ 0	5.4554- 1	8.3964- 1	2.3394- 1
3.0000+ 5 ~ 4.0000+ 5	6.1005+ 0	4.4638+ 0	4.8058- 1	1.1554+ 0	2.8776- 1
4.0000+ 5 ~ 5.0000+ 5	6.2317+ 0	4.4162+ 0	4.5458- 1	1.3612+ 0	3.2526- 1
5.0000+ 5 ~ 6.0000+ 5	6.4299+ 0	4.5268+ 0	4.5253- 1	1.4509+ 0	3.5381- 1
6.0000+ 5 ~ 8.0000+ 5	6.7413+ 0	4.7346+ 0	4.5893- 1	1.5479+ 0	3.9652- 1
8.0000+ 5 ~ 1.0000+ 6	7.0630+ 0	4.9661+ 0	4.7599- 1	1.6209+ 0	4.5572- 1
1.0000+ 6 ~ 1.5000+ 6	7.3207+ 0	5.1827+ 0	5.3769- 1	1.6001+ 0	5.4356- 1
1.5000+ 6 ~ 2.0000+ 6	7.3346+ 0	5.0842+ 0	4.2534- 1	1.8193+ 0	6.3957- 1
2.0000+ 6 ~ 3.0000+ 6	6.8582+ 0	4.5117+ 0	1.3623- 1	2.2034+ 0	7.1109- 1
3.0000+ 6 ~ 4.0000+ 6	6.0471+ 0	3.6864+ 0	4.3100- 2	2.2879+ 0	7.2396- 1
4.0000+ 6 ~ 5.0000+ 6	5.3970+ 0	3.0407+ 0	1.7154- 2	2.3175+ 0	7.1380- 1
5.0000+ 6 ~ 6.0000+ 6	5.0725+ 0	2.7449+ 0	7.3210- 3	2.3181+ 0	7.1438- 1
6.0000+ 6 ~ 8.0000+ 6	4.9029+ 0	2.6110+ 0	2.2955- 3	2.2875+ 0	7.2684- 1
8.0000+ 6 ~ 1.0000+ 7	4.9214+ 0	2.6706+ 0	5.4553- 4	2.2488+ 0	7.6536- 1
1.0000+ 7 ~ 1.5000+ 7	5.3646+ 0	3.0982+ 0	8.9244- 5	2.2658+ 0	8.4858- 1